

University of Windsor

## Scholarship at UWindor

---

Electronic Theses and Dissertations

Theses, Dissertations, and Major Papers

---

1-1-1979

### Behaviour of reinforced and prestressed waffle slabs.

Ibrahim Sayed Ahmed el-Sebakhy  
*University of Windsor*

Follow this and additional works at: <https://scholar.uwindsor.ca/etd>

---

#### Recommended Citation

el-Sebakhy, Ibrahim Sayed Ahmed, "Behaviour of reinforced and prestressed waffle slabs." (1979).  
*Electronic Theses and Dissertations*. 6726.  
<https://scholar.uwindsor.ca/etd/6726>

This online database contains the full-text of PhD dissertations and Masters' theses of University of Windsor students from 1954 forward. These documents are made available for personal study and research purposes only, in accordance with the Canadian Copyright Act and the Creative Commons license—CC BY-NC-ND (Attribution, Non-Commercial, No Derivative Works). Under this license, works must always be attributed to the copyright holder (original author), cannot be used for any commercial purposes, and may not be altered. Any other use would require the permission of the copyright holder. Students may inquire about withdrawing their dissertation and/or thesis from this database. For additional inquiries, please contact the repository administrator via email ([scholarship@uwindsor.ca](mailto:scholarship@uwindsor.ca)) or by telephone at 519-253-3000ext. 3208.

BEHAVIOUR OF REINFORCED AND  
PRESTRESSED WAFFLE SLABS

by

Ibrahim Sayed Ahmed El-Sebakhy

A Thesis  
submitted to the Faculty of Graduate Studies  
through the Department of  
Civil Engineering in Partial Fulfillment  
of the requirements for the degree  
of Master of Applied Science at  
The University of Windsor

Windsor, Ontario, Canada  
1979

UMI Number: EC54719

### INFORMATION TO USERS

The quality of this reproduction is dependent upon the quality of the copy submitted. Broken or indistinct print, colored or poor quality illustrations and photographs, print bleed-through, substandard margins, and improper alignment can adversely affect reproduction.

In the unlikely event that the author did not send a complete manuscript and there are missing pages, these will be noted. Also, if unauthorized copyright material had to be removed, a note will indicate the deletion.

UMI<sup>®</sup>

---

UMI Microform EC54719  
Copyright 2010 by ProQuest LLC  
All rights reserved. This microform edition is protected against  
unauthorized copying under Title 17, United States Code.

---

ProQuest LLC  
789 East Eisenhower Parkway  
P.O. Box 1346  
Ann Arbor, MI 48106-1346

AB 4883

© Ibrahim Sayed Ahmed El-Sebakhy 1979

713340

To my wife and parents

## ABSTRACT

Reinforced concrete waffle slabs have been used quite often in buildings and other structures, resulting in a reduced dead weight and material cost. The use of prestressed concrete waffle slabs for rectangular and skew decks of short and medium span bridges can also lead to further economics in dead weight and material.

In this investigation, a series solution for the analysis of rectangular and skew concrete waffle slabs by the orthotropic plate theory is presented. Single spans of reinforced and prestressed concrete deck bridge models are investigated. The deflection function of the slab is assumed in the form of a Fourier series so as to satisfy the governing differential equation of equilibrium. The arbitrary constants in the deflection function are chosen to satisfy the appropriate boundary conditions. The in-plane prestressing force along the edges and the resulting edge moment are represented by a Fourier series using a graphical technique.

Available computer program for solving orthotropic plates or slabs subjected to lateral loads is modified to compute the stresses and deflection due to the prestressing force. This computer program can be used for reinforced and prestressed concrete waffle slabs of rectangular and skew shapes subjected to uniform as well as concentrated

transverse loads.

The experimental study is carried out on three one-eighth models of reinforced concrete waffle slabs and two one-eighth models of prestressed concrete waffle slabs. The first slab is tested under uniformly distributed load applied by means of air pressure while the remaining slabs are tested under concentrated loads only at various positions; the tests were carried in the elastic domain as bridge slabs and finally to collapse. The effect of concrete cracking on the rigidities of the slabs is studied. The strains and deflections obtained from the tests are found to be in satisfactory agreement with the theoretical solution. Furthermore, theoretical studies are carried out on two types of structures, the waffle-type and the slab-type with a uniform thickness, both structures having the same volume of concrete and reinforcing steel. The comparison of stresses and deflection for the two types of structures show that the waffle type exhibits much smaller deflections and lower stresses, especially for prestressed concrete waffle slabs.

## ACKNOWLEDGEMENTS

The author wishes to express his deep appreciation to his supervisor Dr. J.B. Kennedy, Professor of Civil Engineering at the University of Windsor, for his extremely valuable comments, guidance, encouragement, generous aid and constructive criticism.

The author would like to thank Dr. D.S. Gupta, Chief Engineer at Canadian Bridge Division, Windsor, Ontario, for his assistance and guidance in the computer program.

The aid of Mr. G. Michalczuk and Mr. P. Feimer during the experimental work is greatly appreciated. Thanks are also due to the staff of the computer centre for their assistance and help.

The financial assistance given by the National Research Council of Canada under Grant No. A-1896, and the scholarship granted by the University of Windsor are sincerely appreciated.

Thanks are also due to Mrs. Barbara Denomey for typing the manuscript.



TABLE OF CONTENTS

	PAGE
ABSTRACT.....	iv
ACKNOWLEDGEMENTS.....	vi
TABLE OF CONTENTS.....	vii
LIST OF FIGURES.....	x
LIST OF TABLES.....	xv
LIST OF APPENDICES.....	xvi
LIST OF ABBREVIATIONS.....	xvii
CHAPTER I INTRODUCTION.....	1
1.1 General.....	1
1.2 Objective.....	1
1.3 Scope.....	2
CHAPTER II HISTORICAL REVIEW.....	4
2.1 Review of Literature.....	4
2.2 Prestressed Concrete Slabs.....	6
CHAPTER III FORMULATION.....	9
3.1 General.....	9
3.2 Assumptions.....	10
3.3 Governing Differential Equation For The Lateral Loads and Edge Moments.....	10
3.4 Relation of Stress and Strain For Bending Action.....	12
3.5 Elastic Properties of the Waffle Slab Model.....	13
3.6 Rigidities of Uncracked Sections.....	15
3.6.1 Flexural Rigidities.....	15
3.6.2 Torsional Rigidities.....	18
3.7 Plane Stress Problem Due To Pre- stressing Force.....	21
3.7.1 Elastic Constants for Membrane Action.....	21
3.8 Boundary Conditions.....	23
3.8.1 Bridge Slabs.....	24

		PAGE
CHAPTER IV	ANALYTICAL SOLUTION.....	27
4.1	General.....	27
4.2	Complementary Solution.....	27
	4.2.1 Waffle Slab Which Is Flexurally Strong and Torsionally Weak.....	28
4.3	Particular Solution.....	30
4.4	Symmetric and Anti-Symmetric Loading.....	31
4.5	Expansion of the In-Plane Prestressing Force In A Fourier Series by Graphical Method.....	31
CHAPTER V	SATISFACTION OF BOUNDARY CONDITIONS.....	33
5.1	Symmetric Load.....	33
5.2	Anti-Symmetric Load.....	39
CHAPTER VI	EXPERIMENTAL PROGRAM.....	44
6.1	Scope of the Experimental Program.....	44
6.2	Materials.....	44
	6.2.1 Concrete.....	44
6.3	Steel.....	45
	6.3.1 Mild Steel For Reinforced Concrete Slabs.....	45
	6.3.2 High Tensile Steel For The Pre- Stressed Concrete Slabs.....	46
6.4	Formwork.....	46
6.5	Experimental Equipment.....	47
	6.5.1 Prestressing Equipment.....	47
	6.5.2 End Bearing Plate.....	47
	6.5.3 The Steel Frame For Producing Uniformly Distributed Load.....	48
6.6	The Construction of the Slab Models.....	49
6.7	Instrumentation.....	50
	6.7.1 Strain Gauges On The Reinforcement.....	50
	6.7.2 Strain Gauges on The Concrete....	51
	6.7.3 Mechanical Dial Gauges.....	51
	6.7.4 Load Cells.....	52
	6.7.4(a) Universal Flad Load Cell.....	52
	6.7.4(b) Cylindrical Load Cell.....	52
6.8	Experimental Setup and Test Procedure...	52
	6.8.1 Reinforced Concrete Waffle Slabs, Group A.....	52
	6.8.1(a) Slab A.1.....	52
	6.8.1(b) Slab A.2.....	53
	6.8.1(c) Slab A.3.....	54

	PAGE
6.8.2 Prestressed Concrete Waffle Slabs, Group B.....	55
6.8.2(a) Slab B.1.....	55
6.8.2(b) Slab B.2.....	55
CHAPTER VII DISCUSSION OF RESULTS.....	57
7.1 General.....	57
7.2 Reinforced Concrete Waffle Slabs (Group A).....	57
7.2.1 Rectangular Slab Under Uniform Load (Slab A.1).....	57
7.2.2 Rectangular Slab Under Concen- trated Load (Slab A.2).....	58
7.2.3 45° Skew Slab Under Conentra- ted Load (Slab A.3).....	61
7.3 Prestressed Concrete Waffle Slabs Group B).....	61
7.3.1 Rectangular Slab Under Concen- trated Load (Slab B.1).....	61
7.3.2 45° Skew Slab Under Conentra- ted Load (Slab B.2).....	62
7.4 Comparison Between the Behaviours of a Waffle Slab and a Uniform Thickness Slab Having the Same Volume of Con- crete and Reinforcement.....	63
7.5 Sources of Errors.....	65
CHAPTER VIII CONCLUSIONS AND RECOMMENDATIONS.....	67
8.1 Conclusions.....	67
8.2 Suggestions.....	69
FIGURES.....	70
APPENDIX A.....	143
APPENDIX B.....	149
APPENDIX C.....	153
APPENDIX D.....	155
APPENDIX E.....	160
APPENDIX F.....	169
BIBLIOGRAPHY.....	206
VITA AUCTORIS.....	209

LIST OF FIGURES

FIGURE		PAGE
3.1	Bottom Plan Layout Waffle Slabs A <sub>1</sub> and A <sub>2</sub> .....	71
3.2	Geometric Shape of the Ribs and the Plate for Waffle Slab.....	72
3.3	Orthotropic Rigidities of Waffle Slab....	73
3.4	Lateral Loading Cases for Group A Slabs..	74
3.5	Lateral Loading Cases for Group B Slabs..	75
4.1	Steel Loading Plates.....	75
4.2	Expansion of the Load in Fourier Series..	76
6.1	The Reinforcing Steel and Anchorage System.....	77
6.2	Form Before Casting the Concrete.....	77
6.3	Hydraulic 20 KIP Prestressing Jack.....	78
6.4	End Blocks and Load Cells for Prestressed Skew Slab.....	78
6.5	Loading System for Uniform Load.....	79
6.6	Regulator System and Pressure Gauges.....	79
6.7	Transverse Section for the Loading Frame.....	80
6.8	Longitudinal Section for the Loading Frame.....	81
6.9	Reinforced Concrete Waffle Slab A.1.....	82
6.10	Reinforced Concrete Waffle Slab A.2.....	83
6.11	Reinforced Concrete Skew Waffle Slab A.3, Skew of 45°.....	84
6.12	Prestressed Concrete Waffle Slab B.1.....	85
6.13	Prestressed Concrete Waffle Slab B.2.....	86

FIGURE		PAGE
6.14	Dial Gauges In Position.....	87
6.15	Point Loading System.....	87
6.16	Loading System for Slab A.2.....	88
6.17	Loading System for the Skew Slab A.3.....	88
6.18	Loading System for Prestressed Slab B.1..	89
6.19	Loading System for Prestressed Skew Slab B.2.....	89
6.20	Prestressing Force and Edge Moments For Slab B.1.....	90
6.21	Prestressing Force and Edge Moments For Skew Slab B.2.....	91
7.1	Slab A.1 Failure.....	92
7.2	Slab A.1 Cracks.....	92
7.3	Load Deflection Relationship for Slab A.1.....	93
7.4	Load Deflection Relationship for Slab A.1.....	94
7.5	Transverse Deflection.....	95
7.6	Longitudinal Deflection.....	96
7.7	Load Strain Relationship for Slab A.1 At Centre.....	97
7.8	Load Strain Relationship for Slab A.1 At the Free Edge.....	98
7.9	Deflection Shape for Slab A.2.....	99
7.10	Slab A.2 Cracks.....	99
7.11	Load Deflection Relationship for Slab A.2.....	100
7.12	Load Deflection Relationships for Slab A.2, Load at the Edge.....	101
7.13	Transverse Deflection for Slab A.2 (p = 1 Kip).....	102

FIGURE		PAGE
7.14	Longitudinal Deflection Along Line A-A (p = 1 Kip).....	103
7.15	Load Strain Relationship for Slab A.2, Load at the Centre of Slab.....	104
7.16	Load Strain Relationship for Slab A.2, Load at the Free Edge.....	105
7.17	Strain Distribution for Slab A.2 at Bottom Fibre due to 1 Kip at Centre.....	106
7.18	Crack Development in Slab A.3.....	107
7.19	Bottom Cracks for Slab A.3.....	107
7.20	Load Deflection Relationship for Skew Slab A.3.....	108
7.21	Load Deflection Relationship for Skew Slab A.3.....	109
7.22	Deflection Along Line A-A for Skew Slab A.3 (p = 1 Kip).....	110
7.23	Load Strain Relationship for Skew Slab A.3 At Point 1.....	111
7.24	Load Strain Relationship for Skew Slab A.3 At Point 2.....	112
7.25	Strain Distribution for Skew Slab A.3 at Bottom Fibre for Loading At Centre....	113
7.26	Cracks Development for Slab B.1.....	114
7.27	Cracks Failure For Slab B.1.....	114
7.28	The Upward Deflection in Slab B.1 Due To Prestressing.....	115
7.29	Top Fibre Strain Distribution for Slab B.1 Due to Prestressing.....	116
7.30	Bottom Fibre Strain Distribution for Slab B.1 Due to Prestressing.....	117
7.31	Load Deflection Relationship for Slab B.1.....	118
7.32	Load Deflection Relationship for Slab B.1.....	119

FIGURE		PAGE
7.33	Load Strain Relationship for Slab B.1 at Centre.....	120
7.34	Load Strain Relationship for Slab B.1 (Loading at Point 1).....	121
7.35	Cracks Failure for Slab B.2.....	122
7.36	Cracks Development for Slab B.2.....	122
7.37	Punching Failure of Slab B.2.....	123
7.38	Cracks Failure for Slab B.2.....	123
7.39	Deflection Distribution for Skew Slab B.2 Due to Prestressing Force.....	124
7.40	Strain Distribution in Slab B.2 at Top Fibre due to Prestressing Force.....	125
7.41	Strain Distribution in Slab B.2 at Bottom Fibre due to Prestressing.....	126
7.42	Load Deflection Relationship for Slab B.2.....	127
7.43	Load Deflection Relationship for Slab B.2.....	128
7.44	Load Deflection Relationship for Slab B.2 (Ultimate Load).....	129
7.45	Load Strain Relationship for Slab B.2...	130
7.46	Load Strain Relationship for Slab B.2...	131
7.47	Deflection Pattern for Rectangular Slab Due to Uniform Load of 0.01 lb/in <sup>2</sup> .....	132
7.48	Strain Pattern at Top Fibre due to Uniform Load of 0.01 lb/in <sup>2</sup> .....	133
7.49	Variation of Deflection Along the Transverse for Point Load at 1 and 2.....	134
7.50	Variation of Strains Along the Transverse Axis At Top Fibre due to Concentrated Load 1 Kip at Point 1 and 2.....	135

FIGURE		PAGE
7.51	Variation of Strains Along the Transverse Axis at Bottom Fibre due to Concentrated Load 1 Kip.....	136
7.52	Deflections due to Uniform Load of 0.01 lb/in <sup>2</sup> .....	137
7.53	Strain Pattern at Top Fibre Due to Uniform Load of 0.01 lb/in <sup>2</sup> .....	138
7.54	Deflection Pattern due to Concentrated Load 1 Kip at Point 1 and 2.....	139
7.55	Strain Pattern at Top Fibre Due to 1 Kip at Point 1 and 2.....	140
7.56	Deflection due to Prestressing Force.....	141
E1	Calibration of Reinforcing Steel Wires....	161
E2	Load Deflection for High Tensile Steel Wire.....	162
E3	Load Strain Relationship (Load Cell, 5 Kips).....	163
E4	Load Strain Relationship (Load Cell, 25 Kips).....	164
E5	Load Strain Relationship (1-5, Load Cell)..	165
E6	Load Strain Relationship (6-11, Load Cell).....	166
E7	Load Strain Relationship (12-20, Load Cell).....	167
E8	Load Strain Relationship (21-38, Load Cell).....	168



LIST OF TABLES

TABLE		PAGE
D-1	Properties and Strength of Concrete Mixes .....	156
D-2	Geometry and Properties of Slab Models....	158
D-3	Orthotropic Rigidities of Slab Models.....	159

LIST OF APPENDICES

APPENDIX		PAGE
A	Expressions For Matrix Elements.....	143
B	Fourier Coefficients For Lateral Load.....	149
C	Fourier Expansion for In Plane-Forces..	153
D	Design of Concrete Mix.....	155
E	Calibration of Load Cell.....	160
F	Computer Program (WAFFLE).....	169

## LIST OF ABBREVIATIONS

$A_{j1} - A_{j8}$	Definite integrals (Appendix A)
$A_n$	Arbitrary function in n (Equation 5.1)
$A_s (A'_s)$	Area of tension steel in longitudinal (transverse) rib
a	Skew semi-width of the slab
$B_{j1} - B_{j2}$	Definite integrals defined (Appendix A)
$B_n$	Arbitrary function in n (Equation 5.1)
b	Half span length of the slab
$b_y (b_x)$	Width of longitudinal (transverse) rib
$C_{1n} - C_{16n}$	Arbitrary functions dependent on n
$C_{17} - C_{24}$	Arbitrary constants
c	$\cos\theta$
D	Flexural rigidity of the flange plate with respect to its middle plane
$D_x, D_y$	Flexural rigidities of the slab per unit width and length respectively
$D_{xy}, D_{yx}$	Transverse and longitudinal torsional rigidities respectively
$D_1, D_2$	Coupling rigidities - contribution of bending to torsional rigidity of the slab
d" (d')	Concrete cover to centre of longitudinal (transverse) reinforcement
EI	Flexural rigidity of the edge beam
E	Modulus of elasticity of concrete

$e_x$ ( $e_y$ )	Depths of neutral plane from top fibre for bending in the x - (y) directions
$f'_c$	28-days compressive strength of concrete
$G_{xy}$ , $G_{yx}$	Shear moduli of the orthotropic slab
GJ	Torsional rigidity of the edge beam
H	Effective torsional rigidity of the slab
h	Thickness of flange plate
$I'_x$ ( $I'_y$ )	Moment of inertia of transverse (longitudinal) ribs
$I_{xy}$ , $I_{yx}$	Torsional constants
$M_x$ , $M_y$ , $M_{xy}$	Bending and torsional moments associated with the x and y axis
m	Integer > 1, number of harmonics
n	Integer > 1, number of harmonics
$Q_x$	Shear force per unit width of the plate
q(u,v)	Load function
$S_x$ ( $S_y$ )	Spacing of ribs in transverse (longitudinal) direction
W	Deflection function
$W_c$	Complementary solution
$W_p$	Particular solution
x,y,z	Rectangular axes
$\mu$	Poission's ratio of concrete
$\theta$	Skew angle

$$\alpha_m = m\pi/a$$

$$\alpha_n = n\pi/a$$

$$\beta_m = m\pi/b$$

$$\beta_n = n\pi/b$$

$\epsilon_x, \epsilon_y$  Strain in x and y directions

$\tau_x, \tau_y$  Plane stress per unit width (length)

CHAPTER I  
INTRODUCTION

1.1 General

In recent years reinforced and prestressed concrete waffle slabs have become quite popular in buildings and deck bridges. Orthotropic plate structures are often required as component parts of large scale structures as floor system in buildings, auditoriums, aircrafts, ship bottoms, tunnels, highway structures, etc. The trend towards high-rise buildings, modern highway interchanges and the commercial availability of high strength light-weight concrete have re-focused attention on concrete waffle slabs all over the world. The use of prestressed concrete waffle slabs for rectangular and skew decks of short and medium span bridges can also lead to economical design by having a crack-free concrete wearing surface, lower maintenance costs and better live load distribution.

1.2 Objective

The primary objective of this investigation is to determine the behaviour of reinforced and prestressed concrete waffle slabs over the total range of loading up to the point of collapse, from the standpoint of deformation, stresses, cracking and ultimate strength capacity. A waffle slab can be classified as geometrically orthotropic; as such its orthotropic flexural and twisting rigidities must be accurately predicted before and after cracking of

the concrete in order to reliably estimate its performance under working and collapse loads. In general, the deflection of a concrete waffle slab is rather small in comparison with the thickness of the slab so that for a proper design of such structures a linear (small deflection) analysis is sufficient. An experimental investigation and a theoretical study based on a series solution are undertaken; this solution is found by superimposing three solutions due to three different loadings, namely: the transverse loads (uniform as well as concentrated load at various locations), in-plane edge loads and edge moments, the latter two being due to in-plane prestressing.

### 1.3 Scope

The test of a structural concrete one-eighth scale "direct" model can simulate the behaviour of the prototype both before and after cracking of the concrete. This investigation covers reinforced and prestressed concrete waffle slabs, including both rectangular and skew plan forms and subjected to uniformly distributed, as well as concentrated lateral loads.

A review of the theoretical and experimental studies of orthotropic structures, reinforced and prestressed concrete waffle slabs are presented together with simple expressions for estimating the orthotropic rigidities. Mathematical formulation of the problem using a Fourier series for lateral and in-plane forces are derived.

Analysis and discussion of the theoretical and experimental results from three reinforced and two prestressed concrete waffle slabs are presented in this work. An approximate method is proposed to solve the in-plane stress problem due to the prestressing force along the four sides of the slab.

The experimental work comprises the following two groups:

1) Group A, includes three reinforced concrete waffle slabs. The first and second slabs were rectangular in plan with identical geometry and subjected to uniform and concentrated lateral loads, respectively. The third slab had a skew of  $45^{\circ}$ , and was subjected to a concentrated lateral load.

2) Group B, includes two prestressed concrete waffle slabs, one was rectangular in plan and the other had a skew of  $45^{\circ}$ , and subjected to concentrated lateral loads.

All the slab models are analysed as bridge slabs having two opposite edges simply supported and other two edges free (Group A) or elastically supported (Group B).



## CHAPTER II

### HISTORICAL REVIEW

#### 2.1 Review of Literature

The study of theory of plates goes back to the French mathematician, Sophie Germain (1816), who obtained a differential equation for vibration of plates, but she neglected the work done by warping of the middle surface. The first corrected differential equation for the free vibration of plates was used by Lagrange by adding the missing term in Sophie's equation. This work, which was improved by researchers such as Navier, Poisson and Kirchhoff, is considered to be the basis for the classical thin plate theory. Solutions of many problems in plates of circular, rectangular, skew, triangular shapes are available (see Timoshenko (31) and Szilard (29,30)). The exact solution to a plate problem should satisfy the boundary conditions as well as the governing differential equation of equilibrium or minimize the potential energy of the plate. The deflection function could be in the form of an infinite series and its sum to infinity gives any deflection pattern of the plate which satisfies the imposed geometrical conditions by suitable choice of values for the infinite number of constants of integration.

The development of the modern aircraft industry provided another strong impetus toward more rigorous analytical investigations of plate problems. Plates subjected

to in-plane forces, postbuckling loads, stiffened plates, etc., were analyzed by various scientists and engineers. Most recently, the invention of high-speed electronic computers exerted a considerable influence on the static and dynamic analysis of plates. Probably the first approach used in computer analysis was the finite difference method.

Considerable attention has been given recently to developing methods of designing more economical concrete bridges. Various methods of estimating the load distribution in concrete bridge decks have been proposed to date. In all these methods values of the effective flexural and torsional rigidities of the deck system are required before the analysis can proceed. Little information was available as to how these rigidities might be assessed for many of the bridge-deck systems.

In 1956, Huffington (10) investigated theoretically and experimentally the method for the determination of rigidities for metallic rib-reinforced deck structures. It was applied to the case of equally spaced stiffeners, of rectangular cross section, and symmetrically placed with respect to its middle plane.

Methods of analysing rectangular and skew deck plates with simple boundary conditions have been recently investigated by Kennedy et al. (12,14,15,16). They solved the problem of skew plate under uniform load by means of variational techniques and a series solution were

presented for rib stiffened plates under uniform and concentrated loads; the results were verified with experiments. They observed that critical stresses often occur in obtuse corners of such skew plates.

In 1968 Jackson (11) proposed a method to estimate the torsional rigidities of concrete bridge decks, using the membrane analogy and the estimation of the junction effect. The effect of the continuity of the slab on the flange plate was not accounted for.

In 1972, Perry and Heins (21) studied a series of equations for preliminary design of transverse floor beams in orthotropic deck bridges. The applied loads were represented in the form of a Fourier series. This method is not exact since it neglected the effects of contributions of bending to the torsional rigidities of the plate. Cardens et al (4,5) investigated the in-plane and flexural stiffnesses of isotropically and nonisotropically reinforced concrete plates. Results indicated that the stiffness of such plates was related quantitatively to the relative orientation of the reinforcement with respect to the applied forces.

Mathematical analysis of grid systems with particular regard to bridge type was given by Bares and Massonnet (2) and Rowe (24) together with practical applications.

## 2.2 Prestressed Concrete Slabs

Possibly, Guyon, in the early 1950's was the first

to realize that slabs, prestressed in two directions behaved analogously to the two-way arch action of thin shell structures. In the late 1950's several prestressed slab research projects were undertaken in the United States. Scordelis et al, 1960, (26,27) studied the ultimate strength of continuous prestressed slabs and proposed several design recommendations. They investigated the load distribution between the column and the middle strips and the following conclusions were obtained:

1. The elastic plate theory may be used satisfactorily to predict the behaviour of a prestressed concrete slab loaded within the elastic limit.
2. The slab can sustain a large increase in load before widespread cracking takes place.

Possibly the largest stride in the design of prestressed slabs was taken by Lin (18) who was the first to introduce the Load Balancing Method. It was soon made apparent that the tendon profiles could be designed so that the upward cable force neutralized the vertical downward load. Between 1957 and 1969, many researchers developed the method and studied the load distribution in bridge slabs (Sherman (28), Rowe (24) and Wang (32)). In 1969, Muspratt (20) used the load balancing method on prestressed concrete waffle slabs. For other applications of this method in U.S.A. see references (19) and (23). Another investigation was made by Hondros and Smith (9) on

a post-tensioned diagrid flat plate, simply supported on four edges using the link force method of analysis. The force method applies compatibility but disregards the influence of torsion on the plate.

Burns and Hemakom in 1977 (3), investigated the problem of post-tension flat plate using frame analysis; furthermore, the cracks were predicted and the stresses compared with that obtained by ACI code (318-71), (1).

Although an appreciable amount of work has been done on the analysis of prestressed flat slabs, very little work is available on prestressed concrete waffle slabs. It is beyond the scope of this thesis to give a comprehensive survey of the entire literature in this field. However, a study of the literature shows that no exact solution is available for prestressed concrete waffle slabs under a general type of lateral load and in-plane prestressing force.

## CHAPTER III

### FORMULATION

#### 3.1 General

With reinforced concrete structures cast in-situ, it is common practice to cast the slab and the supporting beam grid at the same time. The grid elements may be either reinforced or prestressed concrete beam or steel girders. Since a reinforced concrete slab has to withstand the local effects of heavy concentrated loads, the slab thickness is usually substantial, and composite action of the grid-and-slab system must be taken into account. Due to the action of concentrated loads, the transverse direction becomes important and the transverse strength of the structures has to be considered carefully. In dealing, herein with orthotropic concrete structures, it is assumed that orthotropy is a result of geometry and not of material, see Figure 3.1.

#### 3.2 Assumptions

The analytical approach to the problem of the orthotropic plate has to be based on some simplifying assumptions related to the form and material of the plate and to the state of strain induced by the external loading. The assumptions for orthotropic plates are based on the same assumptions used in the analysis of isotropic plates, and they are as follows:

- a) The material of the plate is elastic, i.e., the

stress-strain relationship is given by Hooke's law.

- b) The material of the plate is considered to be homogeneous, by transforming the steel area into an equivalent area of concrete.
- c) The thickness of the plate is uniform and small in comparison to the other lateral dimensions of the plate. Thus the shearing and normal stresses to the plane of symmetry are small and can be neglected.
- d) Straight lines normal to the middle plane of the plate remain straight and normal to the middle plane of the plate after bending.
- e) The deflections of the plate are small in comparison with its thickness; and are such that there is no normal strain in planes tangent to the middle plane.

It should be mentioned that the theory of orthotropy is applicable for structures which have a small ratio of stiffness spacing relative to any lateral length of the structure.

### 3.3 Governing Differential Equation For The Lateral Loads And Edge Moments

It is assumed that the material of the plate has three planes of symmetry with respect to its elastic properties. Taking these planes as the coordinate planes, the relations between the moments and deflections are:

$$\begin{aligned}
 M_x &= -(D_x W_{,xx} + D_1 W_{,yy}) \\
 M_y &= -(D_y W_{,yy} + D_2 W_{,xx}) \\
 M_{xy} &= D_{xy} W_{,xy}
 \end{aligned}
 \quad \left. \vphantom{\begin{aligned} M_x \\ M_y \\ M_{xy} \end{aligned}} \right\} (3.1)$$

where,

$D_x, D_y$  = flexural rigidities of the plate per unit width in x and y directions respectively

$D_1, D_2$  = coupling rigidities, measuring the contribution of bending to torsional rigidities of the plate.

$D_{xy}, D_{yx}$  = torsional rigidities of the plate and ribs

Substituting expressions 3.1 in the following general differential equation of equilibrium, given by Timoshenko (31),

$$M_{x,xx} + M_{y,yy} - zM_{xy,xy} = -q(x,y) \quad (3.2)$$

The following fourth order differential equation governing the deflection of the orthotropic plate is obtained in rectangular coordinate:

$$D_x W_{,xxxx} + 2HW_{,xxyy} + D_y W_{,yyyy} = q(x,y) \quad (3.3)$$

where,

$$H = (D_1 + D_2 + D_{xy} + D_{yx})/2$$

and known as the effective torsional rigidity of the plate and characterizes the resistance of the plate element to twisting.



To generalize the solution from the rectangular slab to a skew slab the following transformation is used:

$$\begin{aligned} u &= x/\cos\theta \\ v &= y - x \tan\theta \end{aligned} \quad (3.4)$$

where,  $\theta$  is the skew angle.

Equation 3.3, known as Huber's equation, becomes,

$$\begin{aligned} D_x W_{,uuuu} - E_1 W_{,uuuv} + E_2 W_{,uuvv} - E_3 W_{,uvvv} + E_4 W_{,vvvv} \\ = c^4 q(u,v) \end{aligned} \quad (3.5)$$

where,

$$E_1 = 4sD_x$$

$$E_2 = 2(3D_x s^2 + Hc^2)$$

$$E_3 = 4s(D_x s^2 + Hc^2)$$

$$E_4 = D_x s^4 + 2Hs^2 c^2 + D_y c^4$$

$$c = \cos\theta \quad \text{and} \quad s = \sin\theta$$

### 3.4 Relation of Stress and Strain for Bending Action

Solving equations 3.1 and 3.3 to find  $W_{,xx}$  and  $W_{,yy}$  and substituting these two terms in the following formulae (31) relating strain to curvature,

$$\left. \begin{aligned} \epsilon_x &= -zW_{,xx} \\ \epsilon_y &= -zW_{,yy} \end{aligned} \right\} \quad (3.6)$$

yields the strains in x and y directions in terms of the rigidities and moments:

$$\left. \begin{aligned} \epsilon_x &= z(M_{x D_y} - M_{y D_1}) / (D_x D_y - D_1 D_2) \\ \epsilon_y &= z(M_{y D_x} - M_{x D_2}) / (D_x D_y - D_1 D_2) \end{aligned} \right\} (3.7)$$

$z$  is the depth of the neutral axis from the top fibre.

### 3.5 Elastic Properties of the Waffle Slab Model

As mentioned earlier, the condition of orthotropy for the slabs treated herein, was mainly due to geometry and steel reinforcement. The problem was idealized by assuming that the slab is made of a homogeneous material with different elastic properties in two mutually perpendicular directions. Waffle slab construction considered as a "composite system" consists of two parts, the grid, and the plate. This "composite system" displays a high degree of torsional rigidity, especially for skew slabs. The composite system may be arranged in a sequence of structural forms; the sequence may consist of limiting case having a simple grid with no plate and the other extreme case of a true orthotropic slab; various types of composite systems fall between these two limits.

In addition to the basic assumptions in deriving the governing differential equation for an orthotropic plate, the following assumptions are made with respect to waffle slab construction:

1. The number of ribs in both directions is large enough for the real structure to be replaced by an idealized one with continuous properties.

2. The neutral plane in each of the two orthogonal directions coincides with the centre of gravity of the total section in the corresponding direction.
3. The area of the flange plate is magnified by the factor  $1/(1 - \mu^2)$  due to the effect of Poisson's ratio  $\mu$ .

Since the thickness of the slab is constant and the slab material is continuous, as assumed before, the different elastic properties in two principal directions must be due to different moments of inertia per unit width of the slab. The modulus of elasticity in two perpendicular directions are equal ( $E_x = E_y = E$ ) as well as Poisson's ratio ( $\mu_x = \mu_y = \mu$ ) and the torsional rigidities  $D_{xy}$  and  $D_{yx}$  are equal.

There is no difficulty in determining the flexural rigidities  $D_x$  and  $D_y$  of the slab models, but the difficulty is to find an accurate value for the torsional rigidities. Various methods of estimating the load distribution in concrete bridge decks (2,13,26) have been proposed to date. In all of these methods, values of flexural and torsional rigidities of the deck structures are required before the analysis can proceed. Some of the methods used for estimating the torsional rigidities are very limited in their application and can lead to appreciable errors in the value of the torsional parameter, unless their limitations are recognized. A method of determination of rigidities was

investigated by Huffington (10).

### 3.6 Rigidities of Uncracked Sections

#### 3.6.1 Flexural Rigidities

It is assumed that the neutral planes in each of the two coordinate directions coincides with the centre of gravity of the total section. This is an approximation only, since it can be shown that the location of the neutral surfaces is a function of the deflection as well as the geometry of the section.

Figure 3.2 shows a typical section of a waffle-type slab. Based on the assumptions made before, the orthotropic flexural rigidities  $D_x$  and  $D_y$ , as well as the coupling rigidities  $D_1$  and  $D_2$  due to the Poisson's effect (13) can be put in the form,

$$\left. \begin{aligned} D_x &= D + \left\{ Eh(e_x - h/2)^2 / (1 - \mu^2) \right\} + EI'_x / S_x \\ D_y &= D + \left\{ Eh(e_y - h/2)^2 / (1 - \mu^2) \right\} + EI'_y / S_y \\ D_1 &= \mu D'_x \\ D_2 &= \mu D'_y \end{aligned} \right\} \quad (3.8)$$

where,

$D$  = the flexural rigidity of the flange plate with respect to its middle plane,  $Eh^3/12(1 - \mu^2)$ .

$E$  = modulus of elasticity of the concrete  
 $= 57000\sqrt{f'_c}$  (1)

$f'_c$  = 28 day concrete cylinder strength in psi

$h$  = thickness of the flange plate

$\mu$  = Poisson's ratio of concrete

$$= \sqrt{f'_c}/350 \quad (8,12)$$

$S_y$  = spacing of longitudinal ribs

$S_x$  = spacing of transverse ribs

$e_x$  = depth of neutral plane from top fibre for bending in the x direction

$e_y$  = depth of neutral plane from top fibre for bending in the y direction, i.e.,

$$\left. \begin{aligned} e_x &= \left\{ b_x d_x (h + d_x/2) + (n - 1)A_s (h + d_x - d') + S_x h^2 / \right. \\ &\quad \left. 2(1 - \mu^2) \right\} / \left\{ b_x d_x + (n - 1)A'_s + S_x h / (1 - \mu^2) \right\} \\ e_y &= \left\{ b_y d_y (h + d_y/2) + (n - 1)A_s (h + d_y - d'') + S_y h^2 / \right. \\ &\quad \left. 2(1 - \mu^2) \right\} / \left\{ b_y d_y + (n - 1)A_s + S_y h / (1 - \mu^2) \right\} \end{aligned} \right\} (3.9)$$

$I'_x$  = moment of inertia of transverse rib with respect to the assumed neutral axis

$I'_y$  = moment of inertia of longitudinal rib with respect to the assumed neutral axis, i.e.,

$$\begin{aligned} I'_x &= b_x d_x \left\{ (h + d_x/2) - e_x \right\}^2 + (n - 1)A'_s \left\{ (h + d_x - d') - e_x \right\}^2 \\ &\quad + b_x d_x^3 / 12 \\ I'_y &= b_y d_y \left\{ (h + d_y/2) - e_y \right\}^2 + (n - 1)A_s \left\{ (h + d_y - d'') - e_y \right\}^2 \\ &\quad + b_y d_y^3 / 12 \end{aligned}$$

(3.10)

in which,

$n$  = modular ratio

$$= E_s/E_c$$

$b_y$  = width of longitudinal rib

$b_x$  = width of transverse rib

$d_y$  = depth of the longitudinal rib

$d_x$  = depth of the transverse rib

$d''$  = concrete cover to the centre of the longitudinal reinforcements

$d'$  = concrete cover to the centre of the transverse reinforcements

$A_s$  = area of reinforcement steel in the longitudinal direction

$A'_s$  = area of reinforcement steel in the transverse direction

$D'_x$  = flexural rigidity of the flange plate with respect to the neutral plane of the gross-section associated with bending in the  $x$  direction

$D'_y$  = flexural rigidities of the flange plate with respect to the neutral plane of the gross-section associated with bending in the  $y$  direction

Since it is assumed that the number of ribs in both directions is large, the effective width of the flange plate

acting with one rib is taken as the distance between two adjacent ribs. Most of the investigators who have taken the same effective width have obtained very good results.

### 3.6.2 Torsional Rigidities

Reliable information on the estimation of the torsional rigidities of a bridge deck are very limited. The effective torsional rigidities  $H$ , in Eq. 3.3 is given by,

$$H = (D_{xy} + D_{yx} + D_1 + D_2)/2 \quad (3.11)$$

For the analysis of reinforced concrete slabs with different reinforcements in the two perpendicular directions, Huber recommended the expression,  $H = \sqrt{D_x D_y}$ ; such an expression gives a too high an estimate for T-beam section.

The main problem lies in finding the values of  $D_{xy}$  and  $D_{yx}$ , which are given by

$$\left. \begin{aligned} D_{xy} &= G_{xy} I_{xy} \\ D_{yx} &= G_{yx} I_{yx} \end{aligned} \right\} \quad (3.12)$$

where,

$$\begin{aligned} G_{xy} &= G_{yx} \\ &= \text{shear modulus} \\ &= E/2(1 + \mu) \end{aligned}$$

$I_{xy}$  and  $I_{yx}$  are the torsional constants

A number of investigators have obtained the torsional constants for structural steel and aluminum-alloy sections,

using membrane analogy and/or numerical methods. Massonet and Rowe (2,25) have determined the torsional constants by dividing open section into a number of rectangular areas. Thus the torsional constant is given by,

$$I_{xy} S_x \text{ or } I_{yx} S_y = (\frac{1}{2} k_1 a_1^3 b_1 + \sum_{i=2}^n K_i a_i^3 b_i) \quad (3.13)$$

where,

$S_x, S_y$  = spacing of transverse (longitudinal) ribs

$a_1$  = the smaller dimension of the cut area

$b_1$  = the larger dimension of the cut area

$K$  = factor depend on the ratio  $a_i/b_i$  (31)

Jackson (11) has considered the value mentioned above as not accurate enough since it neglects the junction effect on the torsional rigidity. The twisting rigidity of the uncracked section of concrete waffle-type slab is estimated by means of the membrane analogy method (31) taking into account the stiffening effect afforded by the ribs in the orthogonal direction to the one under consideration. Considering the geometry of the deflected membrane, the torsional constant for the rectangular sections 1, 2 and 3 as shown in Figure 3.3 are calculated to give the total torsional constant,  $I_{xy}$ .

$$I_{xy} = I_{xy_1} + I_{xy_2} + I_{xy_3} \quad (3.14)$$

in which,

$$I_{xy_1} = \frac{1}{2} k_1 S_y h^3$$



$$\begin{aligned}
 I_{xy_2} &= k_1 d_y b_y^3 && (\text{if } d_y > b_y) \\
 &= k_1 b_y d_y^3 && (\text{if } b_y > d_y) \\
 I_{xy_3} &= 4k_1 (n - 1) (A'_s)^2 / \pi && (13)
 \end{aligned}
 \quad \left. \vphantom{\begin{aligned} I_{xy_2} \\ I_{xy_3} \end{aligned}} \right\} (3.15)$$

where,

$I_{xy_1}$  is reduced by factor  $\frac{1}{2}$  which accounts for the continuity of the flange plate. The torsional constant  $I_{xy_1}$  is modified by (Kennedy and Bali (13)) taking into account the effect of transverse ribs in both directions. It is assumed that the presence of the transverse rib will increase the torsional constant of the slab as:

$$I_{xy_1} (\text{modified}) = I_{xy_1} \left( \frac{I_{xy(S+W)}}{I_{xy(S)}} \right) \quad (3.16)$$

in which,

$$I_{xy(S+W)} = \text{torsional rigidity of slab and rib of the transverse or longitudinal ribs}$$

Equation 3.14 becomes

$$I_{xy} = I_{xy_1} (\text{modified}) + I_{xy_2} + I_{xy_3} \quad (3.17)$$

in which,

$$I_{xy_3} = \text{torsional rigidity of transformed section of steel (13)}$$

Similarly, the torsional rigidities  $D_{yx}$  can be calculated in the same way.

### 3.7 Plane Stress Problem Due To Prestressing Force

#### 3.7.1 Elastic Constants For Membrane Action

Assuming the corresponding strains in the flange plate element (deck) and the ribs are equal, and that shearing action is resisted by the flange plate alone, the following relations for equivalent elastic constants can be developed. The stress resultants per unit length in an isotropic flange plate element, shown in Figure 3.2, are:

$$\left. \begin{aligned} (\tau_x)_1 &= \sigma_x h = h(E_x / (1 - \mu^2))(\epsilon_x + \mu\epsilon_y) \\ (\tau_y)_1 &= \sigma_y h = h(E_y / (1 - \mu^2))(\epsilon_y + \mu\epsilon_x) \\ (\tau_{xy})_1 &= \tau_{xy} h = hG\gamma_{xy} \end{aligned} \right\} \quad (3.18)$$

where  $E$ ,  $G$  and  $\mu$  are the material properties of the concrete.

For the same strains in the rib, the stress resultants per unit length, are:

$$\left. \begin{aligned} (\tau_x)_2 &= E_x \epsilon_x A_x^* \\ (\tau_y)_2 &= E_y \epsilon_y A_y^* \\ (\tau_{xy})_2 &= 0 \end{aligned} \right\} \quad (3.19)$$

where  $A_x^*$  and  $A_y^*$  are the cross-sectional areas per unit length of the ribs in the  $x$  and  $y$  directions, respectively. The total stress resultants per unit length of an element are:

$$\begin{Bmatrix} \tau_x \\ \tau_y \\ \tau_{xy} \end{Bmatrix} = h \begin{vmatrix} E_x \frac{1}{(1-\mu^2)} + A_x^*/h & \mu E_y / (1-\mu^2) & 0 \\ \mu E_x / (1-\mu^2) & E_y \frac{1}{(1-\mu^2)} + A_y^*/h & 0 \\ 0 & 0 & G \end{vmatrix} \begin{Bmatrix} \epsilon_x \\ \epsilon_y \\ \gamma_{xy} \end{Bmatrix}$$

$$= h \begin{vmatrix} E'_x & E_1 & 0 \\ E_2 & E'_y & 0 \\ 0 & 0 & G \end{vmatrix} \begin{Bmatrix} \epsilon_x \\ \epsilon_y \\ \gamma_{xy} \end{Bmatrix} \quad (3.20)$$

where,

$$E'_x = E_x (1/(1-\mu^2) + A_x^*/h)$$

$$E_1 = \mu E_x / (1-\mu^2)$$

$$E_2 = \mu E_y / (1-\mu^2)$$

$$E'_y = E_y (1/(1-\mu^2) + A_y^*/h)$$

Based on the directions of the axes, x and y, as shown in Figure 3.2,

$$A_x^* = (b_x)(d - h)/S_x$$

$$A_y^* = (b_y)(d - h)/S_y$$

solving equations 3.20 to find the strains in both directions yields,

$$\left. \begin{aligned} \epsilon_x &= ((\tau_x/h)E'_y - (\tau_y/h)E_2) / (E'_xE'_y - E_1E_2) \\ \epsilon_y &= ((\tau_y/h)E'_x - (\tau_x/h)E_1) / (E'_xE'_y - E_1E_2) \end{aligned} \right\} \quad (3.21)$$

in which  $\epsilon_x$  and  $\epsilon_y$  are the strains in the x and y directions due to the in-plane prestressing.

It should be noted that the deflection due to in-plane stresses is very small and can be neglected. Therefore the total deflection in the slab can be considered to be due to the lateral loads and the edge moments. On the other hand, the total strain in the slab is due to the lateral loads, in-plane forces and edge moments.

### 3.8 Boundary Conditions

A solution for the deflection function  $W_{(x,y)}$  in cartesian coordinates or for  $W_{(u,v)}$  in oblique coordinates to the plate problem must be consistent with the conditions at the edges of the plate. The kind of support is theoretically defined by three "boundary conditions" along each edge. The boundary conditions have to be re-formulated first in terms of the deflection, if the solution is to be based on the deflection. Thus rectangular and skew slabs have 12 boundary conditions which are to be satisfied by the solution of the partial differential equation governing the problem. However, this governing equation is of the fourth order in the variables x and y or u and v, and its solution involves only 8 arbitrary constants. These constants can be made to fit only 8 boundary conditions, two for each edge, so that the three conditions mentioned above must be reduced to two conditions. The boundary conditions for single span waffle slabs are presented below.

### 3.8.1 Bridge Slabs

The simple bridge type shown in Figures 3.4, 3.5 is simply supported along two opposite edges ( $v = \pm b$ ) and free or elastically supported at the remaining two edges ( $u = \pm a$ ).

At the simply supported edges, there is no vertical deflection, and the bending moments about these edge-lines equal the edge moments due to the prestressing. These two boundary conditions can be formulated as follows:

$$1. \quad W_{(v=\pm b)} = 0 \quad \text{for } -a < u < a \quad (3.22)$$

$$2. \quad M_n_{(v=\pm b)} = M_x s^2 + M_y c^2 + (M_{xy} - M_{yx}) sc \quad (v=\pm b)$$

$$= M_{\text{external}}_{(v=\pm b)}$$

or

$$R_1 W_{,uv} + R_2 W_{,vv} = M_{\text{external}} \quad \text{at } v=\pm b \quad \text{for } -a < u < a \quad (3.23)$$

where

$$R_1 = s(2D_x s^2/c^2 + 2D_2 + D_{xy} + D_{yx})$$

$$R_2 = -s^2(D_x s/c^2 + 2H) - c^2 D_y$$

It should be noted that  $W_{,uu} = 0$  and  $W = W_{,u} = 0$  on the simple support

3. According to Timoshenko (31), combining the shear force along the edge with forces replaced by the twisting couples and equating this to the pressure transmitted from the plate to the supporting edge beam, lead to the following

equation:

$$-(Q_x - M_{xy,y}) = EI W_{,yyyy}$$

i.e.,

$$D_x W_{,xxx} + (D_1 + D_{xy} + D_{yx}) W_{,xy} = EI W_{,yyyy}$$

or

$$R_3 W_{,uuu} + R_4 W_{,uuv} + R_5 W_{,uvv} + R_6 W_{,vvv} - EI W_{,vvvv} = 0$$

$$\text{@ } u = \pm a \text{ for } -b < v < b \quad (3.24)$$

where,

$$R_3 = D_x/c^3$$

$$R_4 = -3D_x s/c^3$$

$$R_5 = (3D_x s^2/c^2 + D_1 + D_{xy} + D_{yx})/c$$

$$R_6 = -s(D_x s^2/c^2 + D_1 + D_{xy} + D_{yx})/c$$

EI = flexural rigidities of the edge beam

4. Along the elastically supported edge ( $u = \pm a$ ), equating the external moment due to prestressing force combined with the change in twisting moment in the edge beam to the plate internal moment parallel to the x-axis, yield:

$$-M_x = -GJ(W_{,xy,y}) - M_{\text{ext.}}(u=\pm a)$$

i.e.,

$$D_x W_{,xx} + D_1 W_{,yy} = -GJ(W_{,xyy}) - M_{\text{ext.}}(u=\pm a)$$

or

$$R_7 W,_{uu} + R_8 W,_{uv} + R_9 W,_{vv} + GJW,_{uvv} + R_{10} W,_{vvv} = -cM_{\text{ext.}}$$

$$\text{@ } u = \pm a \text{ for } -b < v < b \quad (3.25)$$

where,

$$R_7 = D_x/c$$

$$R_8 = -2D_x s/c$$

$$R_9 = (D_x s^2 + D_1 c^2)/c$$

$$R_{10} = -sGJ$$

GJ = torsional rigidity of the edge beam

The boundary conditions for the bridge slab where the two edges are free are obtained by putting the rigidities for the edge beams EI and GJ equal to zero.

CHAPTER IV  
ANALYTICAL SOLUTION

4.1 General

The mathematical solution comprises of finding a suitable complementary function which satisfies the governing equation (Eq. 3.5), and a particular solution which satisfies all the given boundary conditions. Combining the two solutions, a complete solution for the slab is obtained as follows:

$$W = W_c + W_p \quad (4.1)$$

where,

- $W$  = The total deflection at a point on the plate
- $W_c$  = Deflection found from the complementary solution of the homogeneous equation (Eq. 3.5)
- $W_p$  = Deflection from the particular solution of the non-homogenous equation.

4.2 Complementary Solution

According to Levy's solution, the deflection of the plate surface is assumed in the form of a Fourier series as

$$W_c = \sum_{n=1}^{\infty} e^{\lambda_n u} (P_n \sin \beta_n v + Q_n \cos \beta_n v) \quad (4.2)$$

where,

$\lambda_n$ ,  $P_n$  and  $Q_n$  are basic functions of the elastic properties and the geometry of the plate; n equals number



of harmonics chosen to make the series closely convergent;  
and,  $\beta_n = n\pi/b$

Solving equations 4.1 and 3.5 for  $q(u,v)$  equals zero, and equating the coefficients of  $\sin \beta_n v$  and  $\cos \beta_n v$ , yields two equations in  $P_n$  and  $Q_n$ . According to Gupta (8) the final expression for  $\lambda_n$  is

$$\lambda_n = \left\{ \pm \left[ (H \pm \sqrt{H^2 - D_x D_y}) / D_x \right]^{0.5} c \pm is \right\} \beta_n \quad (4.3)$$

It can be observed, from equation 4.3, that there are eight possible values for  $\lambda_n$  which give rise to eight possible solutions.

For the slab model considered herein, it is assumed that the slab is flexurally stiff and torsionally weak, i.e., ( $H^2 < D_x D_y$ ). This case includes all T-beam and open rib deck bridges.

#### 4.2.1 Waffle Slab Which is Flexurally Strong and Torsionally Weak

The solution of a waffle slab can be taken as

$$\begin{aligned} W_{cl} = & \sum_{n=1}^{\infty} (C_{1n} \cosh k_3 \beta_n u + C_{2n} \sinh k_3 \beta_n u) \cos(k_4 u + v) \beta_n \\ & + (C_{3n} \cosh k_3 \beta_n u + C_{4n} \sinh k_3 \beta_n u) \sin(k_4 u + v) \beta_n \\ & + (C_{5n} \cosh k_3 \beta_n u + C_{6n} \sinh k_3 \beta_n u) \cos(k_5 u - v) \beta_n \\ & + (C_{7n} \cosh k_3 \beta_n u + C_{8n} \sinh k_3 \beta_n u) \sin(k_5 u - v) \beta_n \end{aligned} \quad (4.4)$$

in which  $\lambda_n$  for this case can be written in the form

$$\lambda_n = \pm(k_1 \pm is) \beta_n \quad \text{or} \quad \pm(k_2 \pm is) \beta_n \quad (4.5)$$

where,

$$k_1 = (c(H + \sqrt{H^2 - D_x D_y})/D_x)^{0.5}$$

$$k_2 = (c(H - \sqrt{H^2 - D_x D_y})/D_x)^{0.5}$$

$C_{1n}$  to  $C_{8n}$  are arbitrary constants dependent on  $n$  and adjusted to satisfy the boundary condition. See references (7,8) and Appendix (A) for a more general representation of the deflection function  $W$ . Another possible complementary solution of  $W$  can be written as;

$$W_{c2} =$$

$$\sum_{n=1}^{\infty} (C_{9n} \cosh x_2 k_3 \alpha_n v + C_{10n} \sinh x_2 k_3 \alpha_n v) \cos(x_2 k_4 v + u) \alpha_n$$

$$+ (C_{11n} \cosh x_2 k_3 \alpha_n v + C_{12n} \sinh x_2 k_3 \alpha_n v) \sin(x_2 k_4 v + u) \alpha_n$$

$$+ (C_{13n} \cosh y_2 k_3 \alpha_n v + C_{14n} \sinh y_2 k_3 \alpha_n v) \cos(y_2 k_5 v - u) \alpha_n$$

$$+ (C_{15n} \cosh y_2 k_3 \alpha_n v + C_{16n} \sinh y_2 k_3 \alpha_n v) \sin(y_2 k_5 v - u) \alpha_n$$

(4.6)

where,

$$\alpha_n = n\pi/a$$

$$x_1 = 1/(k_1^2 + s^2)$$

$$x_2 = 1/(k_2^2 + s^2)$$

The boundary conditions used for the slab are eight in number (two along each edge) and the deflection function is made to satisfy these boundary conditions. Expanding each boundary condition in a Fourier series, will yield three equations and hence 24 equations for the eight

boundary conditions.

To use the same number of arbitrary constants in the deflection function, the following polynomial function is assumed and added:

$$W_{c3} = \left\{ C_{17} + C_{18}u/a + C_{19}v/b + C_{20}u^2/a^2 + C_{21}v^2/b^2 + C_{22}u^3/a^3 + C_{23}v^3/b^3 + C_{24}(Tu^4 - v^4)/b^4 \right\} \quad (4.7)$$

in which,

$$T = (s^4D_x + 2s^2c^2H + c^4D_y)/D_x$$

$C_{17}$  to  $C_{24}$  are arbitrary constants. Thus the total complementary solution becomes,

$$W_c = W_{c1} + W_{c2} + W_{c3} \quad (4.8)$$

### 4.3 Particular Solution

The particular solution has to be determined and added to the complementary solution and must satisfy the boundary conditions. The uniform load or concentrated load acting on a limited area as shown in Figure 4.1 is expanded into double Fourier series over the entire area of the slab. Following Gupta (8) the particular solution can be taken as:

$$W_p = \left\{ (a_0 c^4 / 4E_4) (v^4 / 24 - v^2 b^2 / 4 + 5b^4 / 24) \right. \\ \left. + \sum_1^{\infty} (T_{5m} \cos \alpha_m u + T_{7m} \sin \alpha_m u) \right. \\ \left. + \sum_1^{\infty} (T_{6n} \cos \beta_n v + T_{8n} \sin \beta_n v) \right\}$$

$$\begin{aligned}
& + \sum_1^{\infty} \sum_1^{\infty} (K_{mn} \cos \alpha_m u \cos \beta_n v + P_{mn} \sin \alpha_m u \cos \beta_n v \\
& + Q_{mn} \cos \alpha_m u \sin \beta_n v + L_{mn} \sin \alpha_m u \sin \beta_n v) \} \quad (4.9)
\end{aligned}$$

#### 4.4 Symmetric and Anti-Symmetric Loading

The loading on the structure is divided into symmetric and anti-symmetric components. This division is applied to the lateral load and the prestressing force along the edges of the slab. For symmetric loading odd terms vanish, i.e.,

$$\begin{aligned}
C_{2n} = C_{3n} = C_{6n} = C_{7n} = C_{10n} = C_{11n} = C_{14n} = C_{15n} = \\
C_{18} = C_{19} = C_{22} = C_{23} = Q_{7m} = Q_{8n} = Q_{3mn} = Q_{4mn} = 0 \quad (4.10)
\end{aligned}$$

For the anti-symmetric loading, all even terms vanish, i.e.,

$$\begin{aligned}
C_{1n} = C_{4n} = C_{5n} = C_{8n} = C_{9n} = C_{12n} = C_{13n} = C_{16n} = C_{17} = \\
C_{20} = C_{21} = C_{24} = a_o = Q_{5m} = Q_{6n} = Q_{1mn} = Q_{2mn} = 0 \quad (4.11)
\end{aligned}$$

By superposition, the results for any lateral loading can be obtained with the added advantage that the number of boundary conditions is reduced to four for each loading component.

#### 4.5 Expansion of the In-Plane Prestressing Force In a Fourier Series by Graphical Method

When the equation for a periodic function is not known but a graph of the waveform is available (such as a variable prestressing force along the edges of a slab

bridge), it is possible to obtain an approximate solution for the Fourier coefficients by means of graphical techniques (17,33). Actually this method represents a concept of graphical integration. This is accomplished by dividing one cycle into  $m$  equal divisions. The dependent-variable value (denoted by  $Y_k$ 's) in Figure 4.2 is obtained at the mid-point of each of these intervals. The coefficients of the Fourier series representing the in-plane prestressing force can be shown to be, (See Appendix C),

$$\left. \begin{aligned} a_0 &= (2/m) \sum_{k=1}^m Y_k \\ a_n &= (2/m) \sum_{k=1}^m (-1)^n Y_k \cos(2n\pi/m)(k - \frac{1}{2}) \\ b_n &= (2/m) \sum_{k=1}^m (-1)^n Y_k \sin(2n\pi/m)(k - \frac{1}{2}) \end{aligned} \right\} (4.12)$$

## CHAPTER V

### SATISFACTION OF BOUNDARY CONDITIONS

To obtain the matrix equations, the deflection function must satisfy the boundary conditions for the slab subjected to any arbitrary lateral load. This is accomplished by dividing such a load into symmetric and anti-symmetric loads.

#### 5.1 Symmetric Load

1) The deflection must be zero at the edge  $v = \pm b$ . Substituting equations 3.22, 4.4, 4.6, 4.7, 4.8, 4.9 and 4.10 in equation 4.1, the following equation is obtained (8).

$$\begin{aligned}
 & f_0(u) + \sum_1^{\infty} (f_n(u) + A_n \cos \alpha_n u + B_n \sin \alpha_n u) \\
 = & - \sum_1^{\infty} T_{5m} \cos \alpha_m u - \sum_1^{\infty} (-1)^n T_{6n} - \sum_1^{\infty} \sum_1^{\infty} (-1)^n K_{mn} \cos \alpha_m u \quad (5.1)
 \end{aligned}$$

in which

$$f_0(u) = C_{17} + C_{20} u^2/a^2 + C_{21} + C_{24} [(T u^4/b^4) - 1]$$

$$\begin{aligned}
 f_n(u) = & (-1)^n [C_{1n} \cosh u_{3n} \cos u_{4n} + C_{4n} \sinh u_{3n} \sin u_{4n} \\
 & + C_{5n} \cosh u_{3n} \cos u_{5n} + C_{8n} \sinh u_{3n} \sin u_{5n}]
 \end{aligned}$$

$$A_n = C_{9n} K_{1n} + C_{12n} K_{2n} + C_{13n} L_{1n} + C_{16n} L_{2n}$$

and

$$B_n = -C_{9n} K_{4n} + C_{12n} K_{3n} + C_{13n} L_{4n} - C_{16n} L_{3n}$$

In which,  $u_{3n}$ ,  $u_{4n}$ ,  $u_{5n}$ ,  $K_{1n}$  to  $K_{8n}$  and  $L_{1n}$  to  $L_{8n}$  are defined in Appendix (A).

The function  $f_o(u)$  and  $f_n(u)$  must be expanded in Fourier series to satisfy the boundary condition along the entire length of the edge, thus:

$$\left. \begin{aligned} f_o(u) &= a_{oo} + \sum_1^{\infty} (a_{om} \cos \alpha_m u + b_{om} \sin \alpha_m u) \\ f_n(u) &= c_{no} + \sum_1^{\infty} (c_{nm} \cos \alpha_m u + d_{nm} \sin \alpha_m u) \end{aligned} \right\} (5.2)$$

where,  $a_{oo}$ ,  $a_{om}$ ,  $b_{om}$ ,  $c_{no}$ ,  $c_{nm}$  and  $d_{nm}$  are Fourier coefficient and defined in Appendix (B).

Substituting equation 5.2 in equation 5.1 and equating the coefficients of  $\sin \alpha_m u$  and  $\cos \alpha_m u$  and the constant term to zero, the following three equations are obtained:

$$\left. \begin{aligned} a_{oo} + \sum_1^{\infty} c_{no} &= - \sum_1^{\infty} (-1)^n T_{6n} \\ a_{nm} + \sum_1^{\infty} c_{nm} + A_m &= -T_{5m} - \sum_1^{\infty} (-1)^n K_{mn} \\ B_m &= 0 \quad \text{for each } m. \end{aligned} \right\} (5.3)$$

Substituting the Fourier coefficients in equation 5.3, yields three equations:

$$\begin{aligned} & C_{17} + C_{20/3} + C_{21} + C_{24} [(T a^4/5b^4) - 1] \\ & + \sum_1^{\infty} (-1)^n (C_{1n} W_{1n} + C_{4n} W_{2n} + C_{5n} W_{3n} + C_{8n} W_{4n}) \\ & = - \sum_1^{\infty} (-1)^n T_{6n} \end{aligned} \quad (5.4)$$

$$\begin{aligned}
& C_{20}I_{1m} + C_{24}^T I_{3m} a^4/b^4 \\
& + {}_1\Sigma^{\infty}(-1)^n (C_{1n}A_{j1} + C_{4n}A_{j2} + C_{4n}A_{j2} + C_{5n}A_{j3} + C_{8n}A_{j4}) \\
& + C_{9m}K_{1m} + C_{12m}K_{2m} + C_{13m}L_{1m} + C_{16m}L_{2m} \\
& = -T_{5m} - {}_1\Sigma^{\infty}(-1)^n K_{mn} \tag{5.5}
\end{aligned}$$

$$-C_{9n}K_{4n} + C_{12n}K_{3n} + C_{13n}L_{4n} - C_{16n}L_{3n} = 0 \tag{5.6}$$

2) Boundary condition 3.23 relates the moment normal to the support to the deflection function. Thus,

$$\begin{aligned}
& f_0(u) + {}_1\Sigma^{\infty}(f_n(u) + A_n \cos \alpha_n u + B_n \sin \alpha_n u) \\
& = \sum_{n=1}^{\infty} (-1)^n \beta_n^2 T_{6n} R_2 + \sum_{m=1}^{\infty} \sum_{n=1}^{\infty} (-1)^n \beta_n (R_2 K_{mn} \beta_n - R_1 L_{mn} \alpha_m) \cos \alpha_m u \\
& + (1/m_u) \sum_{k=1}^{m_u} m_k + (2/m_u) \sum_{k=1}^{m_u} \sum_{n=1}^n (-1)^n m_k \cos [n\pi(k - \frac{1}{2})/m_u] \\
& \tag{5.7}
\end{aligned}$$

where,

$$f_0(u) = 2C_{21}R_2/b^2 - 12C_{24}R_2/b^2$$

$$\begin{aligned}
f_n(u) = (-1)^n \beta_n^2 \{ & C_{1n} (A_7 \cosh u_{3n} \cos u_{4n} - R_1 K_3 \sinh u_{3n} \sin u_{4n}) \\
& + C_{4n} (R_1 K_3 \cosh u_{3n} \cos u_{4n} + A_7 \sinh u_{3n} \sin u_{4n}) \\
& + C_{5n} (B_7 \cosh u_{3n} \cos u_{5n} + R_1 K_3 \sinh u_{3n} \sin u_{5n}) \\
& + C_{8n} (-R_1 K_3 \cosh u_{3n} \cos u_{5n} + B_7 \sinh u_{3n} \sin u_{5n}) \}
\end{aligned}$$

$$\begin{aligned}
A_n = \alpha_n^2 \{ & C_{9n} (A_8 K_{1n} + A_9 K_{2n}) + C_{12n} (-A_9 K_{1n} + A_8 K_{2n}) \\
& + C_{13n} (B_8 L_{1n} + B_9 L_{2n}) + C_{6n} (-B_9 L_{1n} + B_8 L_{2n}) \}
\end{aligned}$$



$$B_n = \alpha_n^2 \left\{ C_{9n} (-A_8 K_{4n} + A_9 K_{3n}) + C_{12n} (A_9 K_{4n} + A_8 K_{3n}) \right. \\ \left. + C_{13n} (B_8 L_{4n} - B_9 L_{3n}) + C_{16n} (-B_9 L_{4n} - B_8 L_{3n}) \right\}$$

the values of  $A_7, A_8, \dots, B_9$  are defined in Appendix (A)

$m_u$  = total number of concentrated edge moments (for  $-a < u < a$ ) due to prestressing force ( $m_v$  is for  $-b < v < +b$ ).

$m_k$  = an edge moment at any point along the support.

The second set of three equations due to the boundary condition (Equation 3.23) is obtained using the same procedure. Hence,

$$2C_{21} R_2 / b^2 - 12C_{24} R_2 / b^2 + \sum_{n=1}^{\infty} (-1)^n \beta_n^2 \left\{ C_{1n} (A_7 W_{1n} - R_1 K_3 W_{2n}) \right. \\ \left. + C_{4n} (R_1 K_3 W_{1n} + A_7 W_{2n}) + C_{5n} (B_7 W_{3n} + R_1 K_3 W_{4n}) \right. \\ \left. + C_{8n} (-R_1 K_3 W_{3n} + B_7 W_{4n}) \right\} = \sum_{k=1}^{\infty} (-1)^k \beta_k^2 T_{6n} R_2 + (1/m_u) \sum_{k=1}^{m_u} m_k \quad (5.8)$$

$$\sum_{n=1}^{\infty} (-1)^n \beta_n^2 \left\{ C_{1n} (A_7 A_{j1} - R_1 K_3 A_{j2}) + C_{4n} (R_1 K_3 A_{j1} + A_7 A_{j2}) \right. \\ \left. + C_{5n} (B_7 A_{j3} + R_1 K_3 A_{j4}) + C_{8n} (-R_1 K_3 A_{j3} + B_7 A_{j4}) \right\} \\ + \alpha_m^2 \left\{ C_{9m} (A_8 K_{1m} + A_9 K_{2m}) + C_{12m} (-A_9 K_{1m} + A_8 K_{2m}) \right. \\ \left. + C_{13m} (B_8 L_{1m} + B_9 L_{2m}) + C_{16m} (-B_9 L_{1m} + B_8 L_{2m}) \right\} \\ = \sum_{n=1}^{\infty} (-1)^n \beta_n (R_2 \beta_n K_{mn} - R_1 \alpha_m L_{mn}) + (2/m_u) \\ \sum_{k=1}^{m_u} (-1)^k m_k \cos [2n\pi (k - \frac{1}{2}) / m_u] \quad \text{for } m \geq 1 \quad (5.9)$$

$$\alpha_n^2 \left\{ C_{9n} (-A_8 K_{4n} + A_9 K_{3n}) + C_{12n} (A_9 K_{4n} + A_8 K_{3n}) \right. \\ \left. + C_{13n} (B_8 L_{4n} - B_9 L_{3n}) + C_{16n} (-B_9 L_{4n} - B_8 L_{3n}) \right\} = 0 \quad (5.10)$$

for  $n \geq 1$

3) The third boundary condition (Equation 3.24 for  $-b < v < b$ ) yields the following three equations:

$$24C_{24} (R_3 T_a + EI) / b^4 + \sum_{n=1}^{\infty} (-1)^n \alpha_n^4 \left\{ C_{9n} (A_5 W_{5n} + A_6 W_{6n}) \right. \\ \left. + C_{12n} (-A_6 W_{5n} + A_5 W_{6n}) + C_{13n} (B_5 W_{7n} + B_6 W_{8n}) \right. \\ \left. + C_{16n} (-B_6 W_{7n} + B_5 W_{8n}) \right\} = c^4 a_o EI / 4E_4 \quad (5.11)$$

$$\sum_{m=1}^{\infty} (-1)^m \alpha_m^4 \left\{ C_{9m} (A_5 A_{j5} + A_6 A_{j6}) + C_{12m} (-A_6 A_{j5} + A_5 A_{j6}) \right. \\ \left. + C_{13m} (B_5 A_{j7} + B_6 A_{j8}) + C_{16m} (-B_6 A_{j7} + B_5 A_{j8}) \right\} \\ + \beta_n^3 \left\{ C_{1n} (-EI \beta_n K_{5n} + A_{10} K_{7n} + A_{11} K_{8n}) \right. \\ \left. + C_{4n} (-EI \beta_n K_{6n} - A_{11} K_{7n} + A_{10} K_{8n}) \right. \\ \left. + C_{5n} (-EI \beta_n L_{5n} + B_{10} L_{7n} + B_{11} L_{8n}) \right. \\ \left. + C_{8n} (-EI \beta_n L_{6n} - B_{11} L_{7n} + B_{10} L_{8n}) \right\} \\ = \sum_{n=1}^{\infty} (-1)^n K_{mn} \beta_n^4 EI + T_{6n} \beta_n^4 EI, \quad \text{for } n \geq 1 \quad (5.12)$$

$$-24C_{24} R_6 I_{5n} / b^3 + \sum_{n=1}^{\infty} (-1)^n \alpha_n^3 \left\{ C_{9n} (A_{12} B_{j5} + A_{13} B_{j6}) \right. \\ \left. + C_{12n} (-A_{13} B_{j5} + A_{12} B_{j6}) + C_{13n} (B_{12} B_{j7} + B_{13} B_{j8}) \right. \\ \left. + C_{16n} (-B_{13} B_{j7} + B_{12} B_{j8}) \right\}$$

$$\begin{aligned}
& +\beta_n^3 \{ C_{1n} (A_{11}K_{5n} - A_{10}K_{6n} + EI\beta_n K_{8n}) \\
& + C_{4n} (A_{10}K_{5n} + A_{11}K_{6n} - EI\beta_n K_{7n}) \\
& + C_{5n} (-B_{11}L_{5n} + B_{10}L_{6n} - EI\beta_n L_{8n}) \\
& + C_{8n} (-B_{10}L_{5n} - B_{11}L_{6n} + EI\beta_n L_{7n}) \} \\
& = {}_1\Sigma^\infty (-1)^m \left\{ -\beta_n (R_4\alpha_m^2 + R_6\beta_n^2) K_{mn} + \alpha_n (R_3\alpha_m^2 + R_5\beta_n^2) L_{mn} \right\} \\
& - R_6 c^4 a_o b I_{5n} / 4E_4 - T_{6n} \beta_n^3 R_6 \tag{5.13}
\end{aligned}$$

4) The fourth boundary condition (Equation 3.25) for  $-b < v < b$  gives the following equations:

$$\begin{aligned}
& 2C_{20}R_7/a^2 + 2C_{21}R_9/b^2 + 12C_{24}(R_7Ta^2 - R_9b^2/3)/b^4 \\
& + {}_1\Sigma^\infty (-1)^n \alpha_n^2 \{ C_{9n} (A_{17}W_{5n} + A_{18}W_{6n}) + C_{12n} (-A_{18}W_{5n} + A_{17}W_{6n}) \\
& + C_{13n} (B_{17}W_{7n} + B_{18}W_{8n}) + C_{16n} (-B_{18}W_{7n} + B_{17}W_{8n}) \} \\
& = -R_7 \left\{ {}_1\Sigma^\infty (-1)^m (-T_{5m}\alpha_m^2) \right\} + a_o c^4 b^2 R_9 / 12E_4 - c (1/m_v)_{k=1}^{\Sigma m_u m_k} \\
& \tag{5.14}
\end{aligned}$$

$$\begin{aligned}
& -12C_{24}R_9I_{1n}/b^2 + {}_1\Sigma^\infty (-1)^m \alpha_m^2 \{ C_{9m} (A_{17}A_{j5} + A_{18}A_{j6}) \\
& + C_{12m} (-A_{18}A_{j5} + A_{17}A_{j6}) + C_{13m} (B_{17}A_{j7} + B_{18}A_{j8}) \\
& + C_{16m} (-B_{18}A_{j7} + B_{17}A_{j8}) \} \\
& + \beta_n^2 \{ C_{1n} \{ A_{14}K_{5n} + A_{15}K_{6n} + \beta_n (-GJK_3K_{7n} + A_{16}K_{8n}) \} \\
& + C_{4n} \{ -A_{15}K_{5n} + A_{14}K_{6n} + \beta_n (-A_{16}K_{7n} - GJK_3K_{8n}) \} \\
& + C_{5n} \{ B_{14}L_{5n} + B_{15}L_{6n} + \beta_n (-GJK_3L_{7n} + B_{16}L_{8n}) \}
\end{aligned}$$

$$\begin{aligned}
& +C_{8n} \left\{ -B_{15}L_{5n} + B_{14}L_{6n} + \beta_n (-B_{16}L_{7n} - GJK_3L_{8n}) \right\} \\
& = -c^4 a_o b^2 R_9 I_{1n} / 8E_4 + T_{6n} \beta_n^2 R_9 \\
& + {}_1\Sigma^{\infty} (-1)^m \left\{ (\alpha_m^2 R_7 + \beta_n^2 R_9) K_{mn} - L_{mn} \alpha_m \beta_n R_8 \right\} \\
& - c \left\{ (2/m_v) {}_1\Sigma^{m_v} (-1)^n m_k \cos 2n\pi(k - \frac{1}{2})/m_v \right\} \text{ for } n \geq 1
\end{aligned} \tag{5.15}$$

$$\begin{aligned}
& -24C_{24}R_{10}I_{5n}/b^3 + {}_1\Sigma^{\infty} (-1)^m \alpha_m^3 \left\{ C_{9m} (A_{19}B_{j5} + A_{20}B_{j6}) \right. \\
& + C_{12m} (-A_{20}B_{j5} + A_{19}B_{j6}) + C_{13m} (B_{19}B_{j7} + B_{20}B_{j8}) \\
& + C_{16m} (-B_{20}B_{j7} + B_{19}B_{j8}) \left. \right\} + \beta_n^2 \left\{ C_{1n} \left\{ \beta_n (A_{16}K_{5n} + GJK_3K_{6n}) \right. \right. \\
& + A_{15}K_{7n} - A_{14}K_{8n} \left. \right\} + C_{4n} \left\{ \beta_n (-GJK_3K_{5n} + A_{16}K_{6n}) \right. \\
& + A_{14}K_{7n} + A_{15}K_{1n} \left. \right\} + C_{5n} \left\{ \beta_n (-B_{16}L_{5n} - GJK_3L_{6n}) \right. \\
& - B_{15}L_{7n} + B_{14}L_{8n} \left. \right\} + C_{8n} \left\{ \beta_n (GJK_3L_{5n} - B_{16}L_{6n}) \right. \\
& - B_{14}L_{7n} - B_{15}L_{8n} \left. \right\} \left. \right\} = -c^4 a_o b R_{10} I_{5n} / 4E_4 - T_{6n} \beta_n^3 R_{10} \\
& - {}_1\Sigma^{\infty} (-1)^m \beta_n^2 (R_{10} \beta_n K_{mn} - GJ \alpha_m L_{mn}) \quad \text{for } n \geq 1
\end{aligned} \tag{5.16}$$

## 5.2 Anti-Symmetric Load

1) Proceeding as mentioned before for symmetric loads, the first boundary condition (Equation 3.22) gives the following three equations:

$$C_{19} + C_{23} = 0 \tag{5.17}$$

$$C_{10n}K_{3n} + C_{11n}K_{4n} + C_{14n}L_{3n} + C_{15n}L_{4n} = 0 \text{ for } n \geq 1 \tag{5.18}$$

$$\begin{aligned}
& C_{18} I_{5n}/a + C_{22} I_{7n}/a^3 + \sum_{l=1}^{\infty} (-1)^m \\
& (C_{2m} B_{j1} + C_{3m} B_{j2} + C_{6m} B_{j3} + C_{7m} B_{j4}) \\
& -C_{10n} K_{2n} + C_{11n} K_{1n} + C_{14} L_{2n} - C_{15n} L_{1n} \\
& = -T_{7n} - \sum_{l=1}^{\infty} (-1)^m P_{nm} \quad \text{for } n \geq 1 \tag{5.19}
\end{aligned}$$

2) The second boundary condition (Equation 3.23) along the support gives the following equations:

$$6C_{23} R_2/b^2 = 0 \tag{5.20}$$

$$\begin{aligned}
& \alpha_n^2 \left\{ C_{10n} (A_8 K_{3n} + A_9 K_{4n}) + C_{11n} (-A_9 K_{3n} + A_8 K_{4n}) \right. \\
& \quad \left. + C_{14n} (B_8 L_{3n} + B_9 L_{4n}) + C_{15n} (-B_9 L_{3n} + B_8 L_{4n}) \right\} = 0 \\
& \quad \text{for } n > 1 \tag{5.21}
\end{aligned}$$

$$\begin{aligned}
& \sum_{l=1}^{\infty} (-1)^m \beta_m^2 \left\{ C_{2m} (A_7 B_{j1} - R_1 K_3 B_{j2}) + C_{3m} (R_1 K_3 B_{j1} + A_7 B_{j2}) \right. \\
& \quad \left. + C_{6m} (B_7 B_{j3} + R_1 K_3 B_{j4}) + C_{7m} (-R_1 K_3 B_{j3} + B_7 B_{j4}) \right\} \\
& + \alpha_n^2 \left\{ C_{10n} (A_9 K_{1n} - A_8 K_{2n}) + C_{11n} (A_8 K_{1n} + A_9 K_{2n}) \right. \\
& \quad \left. + C_{14n} (-B_9 L_{1n} + B_8 L_{2n}) + C_{15n} (-B_8 L_{1n} - B_9 L_{2n}) \right\} \\
& = \sum_{l=1}^{\infty} (-1)^m \beta_m (R_2 \beta_m P_{nm} + R_1 \alpha_n Q_{nm}) \\
& + (2/m_u) \sum_{k=1}^{m_u} (-1)^n \sin 2n\pi(k - \frac{1}{2})/m_u \quad \text{for } n \geq 1 \\
& \tag{5.22}
\end{aligned}$$

3) The following three equations result from the third boundary condition (Equation 3.24):

$$\begin{aligned}
& 6C_{22}R_3/a_3^3 + 6C_{23}R_6/b^3 + \sum_{n=1}^{\infty} (-1)^n \alpha_n^3 \left\{ C_{10n} (A_{12}W_{5n} + A_{13}W_{6n}) \right. \\
& + C_{11n} (-A_{13}W_{5n} + A_{12}W_{6n}) + C_{14n} (B_{12}W_{7n} + B_{13}W_{8n}) \\
& \left. + C_{15n} (-B_{13}W_{7n} + B_{12}W_{8n}) \right\} = \sum_{m=1}^{\infty} (-1)^m T_{7m} \alpha_m R_3 \quad (5.23)
\end{aligned}$$

$$\begin{aligned}
& \sum_{n=1}^{\infty} (-1)^m \alpha_n^3 \left\{ C_{10m} (A_{12}A_{j5} + A_{13}A_{j6}) + C_{11m} (-A_{13}A_{j5} + A_{12}A_{j6}) \right. \\
& \quad + C_{14m} (B_{12}A_{j7} + B_{13}A_{j8}) + \\
& \quad \left. + C_{15m} (-B_{13}A_{j7} + B_{12}A_{j8}) \right\} \\
& + \beta_n^3 \left\{ C_{2n} (A_{10}K_{5n} + A_{11}K_{6n} - EI\beta_n K_{7n}) \right. \\
& \quad + C_{3n} (-A_{11}K_{5n} + A_{10}K_{6n} - EI\beta_n K_{8n}) \\
& \quad + C_{6n} (B_{10}L_{5n} + B_{11}L_{6n} - EI\beta_n L_{7n}) \\
& \quad \left. + C_{7n} (-B_{11}L_{5n} + B_{10}L_{6n} - EI\beta_n L_{8n}) \right\} \\
& = T_{8n} \beta_n^3 R_6 + \sum_{m=1}^{\infty} (-1)^m \left\{ \alpha_m (\alpha_m^2 R_3 + \beta_n^2 R_5) P_{mn} \right. \\
& \quad \left. + \beta_n (\alpha_m^2 R_4 + \beta_n^2 R_6) Q_{mn} \right\} \quad \text{for } n \geq 1 \quad (5.24)
\end{aligned}$$

$$\begin{aligned}
& \sum_{n=1}^{\infty} (-1)^m \alpha_m^4 \left\{ C_{10m} (A_5 B_{j5} + A_6 B_{j6}) + C_{11m} (-A_6 B_{j5} + A_5 B_{j6}) \right. \\
& \quad + C_{14m} (B_5 B_{j7} + B_6 B_{j8}) + C_{15m} (-B_6 B_{j7} + B_5 B_{j8}) \left. \right\} \\
& + \beta_n^3 \left\{ C_{2n} (EI\beta_n K_{6n} + A_{11}K_{7n} - A_{10}K_{8n}) \right. \\
& \quad + C_{3n} (-EI\beta_n K_{5n} + A_{10}K_{7n} + A_{11}K_{8n}) \\
& \quad + C_{6n} (-EI\beta_n L_{6n} - B_{11}L_{7n} + B_{10}L_{8n}) \\
& \quad \left. + C_{7n} (-EI\beta_n L_{5n} - B_{10}L_{7n} - B_{11}L_{8n}) \right\}
\end{aligned}$$

$$= \beta_n^4 T_{8n} + {}_1 \Sigma^{\infty} EI \beta_n^4 (-1)^m Q_{mn} \quad \text{for } n \geq 1 \quad (5.25)$$

4) Finally, the following three equations are obtained from the fourth boundary condition (Equation 3.25):

$$\begin{aligned} & 6R_7 C_{22}/a^2 + 6R_{10} C_{23}/b^3 + {}_1 \Sigma^{\infty} (-1)^n \alpha_n^3 C_{10n} (A_{19} W_{5n} + A_{20} W_{6n}) \\ & + C_{11n} (-A_{20} W_{5n} + A_{19} W_{6n}) + C_{14n} (B_{19} W_{7n} + B_{20} W_{8n}) \\ & + C_{15n} (-B_{20} W_{7n} + B_{19} W_{8n}) = 0 \end{aligned} \quad (5.26)$$

$$\begin{aligned} & {}_{m=1} \Sigma^{\infty} (-1)^m \alpha_m^3 \left\{ C_{10m} (A_{19} A_{j5} + A_{20} A_{j6}) + C_{11m} (-A_{20} A_{j5} + A_{19} A_{j6}) \right. \\ & \quad \left. + C_{14m} (B_{19} A_{j7} + B_{20} A_{j8}) + C_{15m} (-B_{20} A_{j7} + B_{19} A_{j8}) \right\} \\ & + \beta_n^2 \left\{ C_{2n} \beta_n (-GJK_3 K_{5n} + A_{16} K_{6n}) + A_{14} K_{7n} + A_{15} K_{8n} \right. \\ & \quad + C_{3n} \beta_n (-A_{16} K_{5n} - GJK_3 K_{6n}) - A_{15} K_{7n} + A_{14} K_{8n} \\ & \quad + C_{6n} \beta_n (-GJK_3 L_{5n} + B_{16} L_{6n}) + B_{14} L_{7n} + B_{15} L_{8n} \\ & \quad \left. + C_{7n} \beta_n (-B_{16} L_{5n} - GJK_3 L_{6n}) - B_{15} L_{7n} + B_{14} L_{8n} \right\} \\ & = T_{8n} \beta_n^3 R_{10} + {}_1 \Sigma^{\infty} (-1)^m \beta_n^2 (GJ \alpha_m P_{mn} + R_{10} \beta_n Q_{mn}), \\ & \quad \quad \quad n \geq 1 \quad (5.27) \end{aligned}$$

$$\begin{aligned} & 6R_9 C_{23} I_{6n}/b^3 + {}_1 \Sigma^{\infty} (-1)^m \alpha_m^2 \left\{ C_{10m} (A_{17} B_{j5} + A_{18} B_{j6}) \right. \\ & \quad + C_{11m} (-A_{18} B_{j5} + A_{17} B_{j6}) + C_{14m} (B_{17} B_{j7} + B_{18} B_{j8}) \\ & \quad \left. + C_{15m} (-B_{18} B_{j7} + B_{17} B_{j8}) \right\} \\ & + \beta_n^2 \left\{ C_{2n} A_{15} K_{5n} - A_{14} K_{6n} + \beta_n (A_{16} K_{7n} + GJK_3 K_{8n}) \right\} \end{aligned}$$

$$\begin{aligned}
& +C_{3n} A_{14}K_{5n} - A_{15}K_{6n} + \beta_n (-GJK_3K_{7n} + A_{16}K_{8n}) \\
& +C_{6n} -B_{15}L_{5n} + B_{14}L_{6n} + \beta_n (-B_{16}L_{7n} - GJK_3K_{8n}) \\
& +C_{7n} -B_{14}L_{5n} - B_{15}L_{6n} + \beta_n (GJK_3L_{7n} - B_{16}L_{8n}) \left. \vphantom{+C_{3n}} \right\} \\
& =\beta_n^2 T_{8n} R_9 + \sum_{m=1}^{\infty} (-1)^m \left\{ R_8 \alpha_m \beta_n P_{mn} + (R_7 \alpha_m^2 + R_9 \beta_n^2) Q_{mn} \right\} \\
& - c \left\{ (2/m_v) \sum_{k=1}^{m_v} (-1)^n \sin[2n\pi(k - \frac{1}{2})/m_v] \right\} \quad n \geq 1 \quad (5.28)
\end{aligned}$$

It should be noted that for one boundary condition,  $(2n+1)$  equations are obtained. For the slab bridge with four boundary conditions,  $(8n+4)$  equations are obtained, so that for each case of loading (symmetric or anti-symmetric) the size of the matrix will be  $(8n+4)$ .

Once the matrix equation is formulated and solved for the unknown constants, the deflection function is known over the entire area of the slab. The moments and strains can be computed readily as follows:

$$M_x = (-D_x/c^2)W_{,uu} + (2D_x s/c^2)W_{,uv} - (D_x s^2/c^2 + D_1)W_{,vv} \quad (5.29)$$

$$M_y = (-D_2/c^2)W_{,uu} + (2D_2 s/c^2)W_{,uv} - (D_2 s^2/c^2 + D_y)W_{,vv} \quad (5.30)$$

$$M_{xy} = (0)W_{,uu} + (D_{xy}/c)W_{,uv} - (D_{xy} s/c)W_{,vv} \quad (5.31)$$

The strain can be obtained from Equation 3.7 by substituting for  $M_x$  and  $M_y$ .



## CHAPTER VI

### EXPERIMENTAL PROGRAM

#### 6.1 Scope of the Experimental Program

To verify the analytical approach proposed in Chapters III, IV and V, tests were carried out on two groups of concrete waffle-type slabs: reinforced and prestressed. The waffle slabs tested were one-to-eight scale models of concrete bridge decks. The tests were aimed at obtaining the deflections, stresses and bending moments at various points and determining the cracking and ultimate loads.

The first group consisted of three reinforced concrete waffle slabs, two were rectangular and the third had a  $45^{\circ}$  skew. One rectangular slab was tested for a uniformly distributed load by means of air pressure and a rubber membrane while the other two slabs were under concentrated loads only. The second group consisted of two post-tensioned rectangular and  $45^{\circ}$ -skew prestressed concrete waffle slabs, each subjected to edge prestressing forces and external concentrated loads applied transversely at various points.

#### 6.2 Materials

##### 6.2.1 Concrete

High Early Strength Portland Cement (CSA) manufactured by Canada Cement Company was used in all slab models. This type of cement provides high strength within a week.

A clean sand free of impurities was used. The maximum size of aggregate was restricted to 0.25 inch (6 mm) since the narrowest dimension between the sides of the formwork was equal to 1.25 inch (32 mm) and the concrete cover to the reinforcing wires was 0.375 inch (10 mm). The combined aggregate was prepared according to the ACI code (1) by mixing 40 to 60% fine aggregates of the total aggregates. This combination gave a well-graded aggregate mix with a fineness modulus equal to 2.50. The coarse aggregates used were crushed stones with hard, clean and durable properties. Natural water having no impurities was used to obtain different concrete pastes and varying maximum strength for the concrete specimens.

Five trial mixes of air-entrained concrete of medium consistency and different water cement ratio varying between 40% to 70% were examined. Mixing was done in an Eerich Counter Current Mixer, Model EA2(2W) with five cu. ft. charging capacity and manually operated. Two batches of concrete mix were required for each slab model, each weighing 700 lbs. The compressive strength of all specimens were measured after seven, fourteen and twenty-eight days as shown in Appendix (D).

### 6.3 Steel

#### 6.3.1 Mild Steel For Reinforced Concrete Slabs

To fulfill the code requirements (1), and using the minimum area of steel, three one-eighth inch (3.2 mm)

in diameter mild steel wires were used. The wires were straightened and twisted in the laboratory, keeping the cross-sectional area the same along the whole length by providing the wires with constant number of pitches per unit length. The wires were cut into different lengths, hooked at both ends and cleaned from rust. The stress-strain relationship for the reinforcing wire is shown in Appendix (E); the yield strength was found to be 33,000 psi (227.7 MN/m<sup>2</sup>). The modulus of elasticity was determined from the calibration test using strain gauges mounted on the wire and was found to be 30,000 ksi (207 GN/m<sup>2</sup>).

### 6.3.2 High Tensile Steel for the Prestressed Concrete Slabs

High tensile steel wire of 0.196 inch (5 mm) in diameter were used for the prestressed concrete waffle slabs. Tensile tests on the wire indicated an ultimate strength of 225,000 psi (1.553 GN/m<sup>2</sup>), and a yield stress of 29,700 psi (204.9 MN/m<sup>2</sup>); see Appendix (E). This wire gave good resistance against slippage from the grips. Figure 6.1 shows the twisted reinforced steel wire and the high tensile steel wire used in the slab models.

### 6.4 Formwork

Two forms were made from plywood, 3/4 inch (19 mm) thick, and wood joists, 2 x 4 inches (51 x 102 mm) cross-sectional dimension, were used as stiffeners. The first form was rectangular in shape and used for casting three

slabs, two reinforced concrete and the third being the prestressed concrete slab. The second form was used for casting the reinforced and prestressed concrete slabs of  $45^\circ$  skew as shown in Figure 6.2. Styrafoam cubes were used for producing the waffle shape; styrafoam plates of 3 inch (76 mm) thickness were cut into cubes of 3 x 4 x 4 inches (76 x 102 x 102 mm) dimensions, to fit the clearance between the ribs.

## 6.5 Experimental Equipment

### 6.5.1 Prestressing Equipment

The prestressing equipment used in prestressing the wires, were manufactured by Cable Covers Ltd., England. A hydraulic jack of twenty kips (89 KN) capacity was used for post-tensioning as shown in Figure 6.3. The mechanical gripping devices of the open grip type and washers shown in Figure 6.1, were very simple and quick to use. Black wax lubricant was applied to the wedges to make it easier to release the grips after completing the prestressing operation.

### 6.5.2 End Bearing Plate

Fifty-eight end bearing plates, 0.25 inch (6.4 mm) thick, with holes of 0.25 inch (6.4 mm) diameter and of 1.5 x 3.0 inches (38 x 76 mm) dimensions, were used to distribute the prestressing force at each end of the rib. Twenty-six steel blocks of 1.5 x 1.5 x 3.0 inches (38 x 38 x 19 mm) were used for the prestressed skew slab.

Each steel block was provided with two perpendicular eccentric holes to fit the wires in two directions. Figures 6.1 and 6.4 show the end bearing plates and the grooves in the concrete skew slab to accommodate the steel blocks.

### 6.5.3 The Steel Frame For Producing Uniformly Distributed Load

The purpose of the steel loading frame, Figures 6.5 and 6.7, was to apply a uniformly distributed load by means of an air chamber and a rubber membrane. The top of the air chamber was made of a stiffened steel plate, 0.25 inch (6.4 mm) thick and, 104.25 x 87.50 inches (2.65 x 2.22 m) in plan. The bottom of the air chamber was a rubber membrane, 0.09 inch (2.4 mm) thick and 134.25 x 117.5 inches (3.41 x 2.98 m) in plan. The steel cover plate was placed on the top of the rectangular steel frame made of two steel channels as shown in Figures 6.5 and 6.6. Figures 6.7 and 6.8 show the longitudinal and transverse sections in the steel loading frame. Two steel rods of 1.25 inch (31.8 mm) diameter, were placed on the top flange of the beams to be used as simple supports for the slab. Styrafoam strips were placed inside the channel of the air chamber to avoid any damage to the rubber membrane from the sharp corners of the steel frame.

All supporting beams were tack-welded onto the floor to avoid any sliding or uplift during the experiment. Two steel rods, 0.25 inch (6.4 mm) in diameter were tack-welded

onto the flange plate around the supporting steel rods to prevent sliding and to allow rotation. Three pressure gauges, two valves and a regulator were fixed on the steel plate to measure and control the air pressure as shown in Figure 6.6. Heavy steel clamps were used to clamp the steel plate and the rubber membrane with the steel frame as shown in Figure 6.5.

### 6.6 The Construction of the Slab Models

Figures 3.2 and 3.3 show the dimension of the cross-sections of the five one-eighth scale model slabs. Figures 6.9 to 6.13 show the layout of the five slabs. The reinforced concrete slabs (Group A) are denoted by A.1, A.2 and A.3, while the prestressed concrete slabs (Group B) are referred to as B.1 and B.2. The required form was prepared as shown in Figure 6.2 and then painted with grease material, Vitrea Oil 150, for easy form release after the concrete has set. The twisted steel wires for group A were placed in the form; they were instrumented with electric strain gauges. The bottom steel layer was supported on steel wire chairs which provided a clear cover of 0.5 inch (12.7 mm) from the bottom. The second steel layer was supported directly over the first layer and fixed with thin wires. All reinforcing wires were hooked at both ends.

For the group B slabs, rubber hoses having an inner diameter of 0.25 inch (6.4 mm) and 0.062 inch (1.6 mm)

thick were used to cover the steel wires during casting of the concrete. The first layer of the steel wires was placed at a distance of one inch from the bottom, and supported on thin steel wires fixed between the styrafoam cubes. The second layer was placed directly over the first layer.

To determine the compressive strength of the concrete, six 3 x 6 inches (76 x 152 mm) cylinders were cast with each model.

All concrete in the slab models was vibrated with a high frequency vibrator. Care was taken during casting and vibrating to ensure that no segregation occurred. The top surface of the slab models was troweled smooth after casting. The slab models and the cylinder specimens were cured in water for 14 and 28 days and then were allowed to dry at least four days before mounting the strain gauges.

## 6.7 Instrumentation

### 6.7.1 Strain Gauges on the Reinforcement

The longitudinal and transverse wires were instrumented with electric strain gauges as shown in Figures 6.10 and 6.11. The gauges used were metal gauges of type EA-06-062AP-120. The surface of the reinforcing wire was prepared by cleaning it using fine silicon carbide paper and acetone. The gauge was mounted using Eastman M-Bond

200 adhesive with 200 catalyst as bonding agent according to the manufacturer's recommendations. The lead wires were then soldered to the gauges and water-proofed with a

plasticised epoxy resin system, Bean Gagekote #3. After curing for 24 hours at room temperature a layer of wax was applied on the gauge and plastic tape for further protection from the wet concrete.

#### 6.7.2 Strain Gauges On The Concrete

To measure the strain on the top and the bottom surfaces of the slab models, electric strain gauges of type EA-06-500 BH-120 were used. Three-legged rosette gauges were used also on the deck surface of the skew model at the obtuse corner. All gauges had a nominal gauge length of 0.50 inch (12.7 mm). The locations of the strain gauges are shown in Figures 6.9 to 6.13.

The concrete surfaces at the locations of the gauges were smoothed using sandpaper, all dust was removed and then the surfaces were cleaned with acetone. Surface cavities were then filled by applying an epoxy of high strength (RTC). This epoxy was mixed by one volume activator B, and the same volume of resin A. After the surface was dry, it was again smoothed and the gauge was mounted, soldered with lead wires and covered by coating epoxy Bean Gagekote #3. The gauges were then connected to a strain indicator, Strainert model TN 20C.

#### 6.7.3 Mechanical Dial Gauges

The deflections were measured using mechanical dial gauges having 0.001 inch (.025 mm) travel sensitivity. The locations of the dial gauges are shown in



Figures 6.9 to 6.13, and are seen in position in Figure 6.14. In group A slabs, the dial gauges were placed at the bottom surface of the slab. In group B slabs, the dial gauges were placed at the top surface of the slab and supported by a light steel frame.

#### 6.7.4 Load Cells

##### a) Universal Flat Load Cell

Two universal flat load cells, having capacities of 5 kips (22.25 KN), and 25 kips (111.3 KN), were used in reinforced and prestressed concrete slabs respectively to determine the value of the applied concentrated load through the hydraulic jack as shown in Figure 6.15. The calibrations of these load cells are given in Appendix (E)

##### b) Cylindrical Load Cell

Thirty-eight cylindrical load cells were used to measure the prestressing force in the wires. The calibration of these load cells is given also in Appendix (E). Figure 6.4 shows the cylindrical load cells in position.

### 6.8 Experimental Setup and Test Procedure

Due to the heavy weight of each slab model and the difficulty in handling, it was decided to cast the slabs near the portal loading frame and in the vicinity of a crane.

#### 6.8.1 Reinforced Concrete Waffle Slabs, Group A

##### a) Slab A.1

Reinforced concrete slab A.1 was subjected to a uniform load, applied by pumping compressed air into a

chamber formed by a rubber membrane and a steel frame as shown in Figures 6.7 and 6.8. The setup was designed and fabricated. Care was taken to insure that the rubber membrane was in contact with the slab's surface, without allowing any tension in the membrane, which might affect the results. Shims were provided along the support rods so that uniform contact was maintained between the supports and the slabs. Clearance of 0.125 inch (3.15 mm) was allowed between the edges of the slab and the edge of the steel frame to allow rotation of the slab during the test. To ensure that the air chamber is totally air tight, heavy steel clamps were used every ten inches along the steel plate.

To measure the air pressure inside the air chamber three pressure gauges of 0.15 lb/in<sup>2</sup> (107 KN/m<sup>2</sup>) accuracy were used at various points as shown in Figure 6.6. A regulator valve was used to control the air pressure and for loading and unloading as shown in Figure 6.6. Forty-two strain gauges were mounted on the concrete, at top of the deck and bottom surface of the longitudinal and transverse ribs and at mid-depth of the rib to observe the strain gradient through the depth of the rib. Nine dial gauges were used to measure the deflections as shown in Figure 6.9.

b) Slab A.2

Slab A.2 was identical in geometric shape and amount of steel to slab A.1, but was tested under transverse

concentrated loads, applied through a rigid portal frame supporting a cross I beam and a hydraulic jack of 20,000 lbs. (89 KN) capacity. The arrangement was such that the concentrated load could be applied anywhere without moving the slab; see Figure 6.16. The transfer of the load from the hydraulic jack to the slab was made through a small rectangular steel plate, 1 inch (25.4 mm) thick and 5 x 6 inches (127 x 152 mm) in plan. Grooves of 0.187 inch (4.8 mm) thickness and 0.75 inch (19 mm) width were made on the bottom of the steel loading plate to avoid contact with the strain gauge located at loading positions. Loading and unloading were applied three times before starting the test, to minimize the residual strains and for proper seating of the slab on the supports. Figure 3.4 shows the loading points: points 1 to 6 for the working load stage, and point 7 up to failure of the model.

The strains were measured by thirty-five electric strain gauges mounted on the concrete and steel. Deflections were measured by sixteen mechanical dial gauges as shown in Figure 6.10. The readings from loading and unloading were recorded and averaged.

c) Slab A.3

The dimensions of this slab are shown in Figure 6.11 and its loading system is shown in Figure 6.17. The loading plate was one inch (25.4 mm) thick and 6x7 inches (152 x 179 mm) in plan as shown in Figures 4.1 and 6.15. The slab was tested under concentrated load at eight

locations, Figure 3.4. Twenty-three electric strain gauges were used to measure the strains in the concrete and steel. Ten mechanical dial gauges were used to measure the deflections; see Figure 6.11.

#### 6.8.2 Prestressed Concrete Waffle Slabs, Group B

This group consisted of two post-tensioned waffle slabs, a rectangular slab B.1 and a  $45^\circ$  skew B.2.

##### a) Slab B.1

Forty-five strain gauges were used to measure the strain on the concrete surfaces and eleven mechanical dial gauges were used to measure the deflections as shown in Figure 6.12. The slab was prestressed by twenty-nine high tensile steel wires, each one connected to a cylindrical load cell to measure the prestressing force.

All care and adequate precautions were taken during the prestressing process. To avoid any distortion in the edge beam and/or local failure, the wires were tensioned in a sequence starting with the odd-numbered wires and followed by tensioning the even-numbered wires. Figures 6.18 and 6.20 show the loading system and the final amount of prestressing force.

The slab was tested under concentrated load through a universal load cell of twenty-five kips capacity. Figure 3.5 shows the loading points: points 1 and 2 for the working load stage, and point 3 up to failure of the model.

##### b) Slab B.2

The slab was mounted with twenty-five strain gauges

to measure the strain on the concrete surfaces and eleven dial gauges to measure the deflections as shown in Figure 6.13. The slab was prestressed by thirty-eight high tensile steel wires in both directions, thirteen wires in the longitudinal direction (parallel to the traffic) and twenty-five wires were perpendicular to the edge beams. To prestress the wires along the skew supports, steel end blocks were placed in ninety degree grooves formed before casting the concrete; see Figure 6.4. The wires were tensioned in the sequence mentioned earlier for slab B.1.

The loading system used is shown in Figure 6.19. The slab was tested at four points; Figure 3.5 shows the loading points: points 1,2,3 and 4 for the working load stage, and again at point 1 up to the failure of the model.

## CHAPTER VII

### DISCUSSION OF RESULTS

#### 7.1 General

The theoretical and experimental results for deflections and strains of reinforced concrete waffle slabs are compared in Figures 7.3 to 7.8, Figures 7.11 to 7.17 and Figures 7.20 to 7.25. The upward deflections (camber) and strains of group B slabs due to prestressing force are presented in Figures 7.28, 7.29, 7.30, 7.39, 7.40 and 7.41.

The comparisons between experimental and theoretical results for stresses and deflections for group B slabs, are given in Figures 7.31 to 7.34 and Figures 7.42 to 7.46.

Finally, comparisons between the results for the waffle slab type and those for the slab type with uniform thickness and having the same volume of concrete and amount of steel, are given in Figures 7.47 to 7.56.

#### 7.2 Reinforced Concrete Waffle Slabs (Group A)

##### 7.2.1 Rectangular Slab Under Uniform Load (Slab A.1)

Figures 7.3 and 7.4 show the comparison between the theoretical and experimental results for the load-deflection relationships at various points on the centre line and on the free edge of the slab. Figures 7.5 and 7.6 show the comparison between the theoretical and experimental deflections for a uniform load of  $0.3 \text{ lb/in}^2$  ( $2 \text{ KN/m}^2$ ) before

cracking. Close agreement is observed in the results before reaching the cracking load, with a maximum difference between the theoretical and experimental results of varying from 5 to 7%.

Load-strain relationships for points at the centre and at the free edge are plotted in Figures 7.7 and 7.8, showing the strains at the top and bottom fibres in the x and y directions. Close agreement between the theoretical and experimental results is observed before cracking of the concrete. Considering the maximum moments due to self-weight of the slab, the microcracking occurs at a strain of approximately  $100 \times 10^{-6}$  in/in, which agrees with the results formed by Evans (6).

Figure 7.2 shows the crack progression during loading of slab A.1, and finally the failure of the slab as shown in Figure 7.1. It can be observed that the cracks appear in the longitudinal ribs between the supports with no cracks in the transverse ribs. Figure 7.8 shows that the maximum strain occurs in the longitudinal ribs, while the strain in the transverse ribs is very small. The final failure of the slab occurs when the maximum tensile stress due to bending is reached at the centre of the slab. The microcracking loads starts at a load equal to one-third the ultimate load.

#### 7.2.2 Rectangular Slab Under Concentrated Load (Slab A.2)

Figure 7.11 shows the load-deflection curves up to

the ultimate load due to a concentrated load at the centre of the slab. A very good agreement is observed between the theoretical and experimental results before microcracking. The microcracking occurs at 0.70 of the experimental cracking load and 0.50 of the ultimate load.

Since the slab was tested first up to 0.60 of the yield stress of the steel for various locations, local cracks occurred near the loading point. It is found that these local cracks reduce the rigidities of the slab by a ratio of 65 to 75%. Figure 7.12 shows the load-deflection curves up to 0.60 yield stress in the steel due to a concentrated load at the central point on the free edge. For this loading case if one accounts for the presence of local cracks by multiplying the experimental deflections by 0.70 (due to reduced rigidity of the slab) the adjusted experimental results become much closer to the theoretical ones.

Figures 7.13 and 7.14 show the theoretical and experimental deflection patterns for a one-kip (4.45 KN) concentrated load at various positions. Curve #1 represents the deflection due to a concentrated load at the centre of the slab and shows good agreement with the theoretical results. Curves #2 and #3 show the theoretical and experimental deflections due to a one-kip load at points 2 and 3; it is observed that 70% of the experimental deflections, gives good agreement with the theoretical deflections; as explained before, this percentage reduction



is applied because of the reduced rigidities at points 1 and 2 due to local cracking resulting from prior loading of the slab at these points.

Figures 7.15 and 7.16 show the load-strain relationships for concentrated loading at the centre and at the free edge. There is better agreement between the theoretical and experimental results for a concentrated load at the centre; comparing the results in Figure 7.15 with the results for uniform loading, Figure 7.7, the orthotropic slab subjected to a concentrated load is more efficient than one loaded by a uniform load. In the case of concentrated load, the transverse ribs are working effectively together with the longitudinal ribs to transmit the load to the supports; which in the case of uniform load the slab acts as a wide beam. The differences in the strains in the transverse ribs for both slabs can also be noted. Figure 7.10 shows the cracks in the bottom fibres of the slab A.2, before failure. It is observed that the majority of the cracks occur in the longitudinal ribs, while only haircracks appear in the transverse ribs.

The strain patterns at the bottom fibre due to a one-kip load at the centre of the slab are shown in Figure 7.17. It can be observed that the strains in the transverse ribs at the loading point equal about 50% of the strains in the longitudinal ribs at the same point. The recorded ultimate load for this slab was 2.25 kips (10 KN) with the corresponding deflection of 2.50 inches (64 mm),

Figure 7.9.

7.2.3 45° Skew Slab Under Concentrated Load  
(Slab A.3)

Figures 7.20, 7.21 and 7.22 show the load-deflection results before and after cracking and the deflection pattern along the transverse direction. A very good agreement between the theoretical and experimental results is obtained before cracking as shown in Figure 7.20. It is observed that the experimental results in Figures 7.21 and 7.22 when scaled down by 70% (due to the reduced rigidities) are in close agreement with the theoretical ones.

Figures 7.23, 7.24 and 7.25 show the load-strain relationships and the strain pattern in both directions and in the top and bottom fibres. A study of Figure 7.23 reveals good correspondence between the theoretical and experimental results and demonstrates that in skew slabs, the transverse ribs work effectively together with the longitudinal ribs to transmit the load to the supports.

Figures 7.18 and 7.19 show the diagonal cracks in the bottom fibre at the free edge. Referring to Figures 7.10 and 7.19 and comparing the two patterns of cracks, it is observed that the cracks in the rectangular slab is due to flexure while the cracks in the skew slab is due predominantly to twisting.

7.3 Prestressed Concrete Waffle Slabs (Group B)

7.3.1 Rectangular Slab Under Concentrated Load  
(Slab B.1)

Figure 7.28 shows the upward deflection due to prestressing force and edge moment, while Figures 7.29 and 7.30 show the strain pattern in the top and bottom fibres of the slab due to prestressing force in both directions. The variation in the strain along the edge beam is due to the variation in the prestressing force.

Figures 7.31 and 7.32 show the load-deflection relationship for a concentrated load at the centre and on the edge beam respectively. It can be observed that there is very good agreement between the theoretical and experimental results before reaching the cracking load with a percentage difference of about 1%.

Load-strain relationships are shown in Figures 7.33 and 7.34 for concentrated loading at the centre of the slab and at the centre of the edge beam. It can be observed that there is close agreement between the theoretical and experimental results. From Figure 7.34 it can be noted that the cracks start due to flexure under the concentrated load, followed by another crack developing in the top fibre leading to the formation of a yield line as shown in Figure 7.26. Figure 7.27 shows the final collapse due to punching shear around the loading plate.

### 7.3.2 45° Skew Slab Under Concentrated Load (Slab B.2)

Figures 7.39, 7.40 and 7.41 show the deflection pattern and strain distribution in the top and bottom fibres over the entire area of the slab. The differences

between the theoretical and experimental deflections (camber) and strains vary between 4 to 6%.

Figures 7.42, 7.43 and 7.44 show the load deflection curves for the theoretical and experimental results; very good agreement is obtained before reaching the cracking load, the difference between the results being less than 2%. Figures 7.45 and 7.46 show the load-strain relationships for concentrated loading at the centre and at the free edge. Point 3 located near the obtuse corner, Figure 7.46, appears to be the critical point on the slab as indicated by the magnitude of strains in the bottom and top fibres. For concentrated loading at the centre of the slab, the cracks start first at the bottom fibre under the load, followed by cracks appearing close to the obtuse corner as shown in Figure 6.4. Figures 7.35 and 7.36 show the development of these cracks. The cracking load for the concentrated load at the centre is 6 kips (26.7 KN) and the slab continues to carry load up to 11 kips (49 KN) and finally fails in punching shear as shown in Figure 7.37. Figure 7.38 shows the number and direction of cracks in the bottom fibre for the same slab under load.

#### 7.4 Comparison Between the Behaviours of a Waffle Slab and a Uniform Thickness Slab Having the Same Volume of Concrete and Reinforcement

An analytical study, using the computer program and the proposed formulae to estimate the rigidities (13) is made on two types of orthotropic slabs. The first type is a waffle slab structure and the second is a slab

structure with uniform thickness, both structures having the same volume of concrete and reinforcing steel. The study includes prestressed concrete waffle slabs as well as reinforced concrete waffle slabs before cracking.

According to the proposed formulae for flexural and torsional rigidities, the values of the flexural rigidities of the orthotropic slab of uniform thickness are approximately one-half of the investigated waffle slabs in both directions; however, the torsional rigidity of the former is four times that of the latter. Figures 7.47 to 7.56 show the results for deflection and strain patterns over the entire area of the slab due to uniform load as well as concentrated load.

Rectangular and skew slabs are considered in this study. The figures show the comparison for deflections and strain between the waffle slab and the slab with uniform thickness. It can be observed from these figures that the waffle slab exhibits much lower stress. For example, the reinforced concrete waffle slabs of rectangular shape and subjected to uniform load have deflections at the centre and centre of the free edge of 43% and 51%, respectively, of those obtained in a slab of uniform thickness. These ratios increase for the skew type to 88% and 94%. The higher flexural rigidities of the waffle slabs produce much smaller deflections and lower stresses, particularly for the rectangular slab. It should also be mentioned that increase in skew leads to a decrease in the

advantages cited above as well as when the concentrated load moves away from the centre of the slab.

One advantage of waffle slabs over slabs of uniform thickness is in prestressed construction. The efficiency of the prestressed waffle slabs in carrying load is much higher than that of slabs of uniform thickness of the same volume of concrete and amount of steel. This is due to the presence of the ribs which contribute to increased eccentricities in waffle slabs for prestressing. Figure 7.56 shows a comparison for the deflection pattern between the two types.

#### 7.5 Sources of Error

The discrepancies between the experimental and theoretical results can be attributed to several sources of error such as:

1. The assumptions made in the theory.
2. Estimates of Poisson's ratio and the modulus of elasticity of concrete by means of empirical formulas.
3. Approximation of the plane stress problem encountered in the prestressed waffle slab.
4. Estimating the strength of the concrete from tests on 3 x 6 inches cylinder.
5. Distortion in the formwork due to effect of water, and lack of complete contact between the support and the test model.
6. Positioning of reinforced and prestress wires.

7. The calibration of load cell, sensitivity and drag in mechanical dial gauges, the stability of strain gauges and the strain gauge measuring device.

## CHAPTER VIII

CONCLUSIONS AND RECOMMENDATIONS8.1 Conclusions

The overall objective of this study was to obtain a better understanding of the behaviour of reinforced and prestressed concrete waffle slabs, before and after cracking of the concrete. A Fourier series method of analysing single span rectangular and skew waffle slabs by orthotropic plate theory was presented; uniform load as well as concentrated loads were considered. Proposed theoretical formulae for calculation of the various orthotropic rigidities were used. The theoretical solutions were supported by the experimental results obtained from tests on prestressed and reinforced concrete models. An analytical study and comparison between the behaviour of a waffle slab and a uniform thickness slab having the same volume of concrete and reinforcement were made.

Based on the results obtained from the theoretical and experimental studies the following conclusions are drawn:

1. The good agreement between the experimental and theoretical results supports the reliability of the proposed formulae for estimating the orthotropic rigidities.
2. The theoretical solution gives good convergence in the results for uniform and concentrated loads at the centre of rectangular



slabs. Such degree of convergency decreases as the concentrated load moves away from the centre of the slab or when the skew angle increases.

3. The discrepancies between the theoretical and the experimental results for reinforced concrete slabs are due to microcracking.
4. Local cracks produced near the concentrated load in reinforced concrete slabs can reduce the stiffness of the slab by as much as 30%.
5. The torsional rigidity of the slab plays an important part on the behaviour of a skew slab as well as when a concentrated load is close to the unsupported edges.
6. The behaviour of prestressed waffle slabs can be much better predicted than that for reinforced concrete waffle slabs; this is due to absence of local cracking and microcracking.
7. The presence of the ribs in waffle slab construction makes it possible to accommodate the prestressing steel more readily and at varying levels of eccentricity, and therefore the realization of its use for longer span, resulting in substantial economy.
8. In general reinforced and prestressed waffle slabs are structurally more efficient than

slabs with uniform thickness.

## 8.2 Suggestions For Future Research

The following suggestions are recommended for future research:

1. An exact solution for the plane stress problem for rectangular and skew prestressed concrete waffle slabs is required for better predictions.
2. The after cracking behaviour of reinforced and prestressed concrete waffle slabs up to failure of the slab should be investigated.
3. The effect of edge beam with different cross sections is of practical interest.
4. An analysis based on a finite element method or finite difference technique should be established to deal with the problem of varying rigidities of the slab due to cracking of the concrete at various locations.

## FIGURES

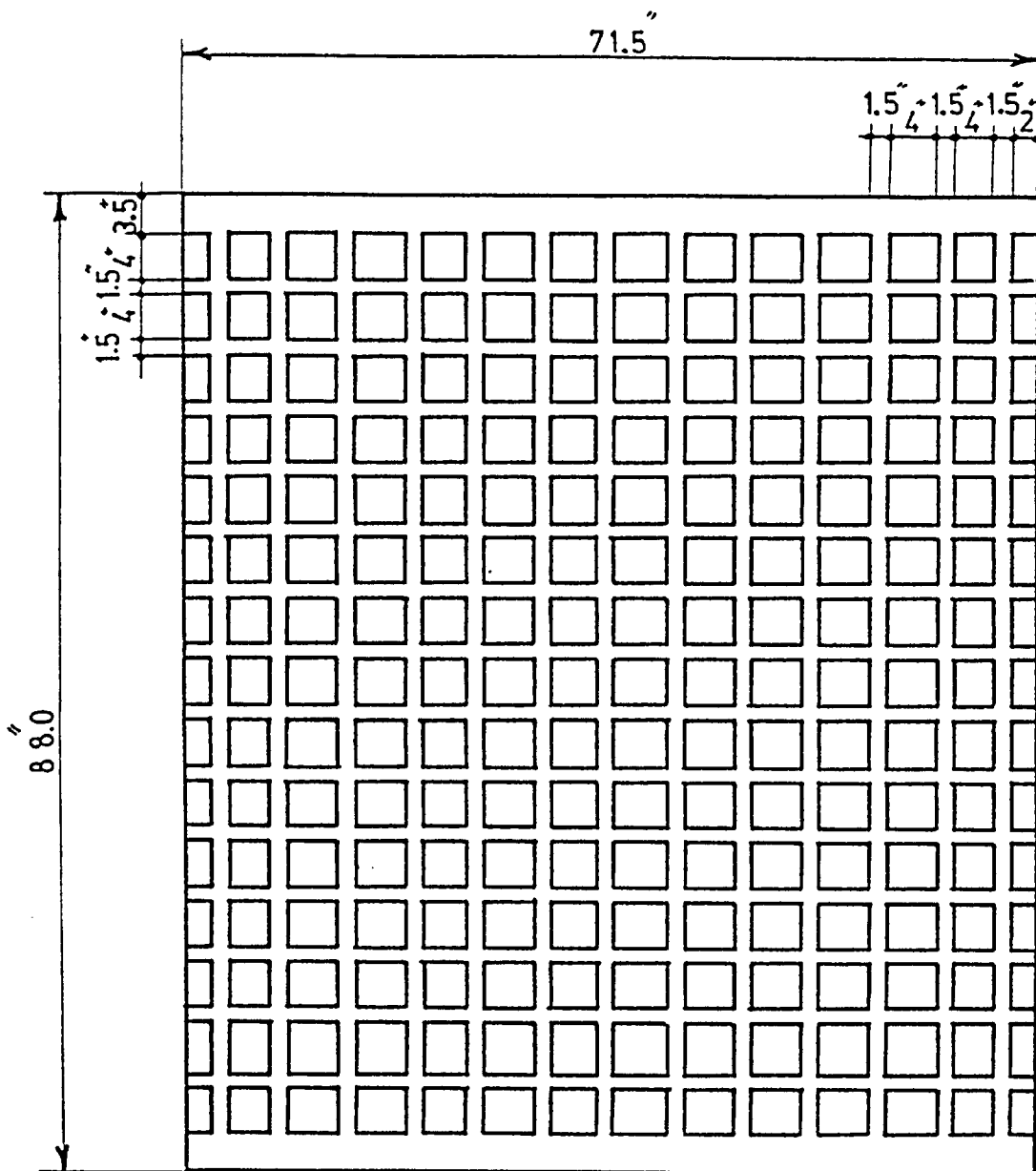


FIGURE 3.1 BOTTOM PLAN LAYOUT WAFFLE SLABS  
A<sub>1</sub> AND A<sub>2</sub>.

(1 in. = 25.4 mm)

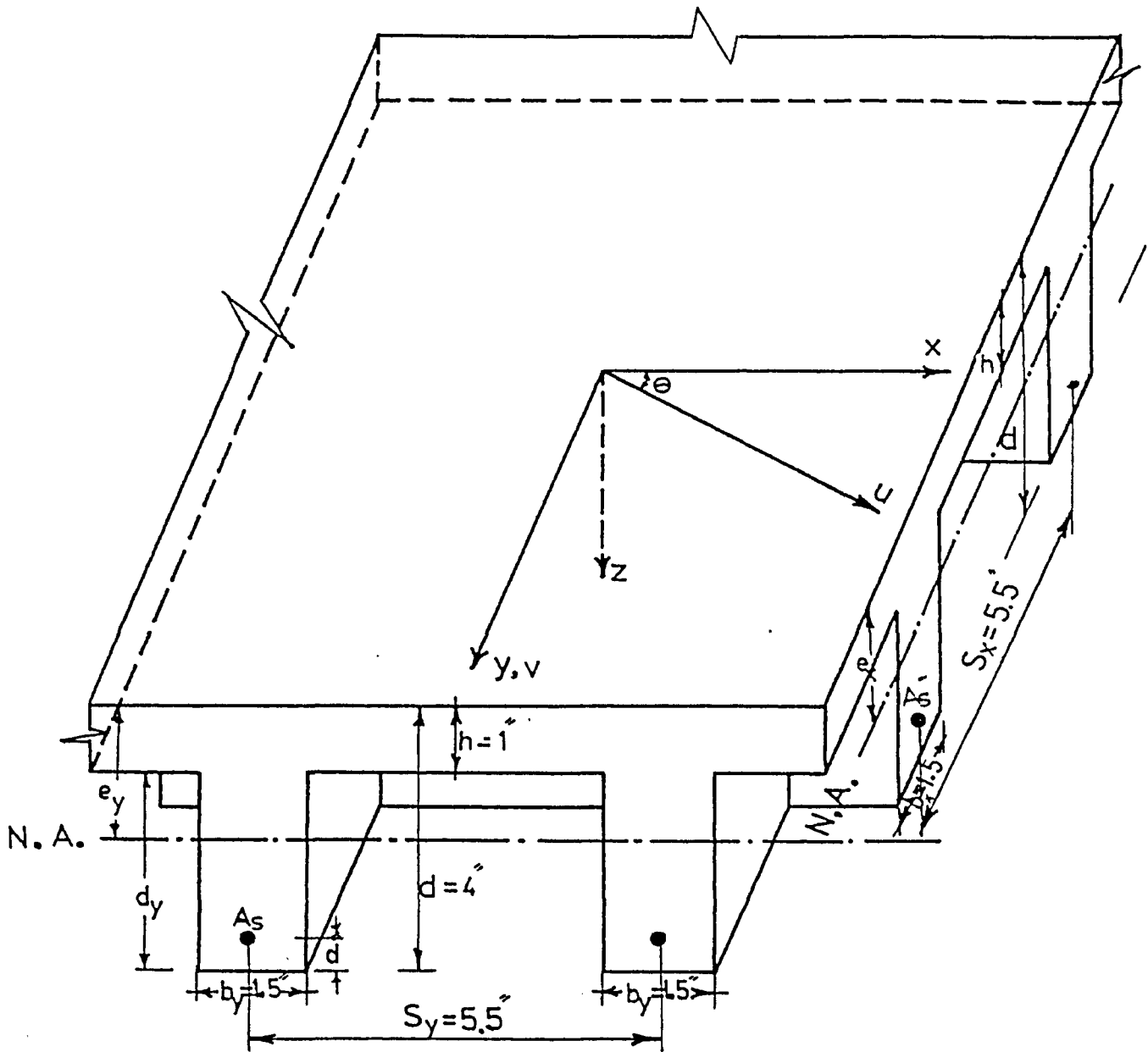
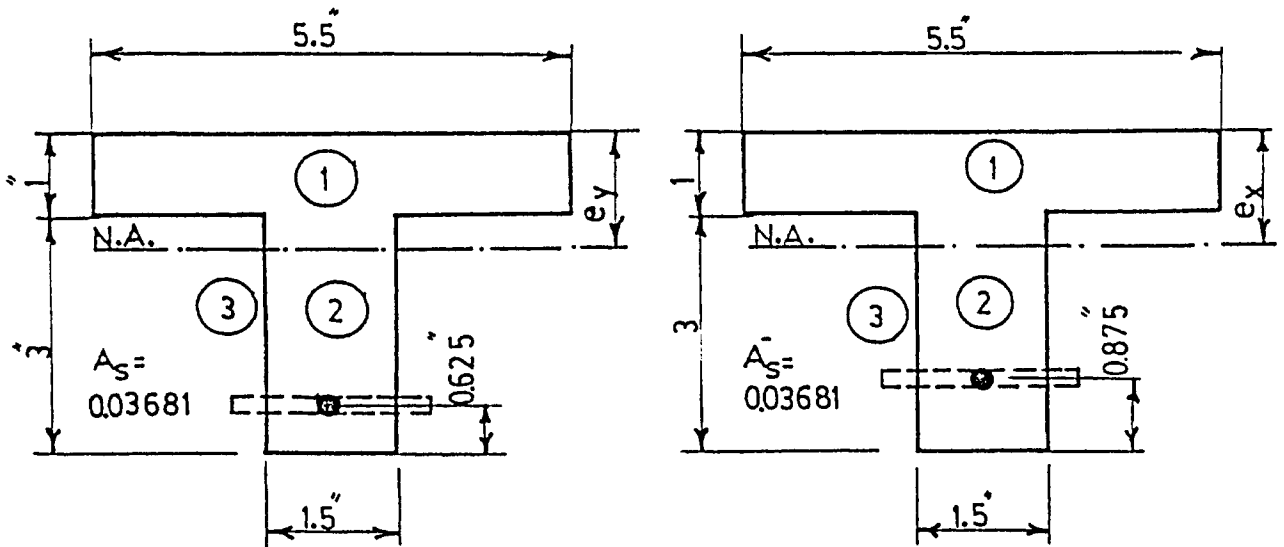


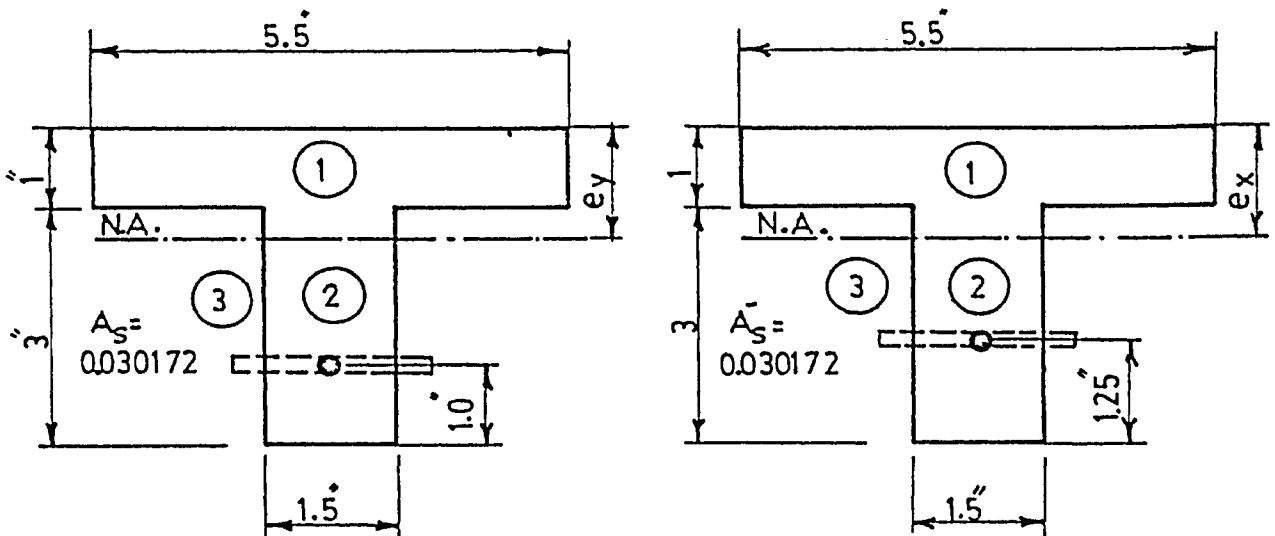
FIGURE 3.2 GEOMETRIC SHAPE OF THE RIBS AND THE PLATE FOR WAFFLE SLAB.

(1 in. = 25.4 mm)



LONGITUDINAL SECTION (y AXIS)      TRANSVERSE SECTION (x AXIS)

a) REINFORCED CONCRETE (GROUP A)



LONGITUDINAL SECTION (y AXIS)      TRANSVERSE SECTION (x AXIS)

b) PRESTRESSED CONCRETE (GROUP B)

FIGURE 3.3 ORTHOTROPIC RIGIDITIES OF WAFFLE SLAB.

(1 in. = 25.4 mm)

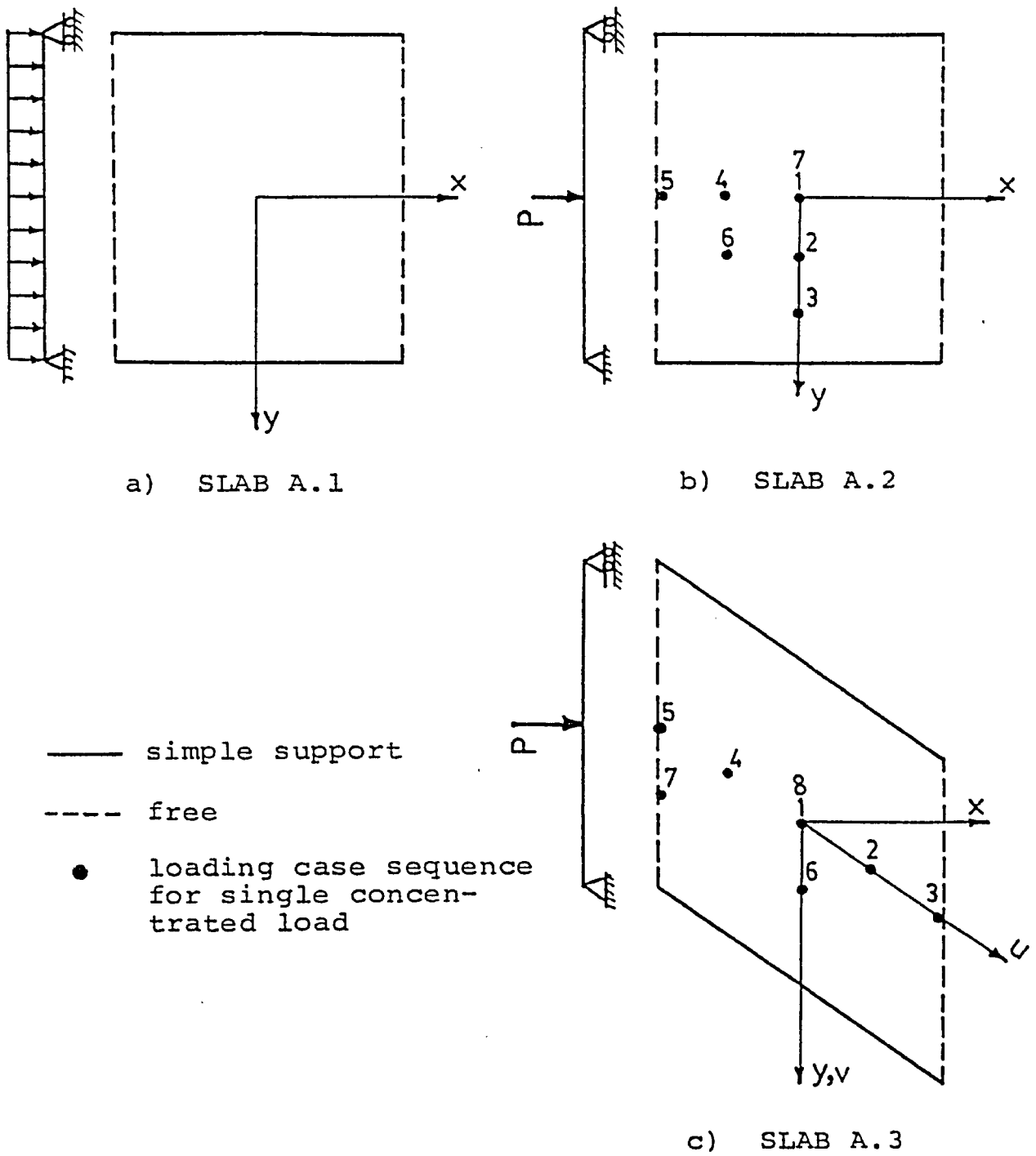


FIGURE 3.4 LATERAL LOADING CASES FOR GROUP A SLABS

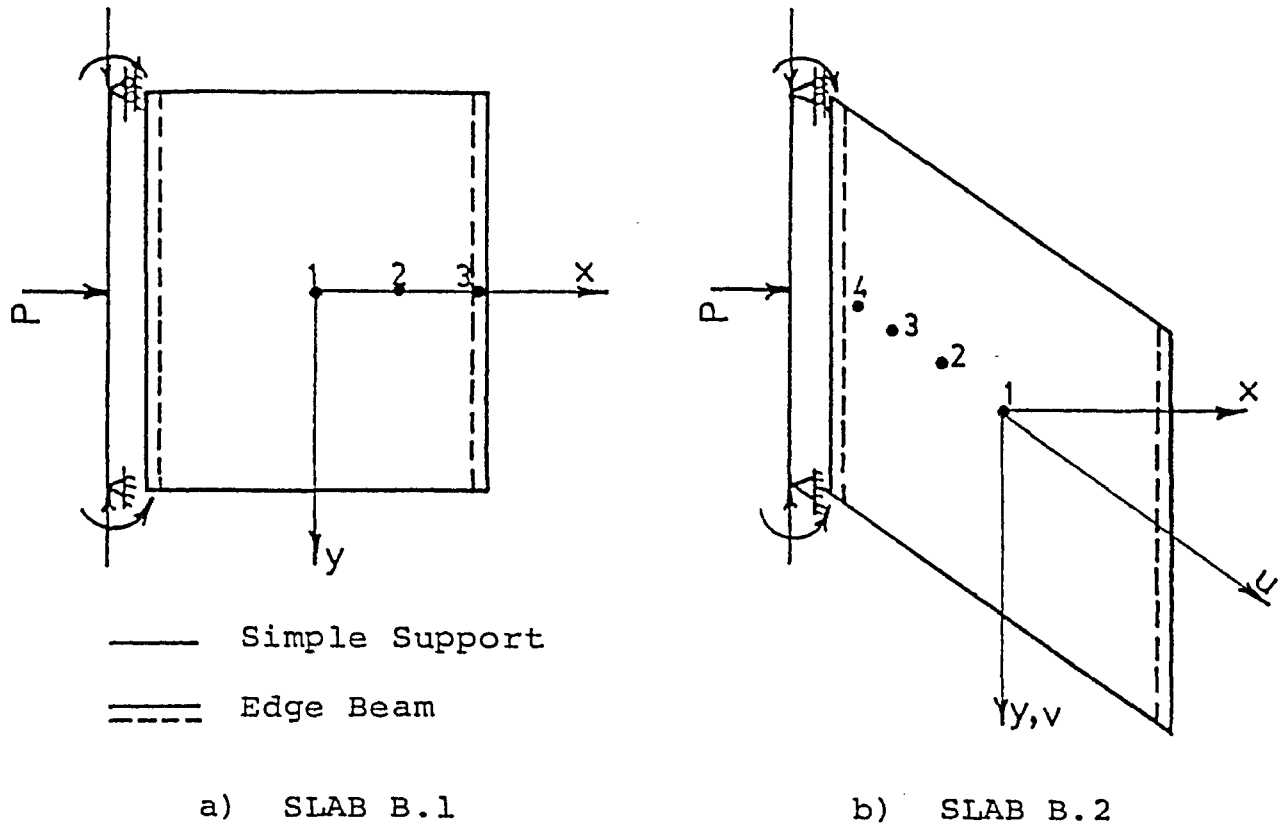


FIGURE 3.5 LATERAL LOADING CASES FOR GROUP B SLABS

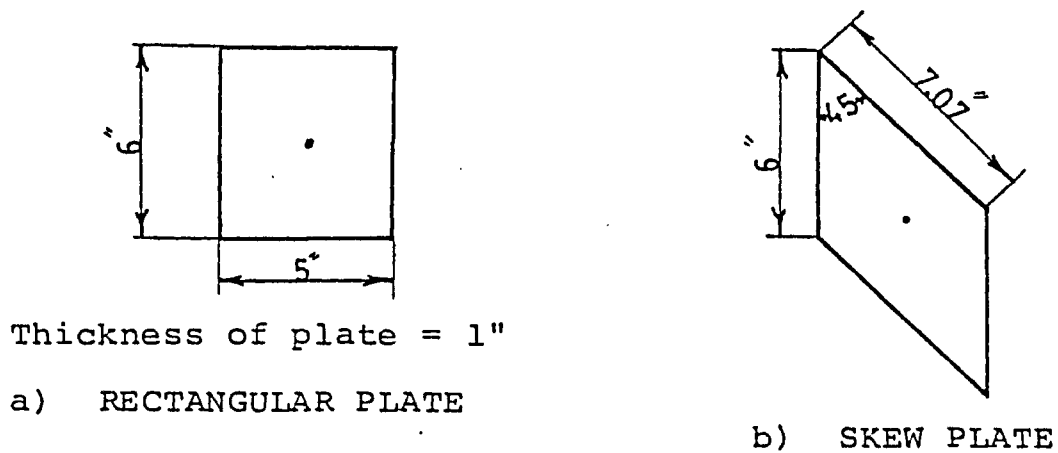


FIGURE 4.1 STEEL LOADING PLATES



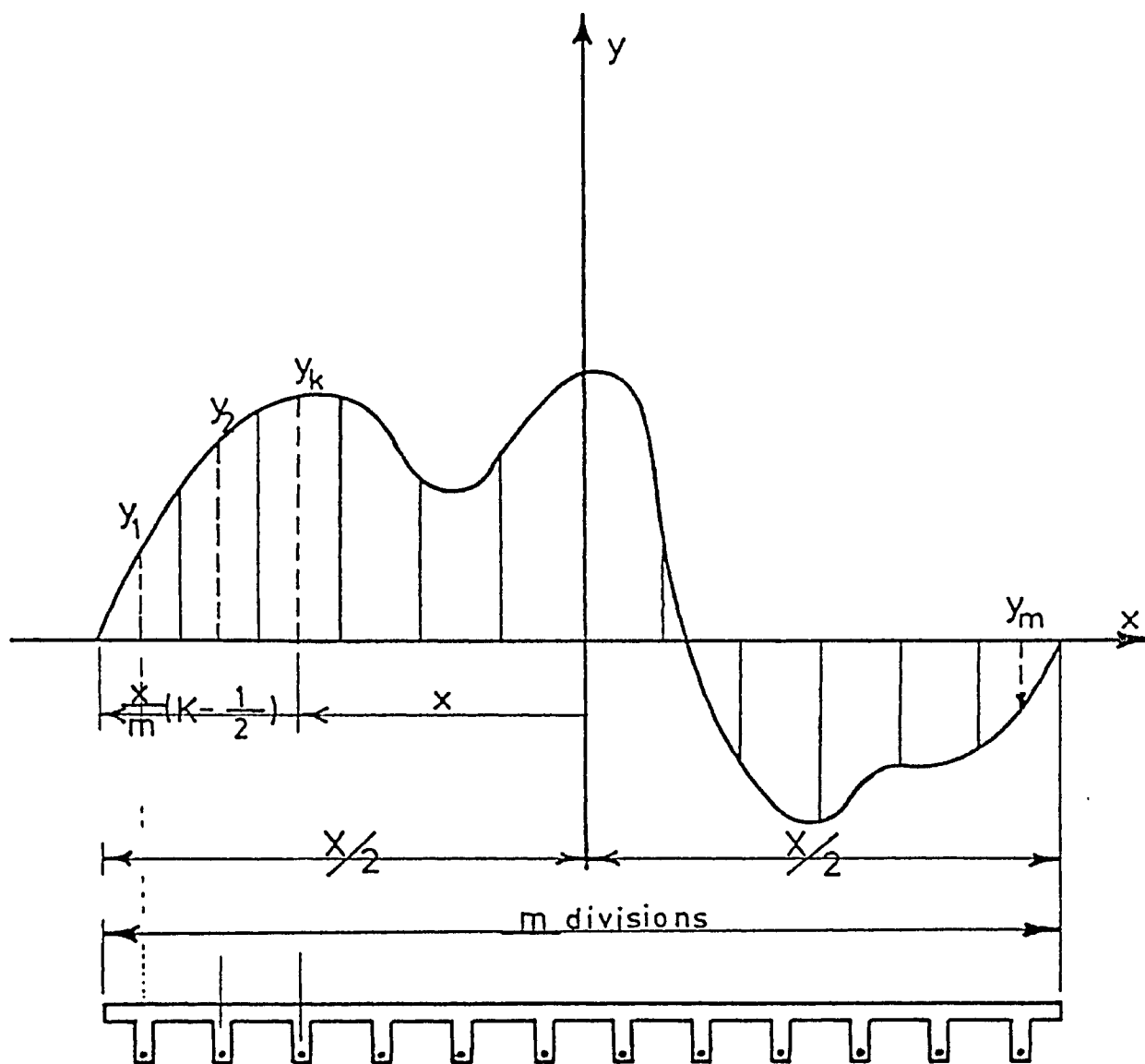


FIGURE 4.2 EXPANSION OF THE LOAD IN FOURIER SERIES.

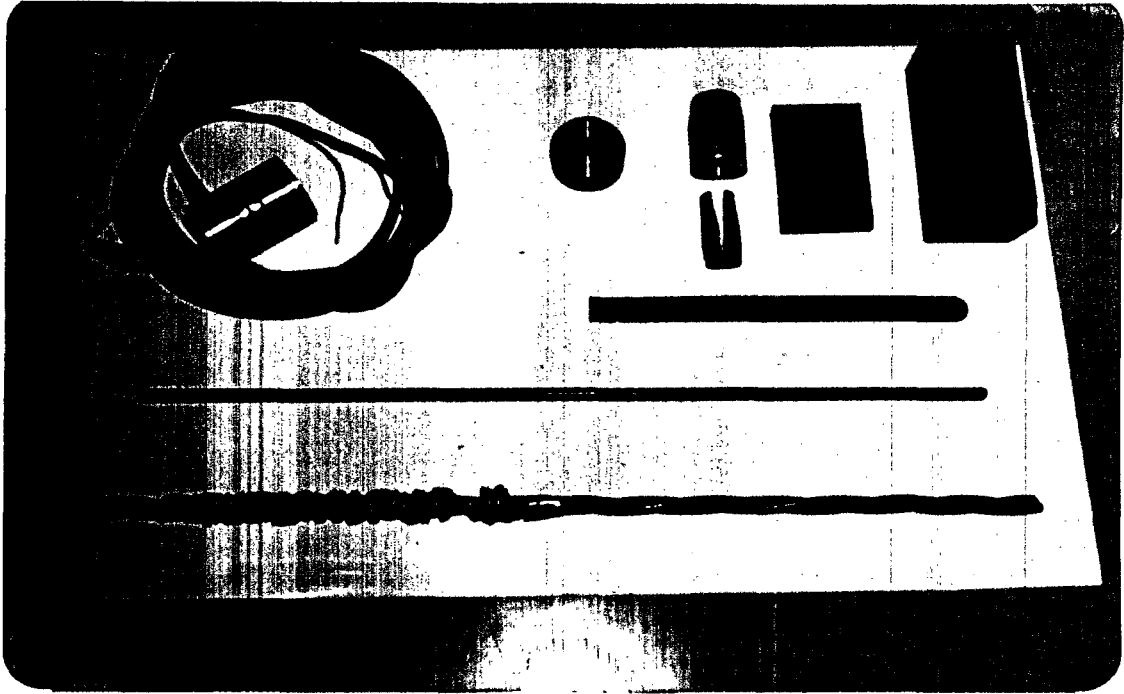


FIGURE 6.1 THE REINFORCING STEEL AND ANCHORAGE SYSTEM.

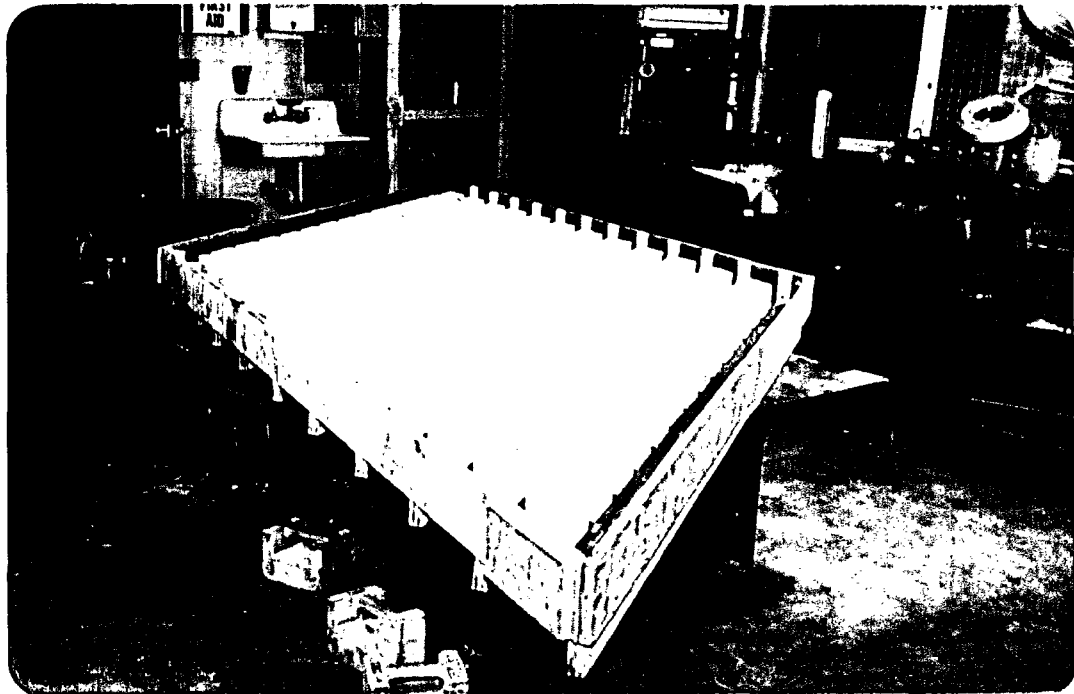


FIGURE 6.2 FORM BEFORE CASTING THE CONCRETE.

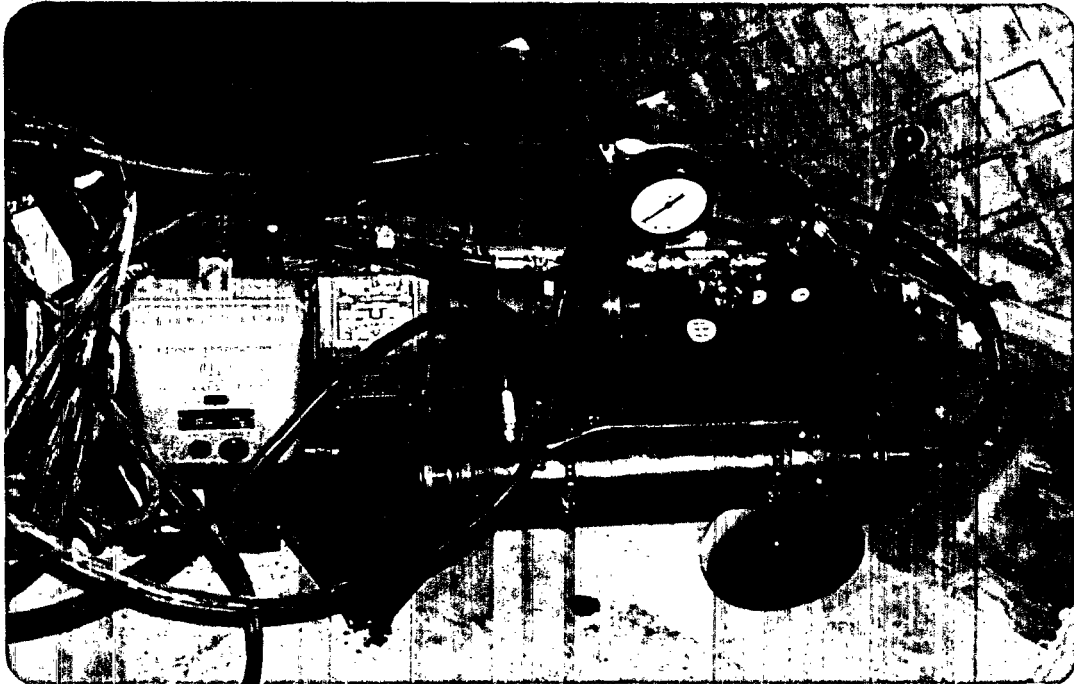


FIGURE 6.3 HYDRAULIC 20 KIP PRESTRESSING JACK.

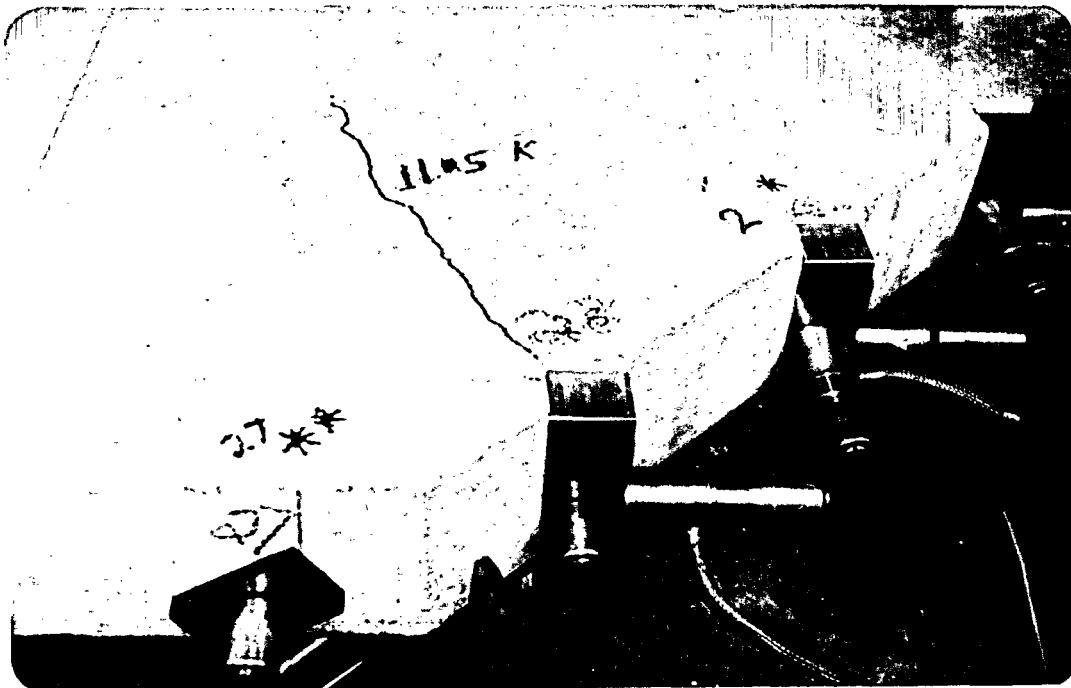


FIGURE 6.4 END BLOCKS AND LOAD CELLS FOR PRESTRESSED SKEW SLAB.

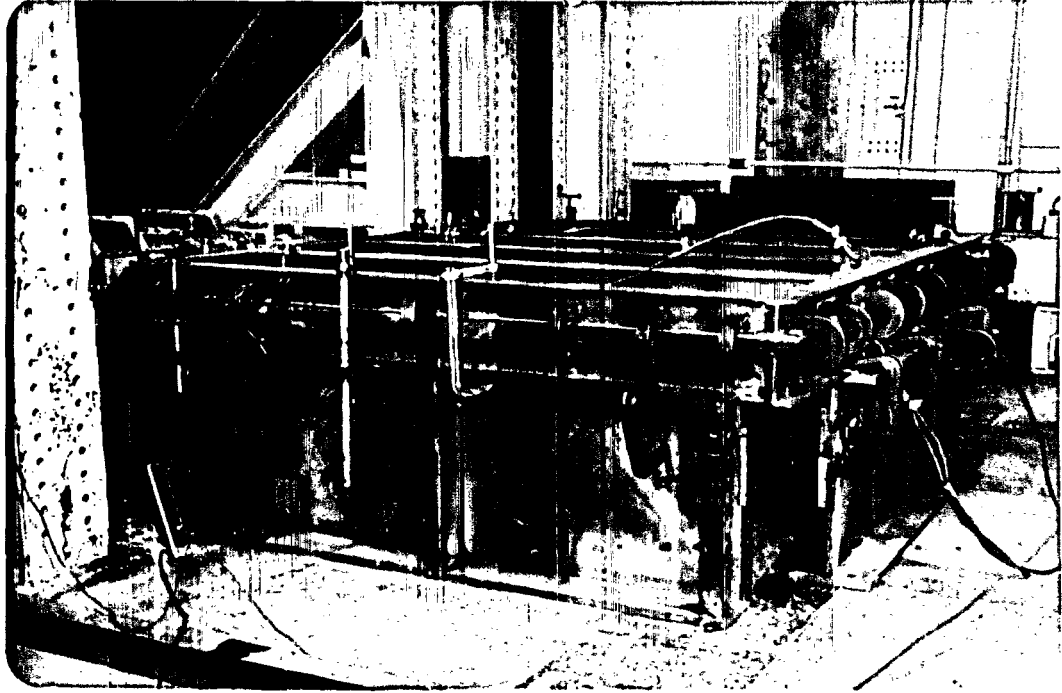


FIGURE 6.5 LOADING SYSTEM FOR UNIFORM LOAD.

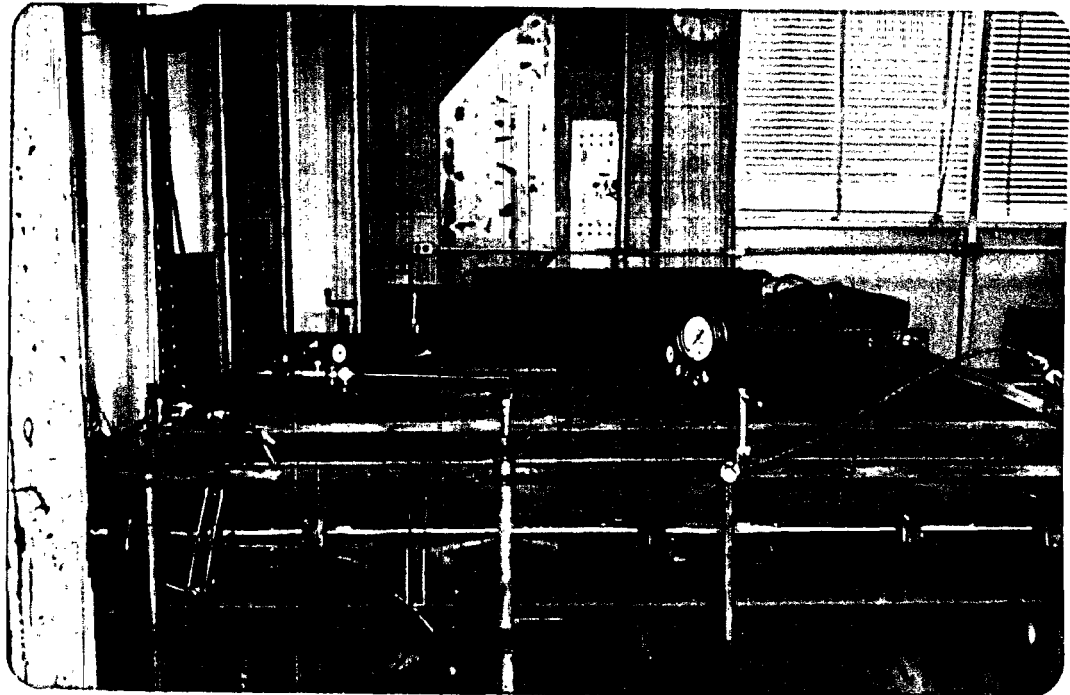


FIGURE 6.6 REGULATOR SYSTEM AND PRESSURE GAUGES.

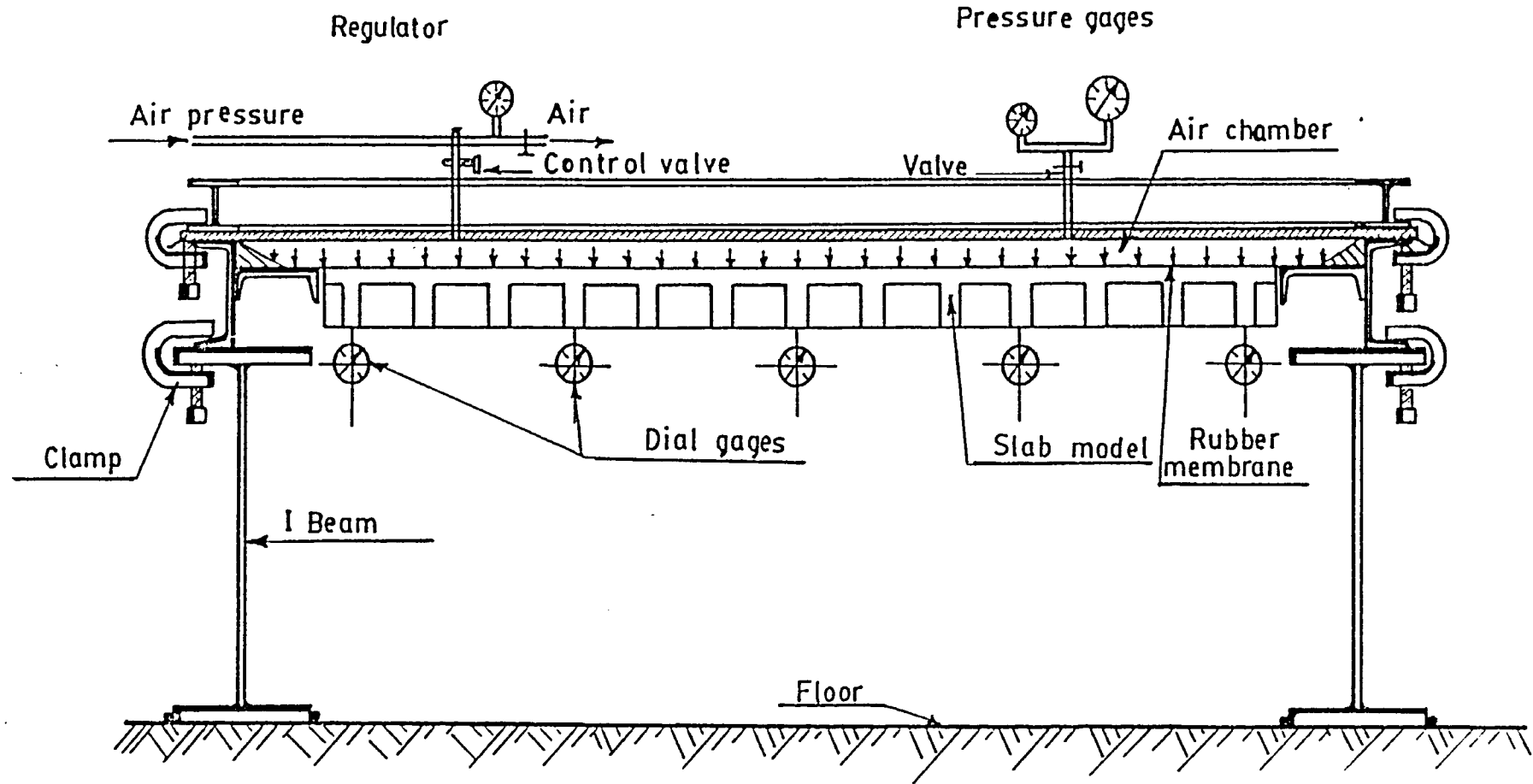


FIGURE 6.7 TRANSVERSE SECTION FOR THE LOADING FRAME.

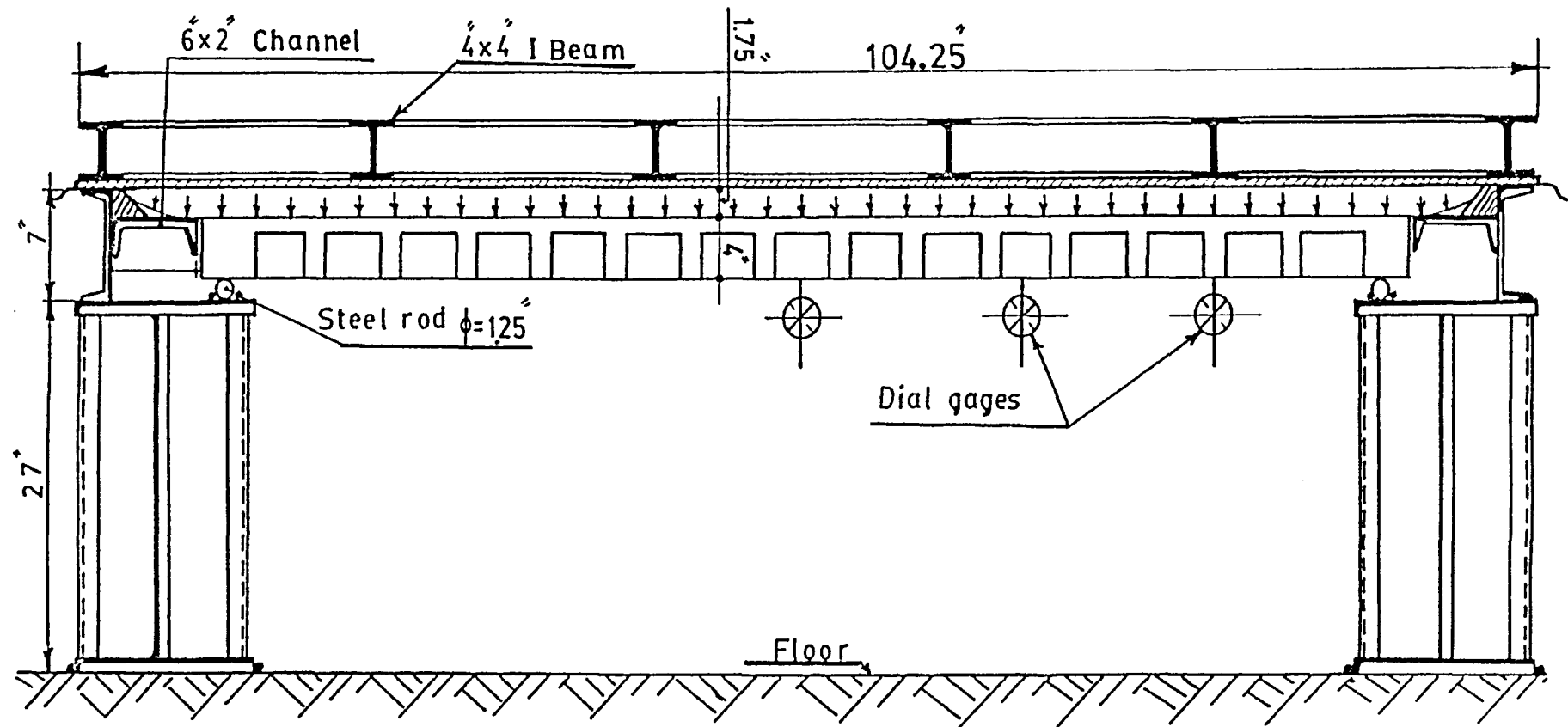


FIGURE 6.8 LONGITUDINAL SECTION FOR THE LOADING FRAME.  
(1 in. = 25.4 mm)

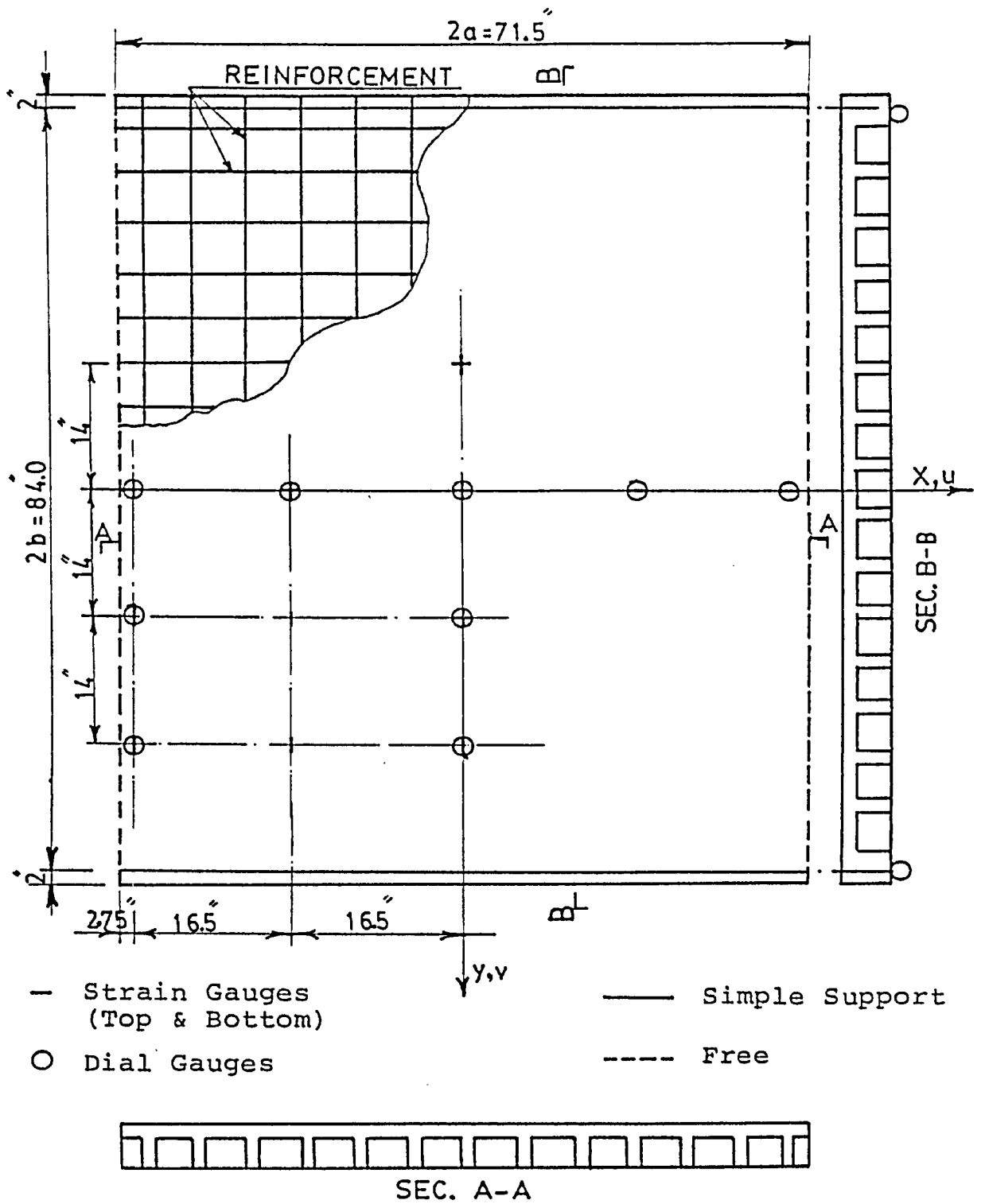


FIGURE 6.9 REINFORCED CONCRETE WAFFLE SLAB A.1

(1 in. = 25.4 mm)

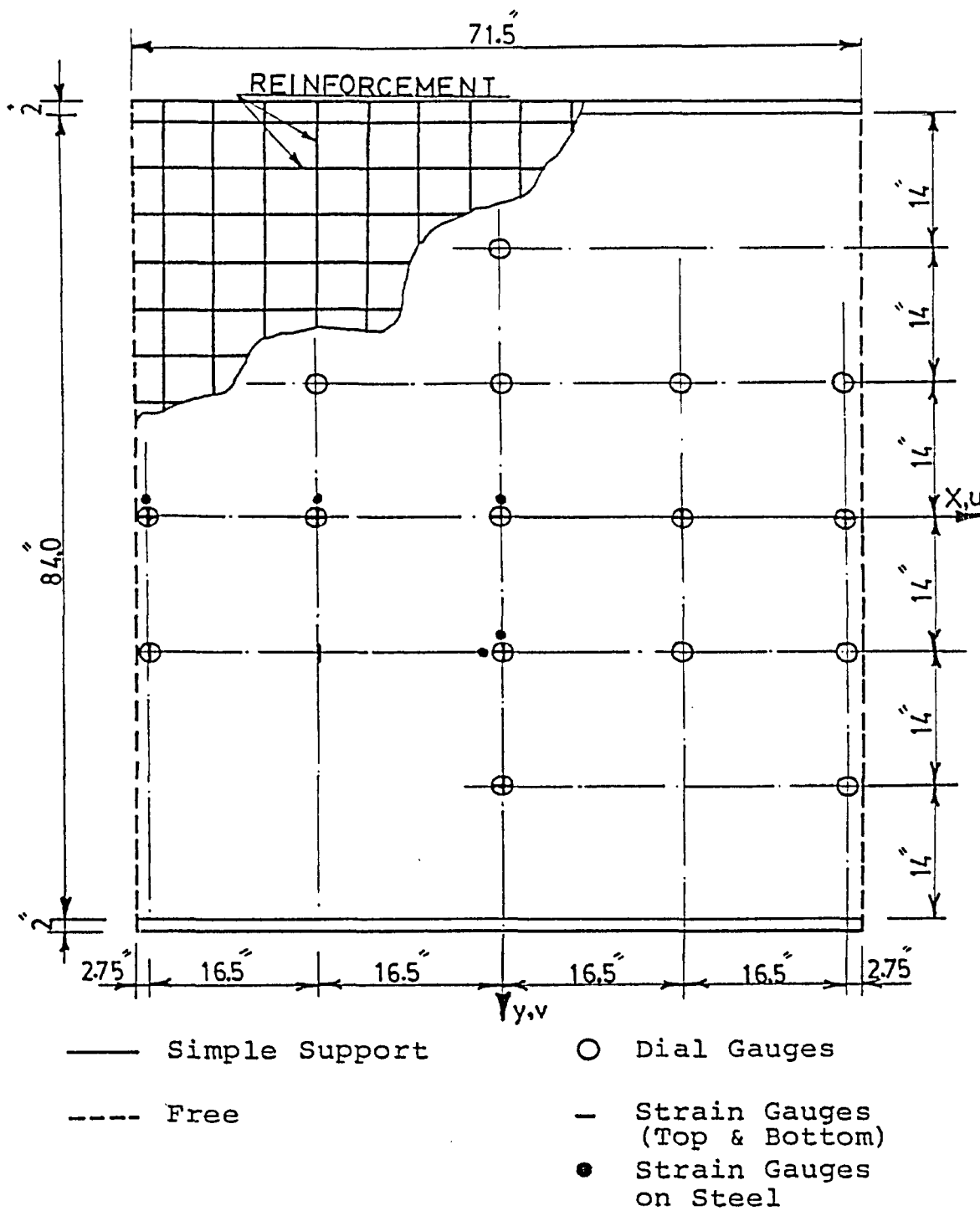


FIGURE 6.10 REINFORCED CONCRETE WAFFLE SLAB A.2.

(1 in. = 25.4 mm)



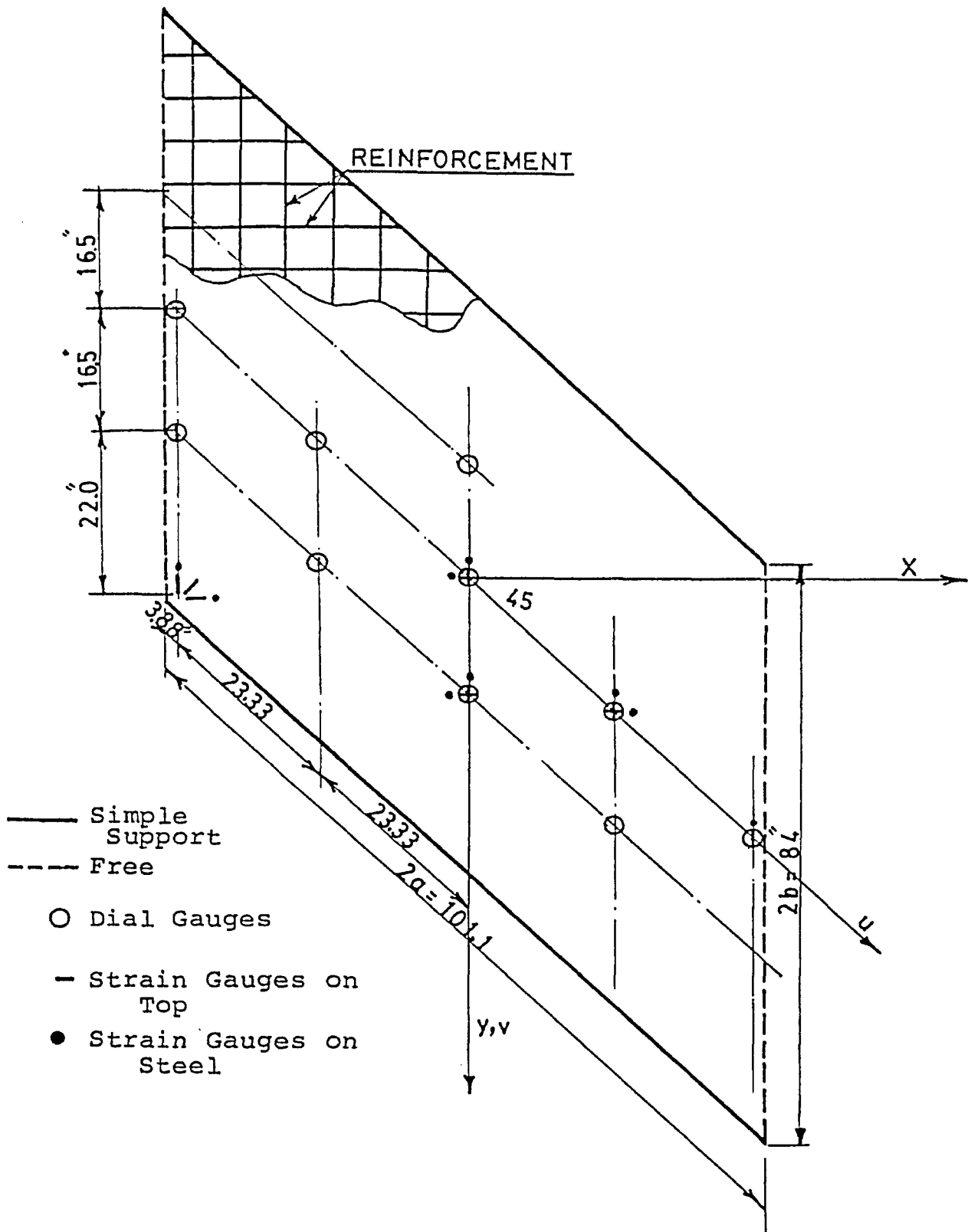
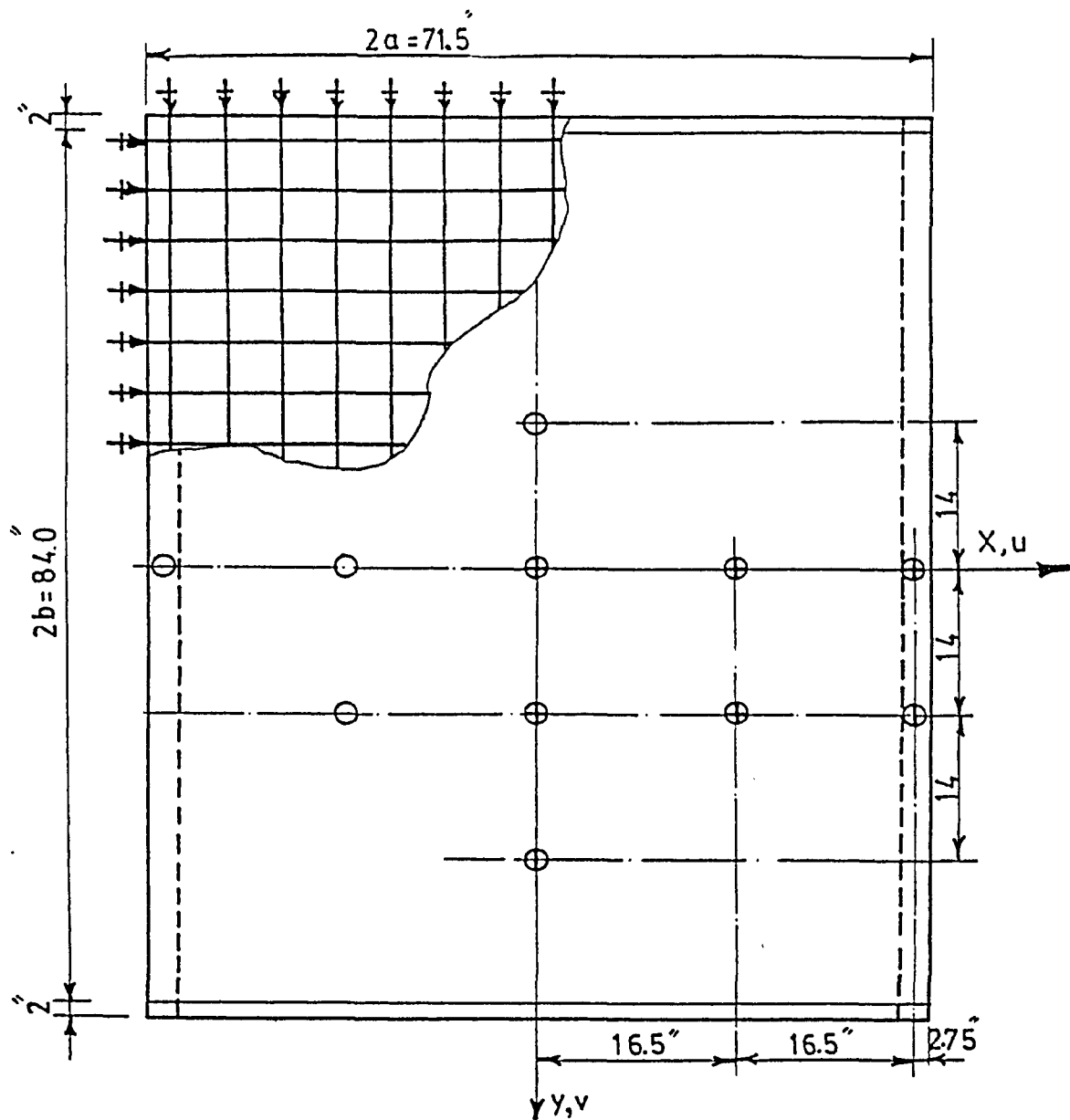


FIGURE 6.11 REINFORCED CONCRETE SKEW WAFFLE SLAB A.3,  
SKEW OF 45°.

(1 in. = 25.4 mm)



- Simple Support
- ||| Elastic Support (Edge Beam)
- Dial Gauges
- Strain Gauges on Top

FIGURE 6.12 PRESTRESSED CONCRETE WAFFLE SLAB B.1.

(1 in. = 25.4 mm)

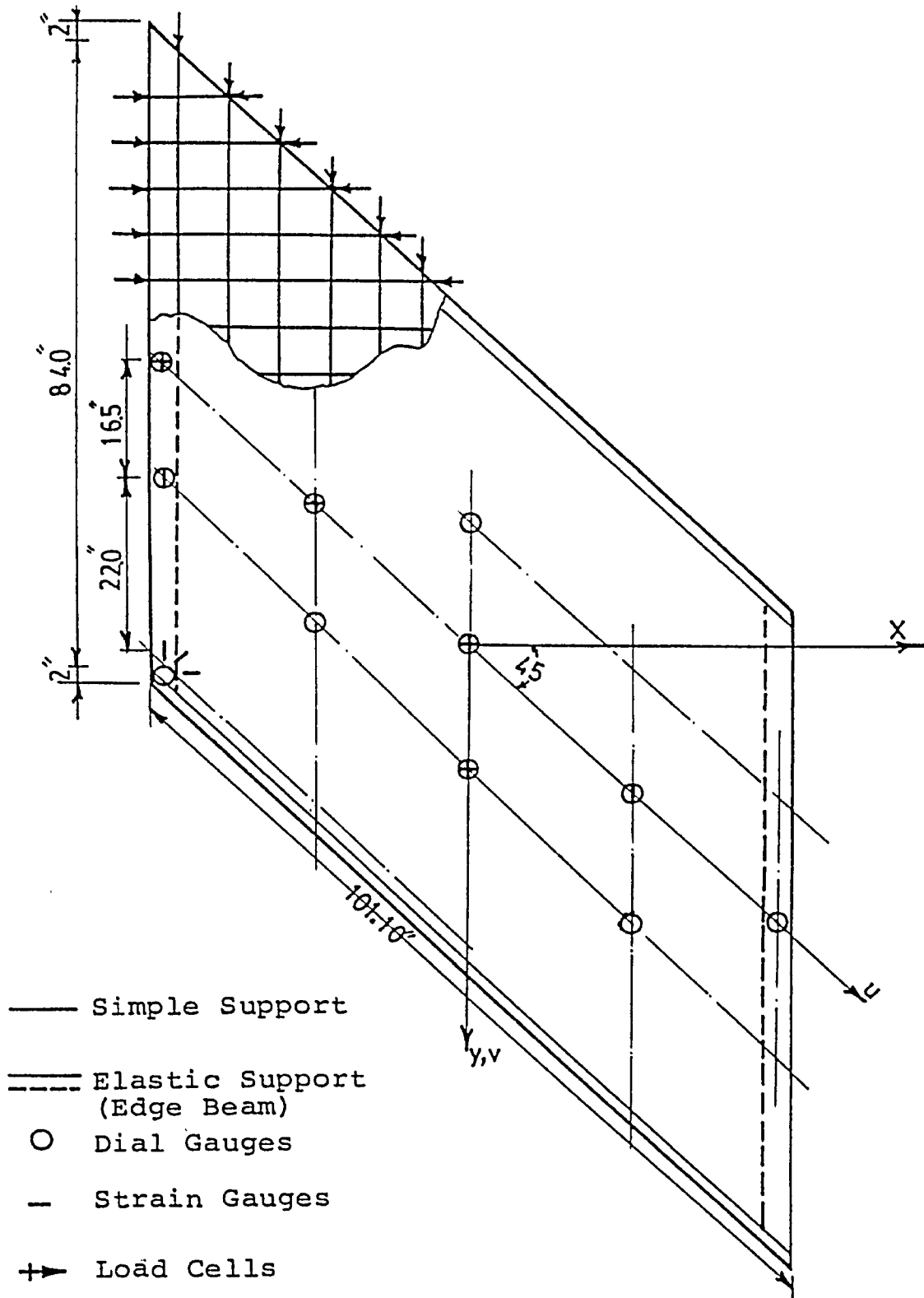


FIGURE 6.13 PRESTRESSED CONCRETE WAFFLE SLAB B.2.

(1 in. = 25.4 mm)

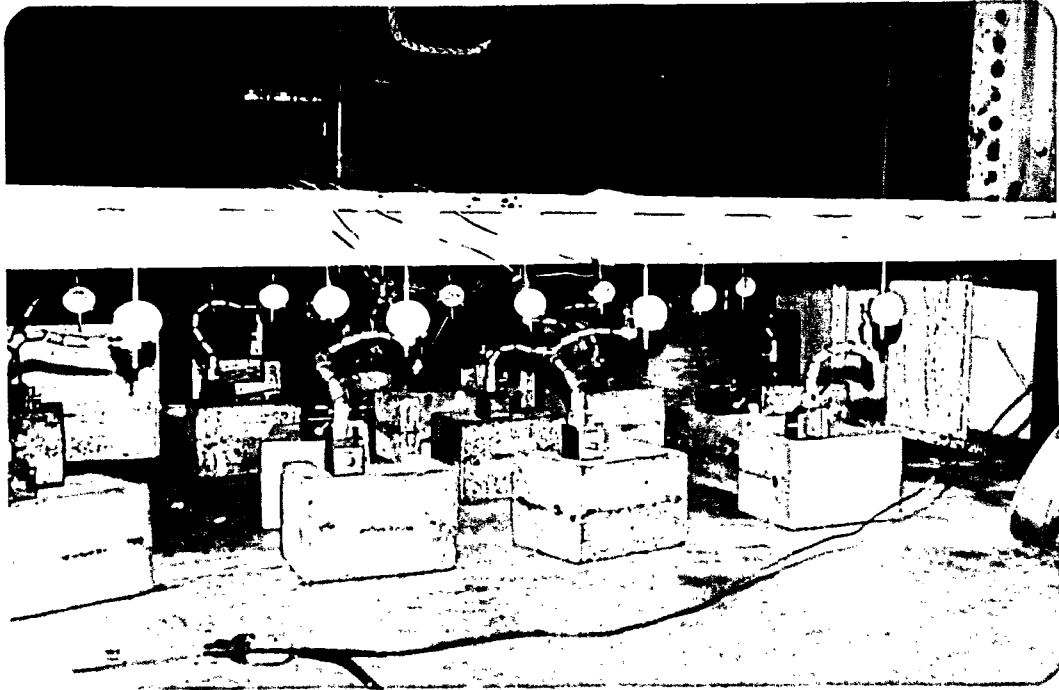


FIGURE 6.14 DIAL GAUGES IN POSITION.

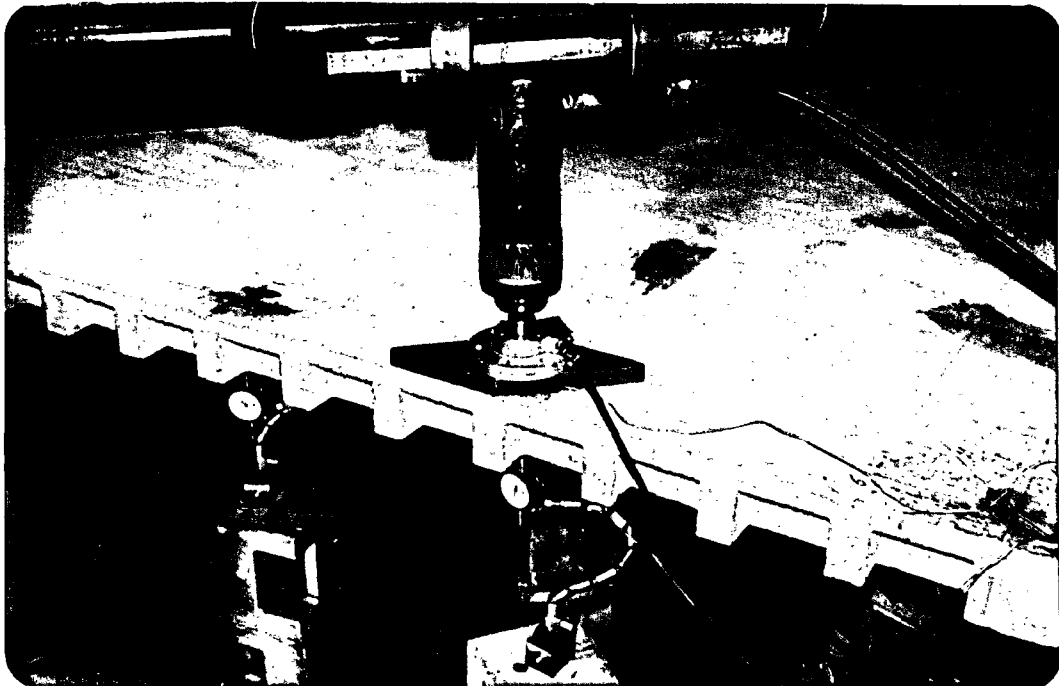


FIGURE 6.15 POINT LOADING SYSTEM.

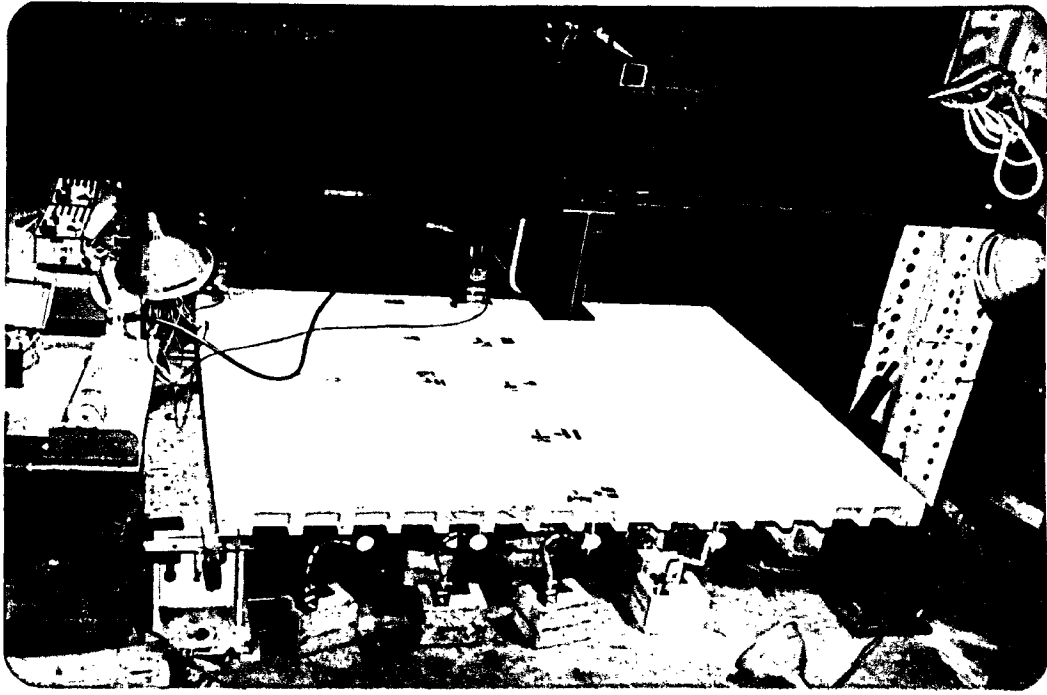


FIGURE 6.16 LOADING SYSTEM FOR SLAB A.2.

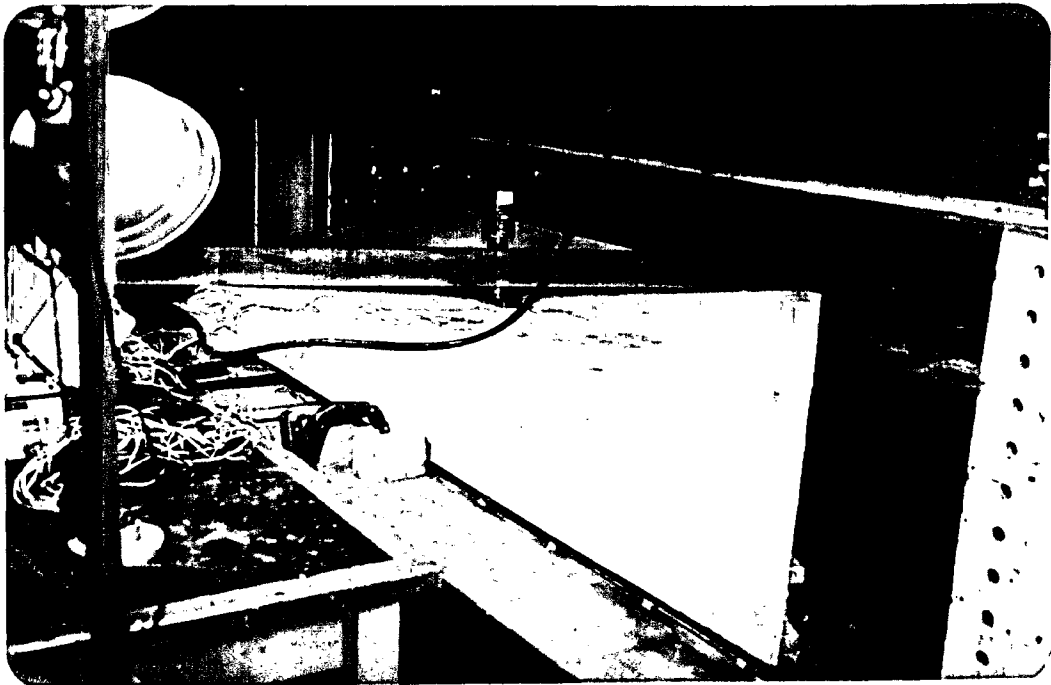


FIGURE 6.17 LOADING SYSTEM FOR THE SKEW SLAB A.3.

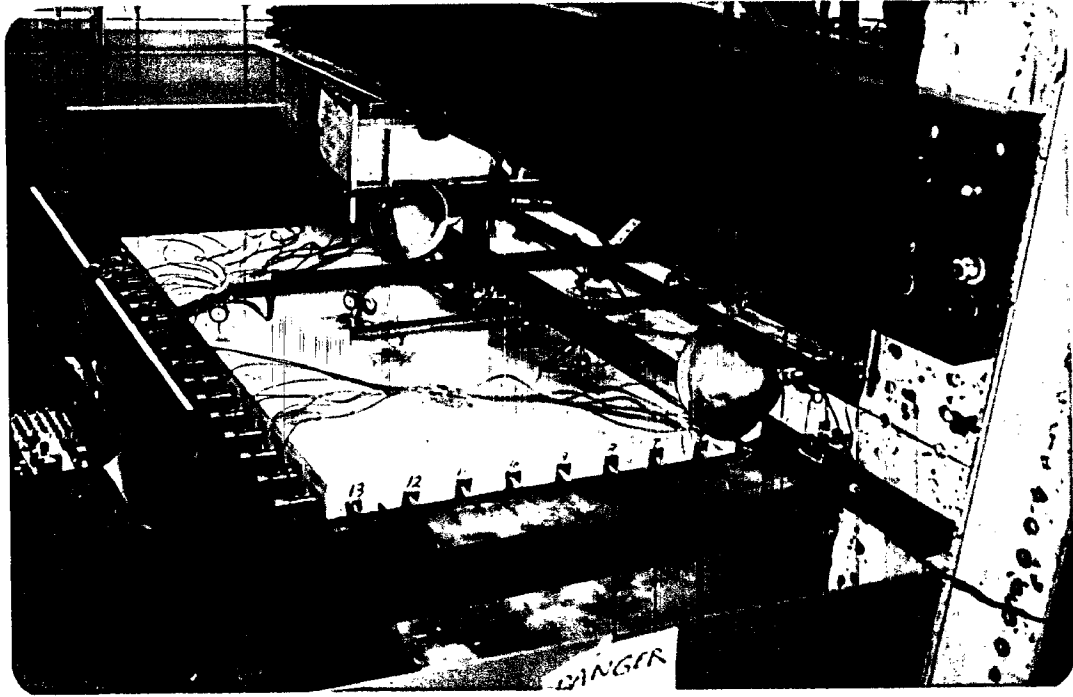


FIGURE 6.18 LOADING SYSTEM FOR PRESTRESSED SLAB B.1.

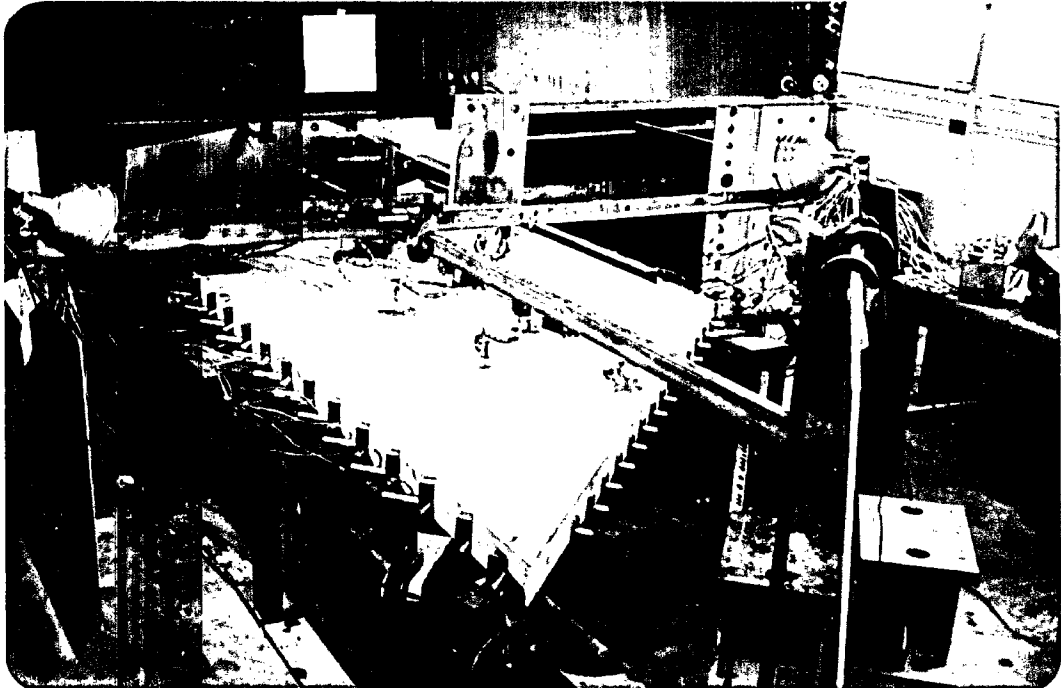


FIGURE 6.19 LOADING SYSTEM FOR PRESTRESSED SKEW SLAB B.2.

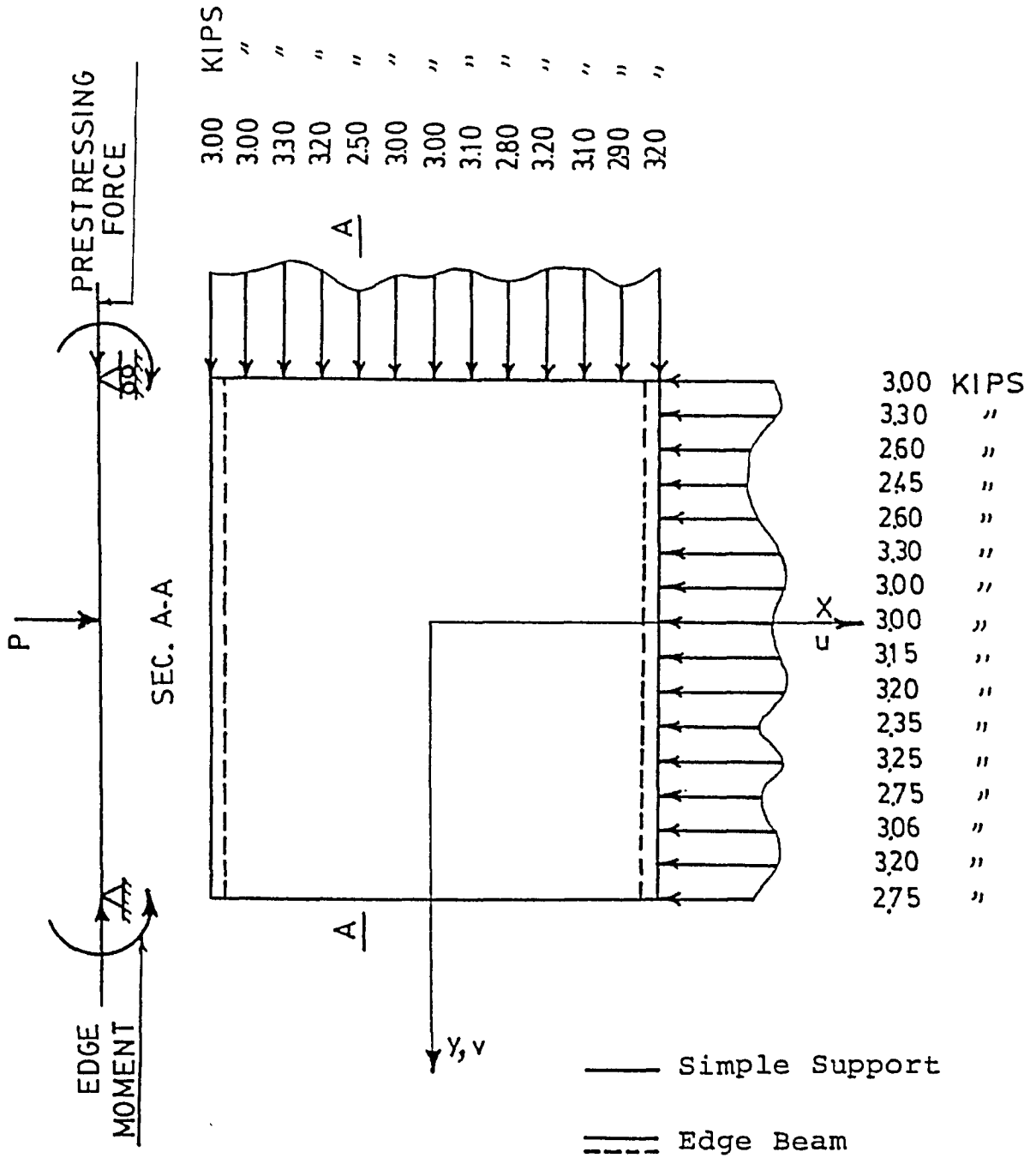


FIGURE 6.20 PRESTRESSING FORCE AND EDGE MOMENTS FOR SLAB B.1.

(1 KIP = 4.45 KN)

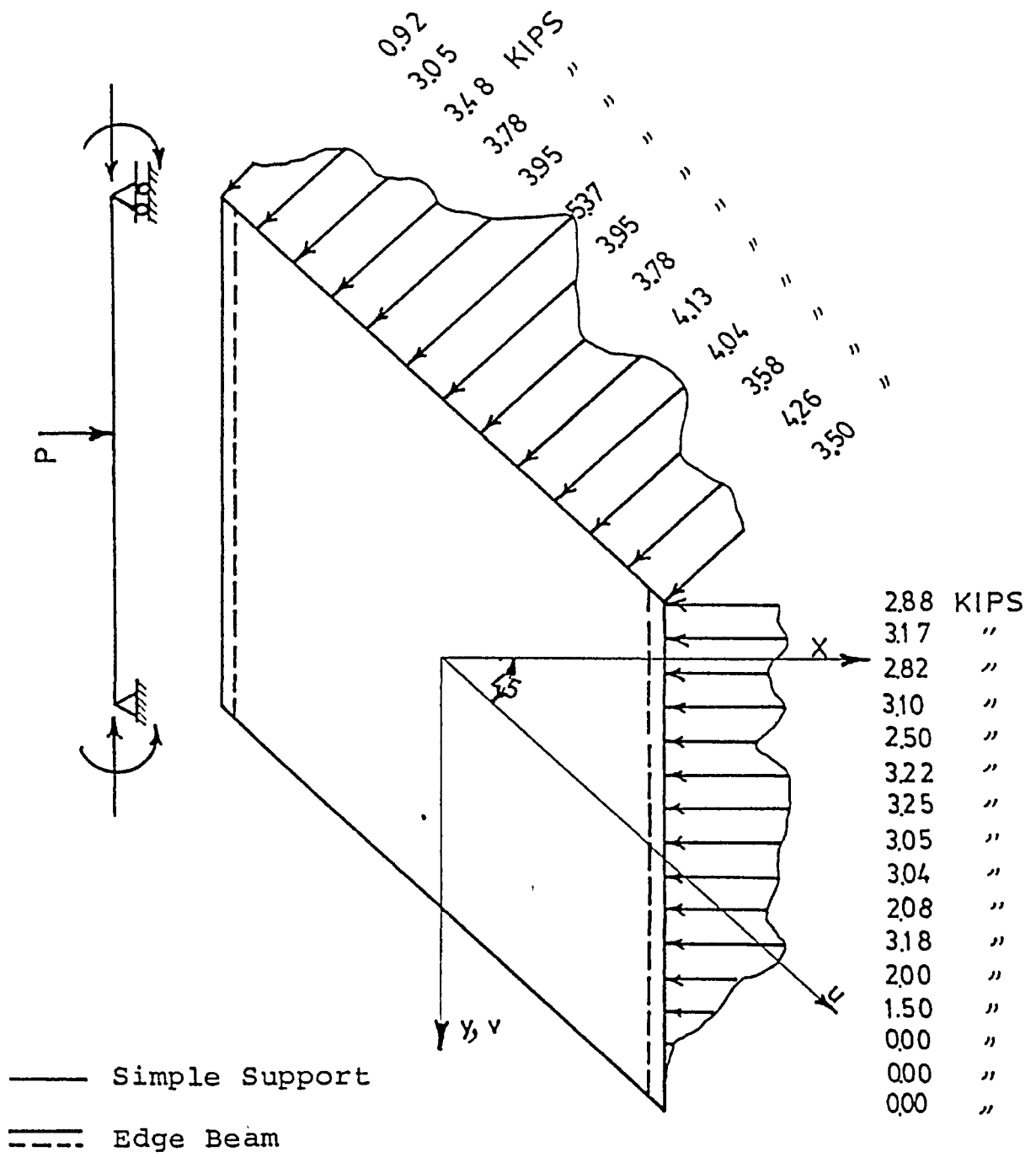


FIGURE 6.21 PRESTRESSING FORCE AND EDGE MOMENTS FOR SKEW SLAB B.2.

(1 KIP = 4.45 KN)



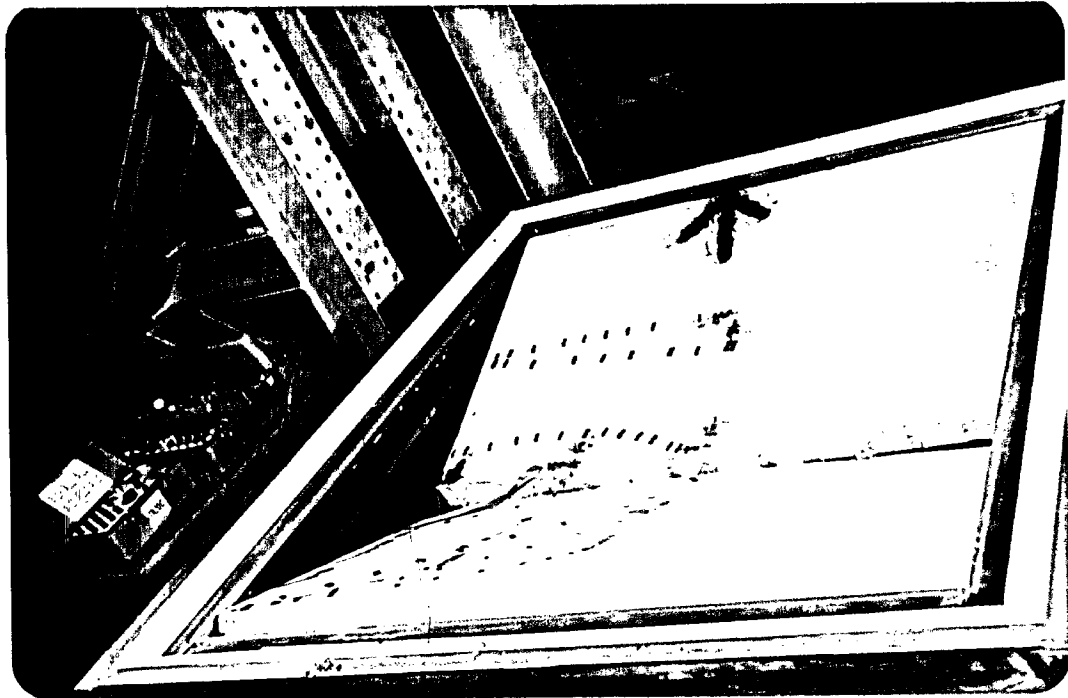


FIGURE 7.1 SLAB A.1 FAILURE.



FIGURE 7.2 SLAB A.1 CRACKS.

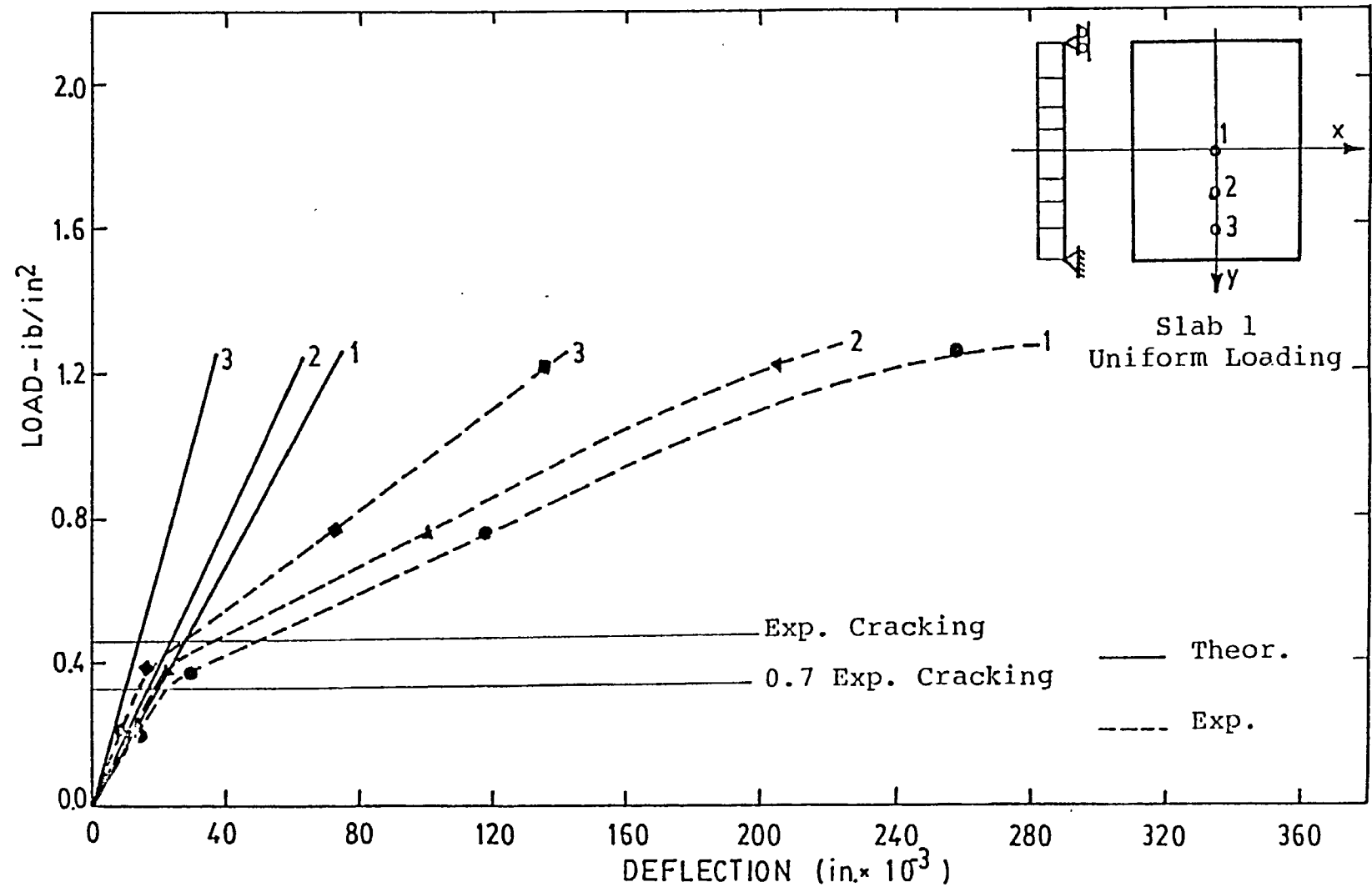


FIGURE 7.3 LOAD DEFLECTION RELATIONSHIP FOR SLAB A.1.

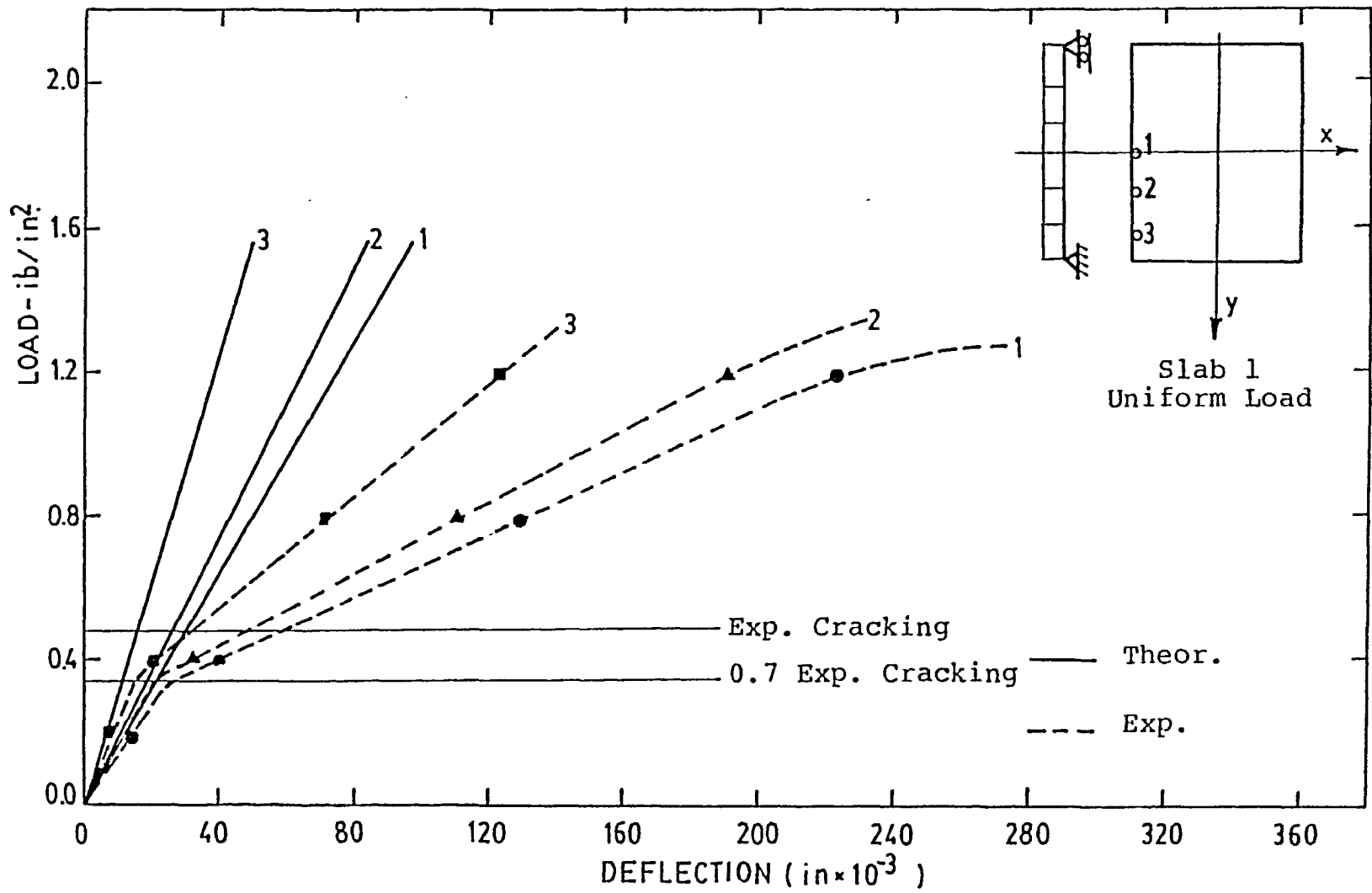


FIGURE 7.4 LOAD DEFLECTION RELATIONSHIP FOR SLAB A.1.

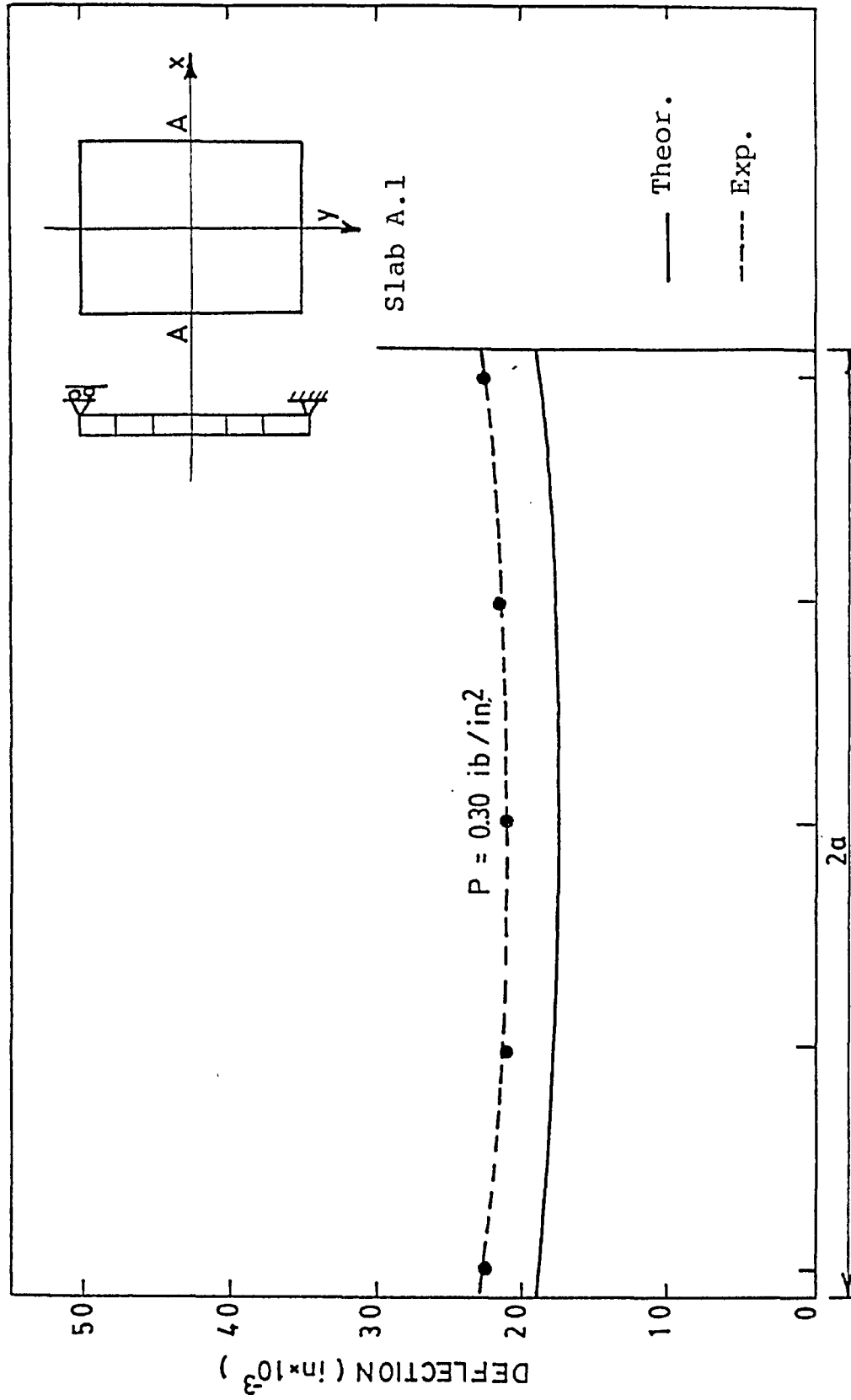


FIGURE 7.5 TRANSVERSE DEFLECTION.

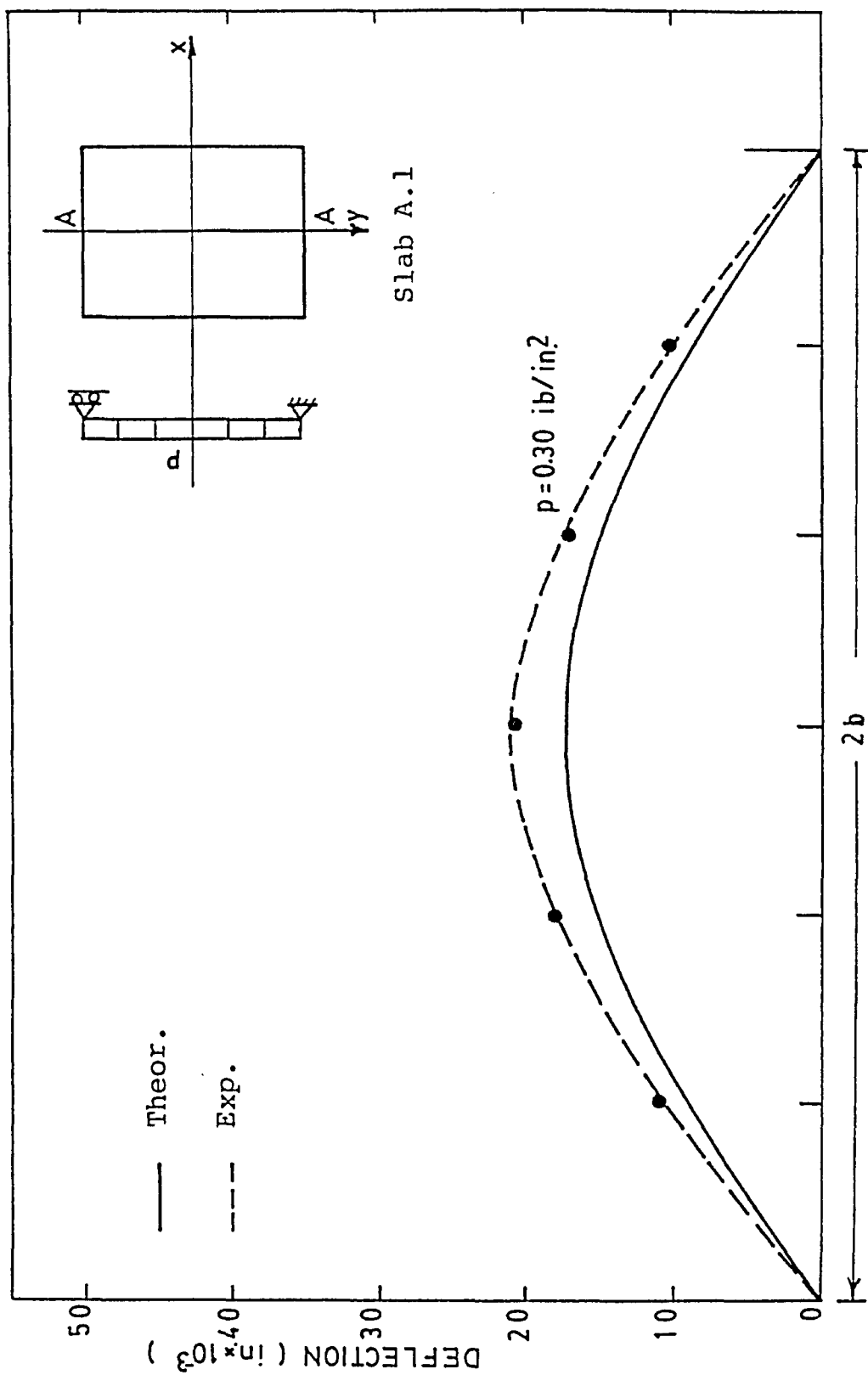


FIGURE 7.6 LONGITUDINAL DEFLECTION.

(1 in. = 25.4 mm)

(1 KIP = 4.45 KN)

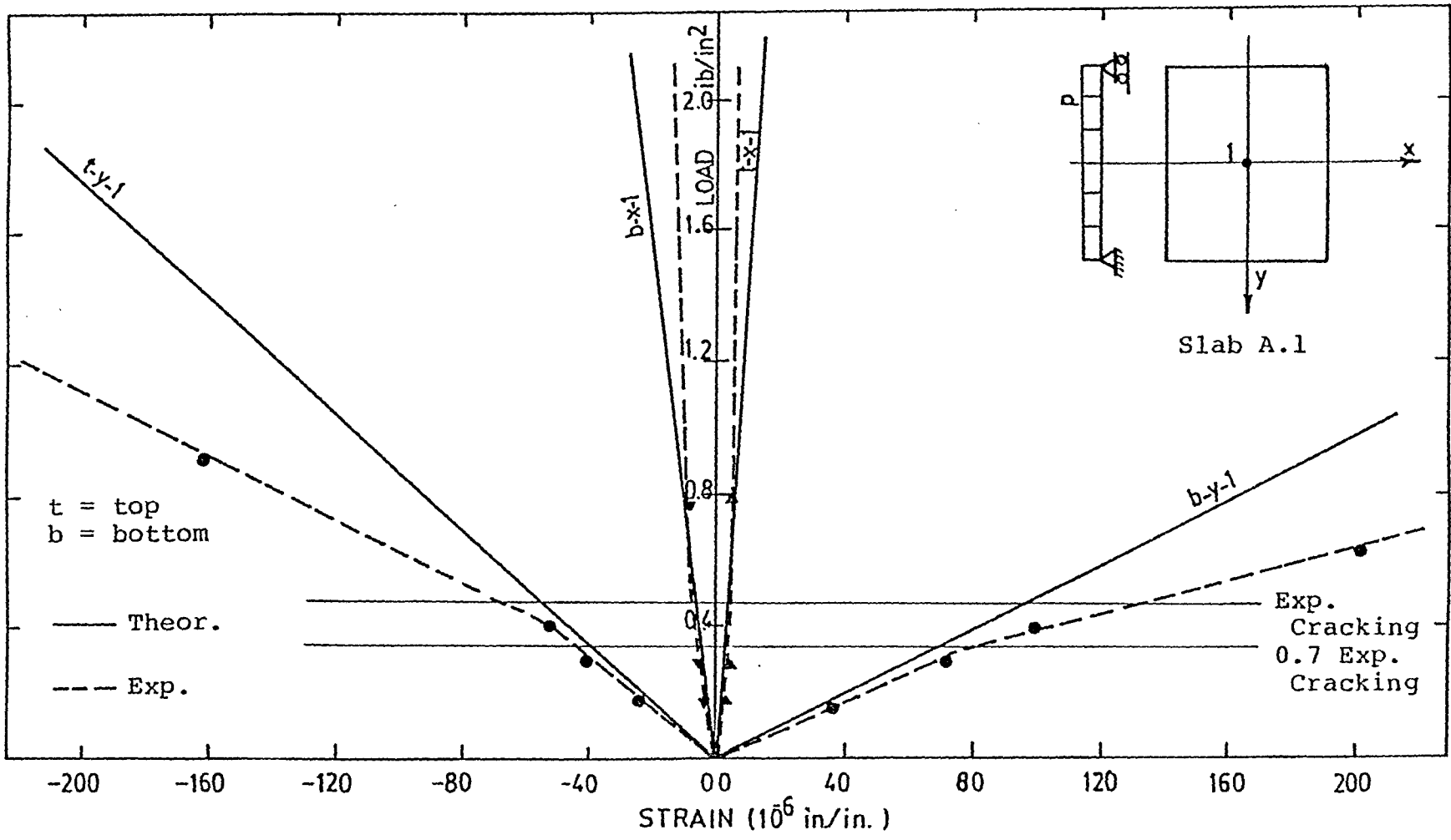


FIGURE 7.7 LOAD STRAIN RELATIONSHIP FOR SLAB A.1 AT CENTRE.

(1 KIP = 4.45 KN)

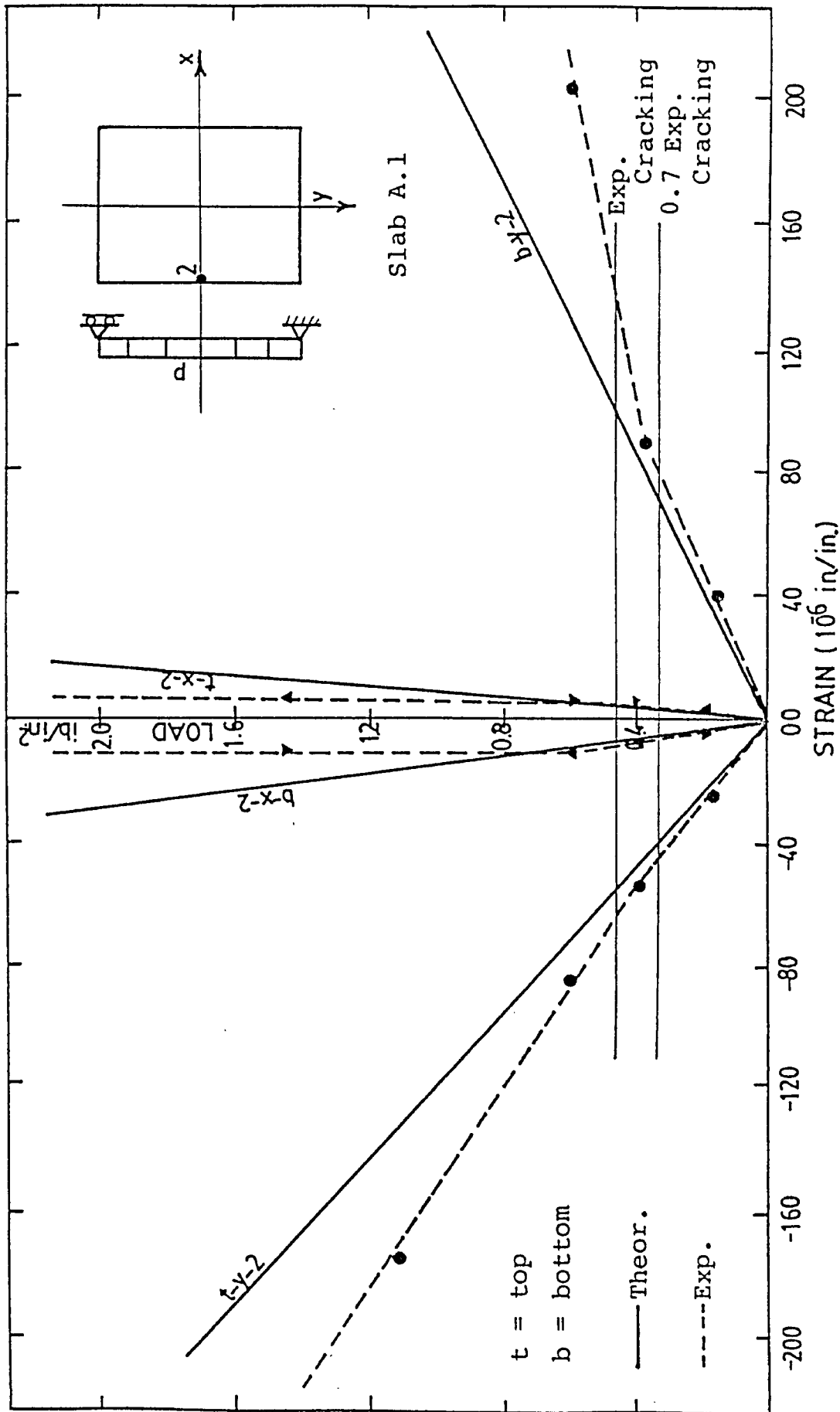


FIGURE 7.8 LOAD STRAIN RELATIONSHIP FOR SLAB A.1 AT THE FREE EDGE.

(1 KIP = 4.45 KN)

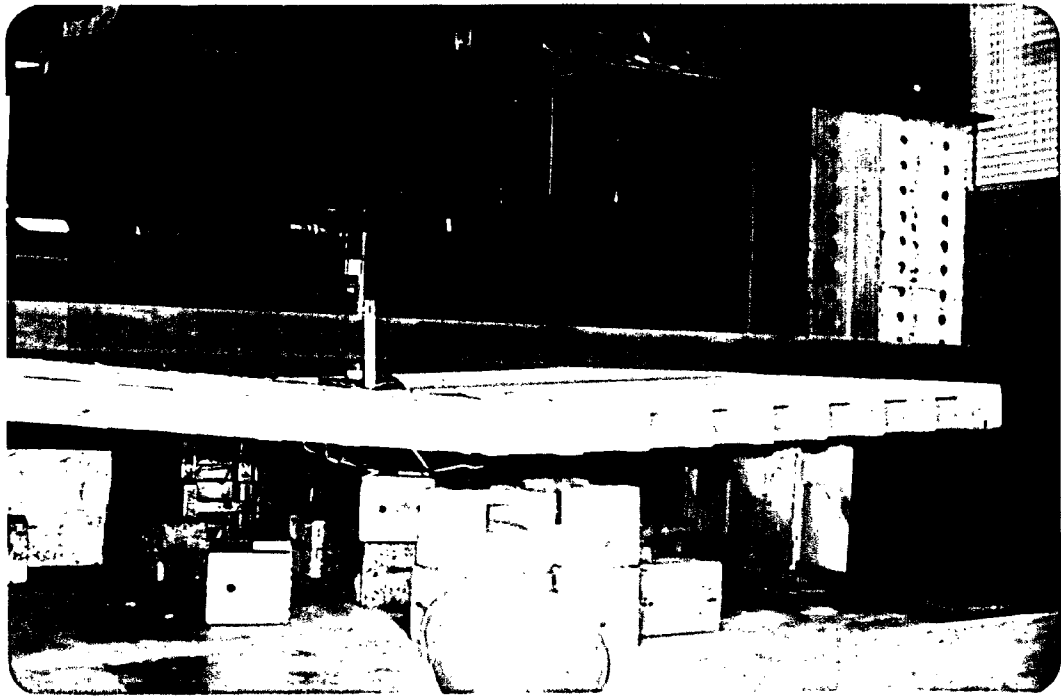


FIGURE 7.9 DEFLECTION SHAPE FOR SLAB A.2.

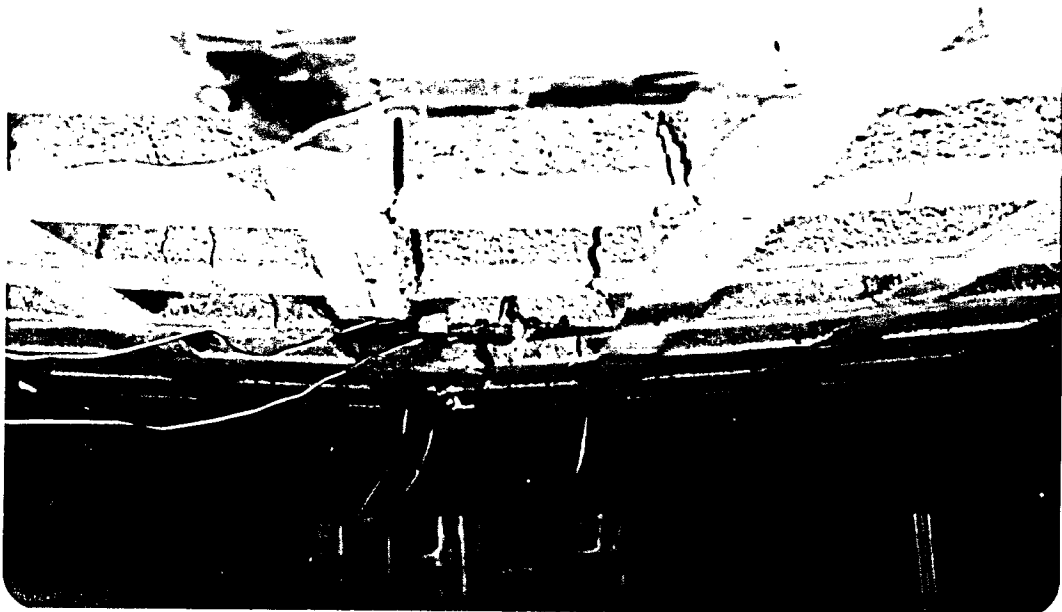


FIGURE 7.10 SLAB A.2 CRACKS.



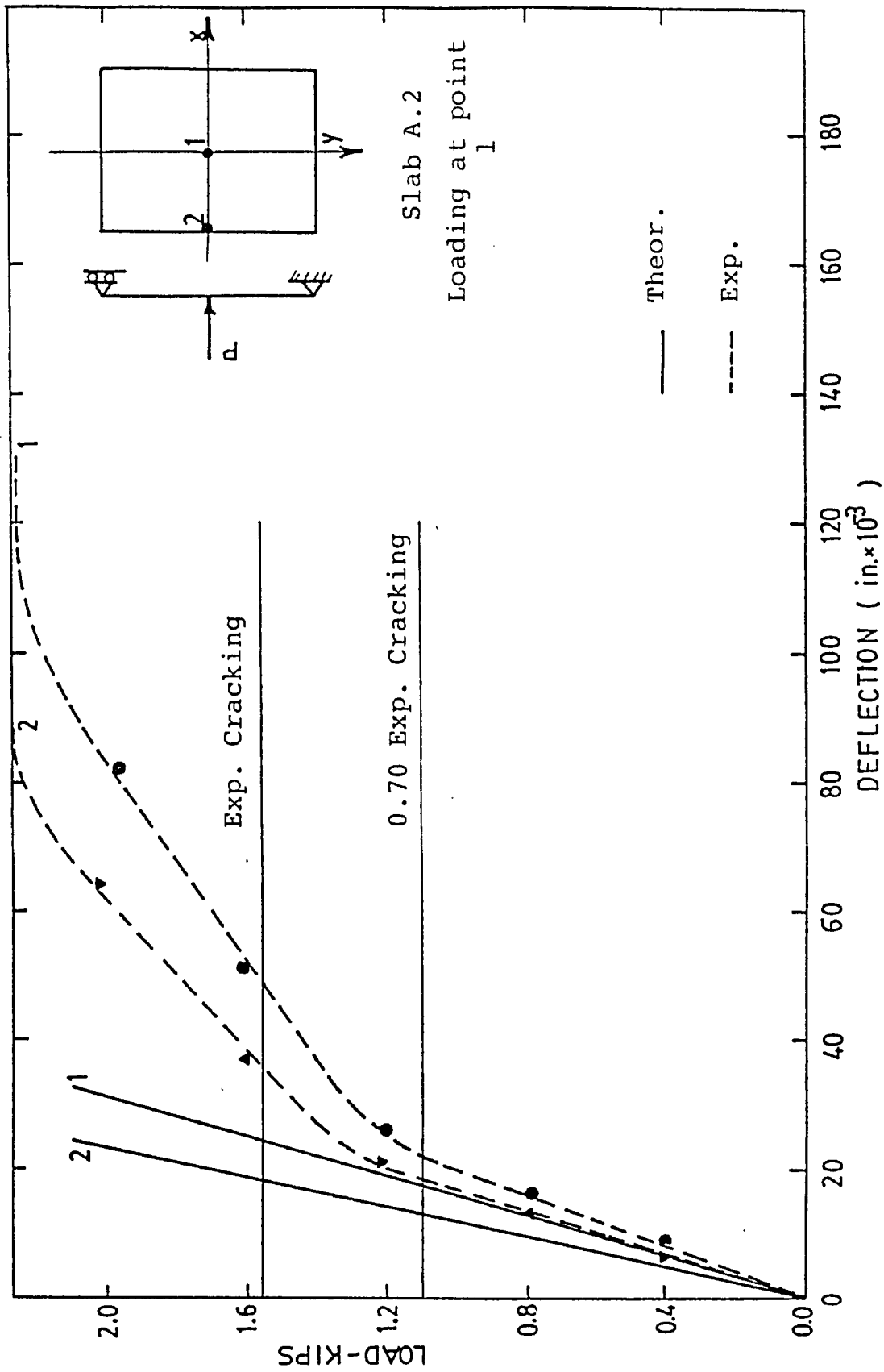


FIGURE 7.11 LOAD DEFLECTION RELATIONSHIP FOR SLAB A.2.

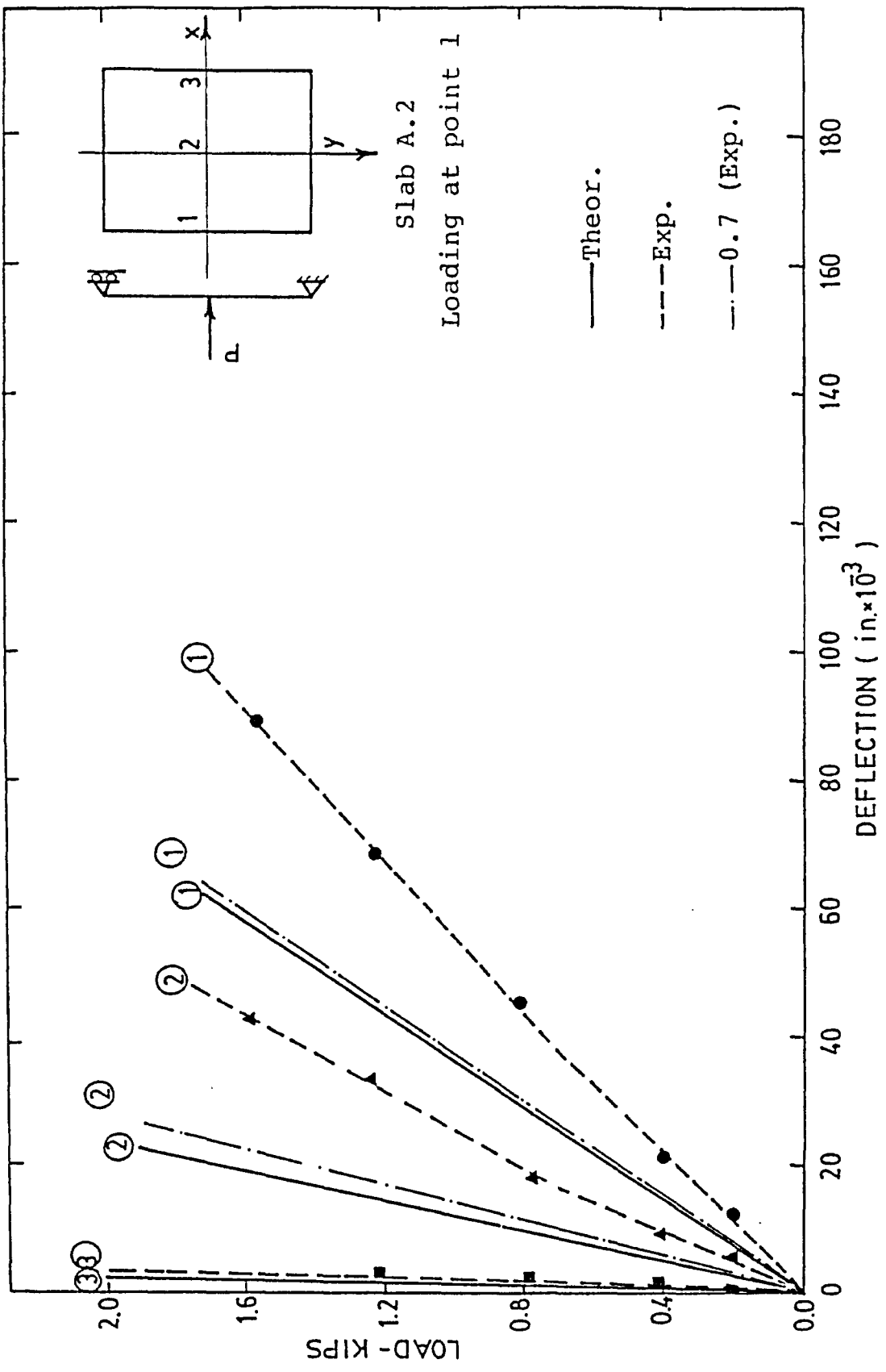


FIGURE 7.12 LOAD DEFLECTION RELATIONSHIP FOR SLAB A.2, LOAD AT THE EDGE.

(1 KIP = 4.45 KN)

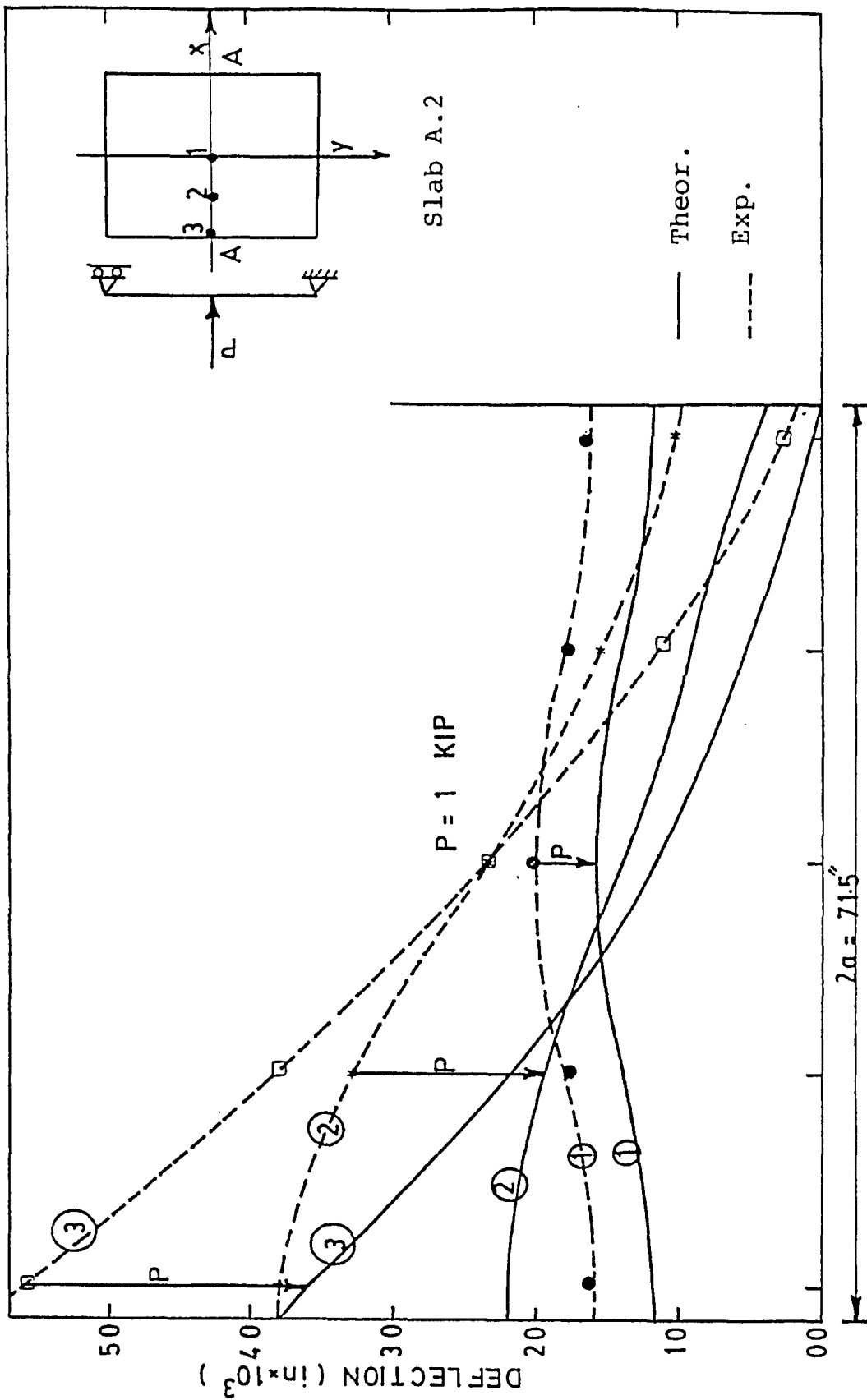


FIGURE 7.13 TRANSVERSE DEFLECTION FOR SLAB A.2 ( $p = 1$  KIP)

(1 in = 25.4 mm)

(1 KIP = 4.45 KN)

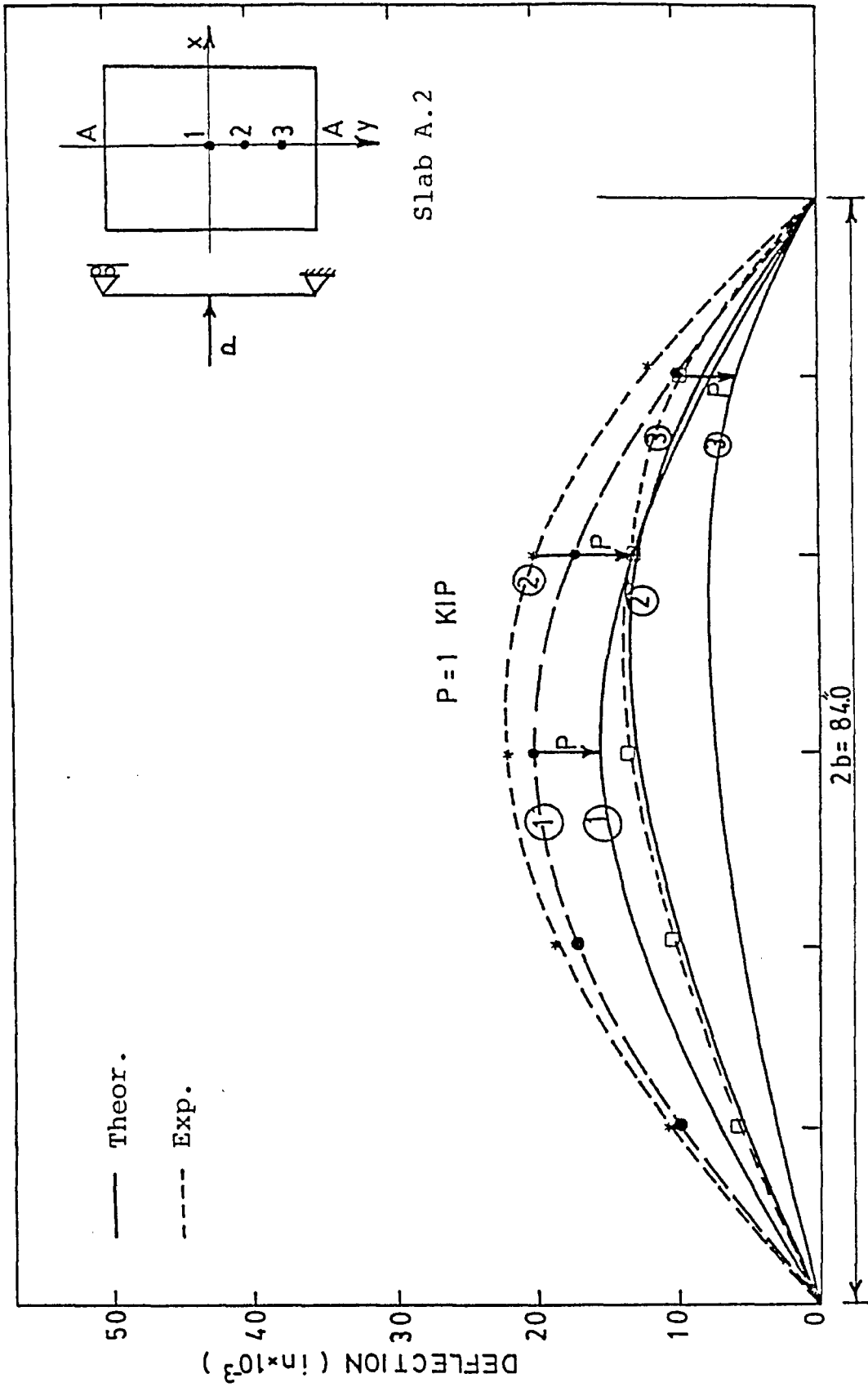


FIGURE 7.14 LONGITUDINAL DEFLECTION ALONG LINE A-A ( $P = 1 \text{ KIP}$ )

(1 in = 25.4 mm)

(1 KIP = 4.45 KN)

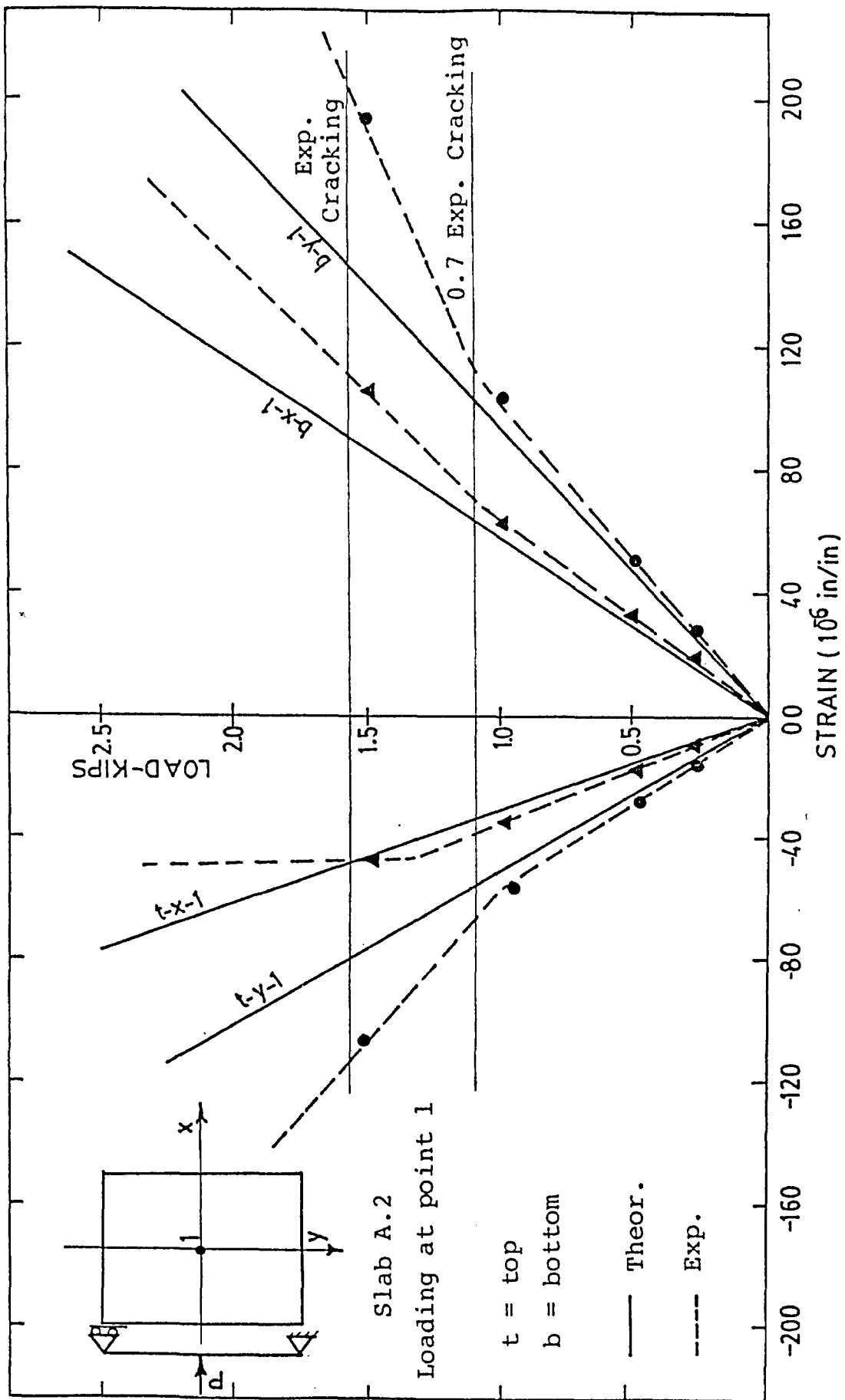


FIGURE 7.15 LOAD STRAIN RELATIONSHIP FOR SLAB A.2, LOAD AT CENTRE OF SLAB.

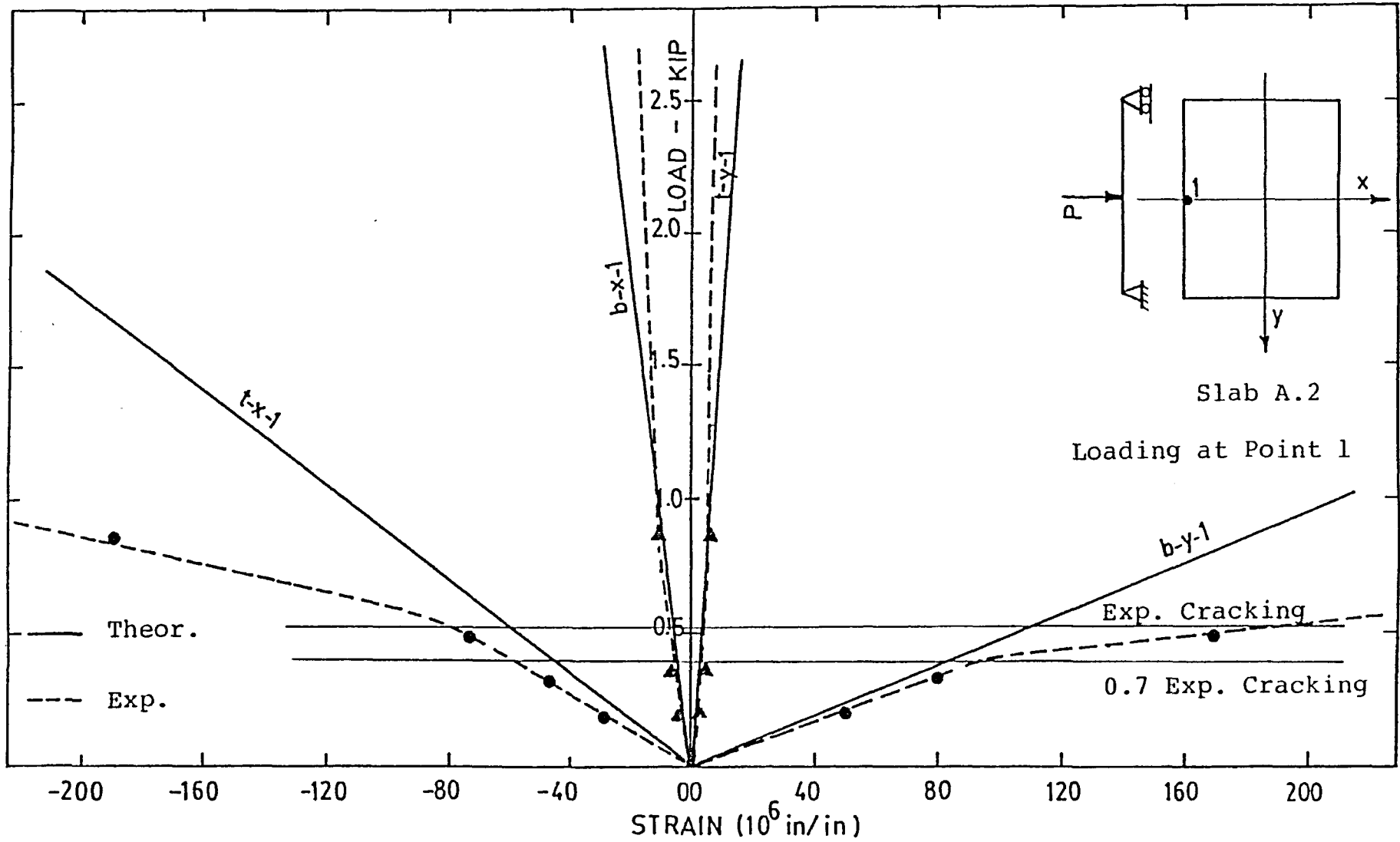


FIGURE 7.16 LOAD STRAIN RELATIONSHIP FOR SLAB A.2, LOAD AT THE FREE EDGE

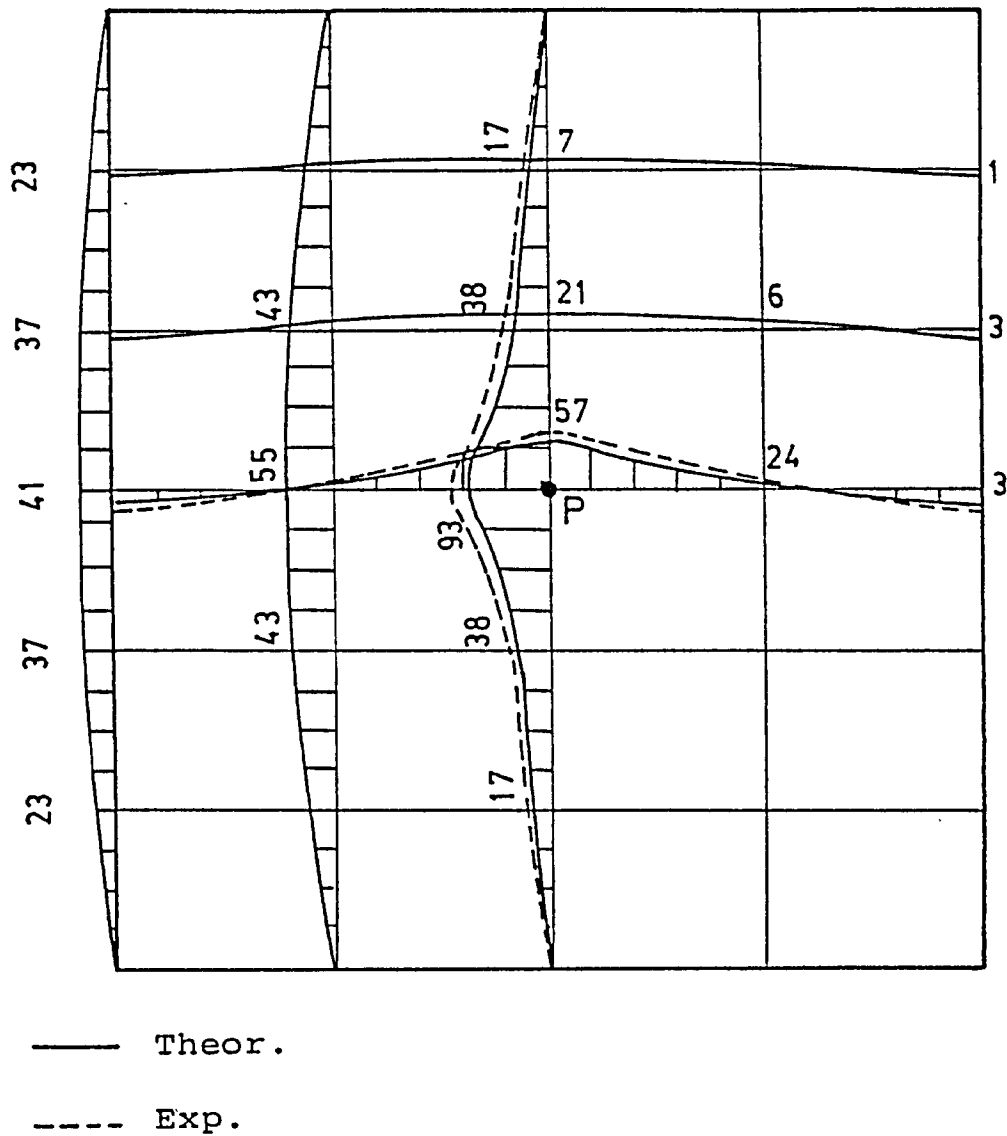


FIGURE 7.17 STRAIN DISTRIBUTION FOR SLAB A.2 AT BOTTOM FIBRE DUE TO 1 KIP AT CENTRE.

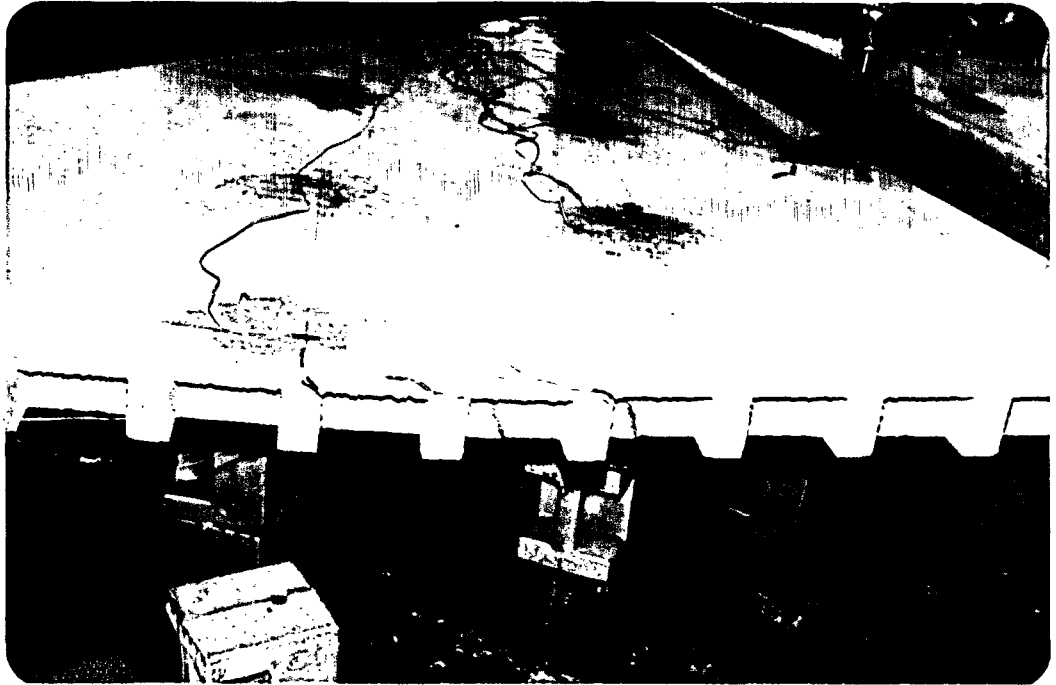


FIGURE 7.18 CRACK DEVELOPMENT IN SLAB A.3.

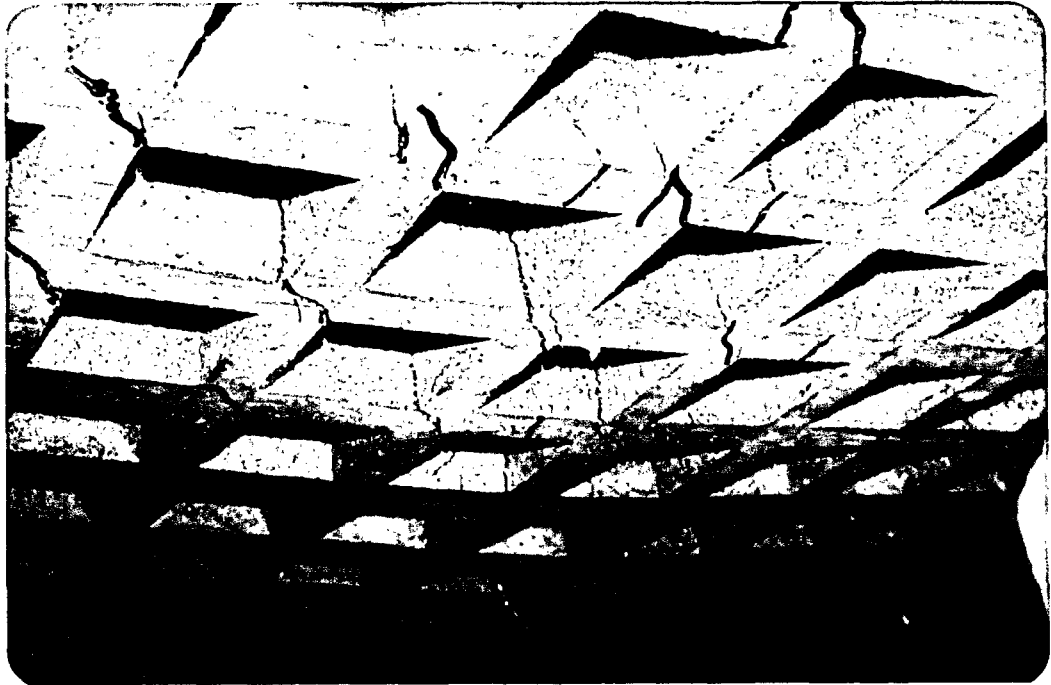


FIGURE 7.19 BOTTOM CRACKS FOR SLAB A.3.



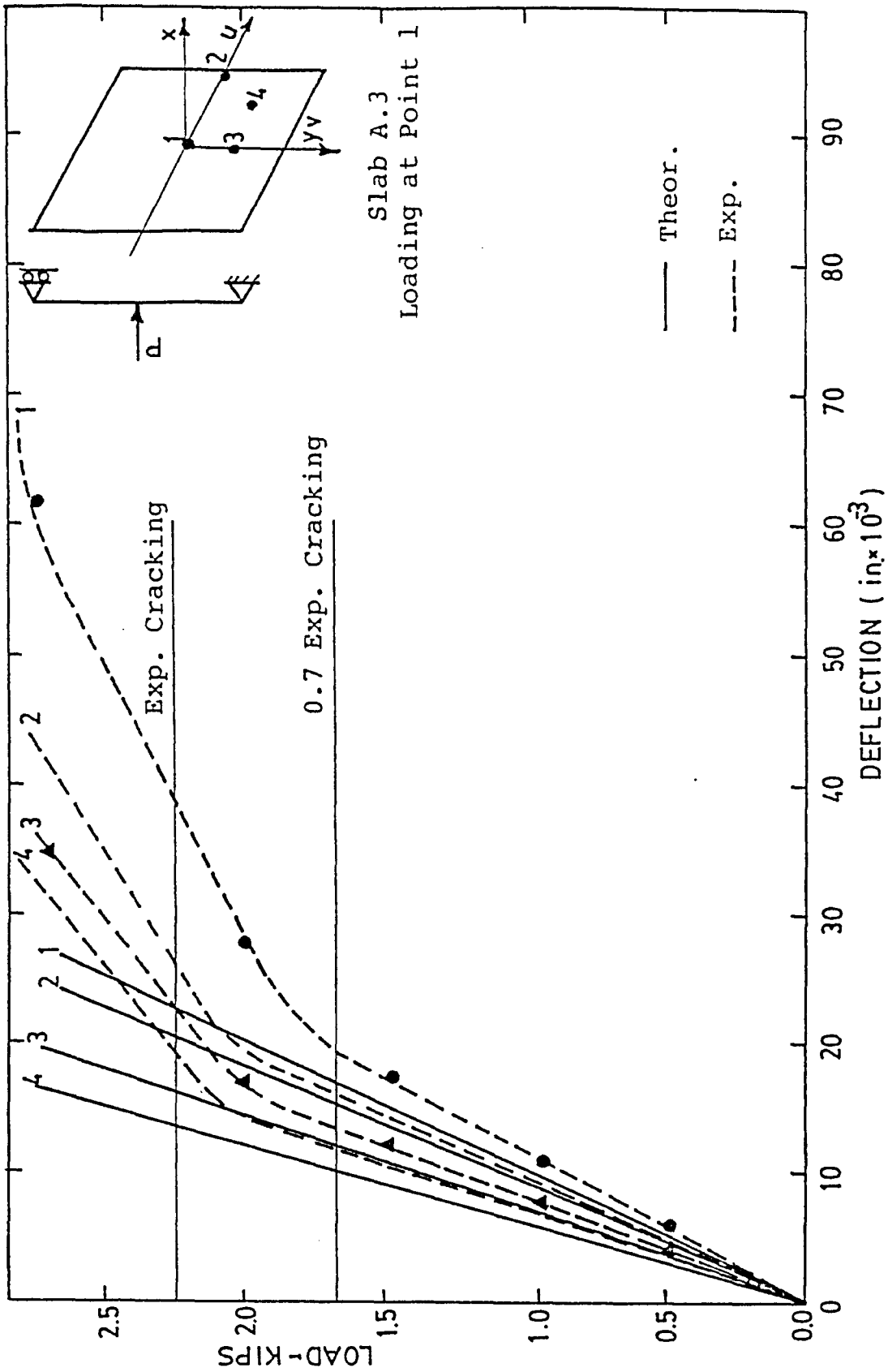


FIGURE 7.20 LOAD DEFLECTION RELATIONSHIP FOR SKEW SLAB A.3.

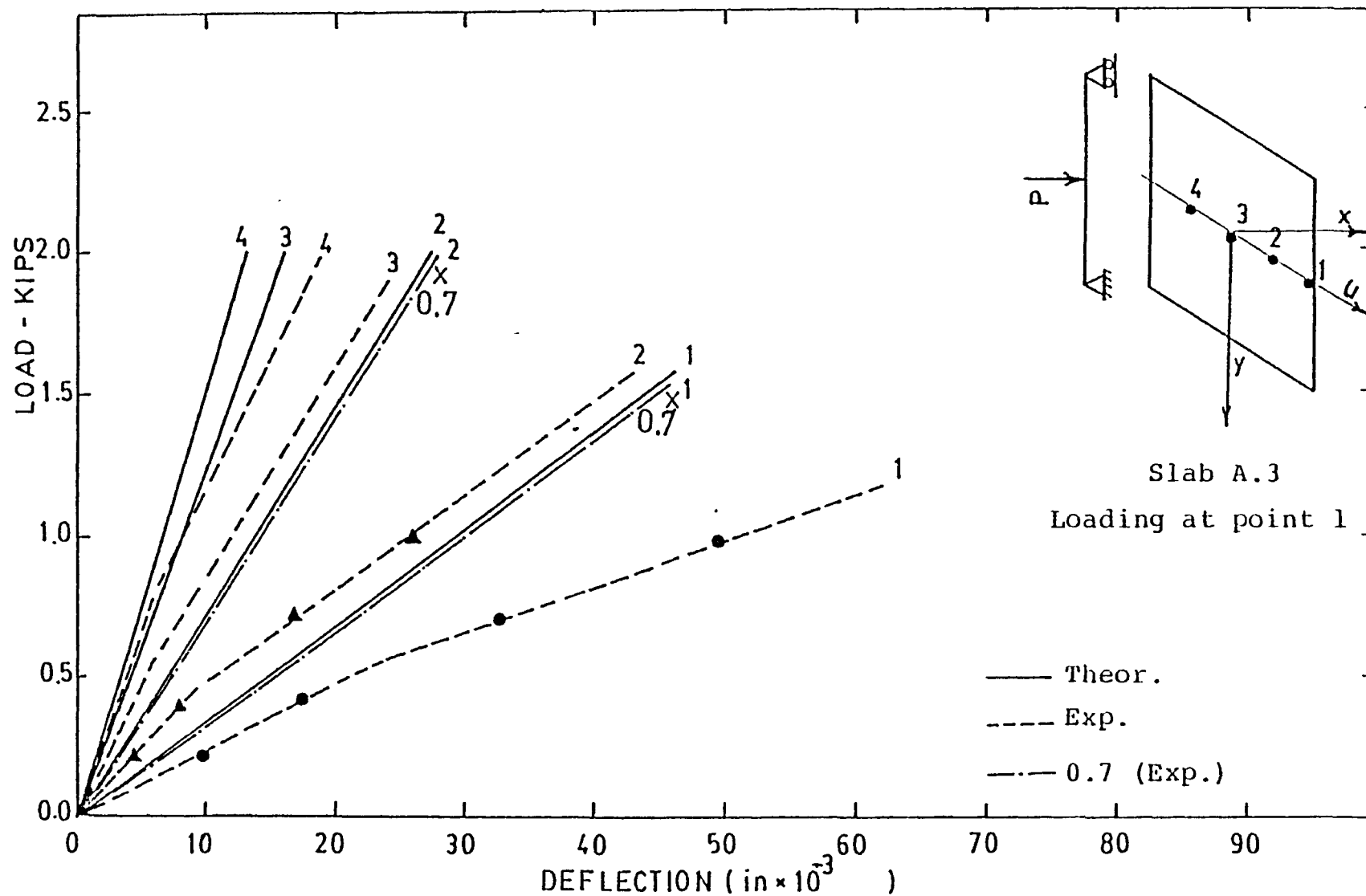


FIGURE 7.21 LOAD DEFLECTION RELATIONSHIP FOR SKEW SLAB A.3.

(1 in = 25.4 mm)

(1 KIP = 4.45 KN)

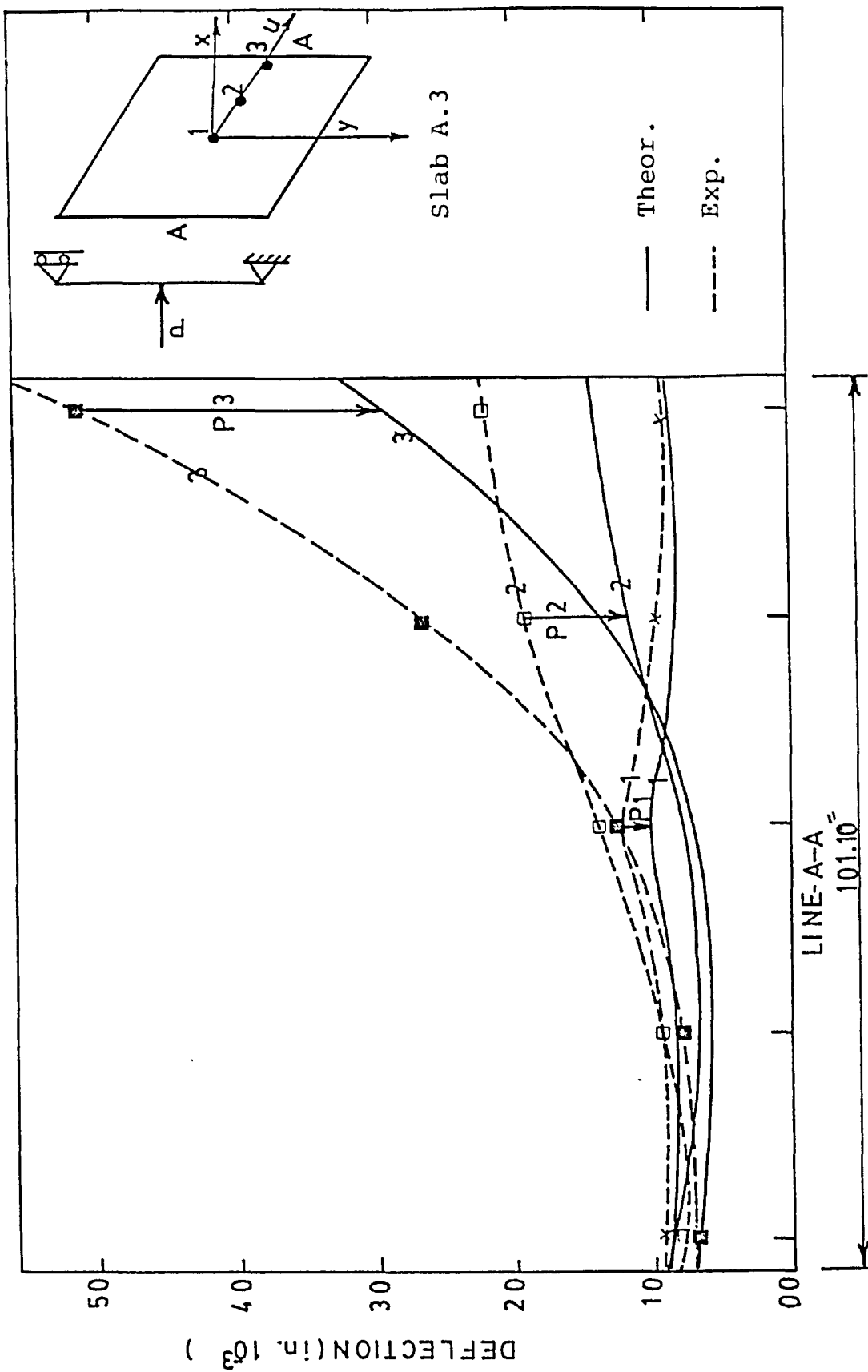


FIGURE 7.22 DEFLECTIONS ALONG LINE A-A FOR SKEW SLAB A.3 ( $p = 1$  KIP)

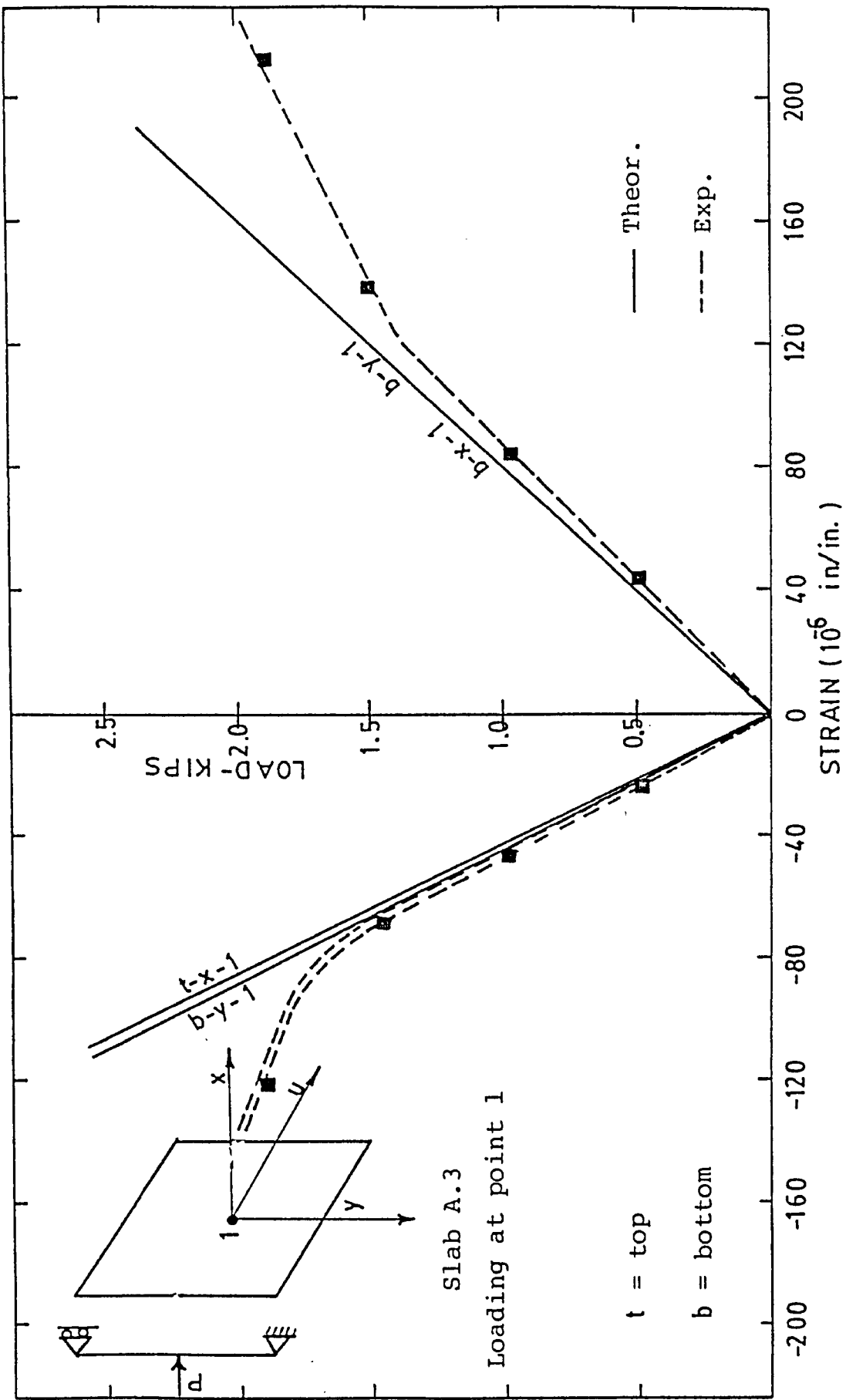


FIGURE 7.23 LOAD STRAIN RELATIONSHIP FOR SKEW SLAB A.3 AT POINT 1.

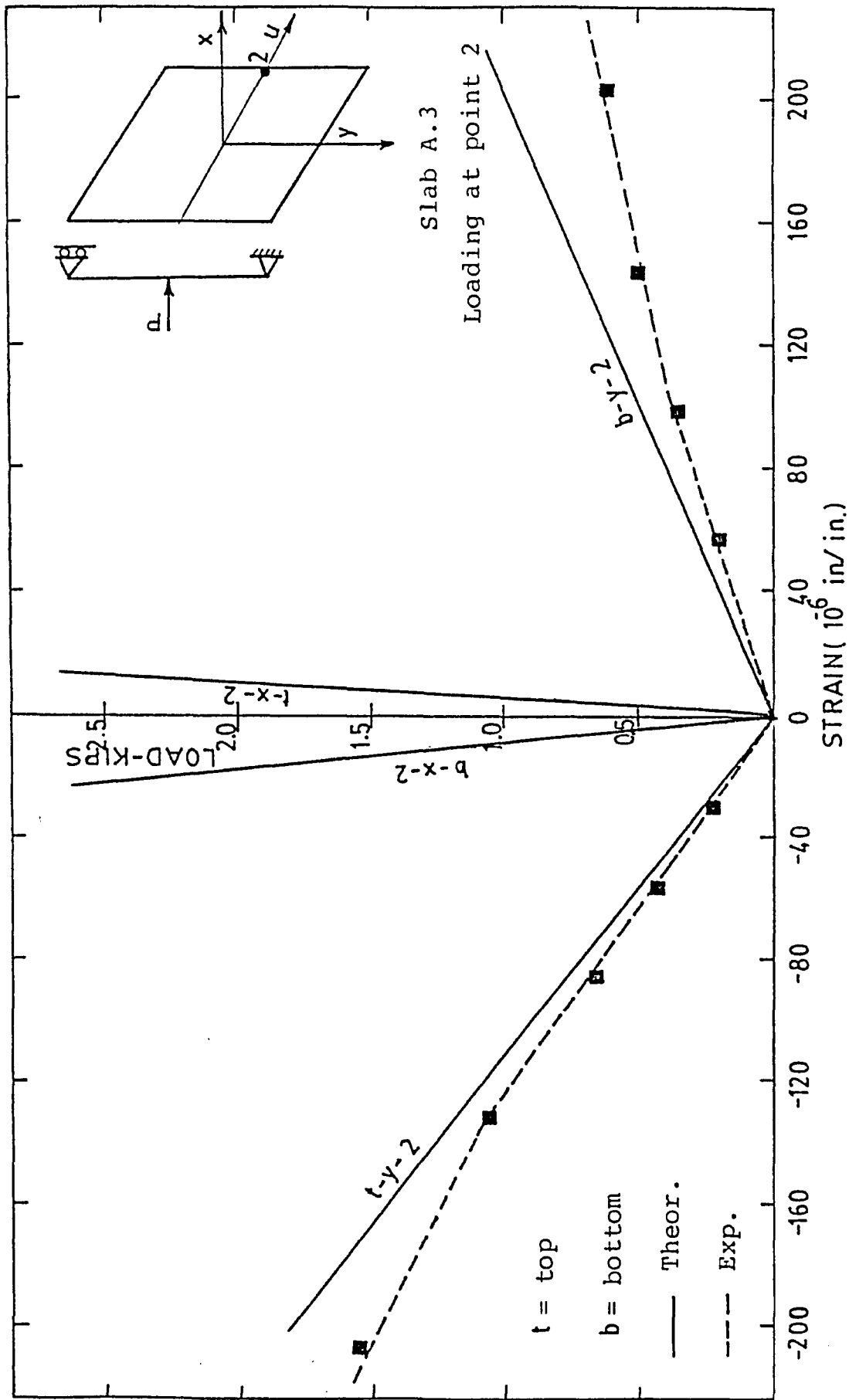


FIGURE 7.24 LOAD STRAIN RELATIONSHIP FOR SKEW SLAB A.3 AT POINT 2.

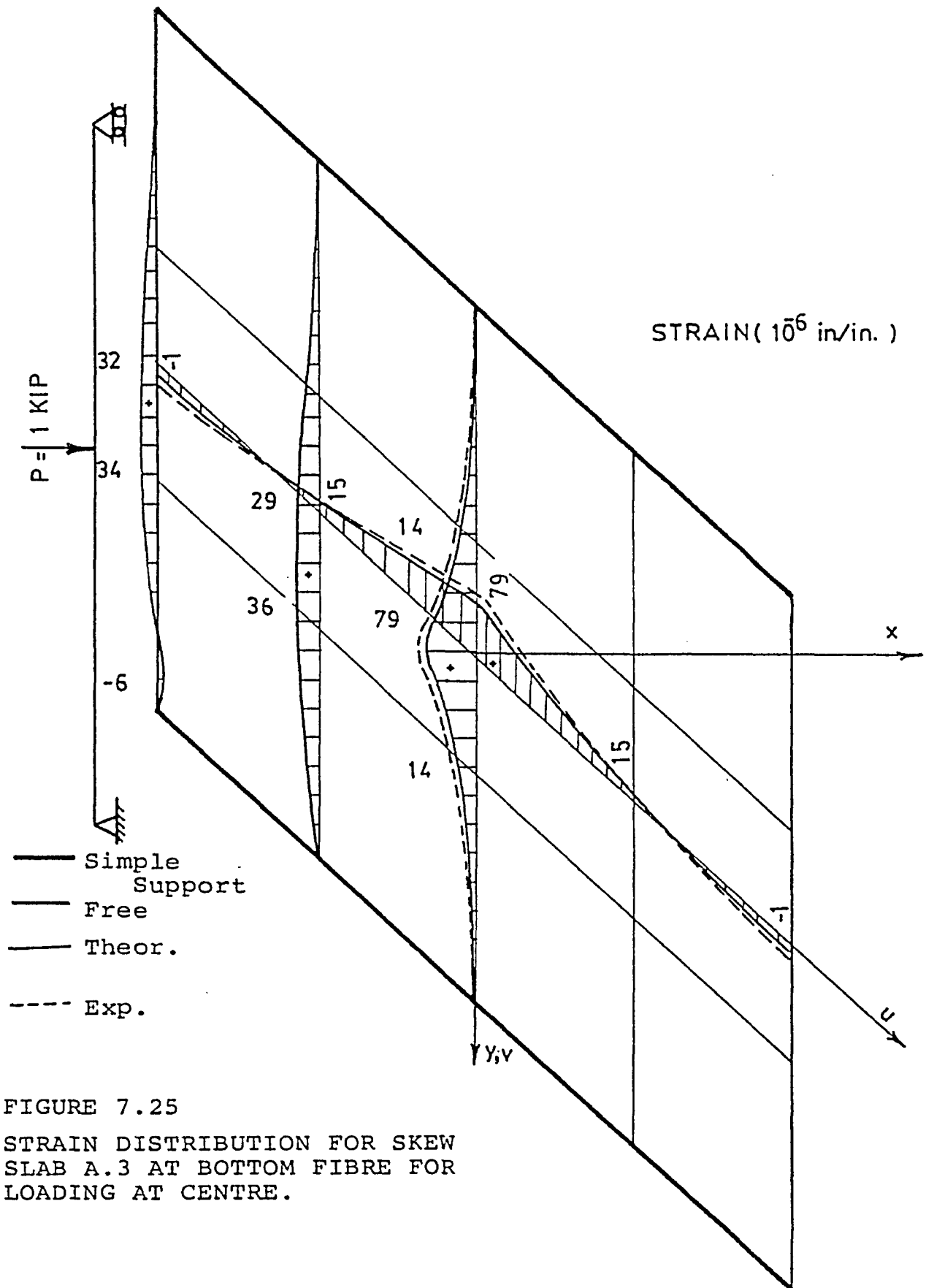


FIGURE 7.25

STRAIN DISTRIBUTION FOR SKEW  
SLAB A.3 AT BOTTOM FIBRE FOR  
LOADING AT CENTRE.

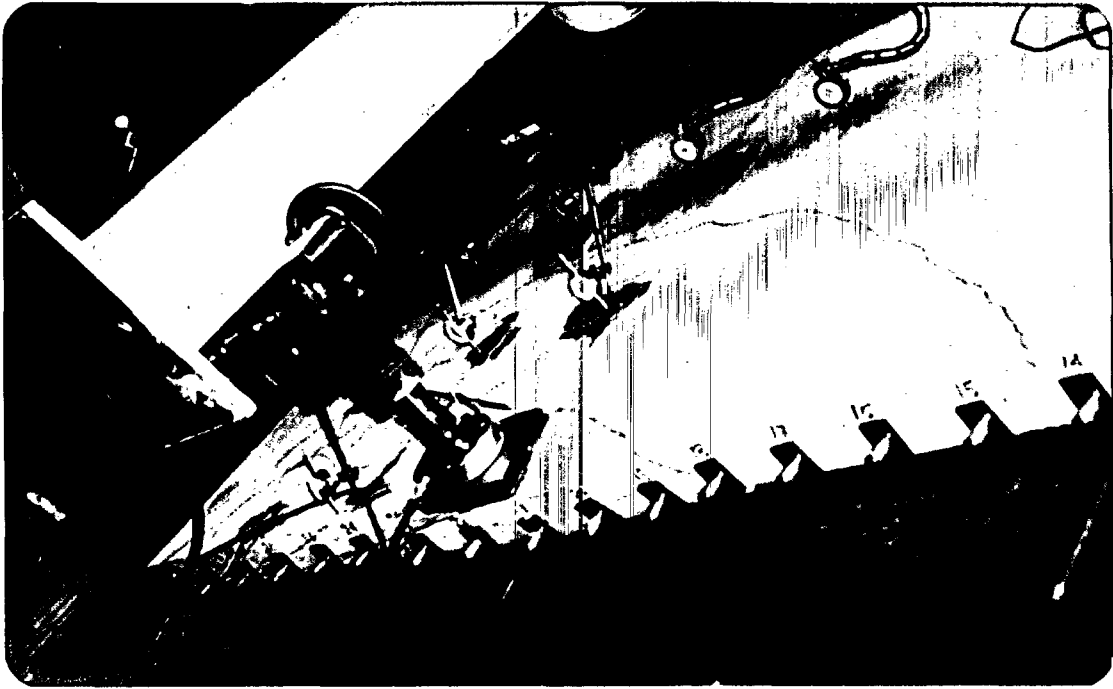


FIGURE 7.26 CRACKS DEVELOPMENT FOR SLAB B.1.

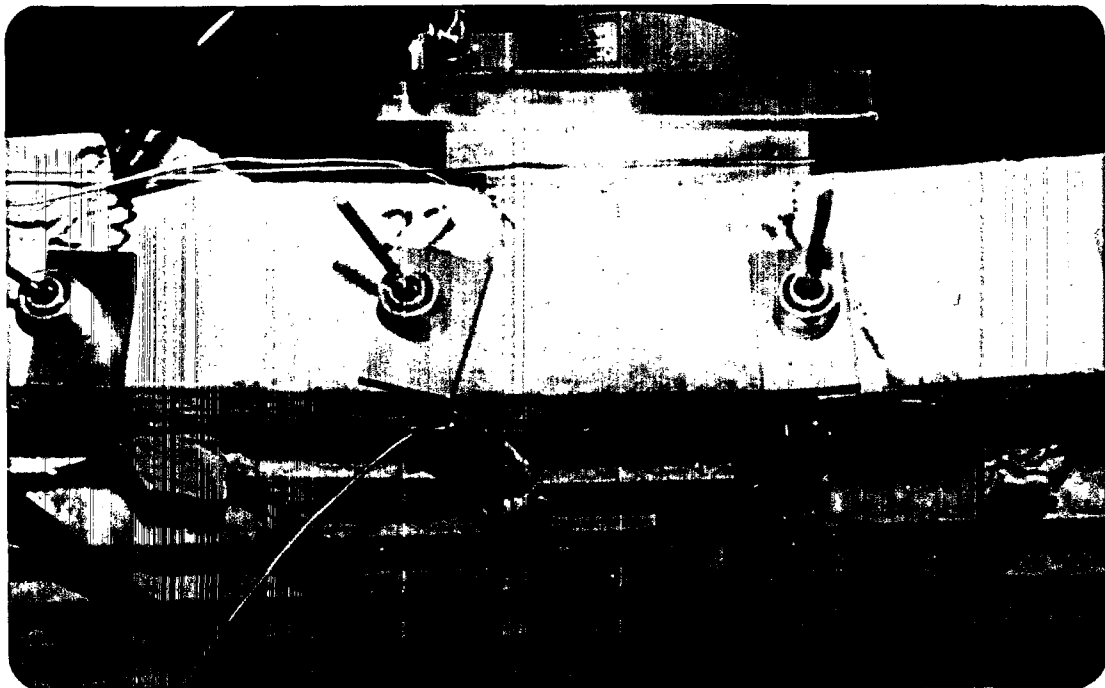


FIGURE 7.27 CRACKS FAILURE FOR SLAB B.1.

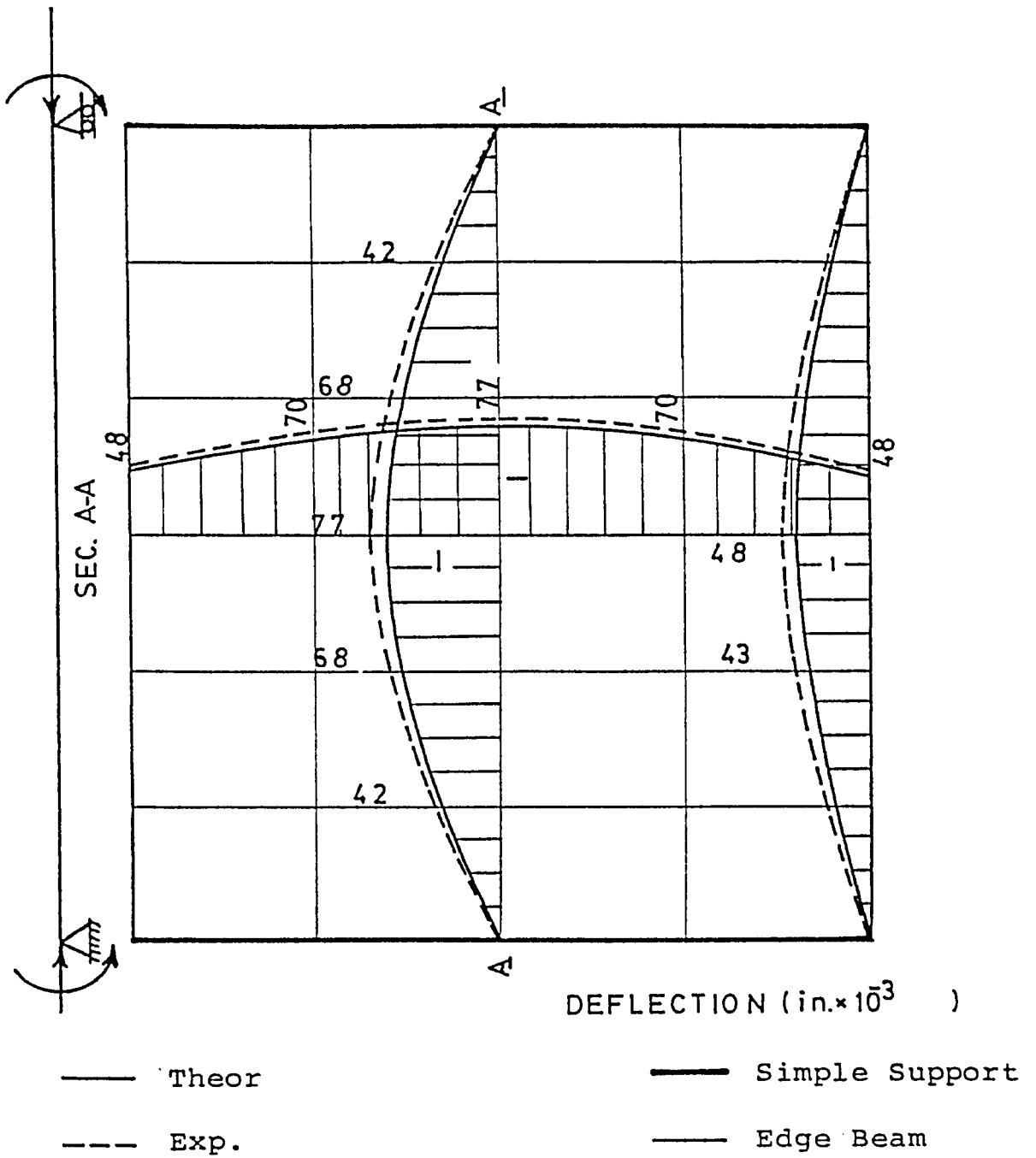


FIGURE 7.28 THE UPWARD DEFLECTION (CAMBER) IN SLAB B.1 DUE TO PRESTRESSING.



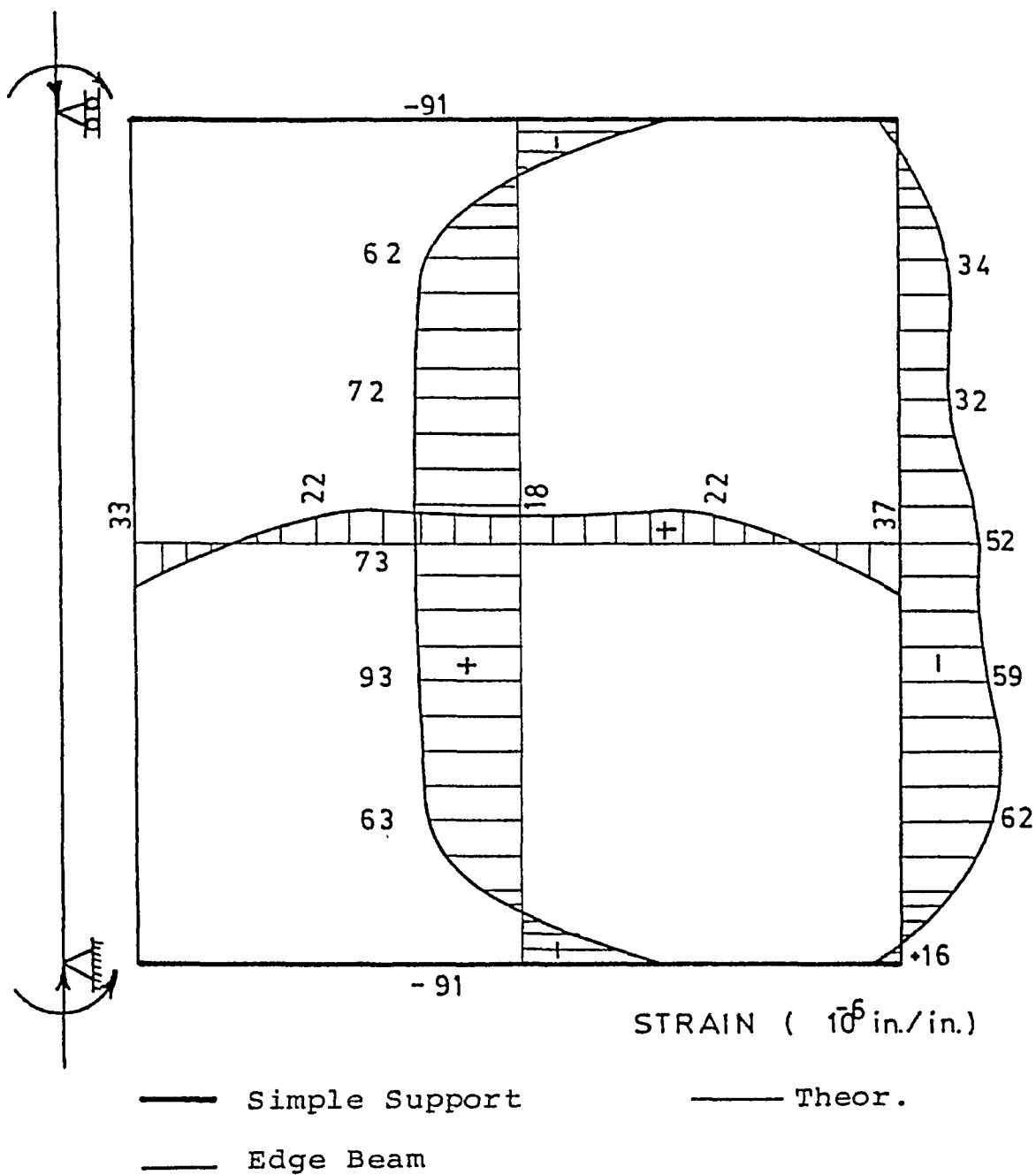


FIGURE 7.29 TOP FIBRE STRAIN DISTRIBUTION FOR SLAB B.1 DUE TO PRESTRESSING.

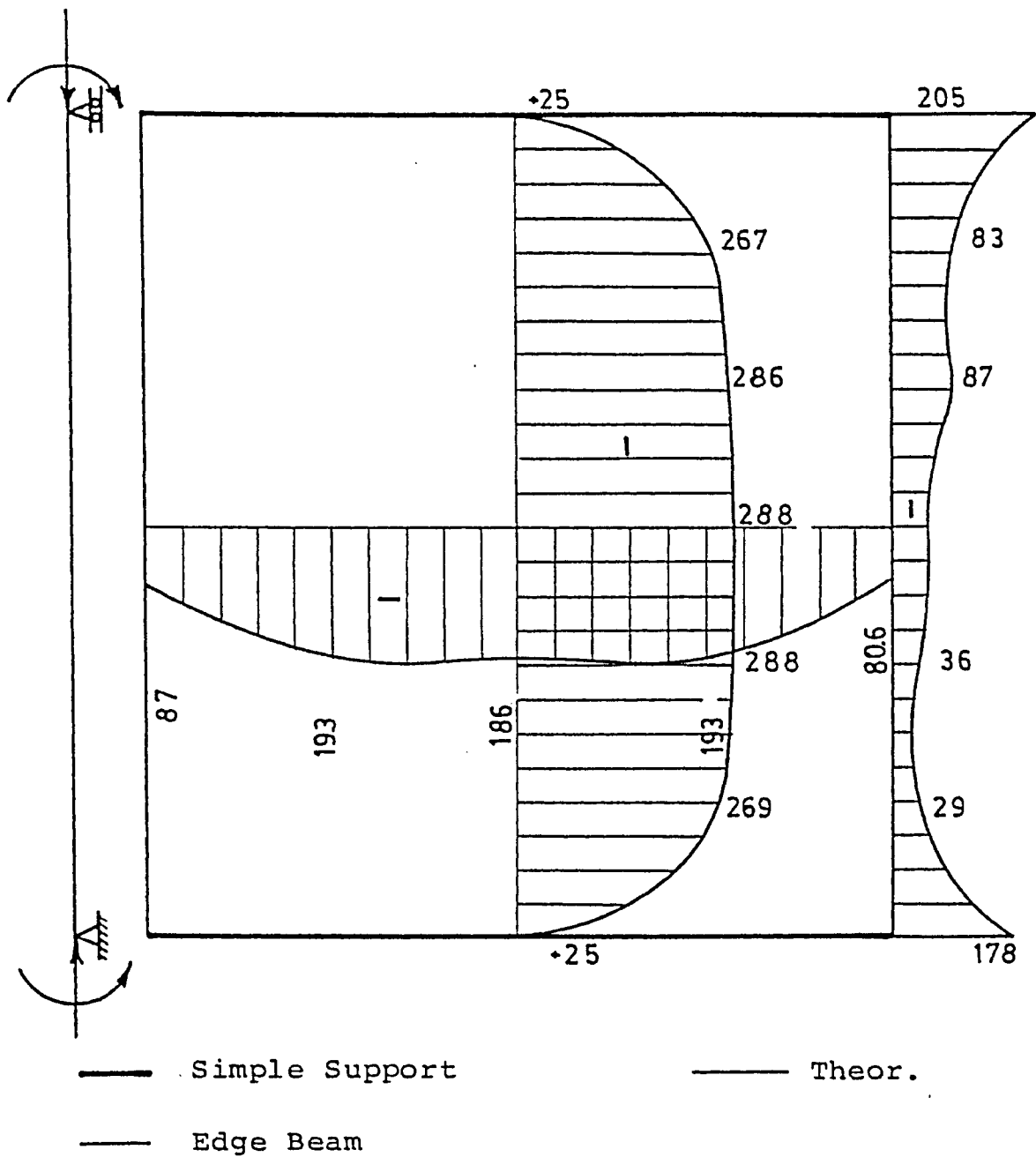


FIGURE 7.30 BOTTOM FIBRE STRAIN DISTRIBUTION FOR SLAB B.1 DUE TO PRESTRESSING.

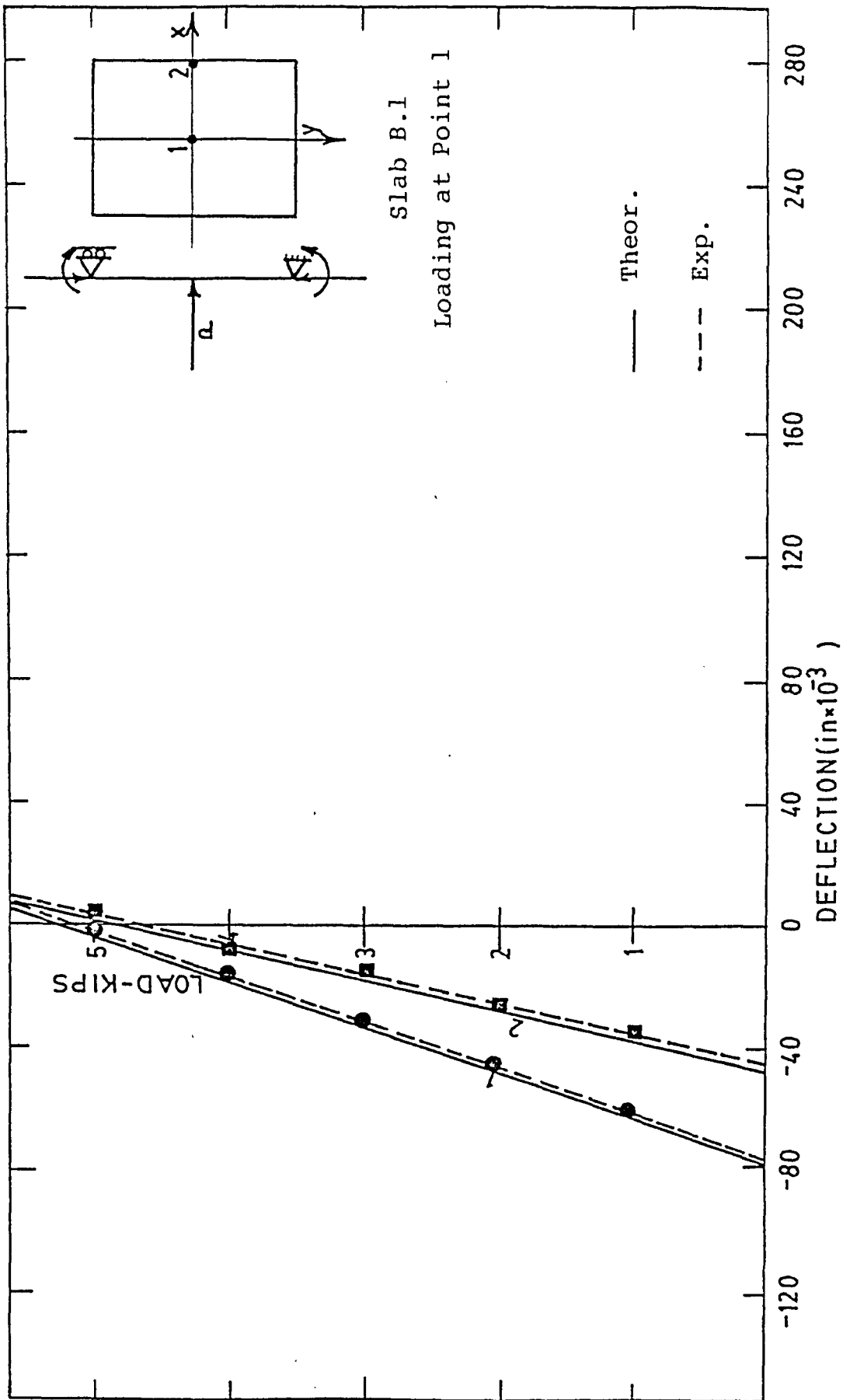


FIGURE 7.31 LOAD DEFLECTION RELATIONSHIP FOR SLAB B.1.

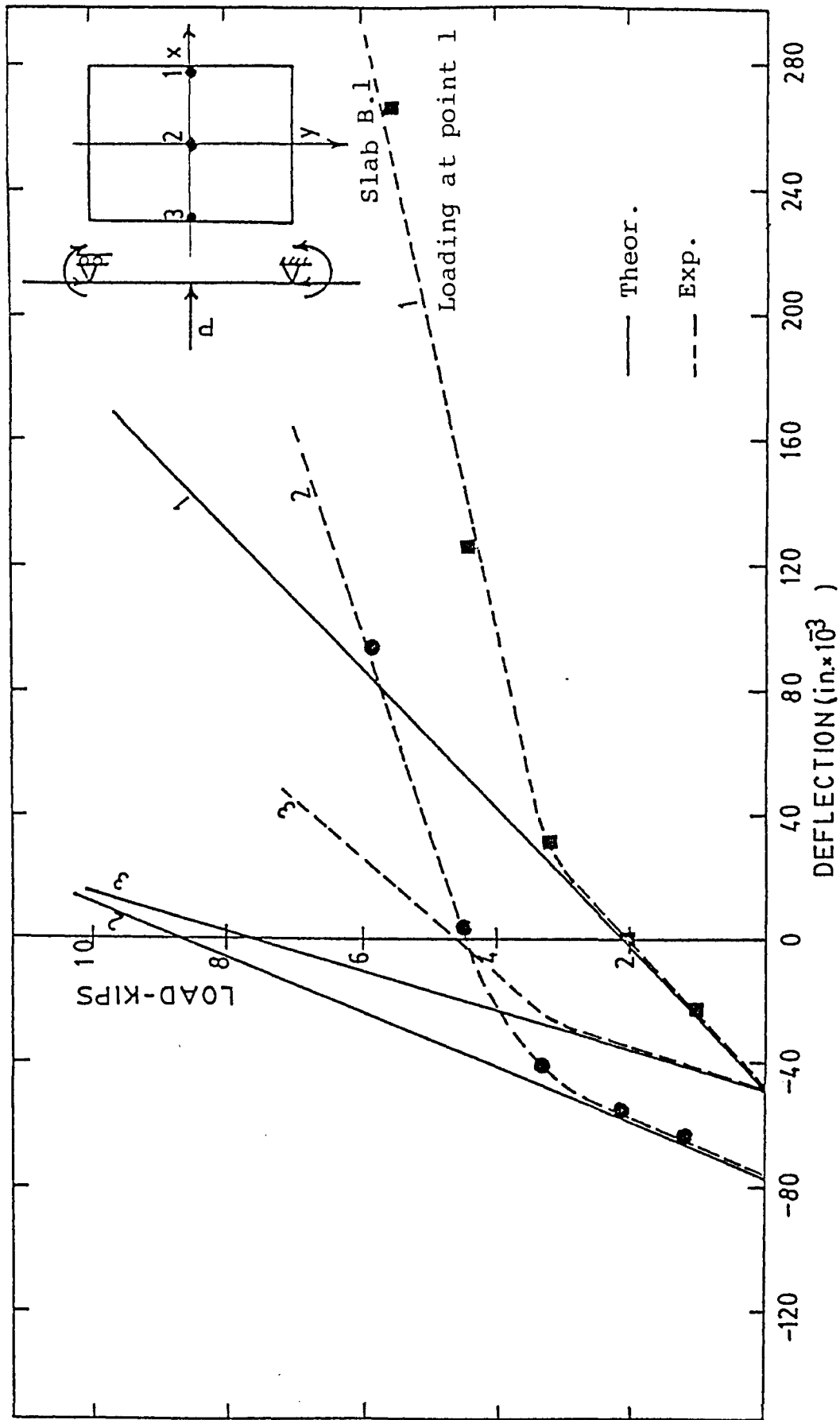


FIGURE 7.32 LOAD DEFLECTION RELATIONSHIP FOR SLAB B.1

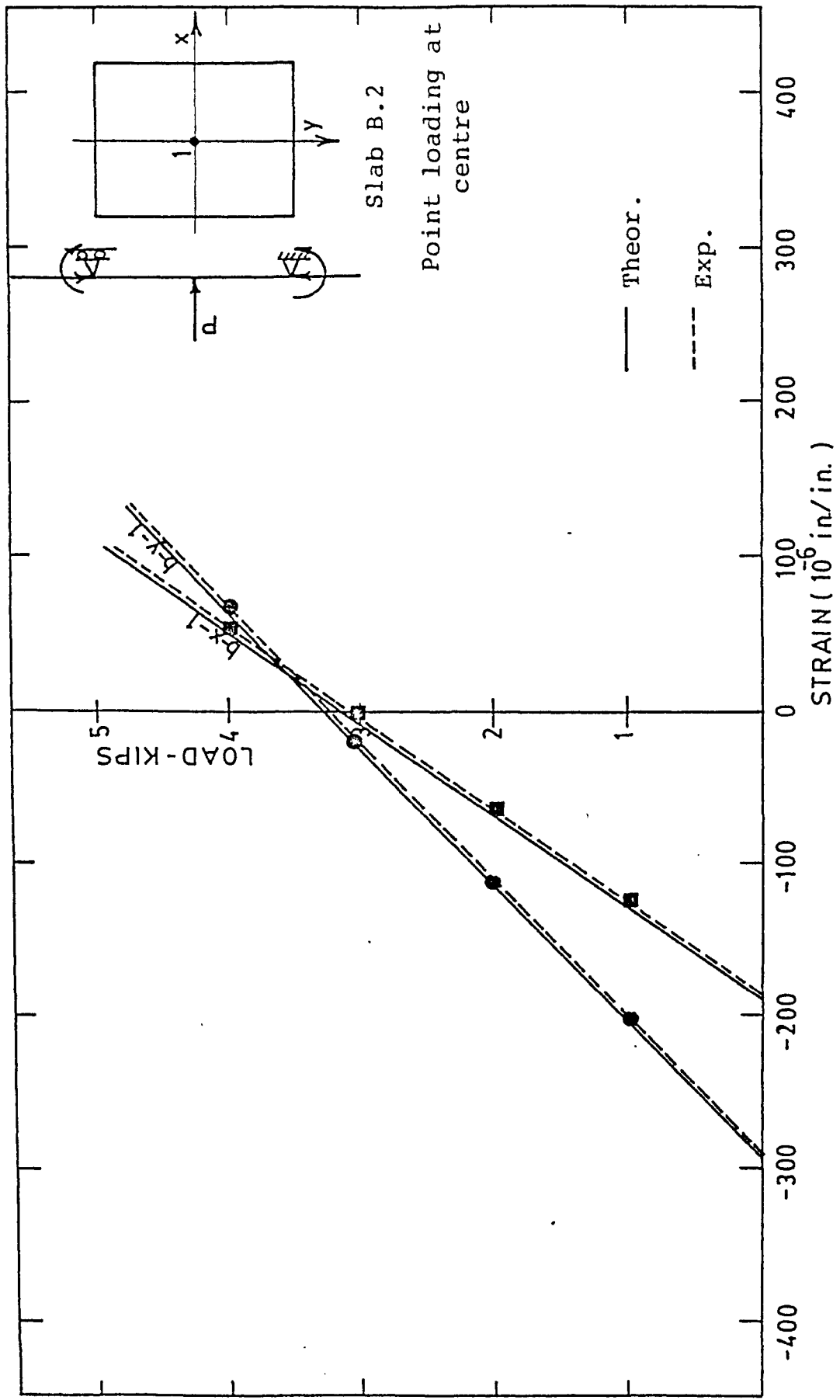


FIGURE 7.33 LOAD STRAIN RELATIONSHIP FOR SLAB B.1 AT CENTRE.

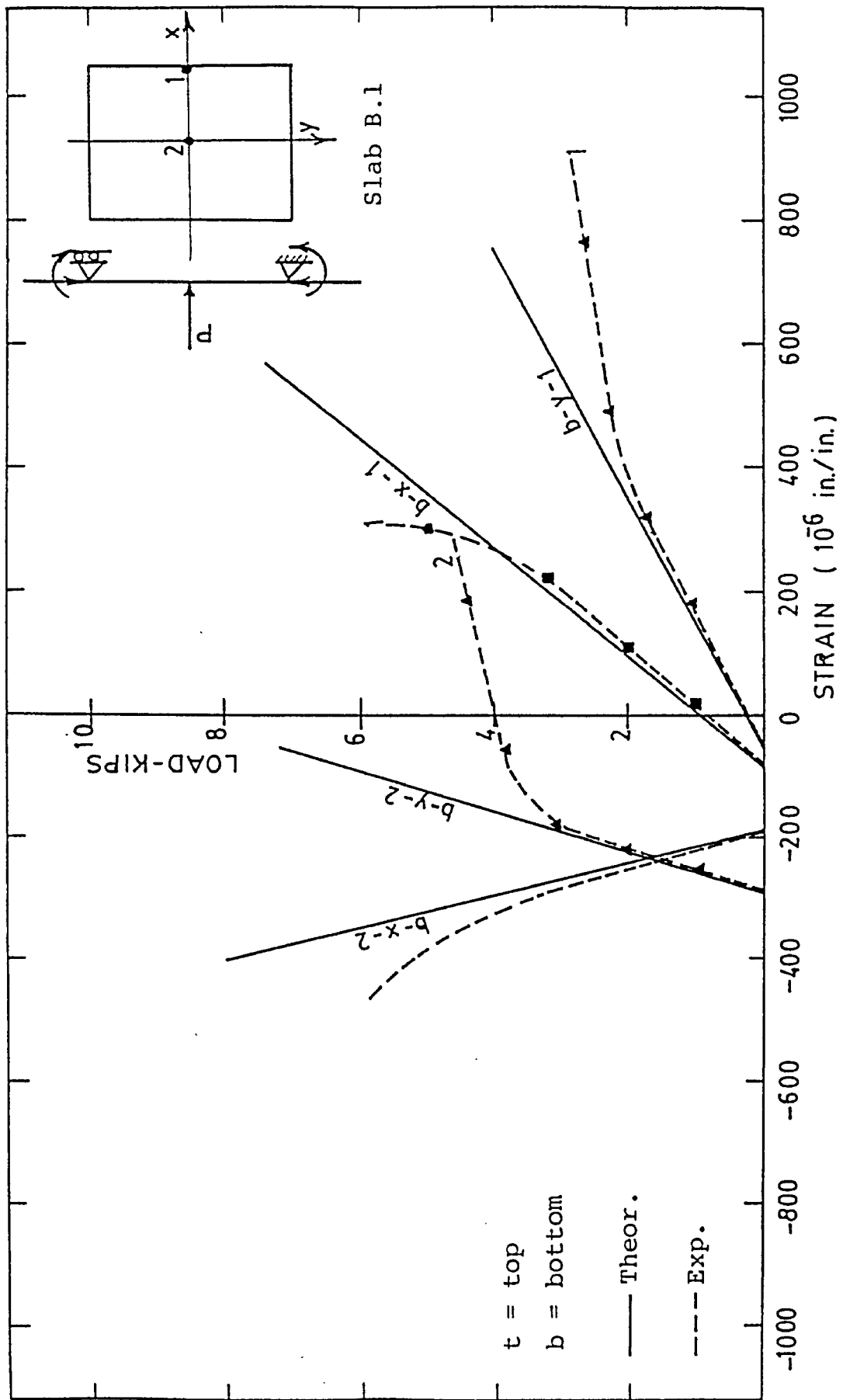


FIGURE 7.34 LOAD STRAIN RELATIONSHIP FOR SLAB B.1 (LOADING AT POINT 1).



FIGURE 7.35 CRACKS FAILURE FOR SLAB B.2.

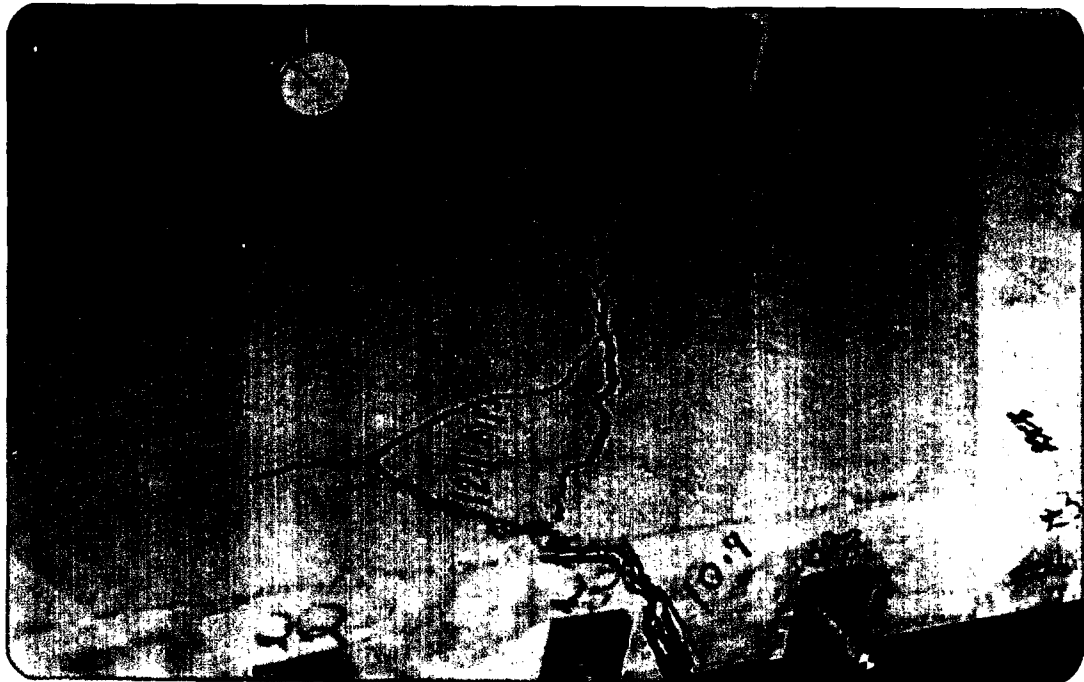


FIGURE 7.36 CRACKS DEVELOPMENT FOR SLAB B.2.

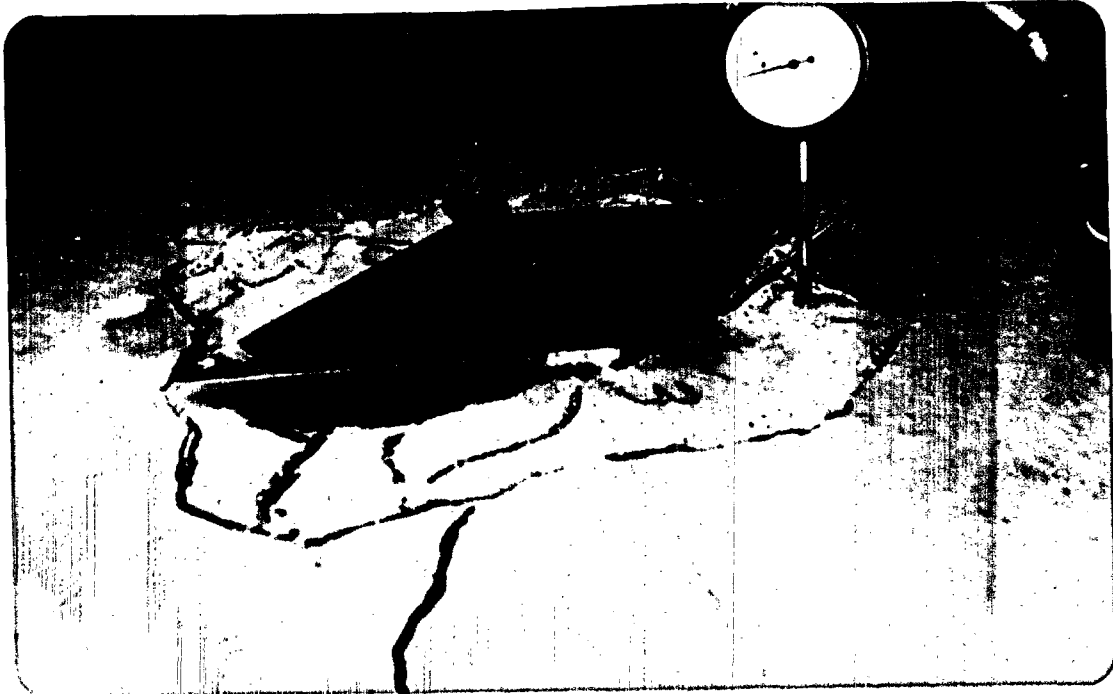


FIGURE 7.37 PUNCHING FAILURE OF SLAB B.2.



FIGURE 7.38 CRACKS FAILURE FOR SLAB B.2.



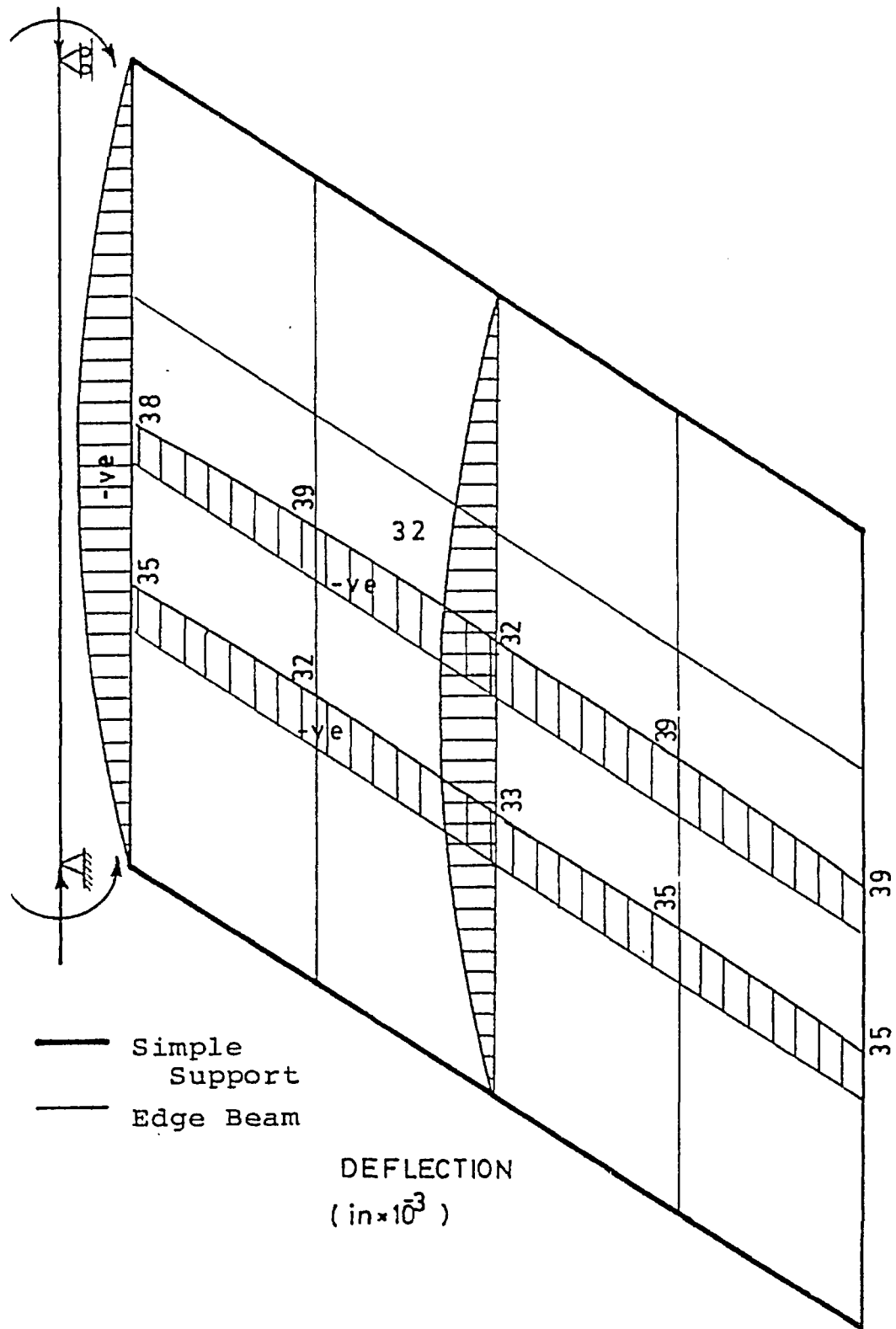


FIGURE 7.39 DEFLECTION DISTRIBUTION FOR SKEW SLAB B.2 DUE TO PRESTRESSING FORCE.

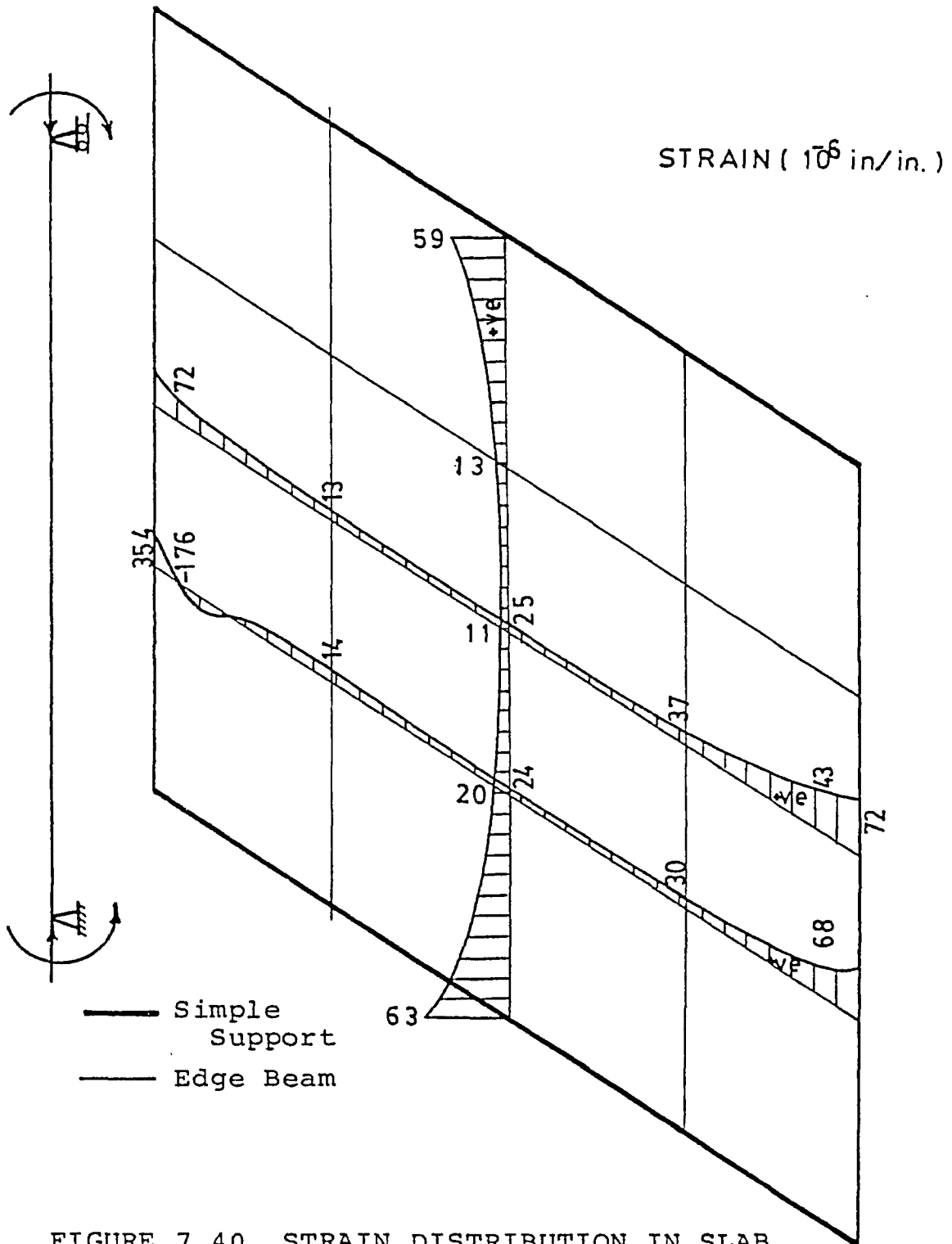
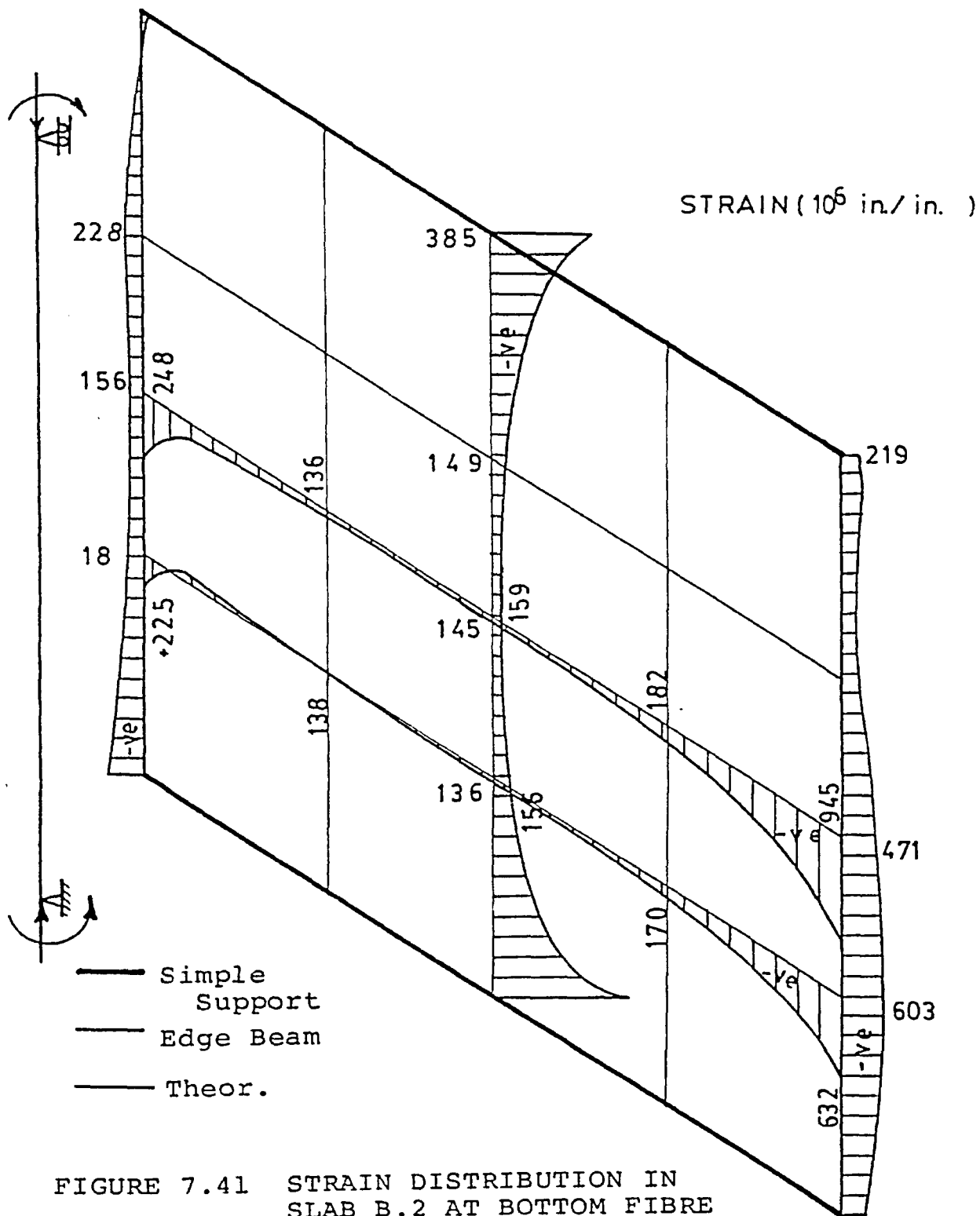


FIGURE 7.40 STRAIN DISTRIBUTION IN SLAB B.2 AT TOP FIBRE DUE TO PRESTRESSING FORCE.



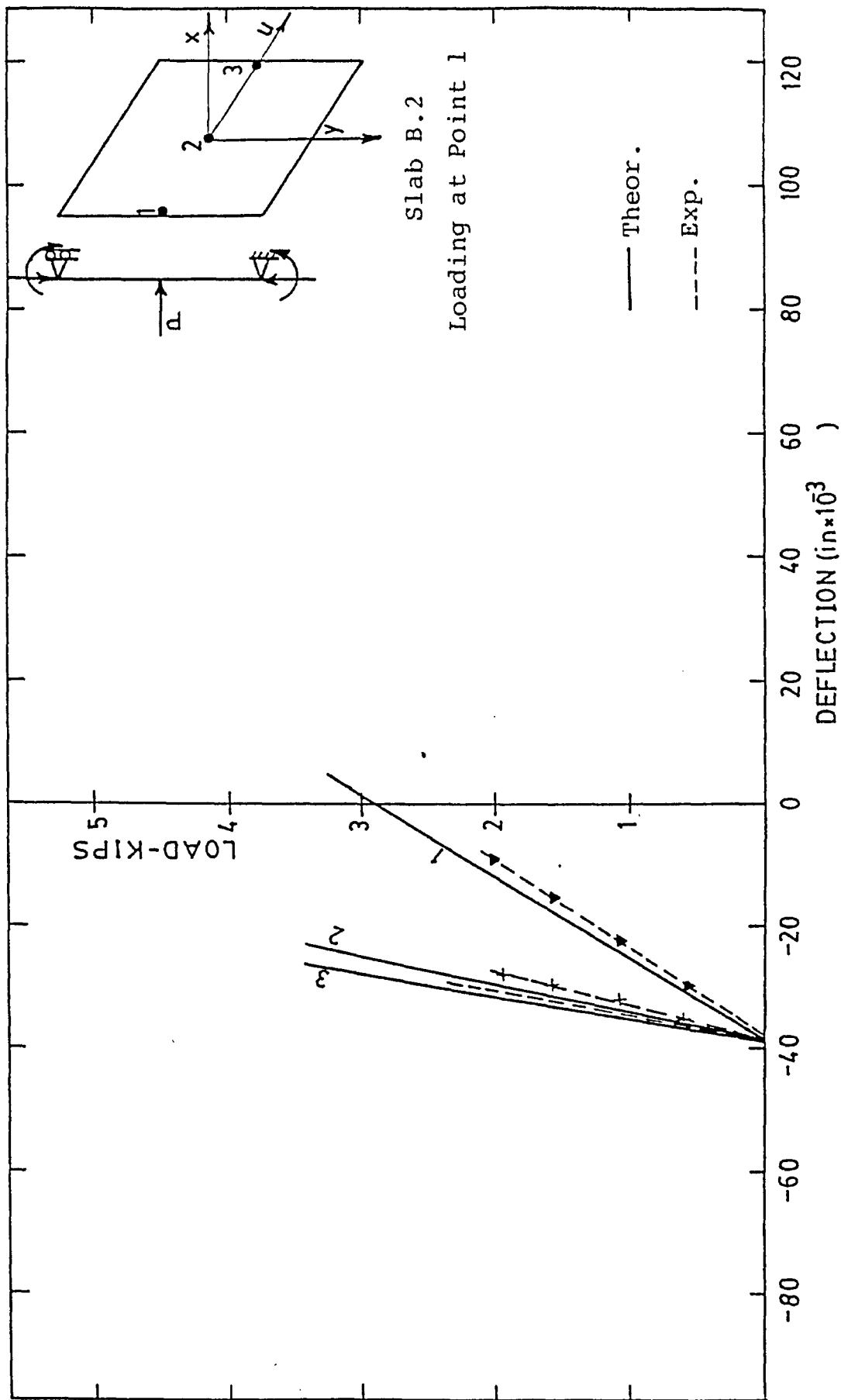


FIGURE 7.42 LOAD DEFLECTION RELATIONSHIP FOR SLAB B.2.

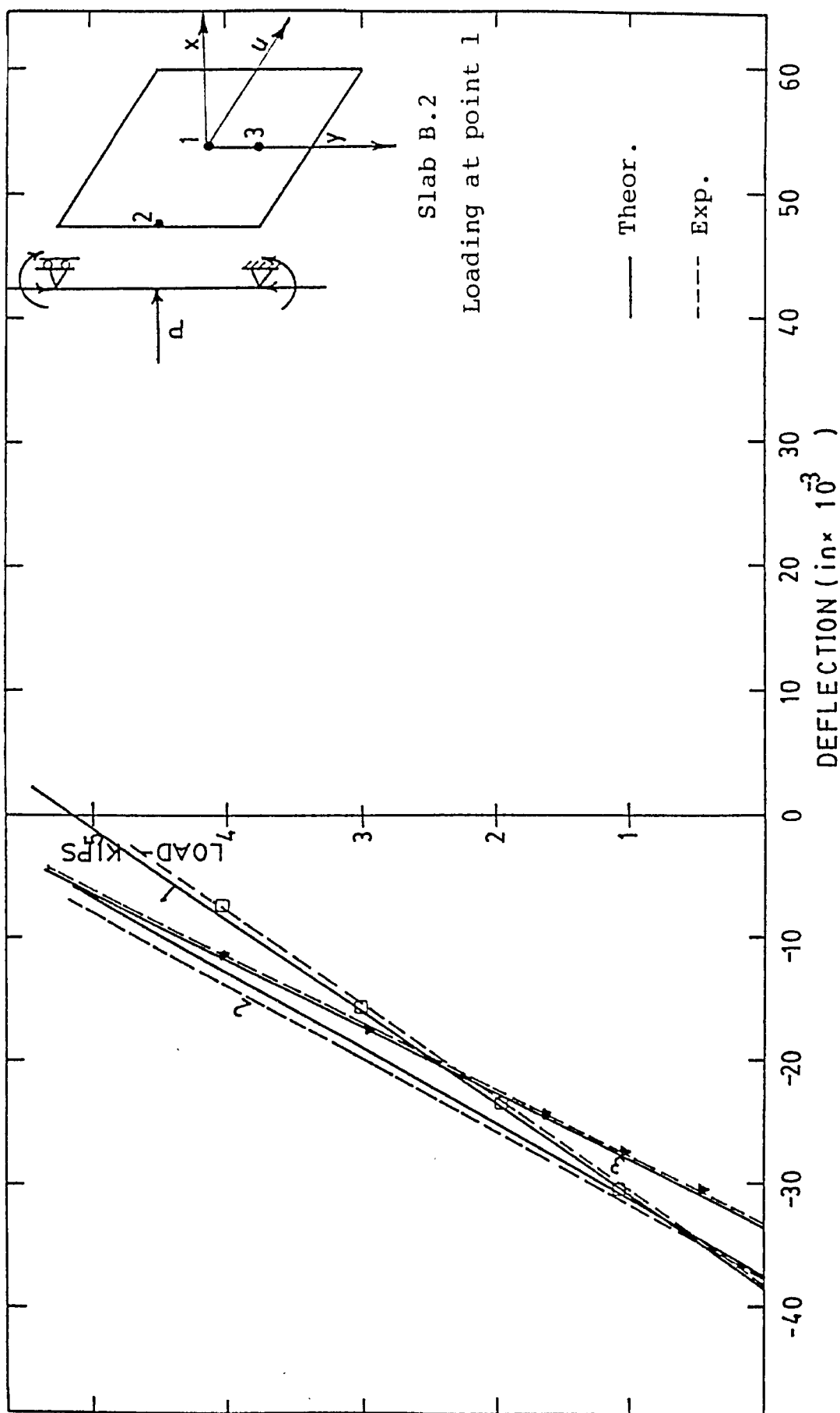


FIGURE 7.43 LOAD DEFLECTION RELATIONSHIP FOR SLAB B.2.

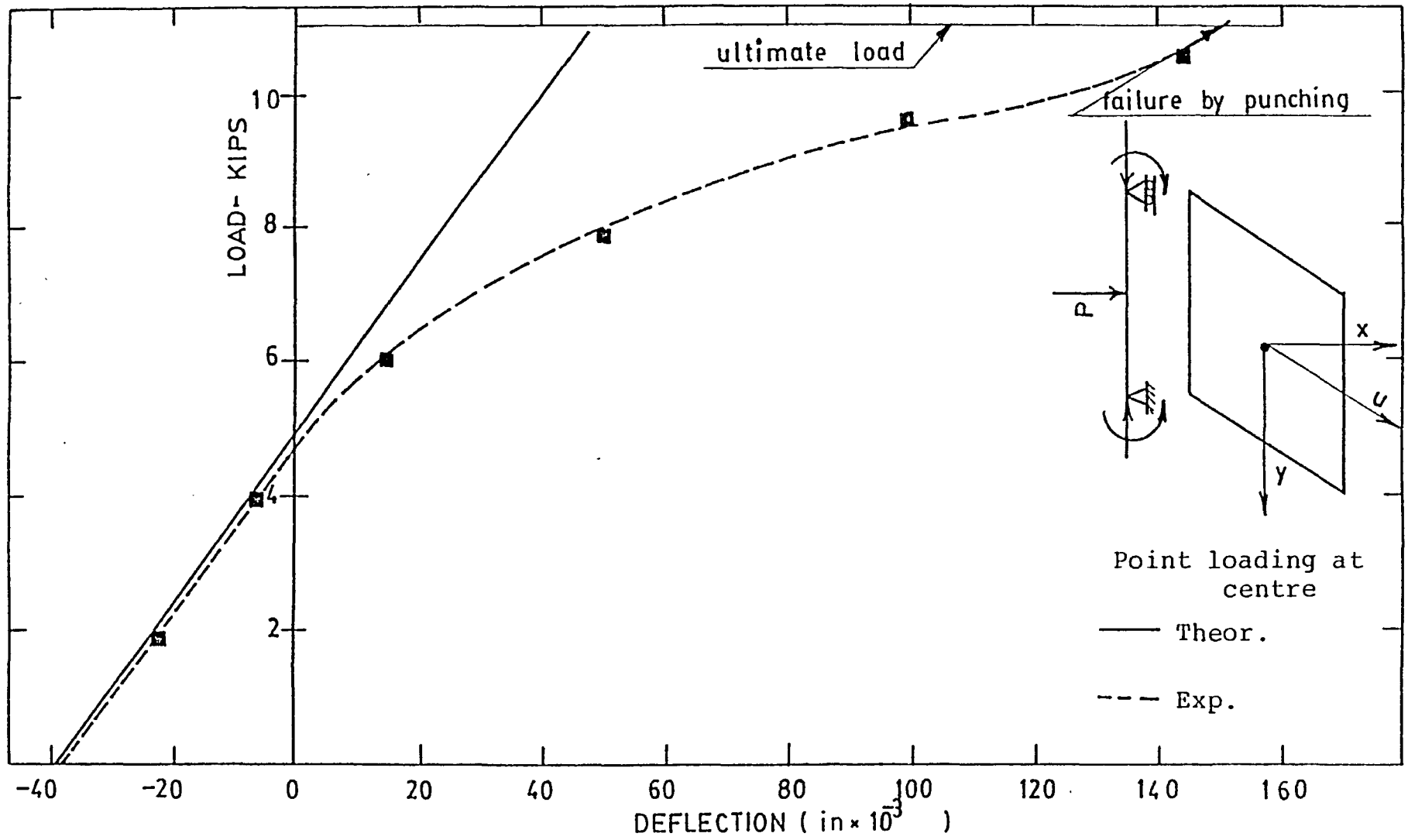


FIGURE 7.44 LOAD-DEFLECTION RELATIONSHIP FOR SLAB B.2 (ULTIMATE LOAD).

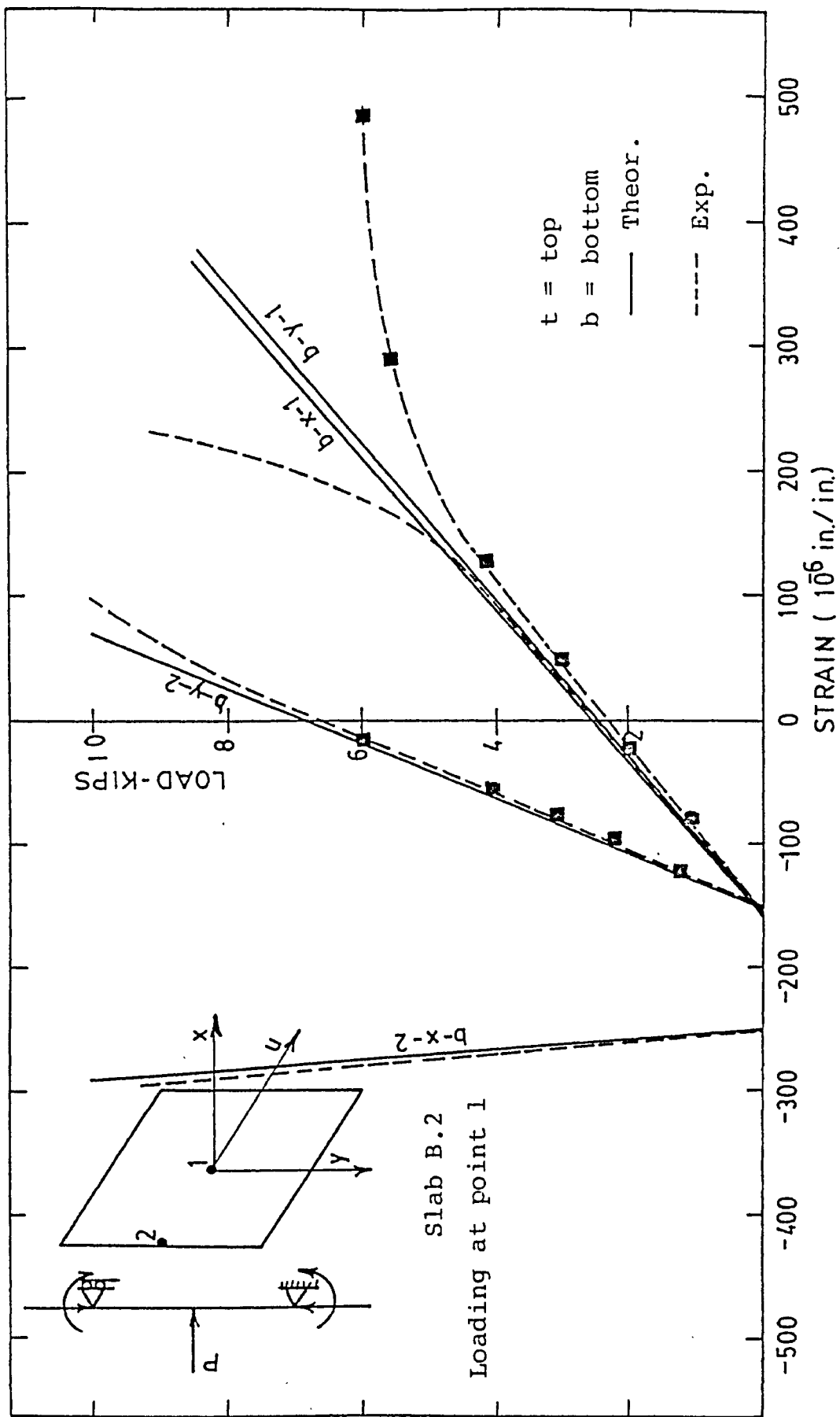


FIGURE 7.45 LOAD STRAIN RELATIONSHIP FOR SLAB B.2.

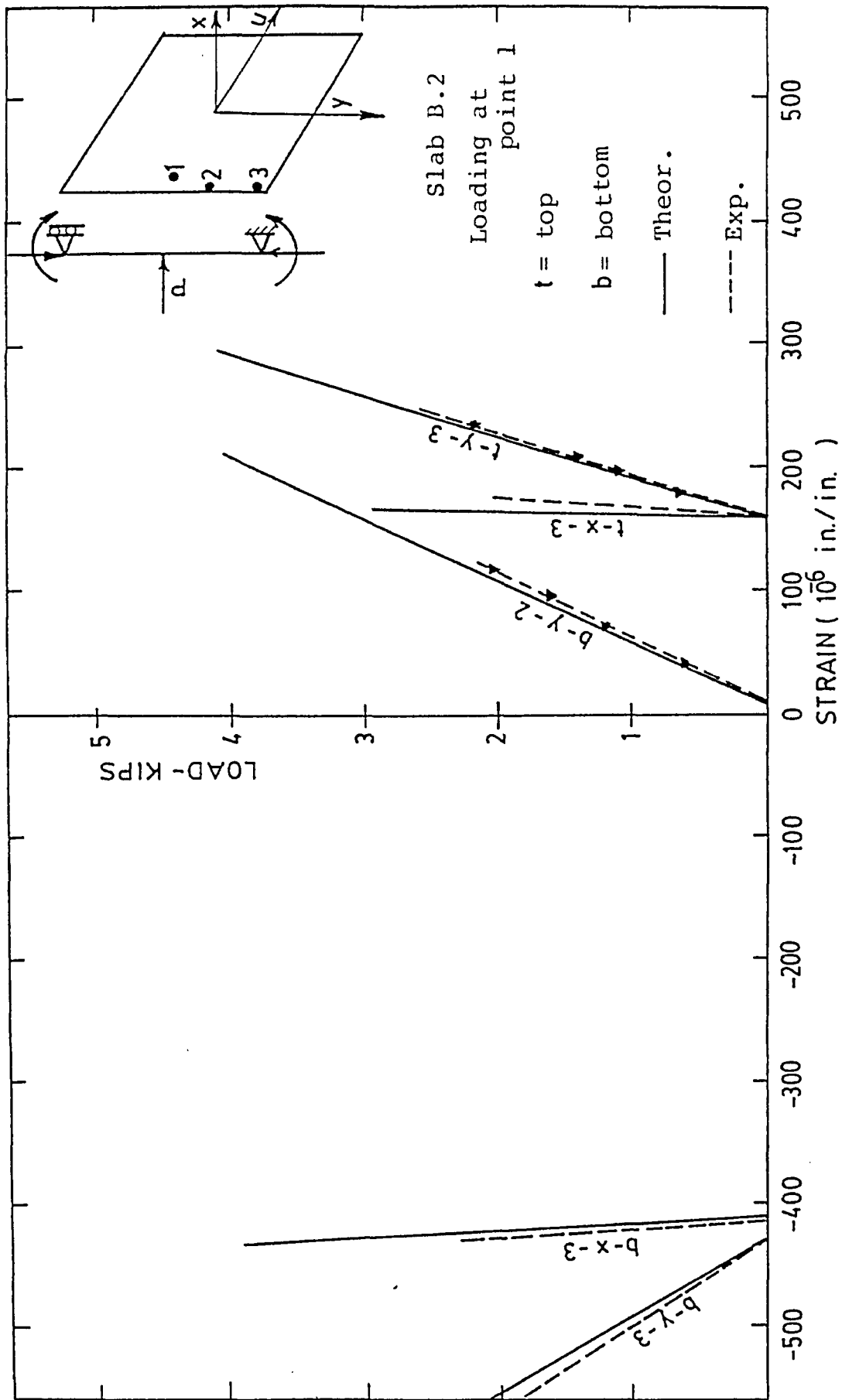


FIGURE 7.46 LOAD STRAIN RELATIONSHIP FOR SLAB B.2.



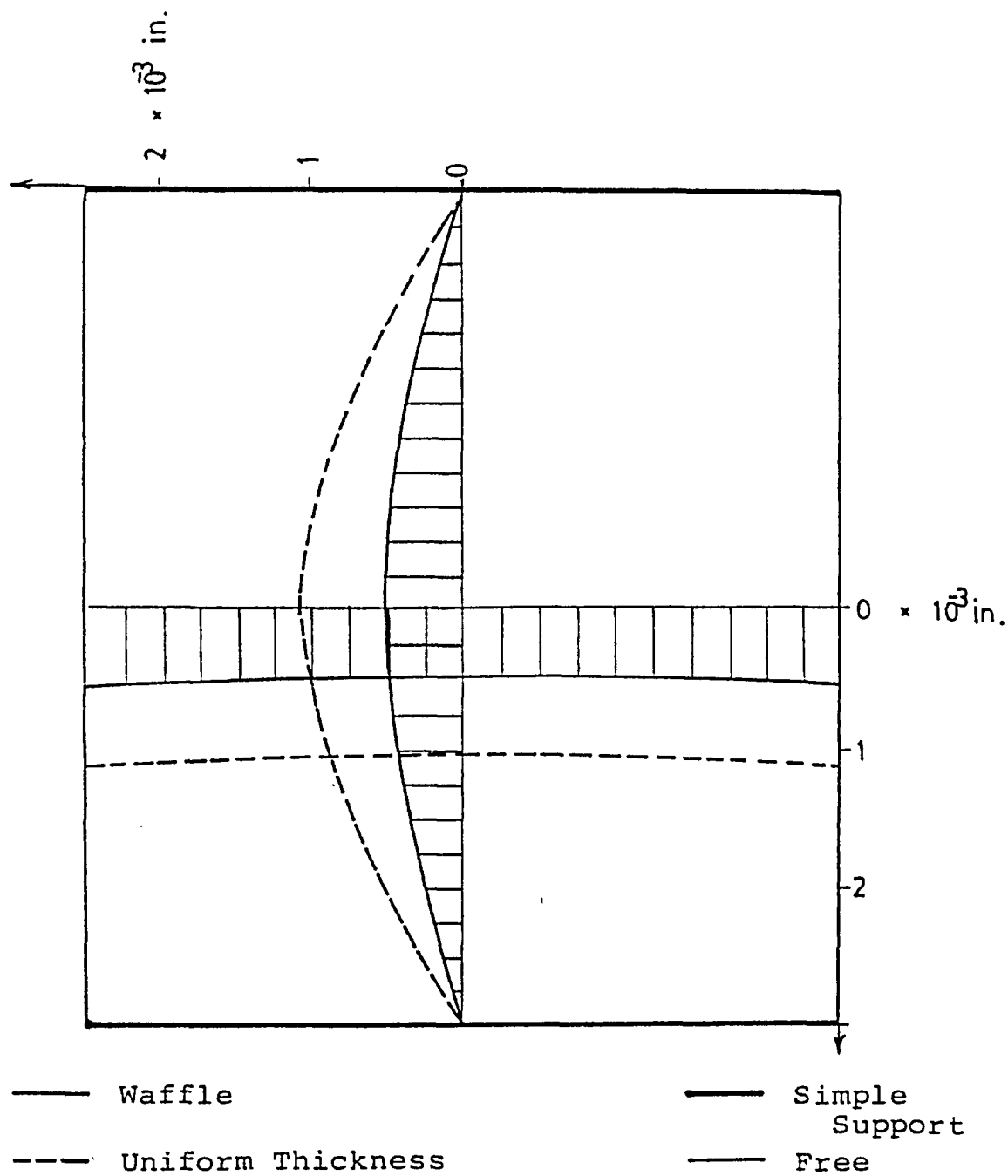


FIGURE 7.47 DEFLECTION PATTERN FOR RECTANGULAR SLAB DUE TO UNIFORM LOAD OF  $.01 \text{ lb/in}^2$ .

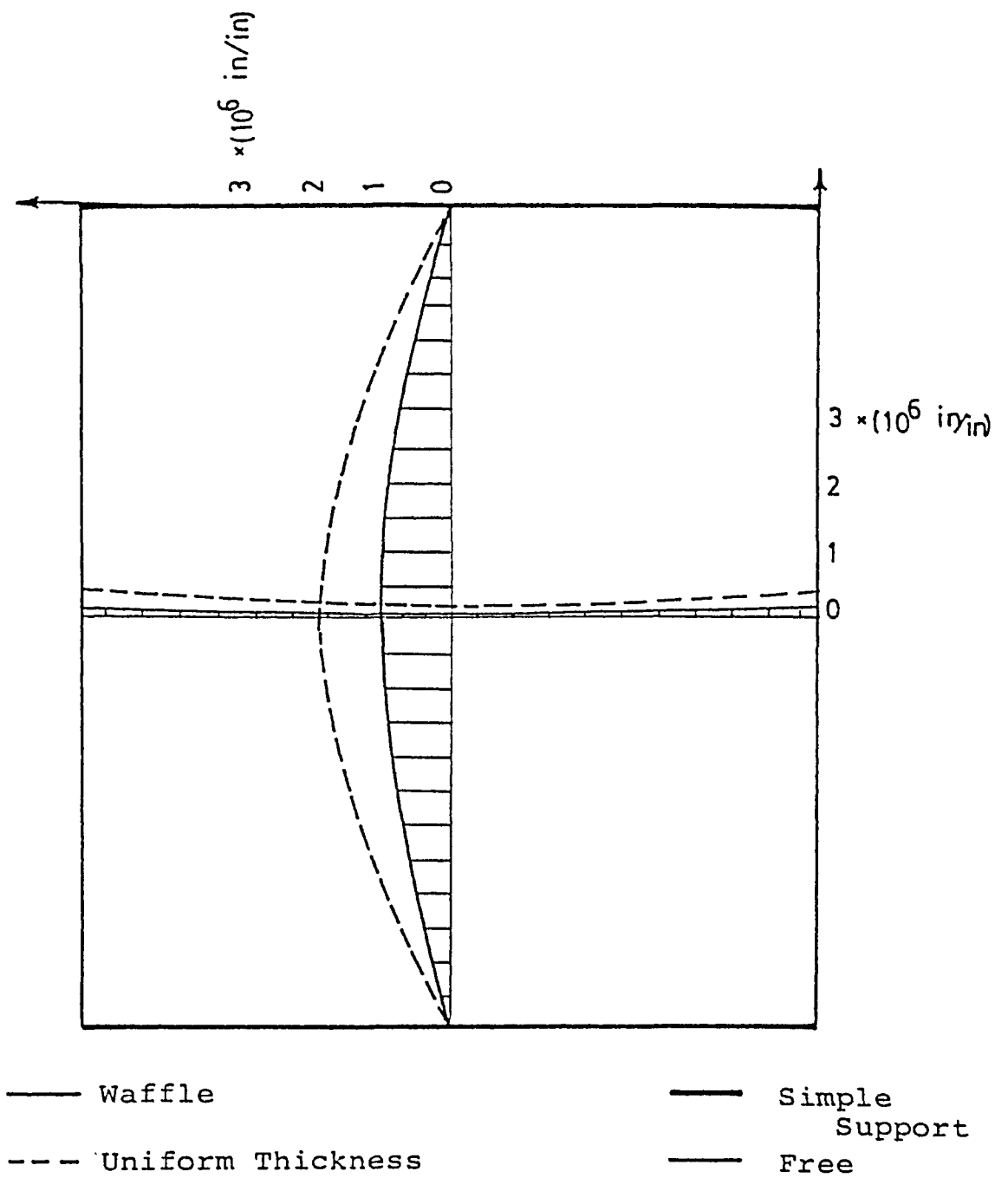


FIGURE 7.48 STRAIN PATTERN AT TOP FIBRE DUE TO UNIFORM LOAD OF .01 lb/in<sup>2</sup>.

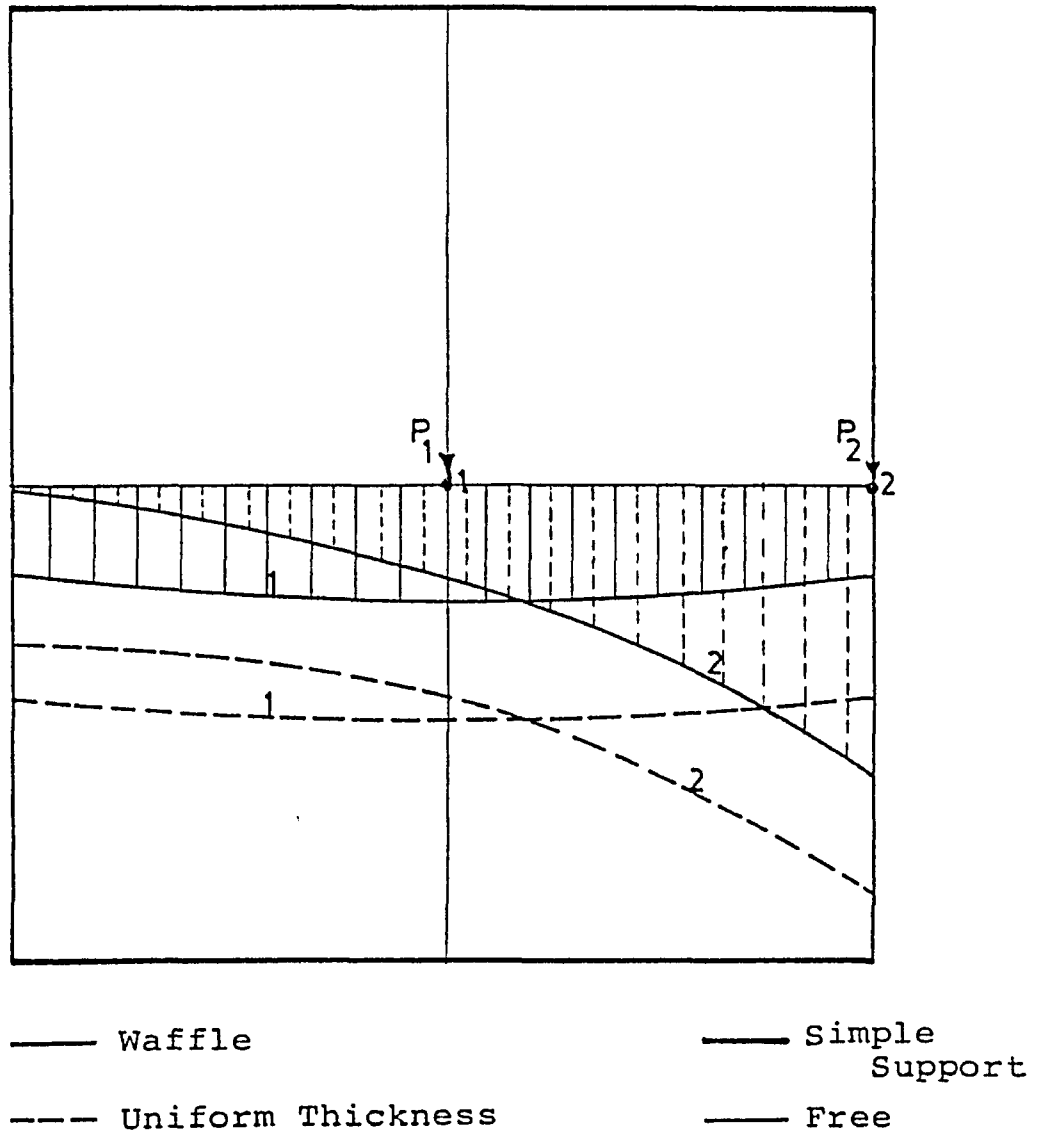


FIGURE 7.49 VARIATION OF DEFLECTIONS ALONG THE TRANSVERSE DIRECTION FOR POINT LOAD AT POINT 1 AND 2.

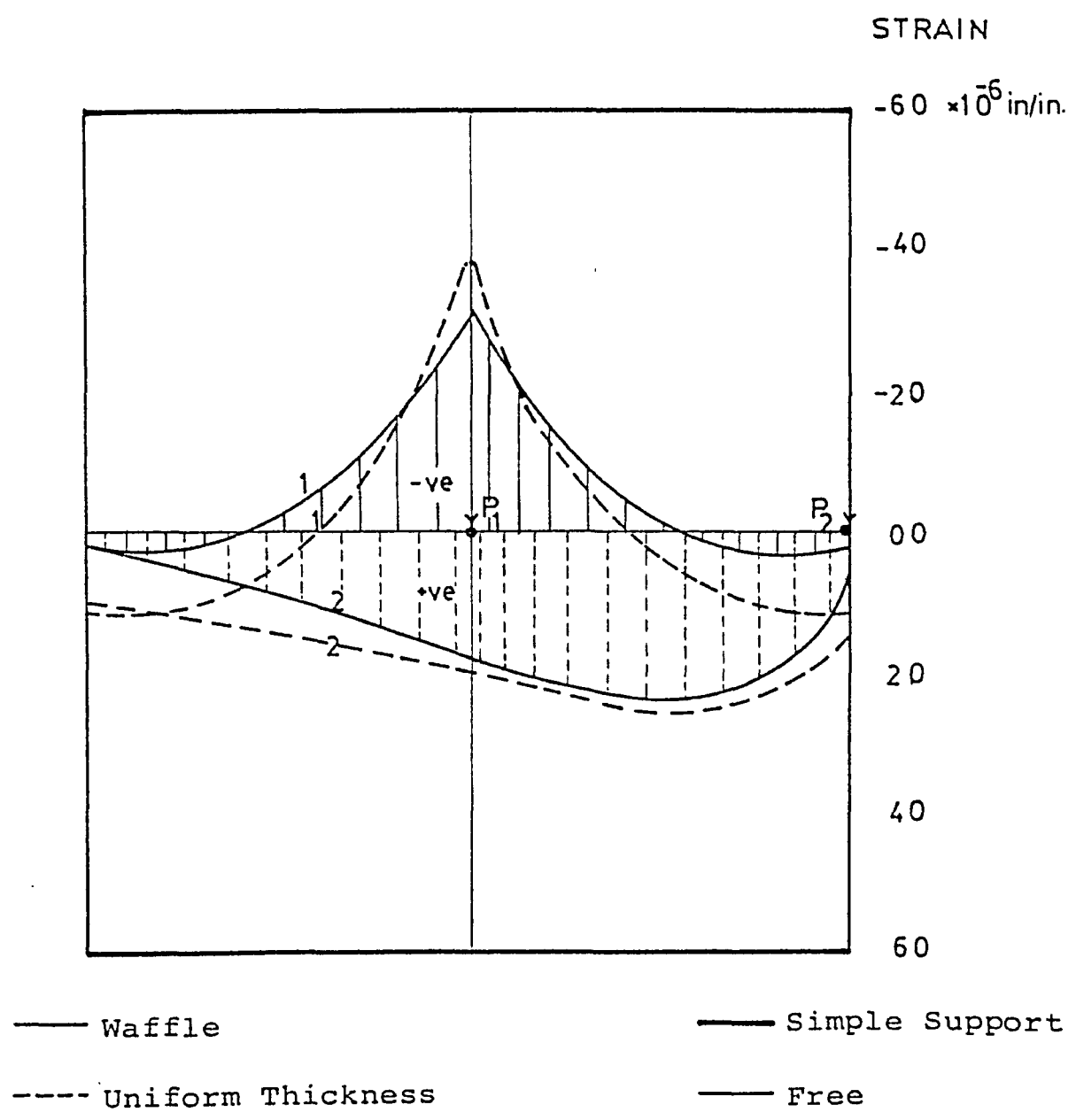


FIGURE 7.50 VARIATION OF STRAINS ALONG THE TRANSVERSE AXIS AT TOP FIBRE DUE TO CONCENTRATED LOAD 1 KIP AT POINT 1 AND 2.



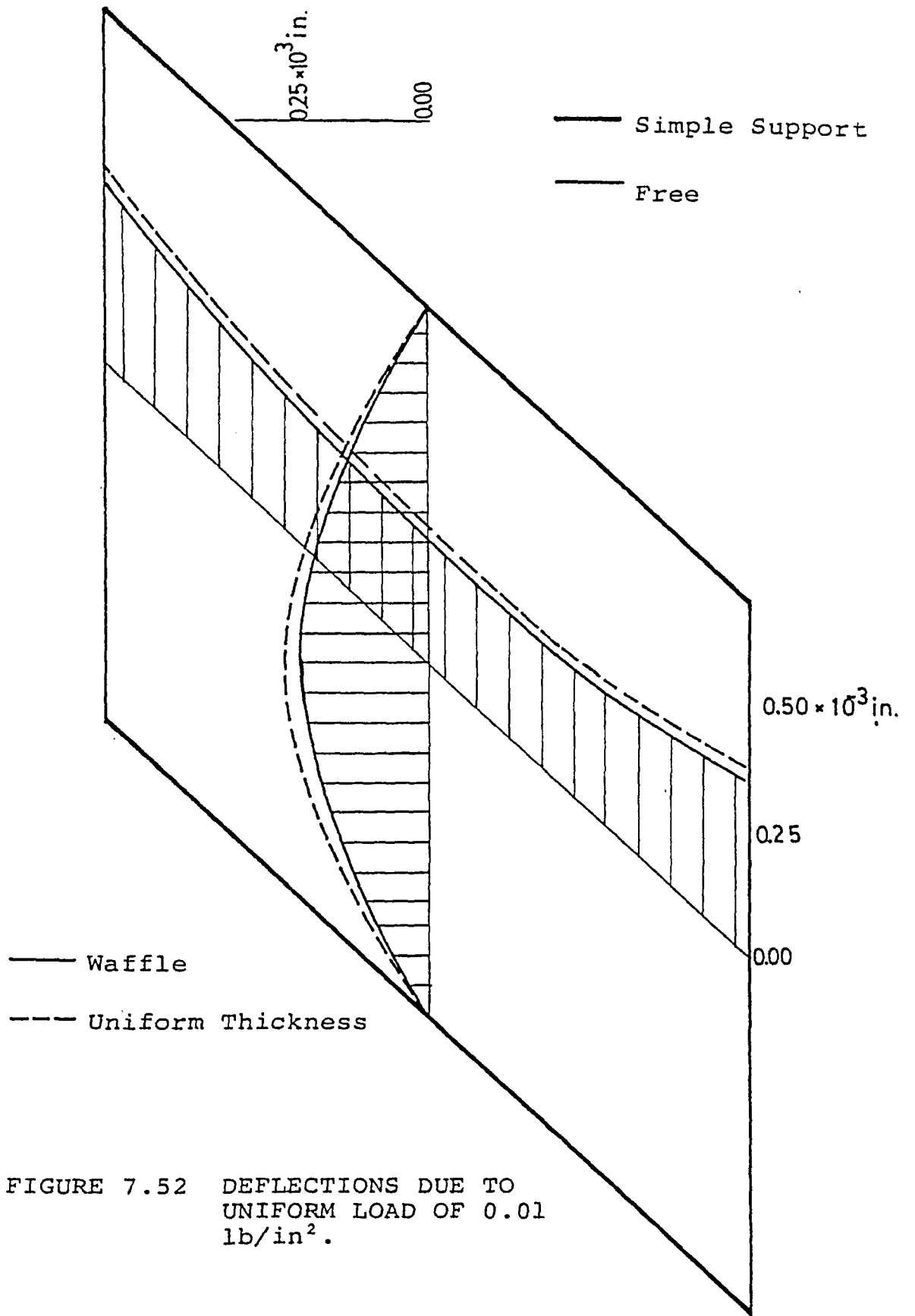


FIGURE 7.52 DEFLECTIONS DUE TO UNIFORM LOAD OF 0.01 lb/in<sup>2</sup>.

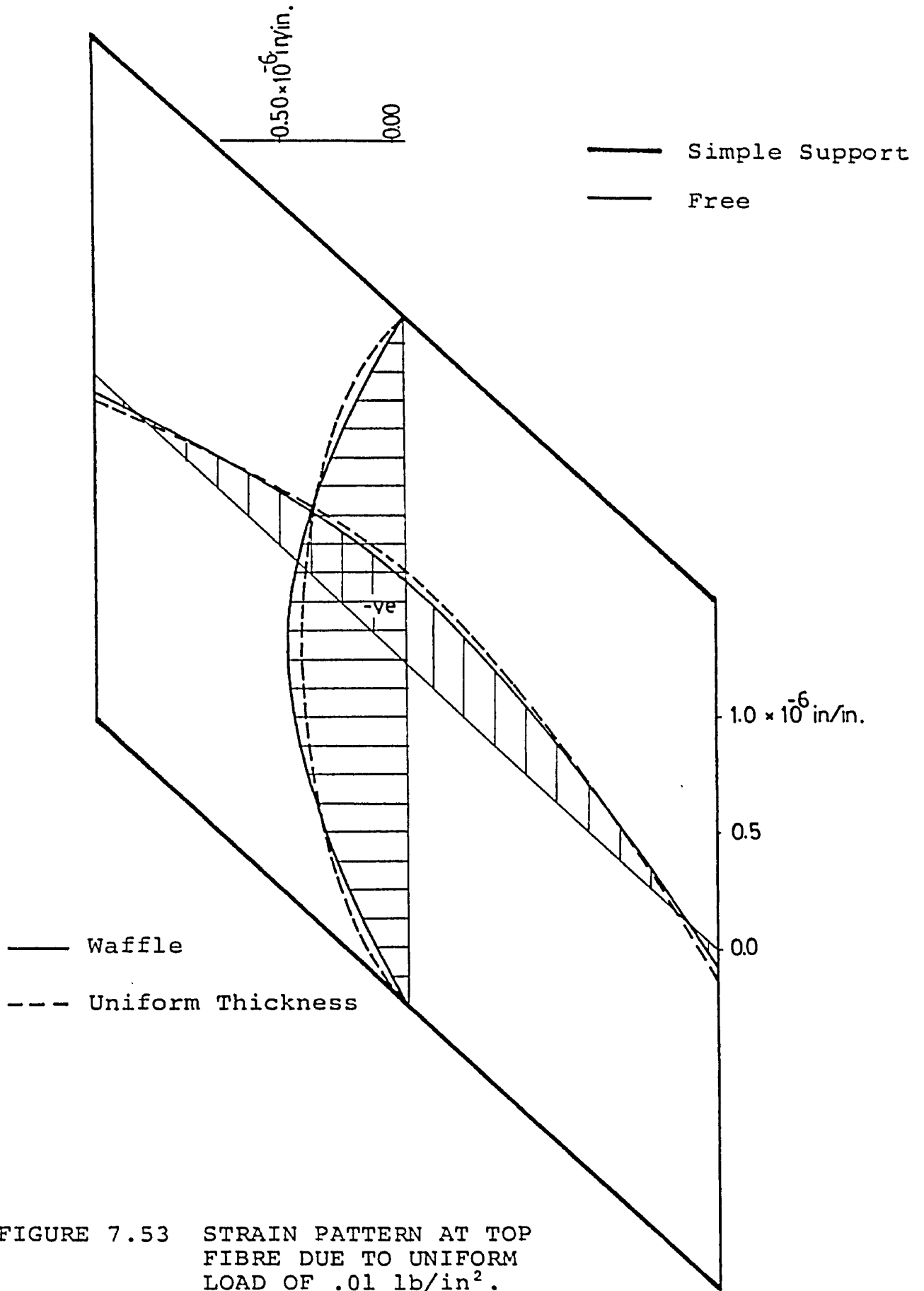


FIGURE 7.53 STRAIN PATTERN AT TOP FIBRE DUE TO UNIFORM LOAD OF .01 lb/in<sup>2</sup>.

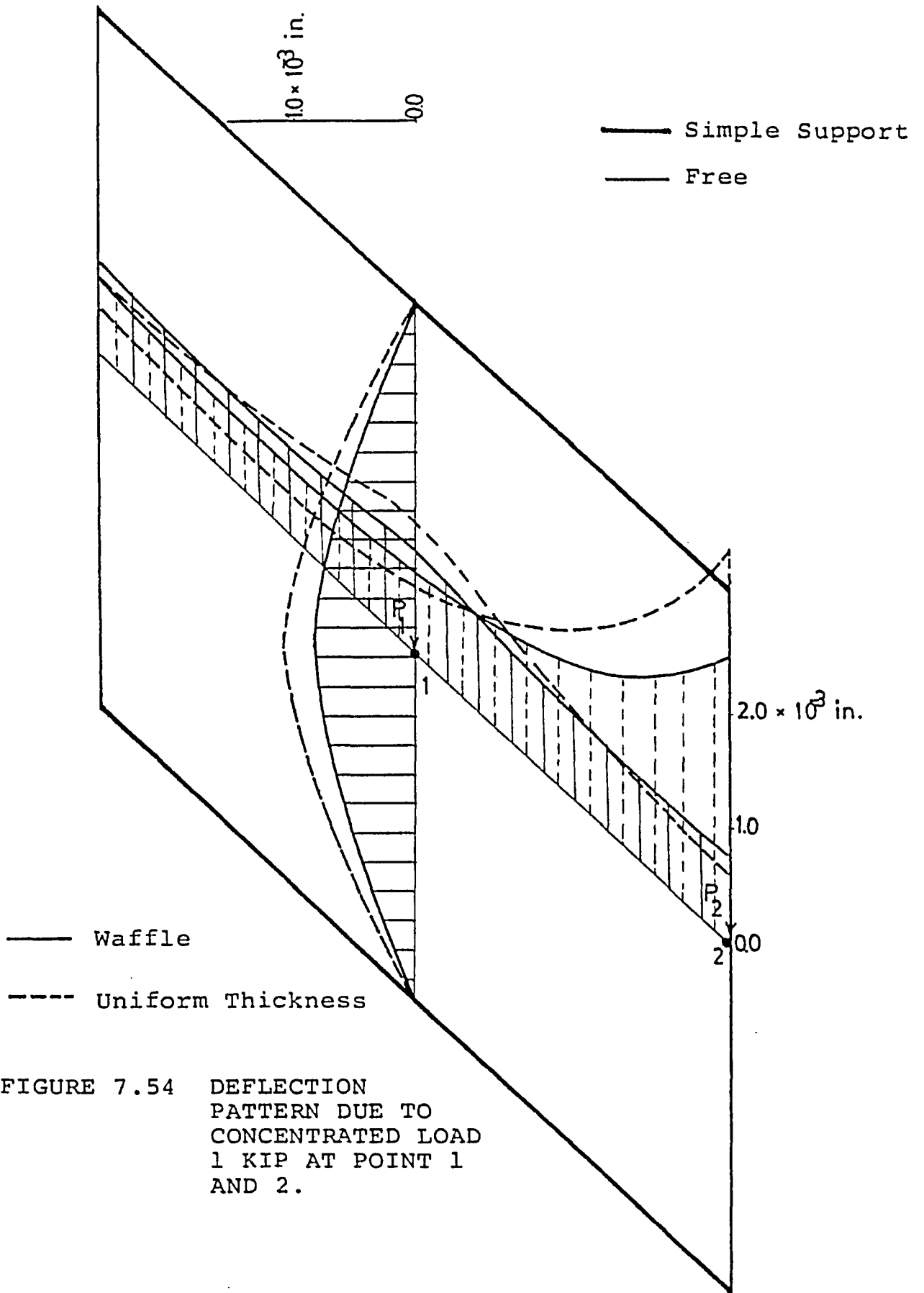


FIGURE 7.54 DEFLECTION PATTERN DUE TO CONCENTRATED LOAD 1 KIP AT POINT 1 AND 2.



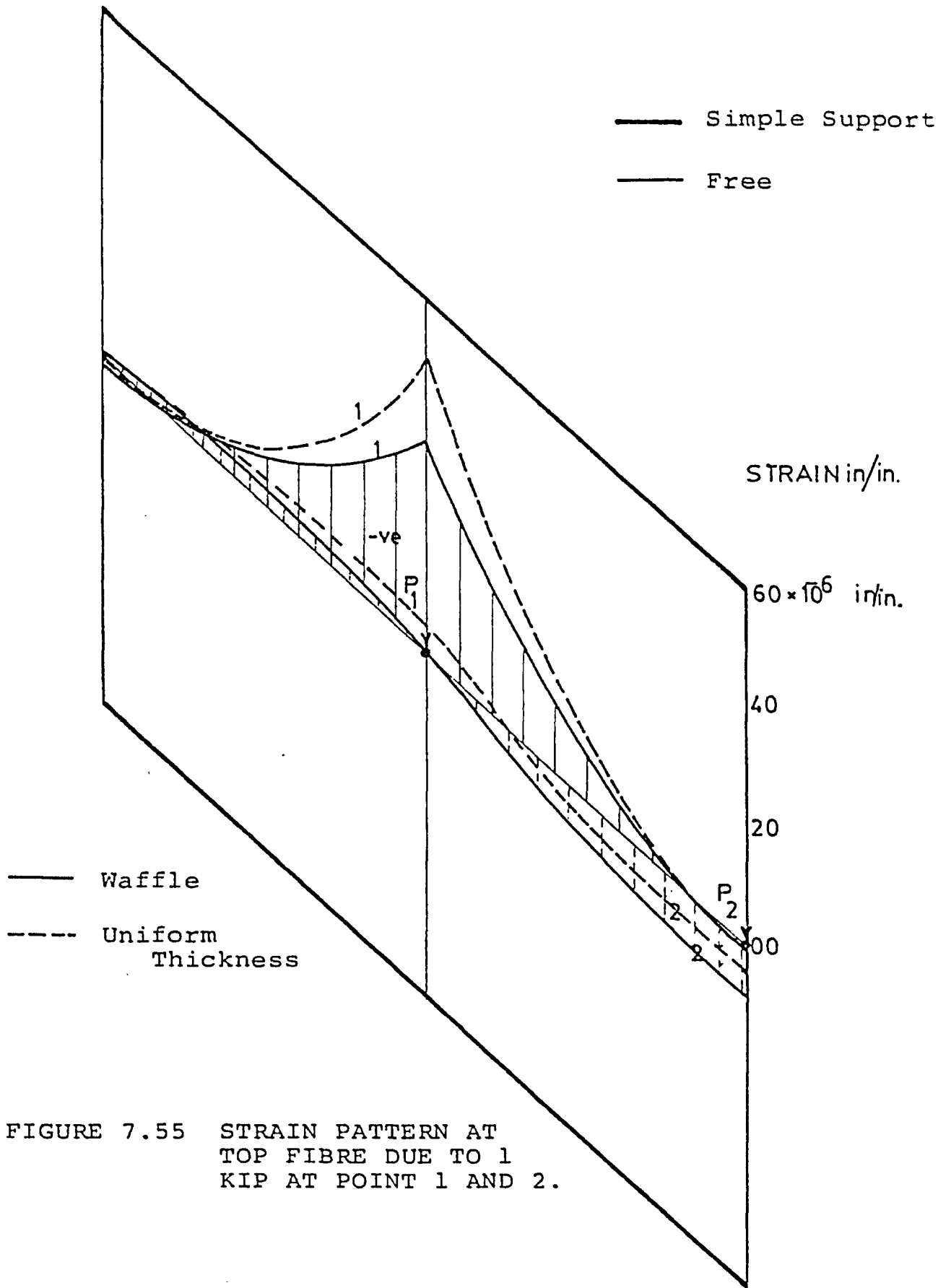


FIGURE 7.55 STRAIN PATTERN AT TOP FIBRE DUE TO 1 KIP AT POINT 1 AND 2.

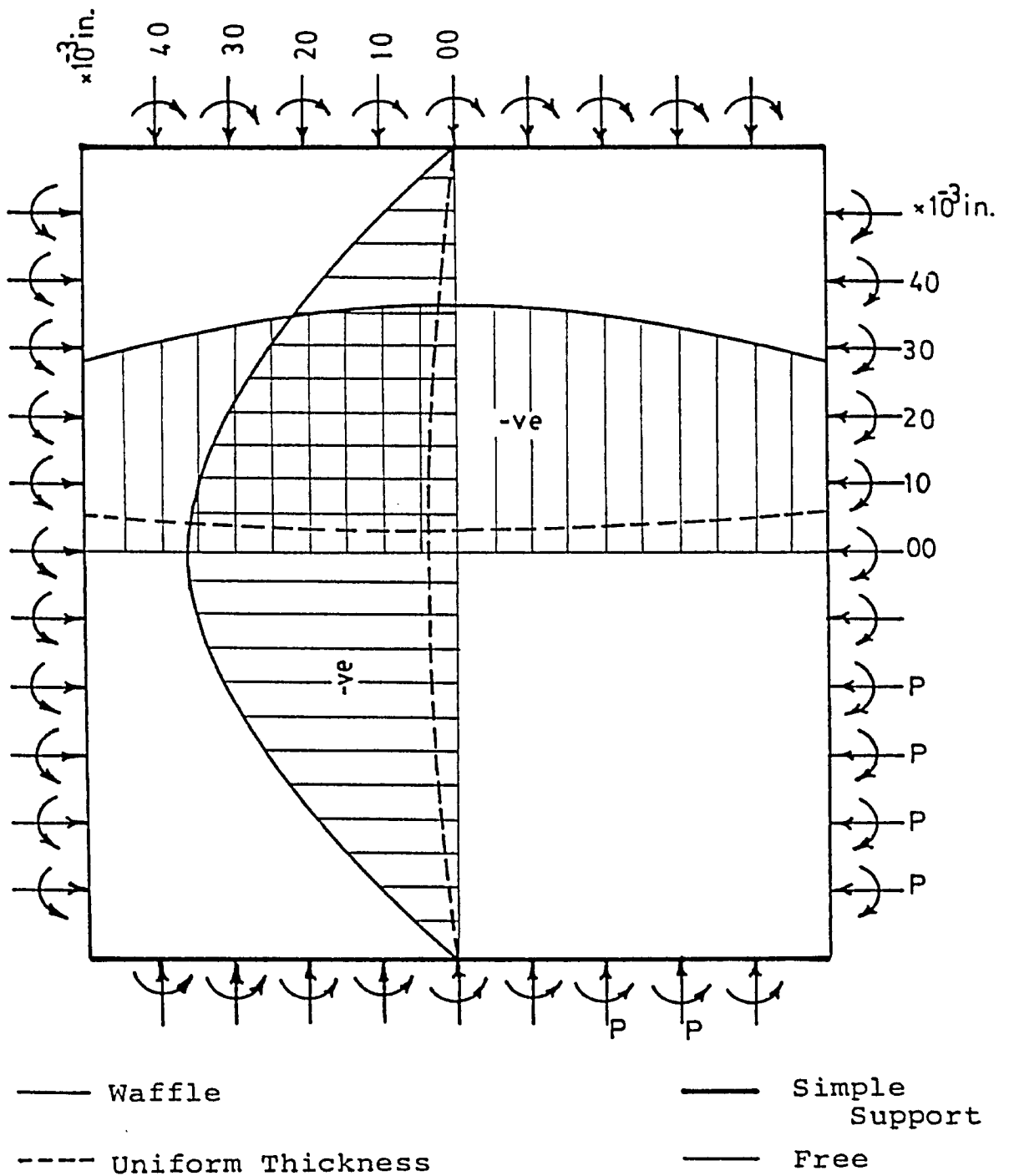


FIGURE 7.56 DEFLECTION (CAMBER) DUE TO PRESTRESSING FORCE.

## APPENDICES

## APPENDIX (A)

### Expressions For Matrix Elements

$$A_1 = 2k_3k_4$$

$$A_2 = k_3^2 - k_4^2$$

$$A_3 = k_3(k_3^2 - 3k_4^2)$$

$$A_4 = k_4(3k_3^2 - k_4^2)$$

$$A_5 = -EI(A_2^2 - A_1^2)x_2^4$$

$$A_6 = 2EIx_2^4A_1A_2$$

$$A_7 = -R_1k_4 - R_2$$

$$A_8 = -x_2(R_1k_4 - R_2x_2A_2)$$

$$A_9 = -x_2(R_1k_3 + R_2x_2A_1)$$

$$A_{10} = R_3A_3 - R_4A_1 - R_5k_3$$

$$A_{11} = -R_3A_4 - R_4A_2 + R_5k_4 + R_6$$

$$A_{12} = -x_2(R_4k_3 + R_5x_2A_1 - R_6x_2^2A_3)$$

$$A_{13} = R_3 + R_4x_2k_4 - R_5x_2^2A_2 - R_6x_2^3A_4)$$

$$A_{14} = R_7A_2 - R_8k_4 - R_9$$

$$A_{15} = -R_7A_1 - R_8k_3$$

$$A_{16} = GJk_4 + R_{10}$$

$$A_{17} = -R_7 - R_8x_2k_4 + R_9x_2^2A_2)$$

$$A_{18} = -x_2(R_8k_3 + R_9x_2A_1)$$

$$A_{19} = -x_2^2(GJA_1 - R_{10}x_2A_3)$$

$$A_{20} = -x_2^2 (GJA_2 + R_{10}x_2A_4)$$

$$A_{21} = -T_n k_3$$

$$A_{22} = T_n k_4 - 1/c$$

$$A_{23} = x_2 k_3 / c$$

$$A_{24} = T_n - x_2 k_4 / c$$

$$A_{25} = k_3 / c$$

$$A_{26} = T_n - k_4 / c$$

$$A_{27} = -T_n k_3 x_2$$

$$A_{28} = -1/c + T_n k_4 x_2$$

$$B_1 = 2k_3 k_5$$

$$B_2 = k_3^2 - k_5^2$$

$$B_3 = k_3 (k_3^2 - 3k_5^2)$$

$$B_4 = k_5 (3k_3^2 - k_5^2)$$

$$B_5 = -EIY_2^4 (B_2^2 - B_1^2)$$

$$B_6 = 2EIY_2^4 B_1 B_2$$

$$B_7 = R_1 k_5 - R_2$$

$$B_8 = Y_2 (R_1 k_5 + R_2 Y_2 B_2)$$

$$B_9 = Y_2 (R_1 k_3 - R_2 Y_2 B_1)$$

$$B_{10} = R_3 B_3 + R_4 B_1 - R_5 k_3$$

$$B_{11} = -R_3 B_4 + R_4 B_2 + R_5 k_5 - R_6$$

$$B_{12} = -Y_2 (R_4 k_3 - R_5 Y_2 B_1 - R_6 Y_2^2 B_3)$$

$$B_{13} = -R_3 + R_4 Y_2 k_5 + R_5 Y_2^2 B_2 - R_6 Y_2^3 B_4$$

$$B_{14} = R_7 B_2 + R_8 k_5 - R_9$$

$$B_{15} = -R_7 B_1 + R_8 k_3$$

$$B_{16} = GJk_5 - R_{10}$$

$$B_{17} = -R_7 + R_8 y_2 k_5 + R_9 y_2^2 B_2$$

$$B_{18} = y_2 (R_8 k_3 - R_9 y_2 B_1)$$

$$B_{19} = y_2^2 (GJB_1 + R_{10} y_2 B_3)$$

$$B_{20} = -y_2^2 (GJB_2 - R_{10} y_2 B_4)$$

$$B_{22} = T_n k_5 + 1/c$$

$$B_{23} = k_3 y_2 / c$$

$$B_{24} = -T_n - k_5 y_2 / c$$

$$B_{26} = -T_n - k_5 / c$$

$$B_{27} = -T_n k_3 y_2$$

$$B_{28} = 1/c + T_n k_5 y_2$$

$$d_{11} = -D_x / c^2$$

$$d_{12} = 2D_x s / c^2$$

$$d_{13} = -(D_x s^2 / c^2 + D_1)$$

$$d_{21} = -D_2 / c^2$$

$$d_{22} = 2D_2 s / c^2$$

$$d_{23} = -(D_2 s^2 / c^2 + D_y)$$

$$d_{31} = 0$$

$$d_{32} = D_{xy} / c$$

$$d_{33} = -D_{xy} s/c$$

$$K_{1n} = \cosh R_{1n} \cos R_{r1}$$

$$K_{2n} = \sinh R_{1n} \cos R_{r1}$$

$$K_{3n} = \sinh R_{1n} \cos R_{r1}$$

$$K_{4n} = \cosh R_{1n} \sin R_{r1}$$

$$K_{5n} = \cosh R_{2n} \cos R_{r2}$$

$$K_{6n} = \sinh R_{2n} \sin R_{r2}$$

$$K_{7n} = \sinh R_{2n} \cos R_{r2}$$

$$K_{8n} = \cosh R_{2n} \sin R_{r2}$$

$$L_{1n} = \cosh S_{1n} \cos S_{s1}$$

$$L_{2n} = \sinh S_{1n} \sin S_{s1}$$

$$L_{3n} = \sinh S_{1n} \cos S_{s1}$$

$$L_{4n} = \cosh S_{1n} \sin S_{s1}$$

$$L_{5n} = \cosh R_{2n} \cos S_{s2}$$

$$L_{6n} = \sinh R_{2n} \sin S_{s2}$$

$$L_{7n} = \sinh R_{2n} \cos S_{s2}$$

$$L_{8n} = \cosh R_{2n} \sin S_{s2}$$

$$R_{r1} = x_2 k_4 \alpha_n^b$$

$$R_{r2} = k_4 \beta_n^a$$

$$R_{1n} = x_2 k_3 \alpha_n^b$$

$$R_{2n} = k_3 \beta_n^a$$

$$S_{aa} = 2/(\beta_n^2 a^2 (\beta_n^2 a^2 / x_2^2 + 2A_2 m^2 \pi^2) + m^4 \pi^4)$$

$$S_{a1} = S_{aa} m \pi (-1)^m$$

$$S_{a2} = S_{aa} \beta_n a (-1)^m$$

$$S_{ba} = 2/(\beta_n^2 a^2 (\beta_n^2 a^2 / y_2^2 + 2B_2 m^2 \pi^2) + m^4 \pi^4)$$

$$S_{b1} = S_{ba} m \pi (-1)^m$$

$$S_{b2} = S_{ba} \beta_n a (-1)^m$$

$$S_{s1} = y_2 k_5 \alpha_n b$$

$$S_{s2} = k_5 \beta_n a$$

$$S_{xa} = 2/(x_2^2 \alpha_n^2 b^2 (\alpha_n^2 b^2 + 2A_2 m^2 \pi^2) + m^4 \pi^4)$$

$$S_{x1} = S_{xa} m \pi (-1)^m$$

$$S_{x2} = S_{xa} \alpha_n b (-1)^m$$

$$S_{ya} = 2/(y_2^2 \alpha_n^2 b^2 (\alpha_n^2 b^2 + 2B_2 m^2 \pi^2) + m^4 \pi^4)$$

$$S_{y1} = S_{ya} m \pi (-1)^m$$

$$S_{y2} = S_{ya} \alpha_n b (-1)^m$$

$$S_{1n} = y_2 k_3 \alpha_n b$$

$$T_{a1} = A_1 \beta_n^2 a^2$$

$$T_{a2} = A_2 \beta_n^2 a^2 + m^2 \pi^2$$

$$T_{a3} = k_3 (\beta_n^2 a^2 / x_2 + m^2 \pi^2)$$

$$T_{a4} = k_4 (\beta_n^2 a^2 / x_2 - m^2 \pi^2)$$

$$T_{b1} = B_1 \beta_n^2 a^2$$

$$T_{b2} = B_2 \beta_n^2 a^2 / y_2 + m^2 \pi^2$$



$$T_{b3} = k_3 (\beta_n^2 a^2 / y_2 + m^2 \pi^2)$$

$$T_{b4} = k_5 (\beta_n^2 a^2 / y_2 - m^2 \pi^2)$$

$$T_{x1} = A_1 \alpha_n^2 b^2 x_2^2$$

$$T_{x2} = A_2 \alpha_n^2 b^2 x_2^2 + m^2 \pi^2$$

$$T_{x3} = x_2 k_3 (x_2 \alpha_n^2 b^2 + m^2 \pi^2)$$

$$T_{x4} = x_2 k_4 (x_2 \alpha_n^2 b^2 - m^2 \pi^2)$$

$$T_{y1} = B_1 \alpha_n^2 b^2 y_2^2$$

$$T_{y2} = B_2 y_2^2 \alpha_n^2 b^2 + m^2 \pi^2$$

$$T_{y3} = k_3 y_2 (y_2 \alpha_n^2 b^2 + m^2 \pi^2)$$

$$T_{y4} = y_2 k_5 (y_2 \alpha_n^2 b^2 - m^2 \pi^2)$$

$$u_{3n} = k_3 \beta_n u$$

$$u_{4n} = k_4 \beta_n u$$

$$u_{5n} = k_5 \beta_n u$$

$$v_{3n} = x_2 k_3 \alpha_n v$$

$$\bar{v}_{3n} = y_2 k_3 \alpha_n v$$

$$v_{4n} = x_2 k_4 \alpha_n v$$

$$v_{5n} = y_2 k_5 \alpha_n v$$

## APPENDIX (B)

### Fourier Coefficients For Lateral Load

The Fourier coefficients of Equation 5.2 are evaluated below:

$$\begin{aligned} a_{00} &= (1/2a) \int_{-a}^a f_0(u) du \\ &= (1/2a) \int_{-a}^a \left\{ C_{17} + C_{20} (u^2/a^2) + C_{21} + C_{24} (Tu^4/b^4 - 1) \right\} du \\ &= C_{17} + 1/3 C_{20} + C_{21} + C_{24} (Ta^4/5b^4 - 1) \end{aligned}$$

$$\begin{aligned} a_{0m} &= (1/a) \int_{-a}^a f_0(u) \cos \alpha_m u du \\ &= C_{20} I_{1m} + C_{24} T I_{3m} a^4/b^4 \end{aligned}$$

The integrals  $I_{1m}$ ,  $I_{3m}$ , etc. are defined at the end of this appendix

$$b_{0m} = (1/a) \int_{-a}^a f_0(u) \sin \alpha_m u du = 0$$

$$\begin{aligned} c_{n0} &= (1/2a) \int_{-a}^a f_n(u) du \\ &= (C_{1n} W_{1n} + C_{4n} W_{2n} + C_{5n} W_{3n} + C_{8n} W_{4n}) (-1)^n \end{aligned}$$

$$\begin{aligned} c_{nm} &= (1/a) \int_{-a}^a f_n(u) \cos \alpha_m u du \\ &= (C_{1n} A_{j1} + C_{4n} A_{j2} + C_{5n} A_{j3} + C_{8n} A_{j4}) (-1)^n \end{aligned}$$

$$d_{nm} = (1/a) \int_{-a}^a f(n) \sin \alpha_n u \, du = 0$$

Fourier Expansions and Definite Integrals

$$I_{1n} = (1/a) \int_{-a}^a (u^2/a^2) \cos \alpha_n u \, du$$

$$= (1/b) \int_{-b}^b (v^2/b^2) \cos \beta_n v \, dv$$

$$= 4(-1)^n / n^2 \pi^2 \quad \text{and so on.}$$

$$I_{3n} = 8(-1)^n (1 - 6/n^2 \pi^2) / n^2 \pi^2$$

$$I_{5n} = -2(-1)^n / n \pi$$

$$I_{7n} = -2(-1)^n (1 - 6/n^2 \pi^2) / n \pi$$

$$W_{1n} = (1/2a) \int_{-a}^a \cosh u_{3n} \cos u_{4n} \, du$$

$$= x_2 (K_3 K_{7n} + K_4 K_{8n}) / a \beta_n$$

$$W_{2n} = x_2 (K_3 K_{8n} - K_4 K_{7n}) / a \beta_n$$

$$W_{3n} = y_2 (K_3 L_{7n} + K_5 L_{8n}) / a \beta_n$$

$$W_{4n} = y_2 (K_3 L_{8n} - K_5 L_{7n}) / a \beta_n$$

$$W_{5n} = (K_3 K_{3n} + K_4 K_{4n}) / b \alpha_n$$

$$W_{6n} = (K_3 K_{4n} - K_4 K_{3n}) / b \alpha_n$$

$$W_{7n} = (K_3 L_{3n} + K_5 L_{4n}) / b \alpha_n$$

$$W_{8n} = (K_3 L_{4n} - K_5 L_{3n}) / b \alpha_n$$

$$\begin{aligned} A_{j1} &= (1/a) \int_{-a}^a \cosh u_{3n} \cos u_{4n} \cos \alpha_m u \, du \\ &= S_{a2} (T_{a3} K_{7n} + T_{a4} K_{8n}) \end{aligned}$$

$$A_{j2} = (S_{a2} (-T_{a4} K_{7n} + T_{a3} K_{8n}))$$

$$A_{j3} = S_{b2} (T_{b3} L_{7n} + T_{b4} L_{8n})$$

$$A_{j4} = S_{b2} (-T_{b4} L_{7n} + T_{b3} L_{8n})$$

$$A_{j5} = S_{x2} (T_{x3} K_{3n} + T_{x4} K_{4n})$$

$$A_{j6} = S_{x2} (-T_{x4} K_{3n} + T_{x3} K_{4n})$$

$$A_{j7} = S_{y2} (T_{y3} L_{3n} + T_{y4} L_{4n})$$

$$A_{j8} = S_{y2} (T_{y4} L_{3n} - T_{y3} L_{4n})$$

$$\begin{aligned} B_{j1} &= (1/a) \int_{-a}^a \sinh u_{3n} \cos u_{4n} \sin \alpha_m u \, du \\ &= S_{a1} (-T_{a2} K_{7n} - T_{a1} K_{8n}) \end{aligned}$$

$$B_{j2} = S_{a1} (T_{a1} K_{7n} - T_{a2} K_{8n})$$

$$B_{j3} = S_{b1} (-T_{b2} L_{7n} - T_{b1} L_{8n})$$

$$B_{j4} = S_{b1} (T_{b1}L_{7n} - T_{b2}L_{8n})$$

$$B_{j5} = S_{x1} (-T_{x2}K_{3n} - T_{x1}K_{4n})$$

$$B_{j6} = S_{x1} (T_{x1}K_{3n} - T_{x2}K_{4n})$$

$$B_{j7} = S_{y1} (-T_{y2}L_{3n} - T_{y1}L_{4n})$$

$$B_{j8} = S_{y1} (T_{y1}L_{3n} - T_{y2}L_{4n})$$

## APPENDIX (C)

The Fourier series is given by

$$y = f(x) = a_0/2 + \sum_{n=1}^{n=\infty} (a_n \cos 2n\pi x/X + b_n \sin 2n\pi x/X)$$

where  $X$  is the total length of the cycle.

The coefficients for Fourier series are obtained by evaluating the following definite integrals (33);

$$a_0 = (2/X) \int_{-X/2}^{X/2} f(x) dx \quad (C.1)$$

$$a_n = (2/X) \int_{-X/2}^{X/2} f(x) \cos(2n\pi x/X) dx \quad (C.2)$$

$$b_n = (2/X) \int_{-X/2}^{X/2} f(x) \sin(2n\pi x/X) dx \quad (C.3)$$

From Figure 4.2,

The width of one division =  $dx = X/m$

$$x = \left\{ (X/m) (k - \frac{1}{2}) - X/2 \right\}$$

$$x/X = \left\{ (1/m) (k - \frac{1}{2}) - \frac{1}{2} \right\}$$

Substituting in Equation (C.1)

$$\begin{aligned} a_0 &= (2/X) \sum_{k=1}^m Y_k (X/m) \\ &= (2/m) \sum_{k=1}^m Y_k \end{aligned} \quad (C.4)$$

Substituting in Equation (C.2)

$$\begin{aligned}
 a_n &= (2/X) \sum_{k=1}^m Y_k \left\{ \cos 2n\pi \left( \frac{1}{m} (k - \frac{1}{2}) - \frac{1}{2} \right) \right\} X/m \\
 &= (2/m) \sum_{k=1}^m (-1)^m Y_k \cos \left\{ (2n\pi/m) (k - \frac{1}{2}) - n\pi \right\} \\
 a_n &= (2/m) \sum_{k=1}^m (-1)^m Y_k \cos (2n\pi/m) (k - \frac{1}{2}) \quad (C.5)
 \end{aligned}$$

Substituting in Equation (C.3) and following the same procedures the final equation is obtained,

$$b_n = (2/m) \sum_{k=1}^m (-1)^m Y_k \sin (2n\pi/m) (k - \frac{1}{2}) \quad (C.6)$$

## APPENDIX (D)

### Design of Concrete Mix

Five trial mixes were made to meet the following conditions: concrete is required for reinforced and pre-stressed concrete waffle slab deck bridges;

Concrete mix must have: 3 to 4 in. range in slump, suitably vibrated and adequately cured.

Cement content: Different cement contents range from 660 to 750 lbs. per cu. yd. and air content of 5% were used in the concrete mixes.

Strength: Two different concrete mixes for strength equal to 4000 and 6000 psi were required for the reinforced and prestressed concrete slab models, respectively.

Aggregates: Maximum size of coarse aggregate was chosen as  $\frac{1}{4}$  in. with a specific gravity equal to 2.65.

Assumptions: According to reference (22, Table 10), the amount of water required per cubic yard was 300 lb. The percentage of fine aggregate to the total aggregate was assumed between 40 to 70% for the different trial mixes.

Quantities per cubic yard: From the information given, the absolute volume occupied by the paste was calculated as:

Cement, abs. vol.	=	$750 / (3.15 \times 62.4)$	=	3.81	cu. ft.
Water, abs. vol.	=	$300 / (1.0 \times 62.4)$	=	4.81	cu. ft.
Air, abs. vol.	=	$5 \times 0.27$	=	1.35	cu. ft.
Paste, total vol.	=	$3.81 + 4.81 + 1.35$	=	9.97	cu. ft.
Aggregate, abs. vol.	=	$27 - 9.97$	=	17.03	cu. ft.



Coarse aggregate, wt. =  $17.6 \times .40 \times 2.65 \times 62.4 = 1126$  lbs.

Fine aggregate, wt. =  $17.6 \times .60 \times 2.65 \times 62.4 = 1689$  lbs.

The above quantities per cubic yard were approximate, and used as a preliminary trial batch.

For 10 lbs. of cement, a trial batch consisted of:

Cement	.....	=	10.00 lbs.
Water	..... $265 \times 10/(750)$	=	4.00 lbs.
Fine aggregate	..... $1746 \times 10/(750)$	=	22.50 lbs.
Coarse aggregate	..... $1164 \times 10/(750)$	=	15.00 lbs.

Based on the workability and maximum strength of this trial mix, four trial mixes with different water/cement ratio and fine aggregate content were made using Figure 32 in reference (22). The following table shows the proportions of the five mixes and their strength after 7, 14 and 28 days.

TABLE (D.1)

Mix No.	Ratio by Weight in lbs.				Strength in psi		
	Cement	Water	Sand	Gravel	7 days	14 days	28 days
1	1.0	0.70	3.00	2.00	4000	4670	5090
2	1.0	0.60	2.50	1.80	5580	5870	6270
3	1.0	0.50	2.00	1.50	6720	6580	7710
4	1.0	0.40	1.40	1.20	7045	7965	8275
5	1.0	0.40	2.25	1.50	6600	7400	7900

The total volume of the slab and cylinders

$$= 10 \text{ ft}^3$$

and the total weight of the concrete mix required

$$= 10 \times 146 = 1460 \text{ lbs.}$$

which was divided into two batches. Mix No. 1 was chosen for the reinforced concrete waffle slabs, and Mix No. 2 for the prestressed concrete waffle slabs.

TABLE D.2

	$E_x = E_y$ $\times 10^6$ psi	Poisson's Ratio $\mu$	Depth of Neutral axis inch		Eccentricity of Prestressing Wire	
			$e_x$	$e_y$	$\bar{e}_x$	$\bar{e}_y$
GROUP	5.00	0.200	1.420	1.425	0	0
A	4.65	0.230	1.405	1.410	0	0
SLABS	3.90	0.195	1.415	1.420	0	0
GROUP	5.00	0.250	1.375	1.380	1.400	1.620
B	5.20	0.260	1.370	1.375	1.400	1.620
SLABS						

GEOMETRY AND PROPERTIES OF SLAB MODELS

TABLE D.3

	Slab	fc28 psi	Span Inch	Width Inch	Skew Angle	D <sub>x</sub>	D <sub>y</sub>	D <sub>1</sub>	D <sub>2</sub>	D <sub>xy</sub>	Edge Beam x10 <sup>6</sup>	
											EI	GJ
GROUP A	A.1	5000	84	71.5	0	10.73	10.88	0.78	0.79	1.65	0	0
	A.2	6635	84	71.5	0	12.47	12.48	1.03	1.02	1.85	0	0
	A.3	4690	84	101.1	45	10.34	10.48	0.74	0.73	1.50	0	0
GROUP B	B.1	7665	84	71.5	0	12.91	12.91	1.13	1.14	1.95	60.00	34.30
	B.2	8285	84	71.5	45	13.35	13.40	1.22	1.22	2.05	62.70	35.35

D<sub>x</sub>, D<sub>y</sub>, D<sub>1</sub>, D<sub>2</sub>, & D<sub>xy</sub> in lb. in<sup>2</sup>/in x 10<sup>6</sup>

ORTHOTROPIC RIGIDITIES OF SLAB MODELS

APPENDIX E  
CALIBRATION OF LOAD CELLS

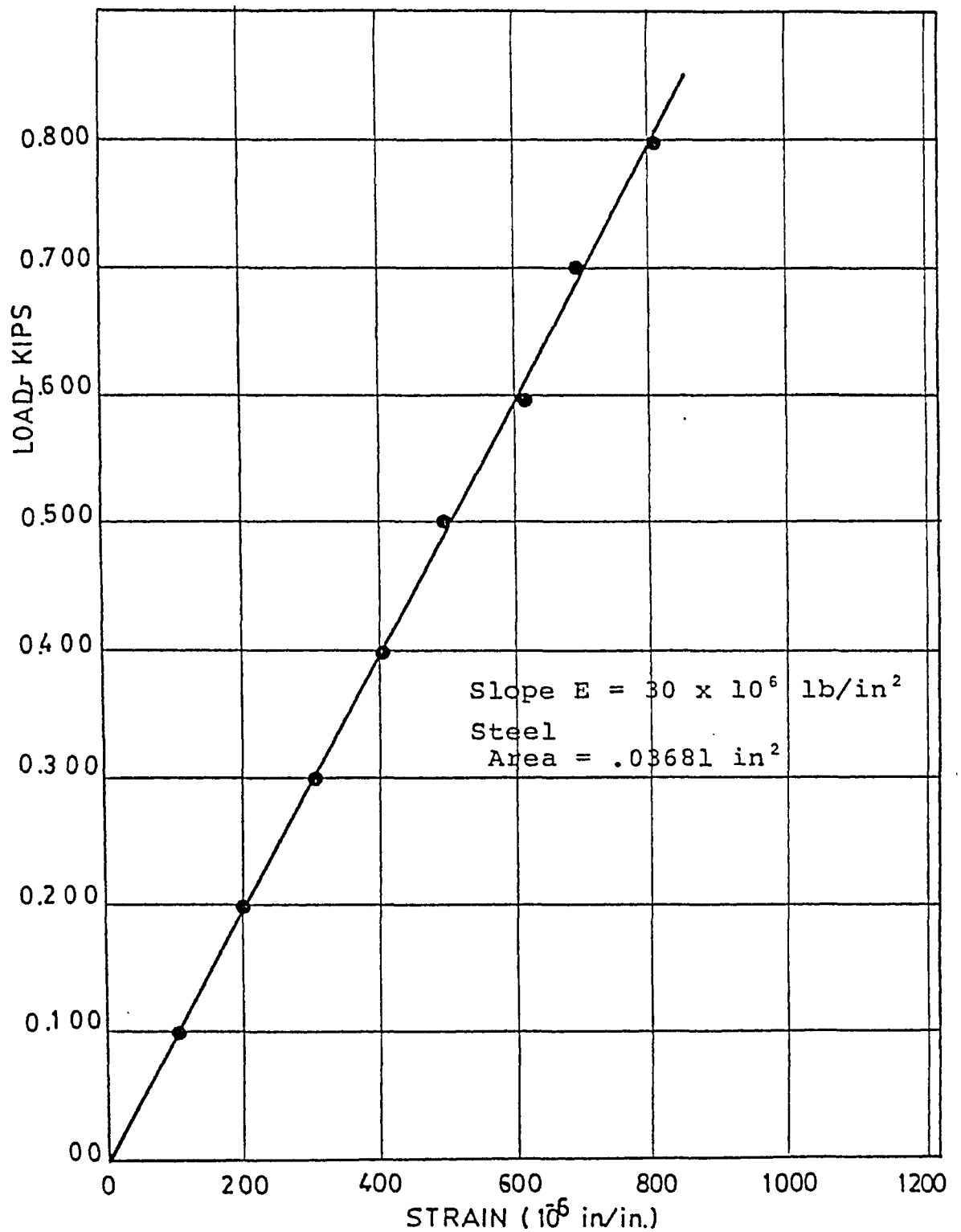


FIGURE (E1) CALIBRATION OF REINFORCING STEEL WIRES.

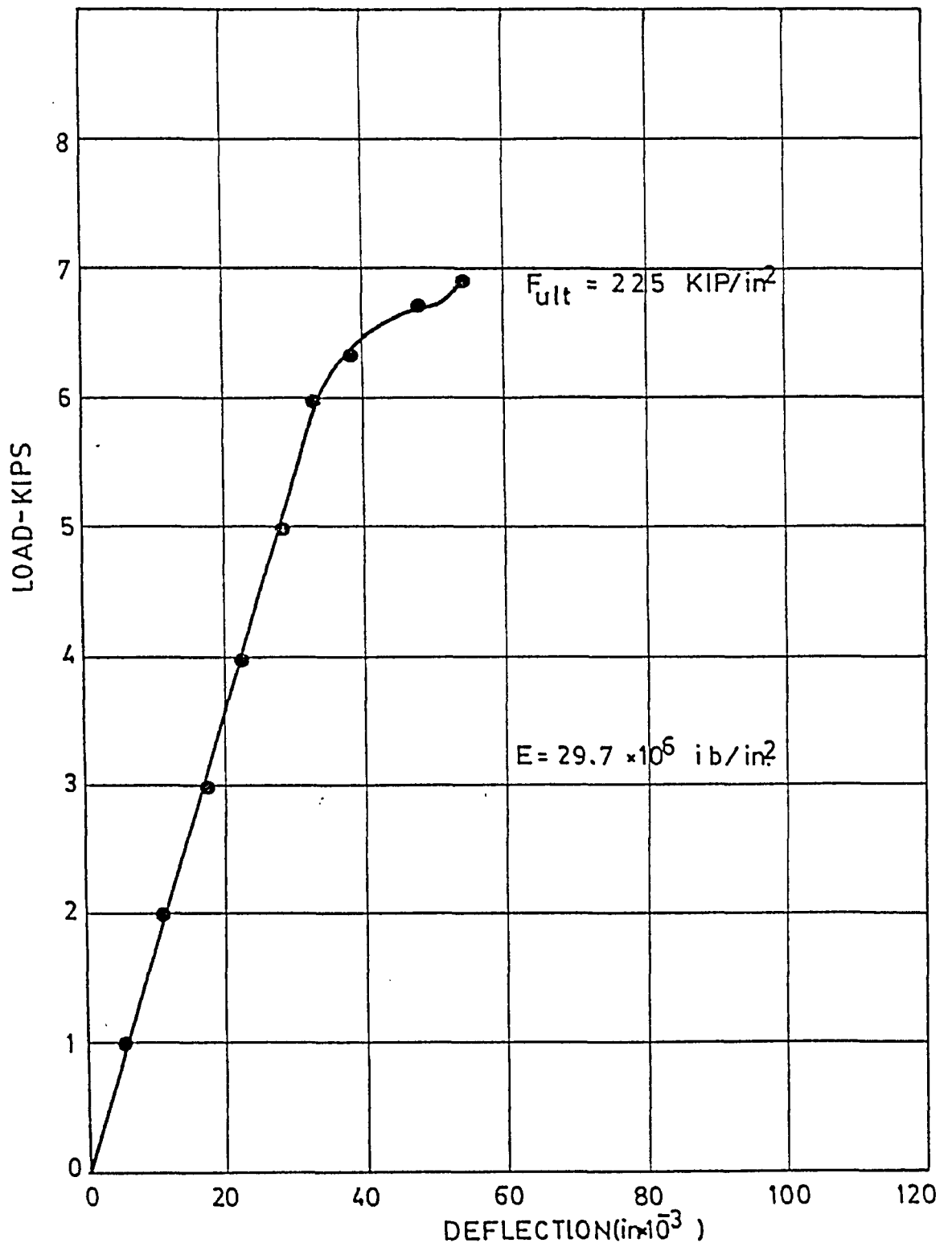


FIGURE (E2) LOAD DEFLECTION FOR HIGH TENSILE STEEL WIRE.

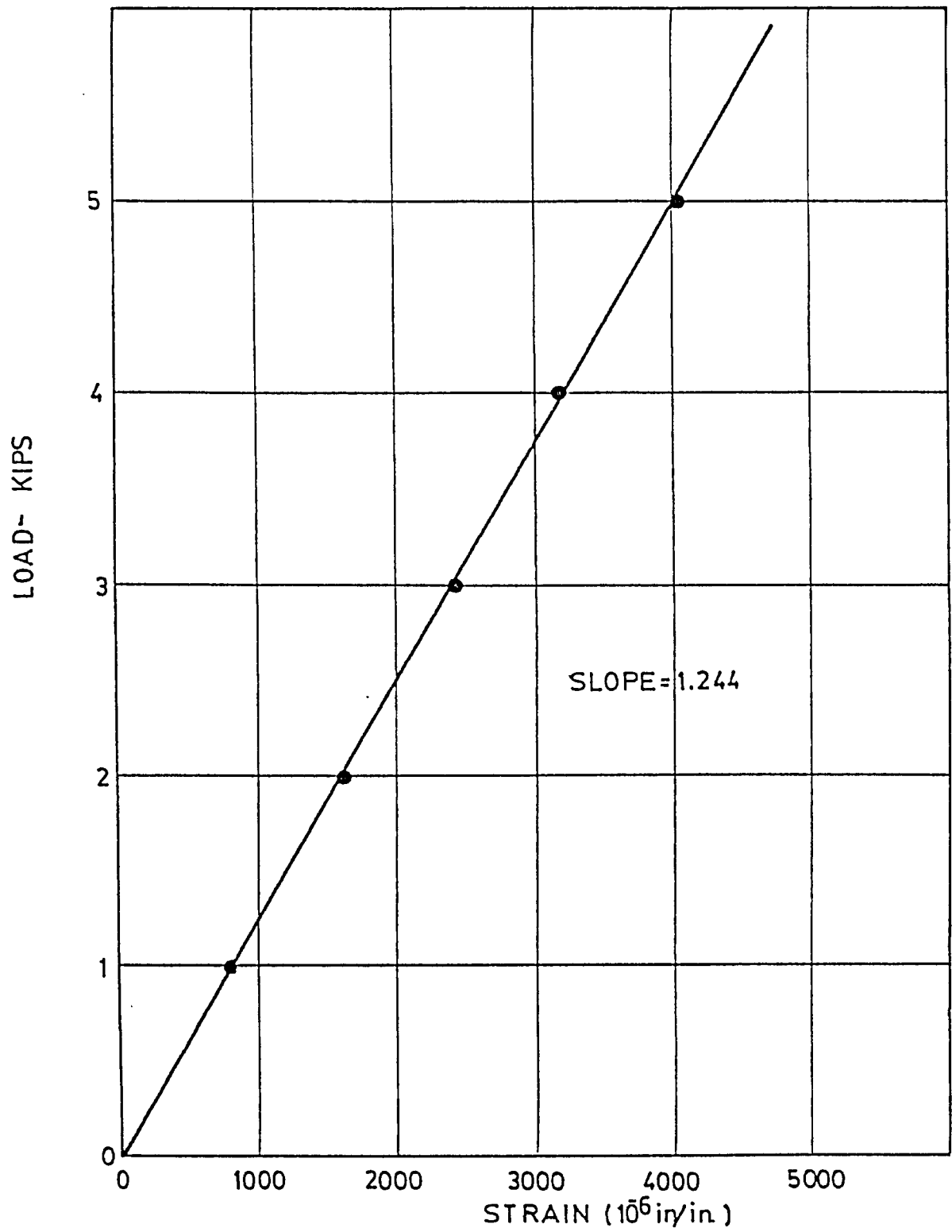


FIGURE (E3) LOAD STRAIN RELATIONSHIP (LOAD CELL 5 KIPS).



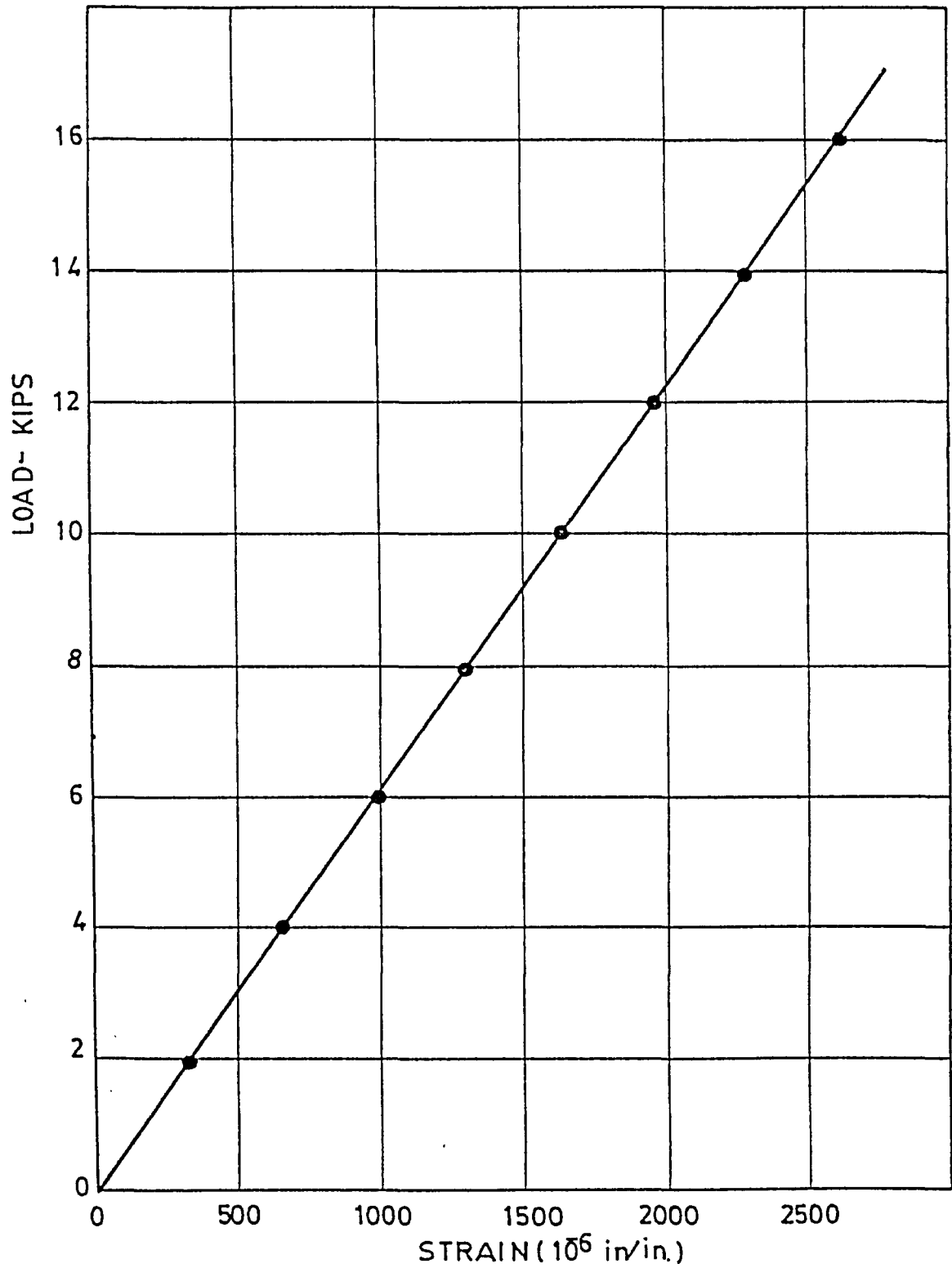


FIGURE (E4) LOAD STRAIN RELATIONSHIP (LOAD CELL 25 KIPS) .

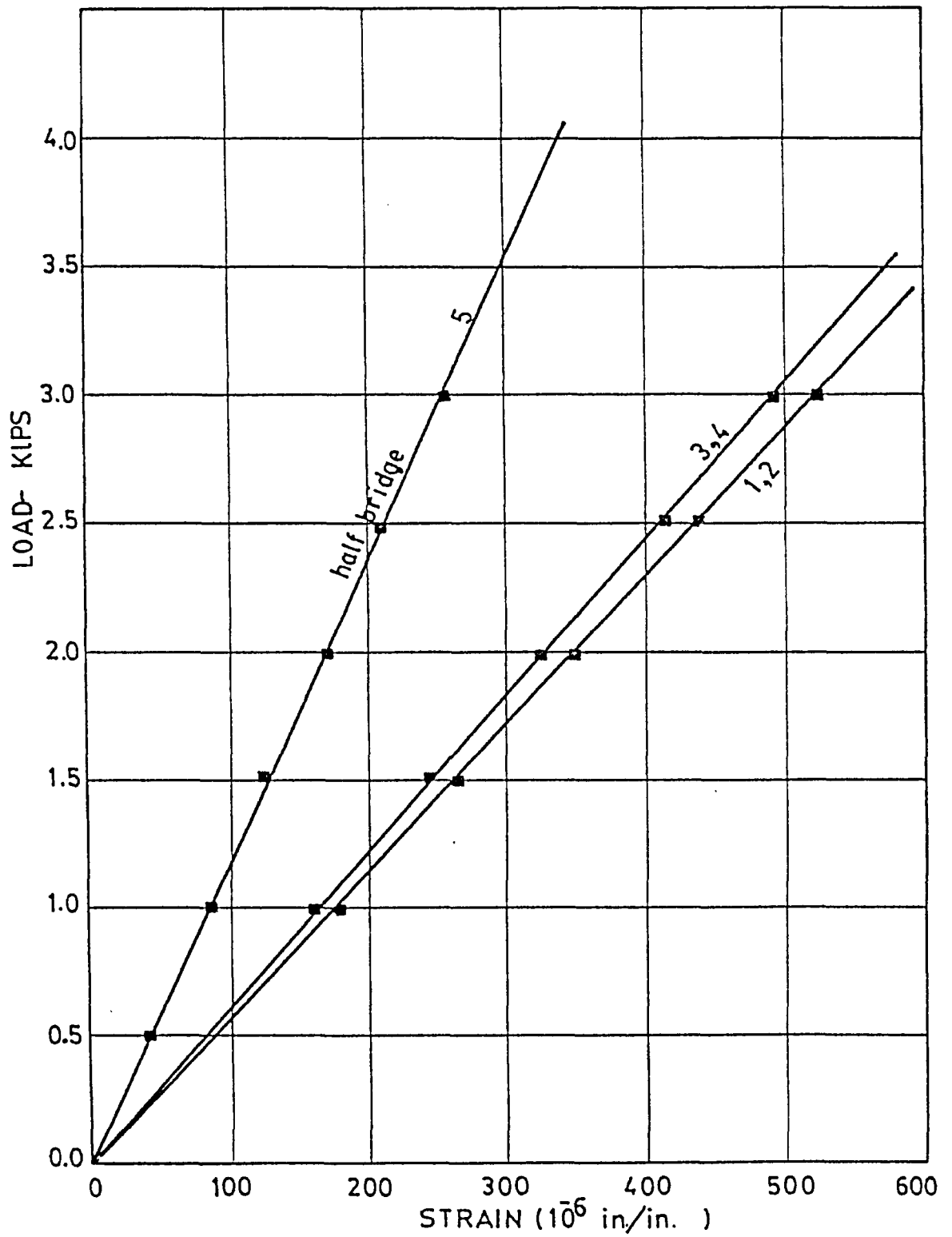


FIGURE (E5) LOAD STRAIN RELATIONSHIP  
(1-15 LOAD CELL).

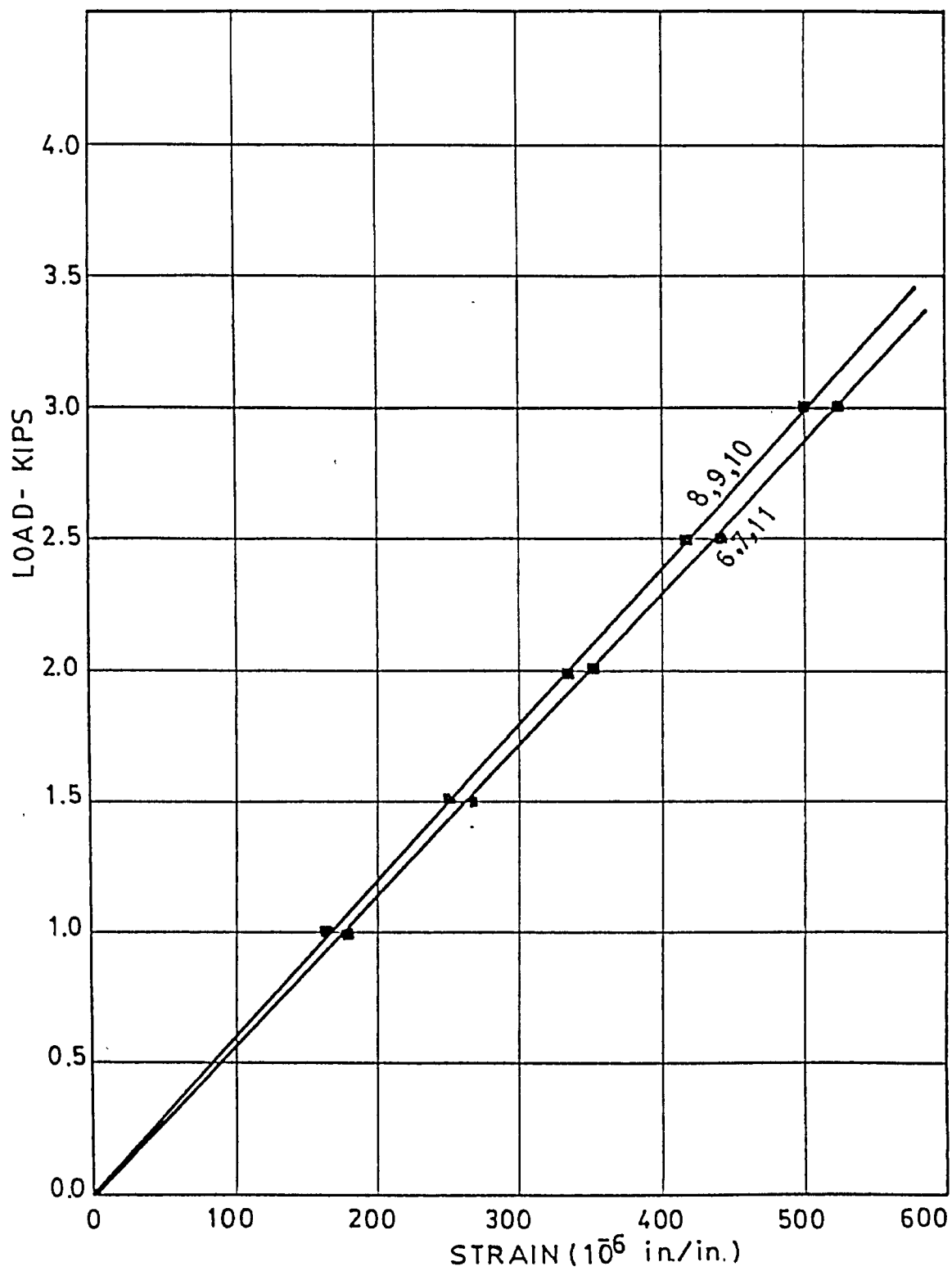


FIGURE (E6) LOAD STRAIN RELATIONSHIP  
(6-11 LOAD CELL).

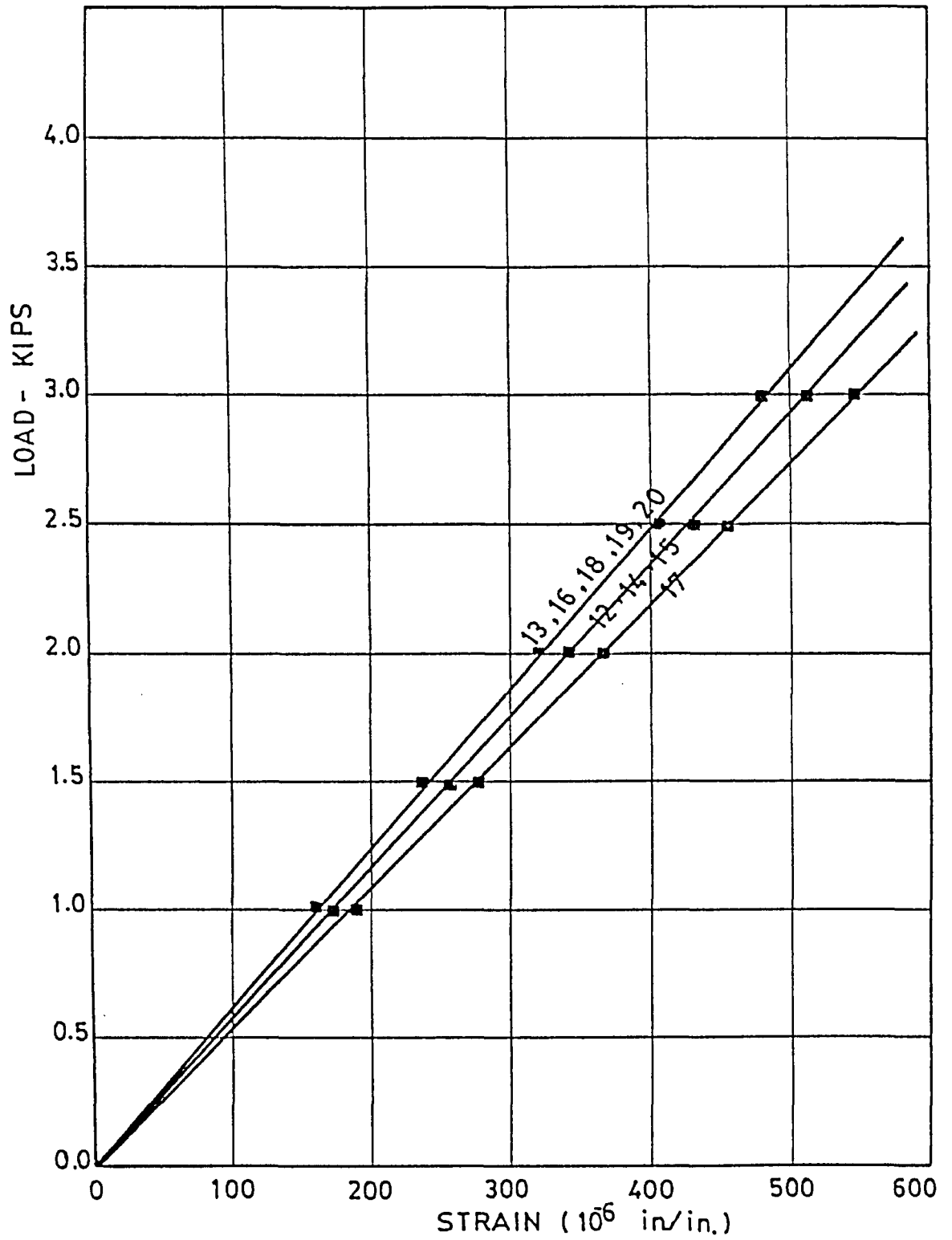


FIGURE (E7) LOAD STRAIN RELATIONSHIP  
(12-20 LOAD CELL).

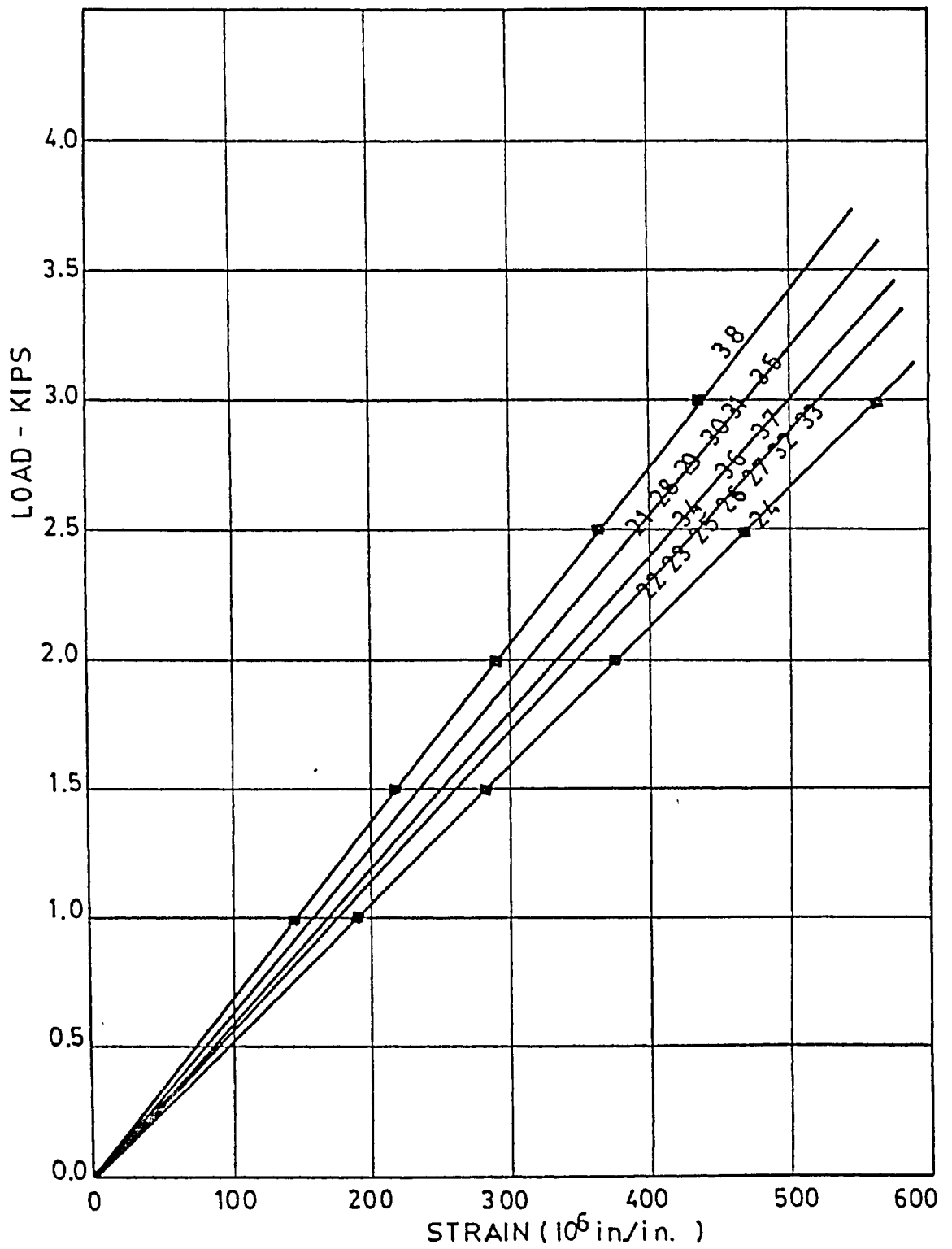


FIGURE (E8) LOAD STRAIN RELATIONSHIP.  
(21-38 LOAD CELL).

APPENDIX F  
COMPUTER PROGRAM  
(WAFFLE)



```

// RAFFLE JOB (XXXXXXXXXX,3,3,3237), 'SEBAKHY', 4SGLEVEL=(1,1), CLASS=B
*****
*REINFORCED & PRESTRESSED CONCRETE RAFFLE SLAB DECK BRIDGES
*****
*COEFFIC DIMENSIONAL ARRAY OF DIMENSION(N,N,S) TO STORE THE MATRIX EQUATION
*OC=I/O DIMENSIONAL ARRAY OF DIMENSION(N,N) TO STORE THE SOL. VECTORS
*STOR=2 DIMENSIONAL ARRAY OF DIMENSION(NST1,NST2) TO STORE SOME OF THE
*ELEMENTS FOR ANTI-SYMMETRIC LOADING
*DIM=VECTORS OF DIMENSION (NS)
*VL=2/DIMENSIONAL ARRAY OF DIMENSION(4,5).THE FIRST DIMENSION IS THE
*SERIAL NUMBER OF THE LOADING CASE AND THE SECOND ONE REPRESENTS U&V
*COORDINATES OF THE CENTRE OF PATCH LOAD,THE WIDTH AND THE LENGTH OF THE
*PATCH LOAD AND THE TOTAL LOAD RESPECTIVELY.
*NS=8N+4
*JS=NS+LN
*NST1=8N+4
*NST2=8N+4+LN
*NSS=NS*NG
*N=MAXIMUM NUMBER OF HARMONIC
*LN=MAXIMUM NUMBER OF LOADING CASES(4).
*N=LESS THAN 3,IF ALL QUANTITIES ARE NEEDED AND GREATER THAN 3,IF INPUT &
*FINAL RESULTS ONLY ARE NEEDED.
*Z=0 OR +VE FOR SYMMETRICAL LOADING ONLY.
*Z=-1 FOR ANTI-SYMMETRICAL LOADING.
*N=0 FOR BRIDGE SLAB.
*II=SLAB NUMBER.
*AS=SEMI WIDTH OF SLAB.
*BS=SEMI SPAN OF THE SLAB.
*GAS=KELV ANGLE IN DEGREE.
*NL=FACTUAL NUMBER OF LOADING CASES TO BE SOLVED.
*MNH=FINAL NUMBER OF HARMONIC TO BE SOLVED.
*NGC=NUMBER OF POINTS AT WHICH THE DEFLECTIONS AND MOMENTS ARE REQUIRED.
*NGPB=THE SERIAL NUMBER OF THE GAGE FOR WHICH THE STRAIN IN THE BOTTOM
*FIBRE OF THE SLAB IS REQUIRED.
*NGPB=0, STRAINS ARE NOT EVALUATED.
*YTP=DEPTH OF NEUTRAL AXIS OF BENDING FROM THE TOP FIBRE IN X-DIRECTION.
*YTB=DEPTH OF NEUTRAL AXIS OF BENDING FROM THE TOP FIBRE IN Y-DIRECTION.
*YTU=DEPTH OF NEUTRAL PLANE FOR TWISTING MOMENTS FROM THE TOP FIBRE
*THK=TOTAL SLAB THICKNESS.
*MU=NO. OF PRESTRESSING FORCES ALONG THE SUPPORT.
*MV=NO. OF PRESTRESSING FORCES ALONG THE FREE EDGE.
*ECU=COEFFICIENCY OF PRESTRESSING FORCE ALONG THE SUPPORTS.
*ECV=COEFFICIENCY OF PRESTRESSING FORCE ALONG THE FREE EDGE.
*FU=PRESTRESSING FORCE ALONG THE SUPPORTS.
*FV=PRESTRESSING FORCE ALONG THE FREE EDGE.
*EXC=MODULUS OF ELASTICITY OF CONCRETE IN X-DIRECTION.
*EYC=MODULUS OF ELASTICITY OF CONCRETE IN Y-DIRECTION.
*AXX=AREA OF ONE RIB PER UNIT WIDTH OF RIB SPACING IN X-DIRECTION
*AYY=AREA OF ONE RIB PER UNIT WIDTH OF RIB SPACING IN Y-DIRECTION
*AMU=POISSON'S RATIO OF SLAB MATERIAL.
*TK=THICKNESS OF FLANGE ONLY.
*****
* HOW TO PUT THE INPUT DATA *
*****
*****
*Z,ZA,ZB,ZC,YTP,YTY,YTU,THK (1X,7F10.0)
*II,A,B,SA,JA,OY,OI (1X,4A,6F10.0)
*O2,OXY,OYX,ZI,GJ,NL,I,NP,O (5F10.0,4IS)
*NGC ,BOTTOM FIBRE(15),IF BOTH OR TOP FIBRE (2(5)
*CENTRE COORDINATES OF THE PATCH LOAD,WIDTH,LENGTH AND TOTAL LOAD OF PATCH
* (12F6.0) 5.....
*EXC,EYC,AXX,AYY,AMU,TK (10X,6F10.3)
*MU,MV,ECU,EV (2110,2F10.3)
*FU(1),FV(1),MU,ECV(I),I=1,MV (2X,12F6.2,6X)
*COORDINATES OF NGC(TOTAL POINTS) ( 12F6.0)
*****
DOUBLE PRECISION CH,OC
COMMON A,PI,SA,C,S,TN,C3,AA,AA3,AA4,Z,SYAS,C3,C3,ST,SF,T,T3,MNH A 51
COMMON /JL/ B,OX,OY,OXY,OYX,O1,O2,ZI,GJ,H,VL(4,5),Z3 A 53
COMMON /BL/ NG,NB3,NC,JC,VB2,NB3,NH4,NH5,NH6,NH7,NH9,NB1,NB2,NH,NL
COMMON /JL/ FM2(3),FM3(108),FM3(71),FM4(94),FM5(123) A 55
COMMON /EX/ UC(24),VC(24),NGC,YA(40,24),NR,CF(9),VR(3),NP(10)
COMMON /AT/ FJ(20),FV(20),MU,MV,FU1,FV1
DIMENSION CJ( 34, 39), OC( 34,4), STOR( 34,43), LI( 34), MI( 34), A 57

```



```

108 ICH( 7035)
DIMENSION F1(10), F2(10), F3(10), F4(10), F5(10), F6(10), F7(10), F8(10), F9(10), F10(10)
1 F1(1), F1(10), F2(1), F2(10), F3(1), F3(10), F4(1), F4(10), F5(1), F5(10), F6(1), F6(10), F7(1), F7(10),
2 F8(1), F8(10), F9(1), F9(10), F10(1), F10(10)
3 F1(1), F1(10), F2(1), F2(10), F3(1), F3(10), F4(1), F4(10), F5(1), F5(10), F6(1), F6(10), F7(1), F7(10),
4 F8(1), F8(10), F9(1), F9(10), F10(1), F10(10)
5 S1(10), V1(10)
DATA TEL, /
READ (5, F1), F2, F3, F4, F5, F6, F7, F8, F9, F10, F11, F12, F13, F14, F
1 F15, F16, F17, F18, F19, F20, F21, F22, F23, F24, F25, F26, F27, F28, F29, F30
2 F31, F32, F33, F34, F35, F36, F37, F38, F39
WRITE (6, F1) F2, F3, F4, F5, F6, F7, F8, F9, F10, F11, F12, F13, F
1 F14, F15, F16, F17, F18, F19, F20, F21, F22, F23, F24, F25, F26, F27, F28, F2
29, F30, F31, F32, F33, F34, F35, F36, F37, F38, F39
READ S6. (H)(1), I(1), J(1), K(1), L(1), M(1), N(1), O(1), P(1), Q(1), R(1), S(1), T(1), U(1), V(1), W(1), X(1), Y(1), Z(1)
WRITE (6, S6) (H)(1), I(1), J(1), K(1), L(1), M(1), N(1), O(1), P(1), Q(1), R(1), S(1), T(1), U(1), V(1), W(1), X(1), Y(1), Z(1)
READ S6. (H)(1), I(1), J(1), K(1), L(1), M(1), N(1), O(1), P(1), Q(1), R(1), S(1), T(1), U(1), V(1), W(1), X(1), Y(1), Z(1)
WRITE (6, S6) (H)(1), I(1), J(1), K(1), L(1), M(1), N(1), O(1), P(1), Q(1), R(1), S(1), T(1), U(1), V(1), W(1), X(1), Y(1), Z(1)
READ S6. (H)(1), I(1), J(1), K(1), L(1), M(1), N(1), O(1), P(1), Q(1), R(1), S(1), T(1), U(1), V(1), W(1), X(1), Y(1), Z(1)
WRITE (6, S6) (H)(1), I(1), J(1), K(1), L(1), M(1), N(1), O(1), P(1), Q(1), R(1), S(1), T(1), U(1), V(1), W(1), X(1), Y(1), Z(1)
READ S6. (H)(1), I(1), J(1), K(1), L(1), M(1), N(1), O(1), P(1), Q(1), R(1), S(1), T(1), U(1), V(1), W(1), X(1), Y(1), Z(1)
WRITE (6, S6) (H)(1), I(1), J(1), K(1), L(1), M(1), N(1), O(1), P(1), Q(1), R(1), S(1), T(1), U(1), V(1), W(1), X(1), Y(1), Z(1)
PI=3.141592653589793
PI=90./PI
N = 10
LN = 4
NS = 3*N + 4
JS = 75 + LN
NST1 = NS
NST2 = 4 * 1 + 4 + LN
NSS = NS * NS
CALL TINIT
READ (5, F1) Z, ZA, ZB, YTP, YTY, YTU, THK
CALL TCSED (ICPU)
CPU=ICPU/1000.
WRITE (5, 103) CPU
108 FORMAT (30X, 'CPU USED =', F3.2, ' SECS')
CALL TINIT
WRITE (6, F1) Z, ZA, ZB, YTP, YTY, YTU, THK
IF (Z.EQ.0.) GO TO 55
READ (5, 200) I1, A, B, SA, OX, OY, O1, O2, OXY, OYX, EI, GJ, NL, MNH,
1 (NP(1), I=1, MNH), NR, NGC, NTP, NGCP
WRITE (6, 200) I1, A, B, SA, OX, OY, O1, O2, OXY, OYX, EI, GJ, NL, MNH,
1 (NP(1), I=1, MNH), NR, NGC
NRC = NR
IF (NR.EQ.0) NRC = 1
READ (3, 58) ((VL(L, J), J=1, 5), L=1, NL), (VR(I), I=1, NRC)
WRITE (6, 58) ((VL(L, J), J=1, 5), L=1, NL), (VR(I), I=1, NRC)
THETA=SA*PI/180.
C=COS(THETA)
S=SIN(THETA)
READ (5, 76) EXC, EYC, AXX, AYY, AMU, TK
WRITE (6, 76) EXC, EYC, AXX, AYY, AMU, TK
76 FORMAT (10X, 3F10.3)
EX=EXC*(1./((1.-AMU**2)+AXX/TK))
EY=EYC*(1./((1.-AMU**2)+AYY/TK))
E1=AMU*EX/(1.-AMU**2)
E2=AMU*EY/(1.-AMU**2)
READ (3, 201) MU, MV, ECU, ECV
WRITE (6, 201) MU, MV, ECU, ECV
201 FORMAT (211J, 2F10.3)
READ (5, 73) (FU(I), I=1, MU)
WRITE (6, 73) (FU(I), I=1, MU)
READ (5, 75) (FV(I), I=1, MV)
WRITE (6, 75) (FV(I), I=1, MV)
75 FORMAT (2X, 12F6.2, 6X)
FUT=0
DO 215 I=1, MU
215 FUT=FUT+FU(I)
PAY=FUT/(L.*A)
FVT=0
DO 216 I=1, MV
216 FVT=FVT+FV(I)
PAX=FVT/(2.*B)
OXY1=(EX*EY/TK-PAY*E1)/OXY1
EYY=(PAY*EX/TK-PAX*E2)/OXY1
DO 202 I=1, MU
202 FU(I)=FU(I)+ECU
DO 203 I=1, MV

```

```

203 FV(I)=FV(I)+ECV
    FUI=0
    DO 204 I=1,MJ
204 FUI=FUI+FJ(I)
    FUI=FUI/(2.*A)
    FV1=0
    DO 205 I=1,MV
205 FV1=FV1+FV(I)
    FV1=-C*FV1/(2.*B)
    NT = MNH=10
    LT=NT*NL
    IF (NGC.NE.J) GO TO 104
    NGC = 12
    DO 100 I=1,J
    RI = I
    UC(I) = J.
    UC(I+4) = (I-1.)*A/4.
    VC(I) = (S-RI)*B/4.
100 VC(I+4) = J.
    UC(10) = J.
    VC(10) = 0.*B
    UC(11) = 0.*A
    VC(11) = J.
    UC(12) = 0.*A
    VC(12) = 0.*B
    GO TO 105
104 READ (8,53)(UC(I),VC(I),I=1,NGC)
    WRITE (6,53)(UC(I),VC(I),I=1,NGC)
    DO 10 I=1,LT
    DO 10 J=1,GC,24
10 YA(I,J)=1000000000.
105 NCTH = 1
    NTHE=4
    NCH = 0
    IF (JYX.EQ.J) GO TO 80
    NCH=J
    GO TO 83
80 NCH = NCH+1
    GO TO (32,J1) , NCH
    OXY = C
    OYX = C
    O1 = C
    O2 = C
    GO TO 81
81 OXY = 0.5*OXY
    OYX = OXY
    O1 = 0.5*O1
    O2 = O1
    GO TO 83
82 OYX = OXY
    O2 = O1
83 IF (SA.GT.J) GO TO 88
    DO 91 L=1,NL
    IF (VL(L,3).EQ.2*A) VLS(L) = VL(L,5)
91 CONTINUE
    NCTH = 4
    NTHE = 1
11 GO TO (34,85,86) , NTHE
    SA = 40.
    GO TO 87
84 SA = 0.004999
    GO TO 87
85 SA = 20.0
    GO TO 87
86 SA = 45.J
    DO 90 L=1,NL
87 IF (VL(L,3).EQ.2*A) VL(L,5)=CDS(SA*P/(180.))*VLS(L)
90 CONTINUE
92 CONTINUE
93 IF (NR.EQ.J) GO TO 106
    DO 107 I=1,J
    RI = I
    UR(I) = (RI-5.)*A/4.
107 UR(I+4) = (I-1.)*A/4.
    DO 101 I=1,MH
101 VR(I) = (1.-VR(I))*B
106 WRITE (6,F11) I,A,B,SA,OXY,OYX,O1,O2,OXY,OYX,EI,GJ
    IF (ZA) J,2,2

```

A 112

A 113

A 116

A 83

A 84

22	WRITE (6,87) IJ,(K,(CD(NJ,NH*(J-1)+K),J=1,8),CD(NJ,NH8+K),K=1,NN)	A	164
	GO TO (23,24,23,24), NH	A	165
	WRITE (6,822) (K,(CD(NJ,NH*(J-1)+K),J=1,8),K=5,NH)	A	166
	GO TO 23	A	167
23	NI=NH+1	A	168
	WRITE (6,823) (CD(NJ,NH8+K),K=NI,4)	A	169
24	WRITE (6,824) (CD(NJ,NC+J),J=1,NL)	A	170
	WRITE (6,844) (HF,I=1,J2)	A	171
		A	172
	*****		
	INVERSE THE MATRIX		A
	*****		
25	CALL MNA (PI,NSS,CD,OC,STOR,NS,JS,LN,NST1,NST2,L1,M1,CH)	A	174
	IF (ZACT,3) GO TO 32	A	175
	WRITE (6,833)	A	176
	DO 31 L=1,NL	A	177
	IF (NH=4) 25,27,27	A	178
26	NN=NH	A	179
	GO TO 29	A	180
27	NN=4	A	181
28	WRITE (6,812) L,(VL(L,I),I=1,5)	A	182
	WRITE (6,831)	A	183
	WRITE (6,844) (HF,I=1,J2)	A	184
	WRITE (6,823) (K,(OC(NH*(J-1)+K,L),J=1,8),OC(NH8+K,L),K=1,NN)	A	185
	IF (NH=4) JJ,31,29	A	186
29	WRITE (6,834) (K,(OC(NH*(J-1)+K,L),J=1,8),K=5,NH)	A	187
	GO TO 31	A	188
30	NI=NH+1	A	189
	WRITE (6,835) (OC(NH8+K,L),K=NI,4)	A	190
31	WRITE (6,844) (HF,I=1,J2)	A	191
		A	192
	*****		
	COMPUTE MOMENTS AND DEFLECTIONS		A
	*****		
32	IF (SYAS) J4,33,33	A	193
33	CALL OS2A (CD,OC,STOR,NS,JS,LN,NST1,NST2)	A	194
	IF(NR.NE.0) CALL OSRA(CD,OC,STOR,NS,JS,LN,NST1,NST2)	A	195
	GO TO 35	A	196
34	CALL O2A (CD,OC,STOR,NS,JS,LN,NST1,NST2)	A	197
	IF(NR.NE.0) CALL O2A(CD,OC,STOR,NS,JS,LN,NST1,NST2)	A	198
35	IF (SYAS) 37,37,36	A	199
36	IF (ZA) 12,37,37	A	201
37	DO 40 L=1,NL	A	202
	LTX=(L-1)*NT+MNH+NHC	A	203
	LTY=LTX+4NH	A	205
	LXY=LTY+MNH	A	206
	LM1=LXY+4NH	A	207
	LM2=LM1+4NH	A	208
	LMT=LM2+4NH	A	209
	DO 40 I=1,12	A	210
	XPY=(YA(LTX,I)+YA(LTY,I))*0.5	A	211
	XMY=(YA(LTX,I)-YA(LTY,I))*0.5	A	212
	XY1=SQRT(XAY**2+(YA(LXY,I))**2)	A	213
	YA(LM1,I)=XPY+XY1	A	214
	YA(LM2,I)=XPY-XY1	A	215
	IF (XMY) 39,39,39	A	216
38	YA(LMT,I)=ATAN(YA(LXY,I)/XMY)*PI9	A	217
	GO TO 40	A	218
39	YA(LMT,I)=0.	A	219
40	CONTINUE	A	220
	IF (YTP) 41,46,41	A	221
41	DSTR=(OX*OY-D1*O2)	A	222
	DO 45 L=1,NL	A	223
	LTX=(L-1)*NT+MNH+NHC		
	LTY=LTX+4NH	A	225
	LXY=LTY+MNH	A	226
	LSX=LTY+4NH*5	A	227
	LSY=LSX+4NH	A	228
	LSUL=SY+4NH	A	229
	DO 44 I=1,MJC	A	230
	IF (I-NTP) +2,42,43	A	231
42	YA(LSX,I)=YTP*(OY*YA(LTX,I)-D1*YA(LTY,I))/DSTR	A	232
	YA(LSY,I)=YTY*(OX*YA(LTY,I)-D2*YA(LTX,I))/DSTR	A	233
	YA(LSU,I)=(YA(LSX,I)+YA(LSY,I))*0.5-2.*YTU*YA(LXY,I)/(OXY+OYX)*1.E	A	234
106	YA(LSX,I)=YA(LSX,I)-EXX	A	235

```

2      PRINT 50
3      GO TO 40
4      PRINT 50
5      WRITE (5,F12) (L,(VL(L,I)),I=1,5),L=1,NL)
6      IF (Z3) 3,6,7
7      PRINT 41
8      GO TO 42
9      PRINT 42
10     GO TO 43
11     PRINT 43
12     THETA=55*PI/180.0
13     C=COS(THETA)
14     S=SIN(THETA)
15     H=(U1+G2+OXY+OYX)/2.0
16     PK=H**2-OXX*Y
17     IF (PK) 9,15,53
18     WRITE (6,F43)
19     Y0X=THX+YTJ
20     Y0Y=THX+YTY
21     Y0Z=THX+YTJ
22     PRINT 64, (NP(I),I=1,4NH)
23
24     *****
25     COMPUTE CONSTANTS OF THE SLAB
26     *****
27
28     CALL CONST(NL)
29     GO TO 46 NHC=1,4NH
30     NH=NP(NHC)
31     NH2=NH+NH
32     NH3=NH+NH+NH
33     NH4=NH+NH+NH+NH
34     NH5=NH+NH+NH+NH+NH
35     NH6=NH+NH+NH+NH+NH+NH
36     NH7=NH+NH+NH+NH+NH+NH+NH
37     NH8=NH+NH+NH+NH+NH+NH+NH+NH
38     NB1=NH8+1
39     NB2=NH8+2
40     NB3=NH8+3
41     NC=NH8+4
42     JC=NC+NL
43
44     *****
45     COMPUTE THE MATRIX
46     *****
47
48     CALL SYLA (NS1,NSL,CD,OC,STOR,NS,JS,LN,NST1,NST2)
49     GO TO 13
50     CALL ASLA (NS1,NSL,SYAS,CD,OC,STOR,NS,JS,LN,NST1,NST2)
51     IF (2,ST,2) GO TO 25
52     IF (3,SYAS) 13,14,14
53     PRINT 15
54     PRINT 16
55     PRINT 15
56     WRITE (5,F21) ((VL(L,I),L=1,2),I=1,2)
57     WRITE (5,F14) (HF,I=1,32)
58     GO TO 20 I=1,3
59     GO TO 20 K=1,4
60     IJ=NH*(I-1)+J
61     GO TO (17,17,17), NH
62     NZ=4
63     GO TO 13
64     NN=NH
65     WRITE (6,F23) I,N,(K,(CD(IJ,NH+(J-1)+K),J=1,3),CD(IJ,NH8+K),K=1,NN
66     1)
67     GO TO (19,19,19,20), NH
68     WRITE (6,F22) (K,(CD(IJ,NH+(J-1)+K),J=1,3),K=5,NH)
69     GO TO 20
70     NI=NH+1
71     WRITE (5,F21) (CD(IJ,NH8+K),K=NH+4)
72     WRITE (5,F24) (CD(IJ,NC+J),J=1,NL)
73     GO TO 20 K=1,4
74     IJ=NH+8
75     NI=NH+4
76     GO TO (21,21,21), NH
77     NZ=4
78     GO TO 22
79     NN=NH

```

A 85  
A 86  
A 87  
A 88  
A 89  
A 90  
A 91  
A 92  
A 93  
A 94  
A 95  
A 96  
A 97  
A 98  
A 99  
A 100  
A 101  
  
A 107  
A 108  
A 109  
A 110  
  
A 118  
A 119  
A 120  
A 121  
A 122  
A 123  
A 124  
A 125  
A 126  
A 127  
A 128  
A 129  
  
A 130  
A 131  
A 132  
A 133  
A 134  
A 135  
A 136  
A 137  
A 138  
A 139  
A 140  
A 141  
A 142  
A 143  
A 144  
A 145  
A 146  
A 147  
A 148  
A 149  
A 150  
A 151  
A 152  
A 153  
A 154  
A 155  
A 156  
A 157  
A 158  
A 159  
A 160  
A 161  
A 162  
A 163

```

YA(LSY,I)=YA(LSY,I)-EYY
GO TO 44
43 YA(LSX,I)=YJL*(OY*YA(LTX,I)-O1*YA(LTY,I))/OSTR A 236
YA(LSY,I)=YJY*(OX*YA(LTY,I)-O2*YA(LTX,I))/OSTR A 237
YA(LSX,I)=(YA(LSX,I)+YA(LSY,I))*O.E-2.*YBU*YA(LXY,I)/(OXY+OYX)*1.E A 238
106 A 239
YA(LSX,I)=YA(LSX,I)-EXX A 240
YA(LSY,I)=YA(LSY,I)-EYY
CONTINUE A 241
CONTINUE
CONTINUE
***** A 248
SUMMARISE THE RESULTS
*****
IF (YTP) 49,48,49 A 250
48 KX=7 A 252
GO TO 50 A 253
49 KX=10 A 254
NTP1=NTP+1 A 255
PRINT 68, YTP, YTY, YTU, THK, NTP, NTP1, NGC A 256
50 00100 L=1,4
LT=(L-1)*NT A 258
WRITE (6, F4.2) L, (VL(L,I), I=1,5) A 259
WRITE (6,63) (HI, I=1,32), HJ, HJ, (I, HJ, I=1,12) A 264
WRITE (6,73) (HI, I=1,32), HJ, HJ, (UC(I), HJ, I=1,12), HJ, HJ, (VC(I), HJ, I=1,12), (HI, I=1,32) A 265
DO 52 K=1, K1 A 266
KX=(K-1)*8 A 260
LX=LT+(K-1)*MNH A 262
WRITE (6, F4.2) (HA(KX+I), I=1,8) A 263
WRITE (6,71) (HJ, NP(N), (HJ, YA(LK+N,I), I=1,12), HJ, [3L, N=1, MNH)
51 IF (NGC-13) 52,52,51 A 268
WRITE (6, F4.2) (HI, I=1,32) A 269
PRINT 72 A 270
WRITE (6,69) (HI, I=1,32), HJ, HJ, (I, HJ, I=13,24) A 271
WRITE (6,70) (HI, I=1,32), HJ, HJ, (UC(I), HJ, I=13,24), HJ, HJ, (VC(I), HJ, I=13,24), (HI, I=1,32) A 272
WRITE (6,71) (HJ, NP(N), (HJ, YA(LK+N,I), I=1,12), HJ, [3L, N=1, MNH)
C 52 WRITE (6, F4.2) (HI, I=1,32)
52 CONTINUE
IF (NCH.EJ.J) GO TO 103
PRINT 73
DO 102 K=1,42
LX=LT+(K+6)*MNH
WRITE (6,69) (HI, I=1,32), HJ, HJ, (I, HJ, I=1,12)
WRITE (6,70) (HI, I=1,32), HJ, HJ, (UR(I), HJ, I=1,9), UR(1), HJ, JR(9), HJ, UR(3), HJ, HJ, HJ, (VR(K), HJ, I=1,12), (HI, I=1,32)
WRITE (6,71) (HJ, NP(N), (HJ, YA(LK+N,I), I=1,12), HJ, [3L, N=1, MNH)
102 WRITE (6, F4.2) (HI, I=1,32)
103 CONTINUE
IF (NCTH.NE.1) GO TO 110
IF (NCT.EJ.J) GO TO 1
GO TO 50
110 IF (SA.NE.EJ.O) GO TO 74
DO 59 L=1,4
IF (VL(L,3).EQ.2*4) VL(L,5)=VLS(L)
89 CONTINUE
74 NTHE = NTHE+1
IF (NTHE.LT.3) GO TO 11
SA = 1.0
IF (NCH.LT.J) GO TO 30
GO TO 1
53 WRITE (6, F4.2) A 276
GO TO 1 A 277
54 WRITE (6, F4.2) A 278
GO TO 1 A 279
55 STOP A 280
***** A 281
*****
56 FORMAT (13A+.8X) A 282
57 FORMAT (15I1) A 283
58 FORMAT (12F5.2,3X) A 284
59 FORMAT (/54X'.3Y44METRIC LOADING ONLY') A 285

```

```

60   FORMAT (/42X 'GENERAL LOAD (NG(SYMMETRIC & ANTISYMMETRIC LOADS))' )      A 287
61   FORMAT (/50X 'THE SLAB IS CLAMPED ON ALL EDGES' )                        A 288
62   FORMAT (/40X 'THE SLAB IS ELASTICALLY SUPPORTED ON TWO EDGES' )          A 289
63   FORMAT (/45X 'THE SLAB IS SIMPLY SUPPORTED ON ALL EDGES' )              A 290
64   FORMAT (/45X 'NUMBER OF HARMONICS ANALYSED',4X(2,10(' ','[2]//))        A 291
65   FORMAT (/54X 'SYMMETRIC LOAD SYSTEM' )                                  A 292
66   FORMAT (/51X 'ANTI-SYMMETRIC LOAD SYSTEM' )                             A 293
67   FORMAT (/13,14,9F14,3/(17,9F14,3))                                     A 294
68   FORMAT (/45X 'DEPTHS OF N.A. FROM TOP FIBRE',3F10,4/                    A 295
    1   45X 'SLAB THICKNESS =',F10,4,' INS' /45X 'TOP GAGES'                A 296
    1   ',25X',11H1U',15/45X 'BOTTOM GAGES',12S,' THRU',15/                A 297
69   FORMAT (2X32A4/2X11,6X11,12(16,3X11))                                   A 298
70   FORMAT (2X32A4/2X11,4X'U=',A1,12(F9,2,1X,A1)/2X11,4X'V=',A1,12(F9,   A 299
    12,1X,A1)/2X32A4)                                                        A 300
71   FORMAT (2X11,1X'NH=',12,12(A1,F9,4),A1/(A2,A1,16,12(A1,F9,4),A1))    A 301
72   FORMAT (50X 'CONTINUED' )                                              A 302
73   FORMAT (/60X 'REACTIONS'//)
200  FORMAT (1X4,6E10,3/5E10,3,4(5,10X/14(5,10X))
    END                                                                    A 303-

```

```

C *****
C SUBROUTINE CONST (NL)
REAL XJ,K4,K5
COMMON A,P1,SA,C,S,TN,C1,AA,AAJ,AA4,Z,SYAS,C2,CJ,ST,SF,T,TB,MNH
COMMON /JLJ/ B,OX,OY,OXY,OYX,O1,O2,ZI,CJ,H,VL(4,5),TB
COMMON /JL1/ P,CJ(4),CJS(4),KJ,K4,K5,SB,SBJ,SB4,X2,Y2,A1,A2,A3,A4,
1 B1,B2,B3,B4,SCA,SCB,SCC,SCD,S1(4),S2(4),S3(4),S4(4),S5(4),S6(4),
2 S7(4)
COMMON /BLJ/ R1,R2,R3,R4,R5,R6,R7,R8,R9,R10,R11,R12,R13,X22,X23,X
124,Y22,Y23,Y24,A5,A6,A7,A8,A9,A10,A11,A12,A13,A14,A15,A16,A17,A19,
2A20,A21,A22,A23,A24,AC,CS,CS,CS,CS,C9,B10,B11,B12,B13,B14,B15,B16,
JB17,B18,B19,B20,B22,B23,B24,A18
COMMON /BLJ/ FM2(J),F18(108),F38(71),F19(94),F20(125)
COMMON /SPL/ A25,A26,A27,A28,B25,B27,B28,CI,TNA,TNAJ,TNB,TNA4,BC2,
1 B8C,B8TN,R2J,R7A
COMMON /PMT/PU(20),FV(20),MU,MV,FU1,FV1
P=A/B
C2=C*C
CJ=C2*C
C4=C2*C2
ST=S*S
SF=ST*ST
SCA=(J,J*ST*OX+C2*H)*2.0
SCB=SF*OX+2.0*ST*C2*H+C*OY
SCC=4.0*S*OX
SCD=(ST*OX+C2*H)*4.0*S
DO I=L-1,N
CC(I)=CJ/ALJ*VL(L,5)
COS(L)=CJ(L)/SCB
CONTINUE
AA=AA*A
AA2=AA*AA
AA4=AA*AA
BB=BB*B
BBJ=BB*B
BB4=BB*BB
OXY=SQRT(OX*OY)
OX2=OX*2.
YA=(OX*OY+H)/OX2
PKKJ=C2*YJ
KJ=C*SQRT(YA)
PKK1=C*SQRT((OX*OY-H)/OX2)
K4=PKK1+J
K5=PKK1+S
PKK4=K4**2
PKK5=K5**2
X2=1./(PKKJ+PKK4)
Y2=1./(PKKJ+PKK5)
X22=X2*X2
X23=X22*X2
X24=X23*X2
Y22=Y2*Y2
Y23=Y22*Y2
Y24=Y23*Y2
OO=O1+OXY*OYX
TN=S/C
OXT=OX*TN**2
R1=S*(2.+OXT+2.*O2+OXY+OYX)
R2=- (ST*(OXT+2.*H)+OY*C2)
R3=OX/CJ
R4=J,C*5*J
R5=(J.*OXT+J)/C
R6=-S*(OXT+J)/C
R7=OX/C
R8=-2.0*S**2
R9=(ST*O1*C2/OX)*R7
R10=S*J
R11=H*J
R12=H*J
R13=H*J
R14=H*J
R15=H*J
R16=H*J
R17=H*J
R18=H*J
R19=H*J
R20=H*J
R21=H*J
R22=H*J
R23=H*J
R24=H*J
R25=H*J
R26=H*J
R27=H*J
R28=H*J
R29=H*J
R30=H*J
R31=H*J
R32=H*J
R33=H*J
R34=H*J
R35=H*J
R36=H*J
R37=H*J
R38=H*J
R39=H*J
R40=H*J
R41=H*J
R42=H*J
R43=H*J
R44=H*J
R45=H*J
R46=H*J
R47=H*J
R48=H*J
R49=H*J
R50=H*J
R51=H*J
R52=H*J
R53=H*J
R54=H*J
R55=H*J
R56=H*J
R57=H*J
R58=H*J
R59=H*J
R60=H*J
R61=H*J
R62=H*J
R63=H*J
R64=H*J
R65=H*J
R66=H*J
R67=H*J
R68=H*J
R69=H*J
R70=H*J
R71=H*J
R72=H*J

```





```

S4(2) = J.0
S5(2) = S1(2) - S2(2) / C
S6(2) = -S3(2) * M.3 * S
S7(2) = -JY - (O2 + OXY) * (TN) ** 2
IF (OXY.EJ.J.0) GO TO 4
OYXD = OYX / XY
GO TO 4
OYXD = J.0
S1(4) = (S1(1) - S1(2)) * C * S + S1(J) * (1. - ST + OYXD) * C2
S2(4) = (S2(1) - S2(2)) * C * S + S2(J) * (1. - ST + OYXD) * C2
S3(4) = (S3(1) - S3(2)) * C * S + S3(J) * (1. - ST + OYXD) * C2
S4(4) = (S1(1) - S1(2)) * C * S + S1(J) * (ST + OYXD) * C2 + S5(1) * S - S5(2) * C
S5(4) = (S2(1) - S2(2)) * C * S + S2(J) * (ST + OYXD) * C2 + S6(1) * S - S6(2) * C
S6(4) = (S3(1) - S3(2)) * C * S + S3(J) * (ST + OYXD) * C2 + S7(1) * S - S7(2) * C
S7(4) =
IF (Z-2) 3,4,3
WRITE (6, F13) C, S, P, C2, H, SCA, SCB, SCC, SCD, AA, BB, TN, X2, Y2, XJ, X4, X5, R
1, R2, R1, R4, R5, R6, R7, R8, R9, R10, R1KJ, R1K4, R1K5, T, A1, A2, A3, A4, A5, A6, A
27, A8
WRITE (6, F13) A9, A10, A11, A12, A13, A14, A15, A16, A17, A18, A19, A20, A0, B1
1, B2, B3, B4, B5, B6, B7, B8, B9, B10, B11, B12, B13, B14, B15, B16, B17, B18, B19, B
220, (S1(I), S2(I), S3(I), I=1, J)
RETURN
END

```

001970  
001980  
001990  
001900

B 147  
B 148  
B 149  
B 150  
B 151  
B 152  
B 153  
B 154  
B 155-

```

*****
SUBROUTINE SYLA (NS1,NSL,CD,DC,STOR,MS,JS,LN,NST1,NST2)
*****
DOUBLE PRECISION CH,OC
REAL X1N,X2N,K1N,K2N,K3N,K4N,K5N,K6N,K7N,K8N,L1N,L2N,L3N,L4N,L5N,L6N,L7N,L
18N,I1N,I2N,I3N,I4N,I5N,I6N,KJ,K4,K5,KMN,LMN
COMMON A,PI,SA,C,S,TN,C2,AA,AAJ,AAA,Z,SYAS,C2,CJ,ST,SF,T,TB,MNH
COMMON /BL0/ B,OX,OY,OXY,OYX,O1,O2,EI,GJ,H,VL(4,5),Z3
COMMON /BL1/ P,CD(4),CS(4),KJ,K4,K5,BB,BB3,BB4,X2,Y2,A1,A2,A3,A4,
181,B2,B3,B4,SCA,SCB,SCC,SCJ,S1(4),S2(4),S3(4),S4(4),S5(4),S6(4),
2 S7(4)
COMMON /BL2/ R1,R2,R3,R4,R5,R6,R7,R8,R9,R10,R11,R12,RIKJ,X22,X23,X
124,Y22,Y23,Y24,A5,A6,A7,A8,A9,A10,A11,A12,A13,A14,A15,A16,A17,A19,
2A20,A21,A22,A23,A24,AG,B5,B6,B7,B8,B9,B10,B11,B12,B13,B14,B15,B16,
3B17,B18,B19,B20,B22,B23,B24,A18
COMMON /BL5/ NHC,NB3,NC,JC,NH2,NH3,NH4,NH5,NH6,NH7,NH8,NB1,NB2,NH,NL
COMMON /BL7/ FM2(3),F13(108),F33(71),F19(94),F20(125)
COMMON /SPL/ A25,A26,A27,A28,B25,B27,B28,CI,TA,TAJ,TNB,TNB4,BC2,
1DDC,BBTN,R23,R7A
COMMON /PMT/ FV(20),FU,MV,FU1,FV1
DIMENSION CJ(NS,JS),DC(NS,LN),STOR(NST1,NST2)
DIMENSION N1(8),AJ(3),BJ(3)
DIMENSION JMC(4),VMC(4),UMC1(4),VMC1(4)
NS1=NH4+1
NS2=NH4+2
NS3=NH4+3
NS4=NH4+4
NSL=NS4+NL
DO 2 I=1,NC
DO 1 J=1,NSL
STOR(I,J)=0.
CONTINUE
DO 2 J=1,JC
DO (I,J)=0.0
CD(NB1,NJ1)=1.0
CD(NB1,NB2)=0. JJJJJJJJJJJJJJJ
CD(NB1,NB3)=1.0
CD(NB1,NC)=T*AAA/BB4/S.-1.
STOR(NB3,NS2)=1.
STOR(NB1,NJ4)=1.
IF (ZB) 7,5,5
CD(NB2,NB2)=2./A/C
CD(NB2,NC)=+. *T*AAJ/BB4/C
CD(NB3,NB3)=BC2
CD(NB3,NC)=-BC2*2.
STOR(NB2,NS1)=1./A/C
STOR(NB2,NS2)=-TN/3
STOR(NB2,NS3)=3./A/C
STOR(NB2,NS4)=-TN/3
STOR(NC,NS1)=-TN/A
STOR(NC,NS2)=1./B/C
STOR(NC,NS3)=-TN/A
STOR(NC,NS4)=3./B/C
CD(NC,NJ1)=1.
CD(NC,NB2)=1.
CD(NC,NB3)=0. JJJJJJJJJJJJJJJ
CD(NC,NC)=T*AAA/BB4-S.2
STOR(NS1,NS1)=1.
STOR(NS1,NSJ)=1.
IF (ZB) 7,5,5
CD(NC,NC)=4.0*(R3*T*AA+EI)/BB4
STOR(NB1,NSJ)=6.*R3/AA3
STOR(NB1,NJ4)=6.*R6/BB3
STOR(NB2,NS4)=6.*R10/BB3
CD(NB2,NJ2)=2.*R7A
CD(NB2,NB3)=2.*R9/B3
CD(NB2,NC)=-4.*R9/B3+12.*R7*T*AA/BB4
CD(NB3,NB3)=R23
CD(NB3,NC)=-R23*6.
STOR(NB2,NSJ)=6.*R7A
STOR(NC,NS4)=R28*3.
DO 210 I=1,+
VMC(I)=0
VMC1(I)=0
VMC1(I)=0
210 UMC(I)=0

```







```

TY1=ANY2=#I
IF (Z-1) 23,24,25
IF (NH=MMH) 25,26,28
WRITE (5,61) NH,N,ON,AN,BN,AN2,BN2,ANJ,BNJ,ANA,IN,IJN,SN,FIN,R2
IN,SIN,XIN,KIN,KJN,KAN,K5N,K6N,K7N,K8N,RR1,RR2,SS1,L1N,L2N,L3N,L4N,
2LSN,LSN,L7N,L8N,RR2
PRINT 59, R,P,RNPD,RNP5,BNA2,ANB2,ANX2,BNY2,ANX2,ANY2,ANBN,SNBN,AR
LAX,BY,BNX,BNY,ANX,ANY,TAI,TBI,TX1,TY1,(I,I=1,3),(JI(I),I=1,3)
OM=1.0
OO 37 #=1.1M
CM=-CM
RM=RM
RMP2=RM+PI
RM22=RM+P2=RAD2
RM24=RM+P2=RAD2
SAA=2./(BNA1*(BNX2+2.*A2*RM22)+RM24)
SBA=2./(BNA1*(BNY2+2.*B2*RM22)+RM24)
SXA=2./(ANX1*(ANB2+2.*A2*RM22)+RM24)
SYA=2./(ANY1*(ANB2+2.*B2*RM22)+RM24)
SA1=SAA*RV*PI*CM
SB1=SBA*RV*PI*CM
SX1=SXA*RV*PI*CM
SY1=SYA*RV*PI*CM
SA2=SAA*BN*RV*PI*CM
SB2=SBA*BN*RV*PI*CM
SX2=SXA*AN*RV*PI*CM
SY2=SYA*AN*RV*PI*CM
TA2=AN*RV*PI*CM
TB2=AN*RV*PI*CM
TX2=AN*RV*PI*CM
TY2=AN*RV*PI*CM
TA3=(BNX+RM22)*KJ
TA4=(BNX+RM22)*KA
TB3=(BNY+RM22)*KJ
TB4=(BNY+RM22)*KA
TX3=(ANX+RM22)*KJ
TX4=(ANX+RM22)*KA
TY3=(ANY+RM22)*KJ
TY4=(ANY+RM22)*KA
AJ(1)=SA1*(TAJ*K7N+TA4*K8N)
AJ(2)=SA2*(-TA4*K7N+TAJ*K8N)
AJ(3)=SB2*(TBJ*L7N+TB4*L8N)
AJ(4)=SB1*(-TB4*L7N+TBJ*L8N)
AJ(5)=SX2*(TXJ*KJN+TX4*K8N)
AJ(6)=SX1*(-TX4*KJN+TXJ*K8N)
AJ(7)=SY2*(TYJ*LJN+TY4*L8N)
AJ(8)=SY1*(-TY4*LJN+TYJ*L8N)
BJ(1)=SA1*(-TA2*K7N-TX1*K8N)
BJ(2)=SB1*(TA1*K7N-TA2*K8N)
BJ(3)=SA1*(-TB2*L7N-TB1*L8N)
BJ(4)=SB1*(TB1*L7N-TB2*L8N)
BJ(5)=SX1*(TX1*KJN-TX2*K8N)
BJ(6)=SX1*(TX1*KJN-TX2*K8N)
BJ(7)=SY1*(-TY2*LJN-TY1*L8N)
BJ(8)=SY1*(TY1*LJN-TY2*L8N)
IF (Z-1) 23,26,28
IF (NH=MMH) 28,27,28
WRITE (5,59) NH,N,M
PRINT 50, R,P,RNPD,RMP2,RM24,RM25,CMR,SAA,SB1,SXA,SYA,SA1,SB1,SX1,
SY1,SA2,SB2,SX2,SY2,TA2,TB2,TX2,TY2,TAJ,TBJ,TXJ,TYJ,TA4,TB4,
TX4,TY
WRITE (5,61) (I,I=1,3),(AJ(I),I=1,3),(BJ(I),I=1,3)
NHX=NH+M
NH2X=NH2+M
NH3X=NH3+M
NH4X=NH4+M
NH5X=NH5+M
NH6X=NH6+M
NH7X=NH7+M
CO(NH4X,N)=I*AJ(1)
CO(NH4X,NH2)=ON*AJ(2)
CO(NH4X,NH3)=ON*AJ(3)
CO(NH4X,NH4)=ON*AJ(4)
STOR(NH5X,1)=ON*BJ(1)
STOR(NH5X,N4)=ON*BJ(2)
STOR(NH5X,NH2N)=ON*BJ(3)
STOR(NH5X,NH3N)=ON*BJ(4)
IF (Z) 29,31,30

```

24

25

26

27

28

```

UUUUUUUUUU 303
UUUUUUUUUU 304
UUUUUUUUUU 305
UUUUUUUUUU 306
UUUUUUUUUU 307
UUUUUUUUUU 308
UUUUUUUUUU 309
UUUUUUUUUU 310
UUUUUUUUUU 311
UUUUUUUUUU 312
UUUUUUUUUU 313
UUUUUUUUUU 314
UUUUUUUUUU 315
UUUUUUUUUU 316
UUUUUUUUUU 317
UUUUUUUUUU 318
UUUUUUUUUU 319
UUUUUUUUUU 320
UUUUUUUUUU 321
UUUUUUUUUU 322
UUUUUUUUUU 323
UUUUUUUUUU 324
UUUUUUUUUU 325
UUUUUUUUUU 326
UUUUUUUUUU 327
UUUUUUUUUU 328
UUUUUUUUUU 329
UUUUUUUUUU 330
UUUUUUUUUU 331
UUUUUUUUUU 332
UUUUUUUUUU 333
UUUUUUUUUU 334
UUUUUUUUUU 335
UUUUUUUUUU 336
UUUUUUUUUU 337
UUUUUUUUUU 338
UUUUUUUUUU 339
UUUUUUUUUU 340
UUUUUUUUUU 341
UUUUUUUUUU 342
UUUUUUUUUU 343
UUUUUUUUUU 344
UUUUUUUUUU 345
UUUUUUUUUU 346
UUUUUUUUUU 347
UUUUUUUUUU 348
UUUUUUUUUU 349
UUUUUUUUUU 350
UUUUUUUUUU 351
UUUUUUUUUU 352
UUUUUUUUUU 353
UUUUUUUUUU 354
UUUUUUUUUU 355
UUUUUUUUUU 356
UUUUUUUUUU 357
UUUUUUUUUU 358
UUUUUUUUUU 359
UUUUUUUUUU 360
UUUUUUUUUU 361
UUUUUUUUUU 362
UUUUUUUUUU 363
UUUUUUUUUU 364
UUUUUUUUUU 365
UUUUUUUUUU 366
UUUUUUUUUU 367
UUUUUUUUUU 368
UUUUUUUUUU 369
UUUUUUUUUU 370
UUUUUUUUUU 371
UUUUUUUUUU 372
UUUUUUUUUU 373
UUUUUUUUUU 374
UUUUUUUUUU 375
UUUUUUUUUU 376
UUUUUUUUUU 377
UUUUUUUUUU 378
UUUUUUUUUU 379
UUUUUUUUUU 380

```

```

29  CO(NH13M,NH14A)=OAI*(A27*BJ(5)+A28*BJ(6))
    CO(NH13M,NH15A)=OAI*(A29*BJ(5)+A27*BJ(6))
    CO(NH13M,NH16A)=OAI*(B27*BJ(7)+B29*BJ(3))
    CO(NH13M,NH17A)=OAI*(B29*BJ(7)+B27*BJ(3))
    CO(NH7M,N)=BJ1*(A21*BJ(1)+A22*BJ(2))
    CO(NH7M,NH2A)=OB1*(A22*BJ(1)+A21*BJ(2))
    CO(NH7M,NH2A)=OB1*(A21*BJ(3)+B23*BJ(4))
    CO(NH7M,NH3A)=OB1*(B22*BJ(3)+A21*BJ(4))
    STOR(NH2M,N)=OAI*(A27*AJ(5)+A28*AJ(6))
    STOR(NH2M,NH1N)=OAI*(A29*AJ(5)+A27*AJ(6))
    STOR(NH2M,NH2N)=OAI*(B27*AJ(7)+B29*AJ(3))
    STOR(NH2M,NH3N)=OAI*(B29*AJ(7)+B27*AJ(3))
    STOR(NH6M,N)=OB1*(A21*AJ(1)+A22*AJ(2))
    STOR(NH6M,NH1N)=OB1*(A22*AJ(1)+A21*AJ(2))
    STOR(NH6M,NH2N)=OB1*(A21*AJ(3)+B22*AJ(4))
    STOR(NH6M,NH3N)=OB1*(B22*AJ(3)+A21*AJ(4))
30  CO(X,NH4A)=ON*AJ(5)
    CO(X,NH5A)=ON*AJ(6)
    CO(X,NH6A)=ON*AJ(7)
    CO(X,NH7A)=ON*AJ(3)
    STOR(NH4M,N)=ON*BJ(5)
    STOR(NH4M,NH1A)=ON*BJ(6)
    STOR(NH4M,NH2A)=ON*BJ(7)
    STOR(NH4M,NH3A)=ON*BJ(3)
    IF (ZB) J1,J1,J2
31  CO(M,NH4N)=J1A*(A5*AJ(5)+A6*AJ(6))
    CO(X,NH5N)=J1A*(-A6*AJ(5)+A5*AJ(6))
    CO(X,NH6N)=J1A*(B5*AJ(7)+B6*AJ(3))
    CO(X,NH7N)=J1A*(-B6*AJ(7)+B5*AJ(3))
    CO(NH4M,NH4A)=OAJ*(A12*BJ(5)+A13*BJ(6))
    CO(NH4M,NH5A)=OAJ*(-A13*BJ(5)+A12*BJ(6))
    CO(NH4M,NH6A)=OAJ*(B12*BJ(7)+B13*BJ(3))
    CO(NH4M,NH7A)=OAJ*(-B13*BJ(7)+B12*BJ(3))
    CO(NH13M,NH4A)=OAJ*(A19*BJ(5)+A20*BJ(6))
    CO(NH13M,NH5A)=OAJ*(-A20*BJ(5)+A19*BJ(6))
    CO(NH13M,NH6A)=OAJ*(B19*BJ(7)+B20*BJ(3))
    CO(NH13M,NH7A)=OAJ*(-B20*BJ(7)+B19*BJ(3))
    STOR(X,N)=J1A*(A12*AJ(5)+A13*AJ(6))
    STOR(X,NH1N)=OAJ*(-A13*AJ(5)+A12*AJ(6))
    STOR(X,NH2N)=OAJ*(B12*AJ(7)+B13*AJ(3))
    STOR(X,NH3N)=OAJ*(-B13*AJ(7)+B12*AJ(3))
    STOR(NH4M,N)=J1A*(A5*BJ(5)+A6*BJ(6))
    STOR(NH4M,NH1A)=OAJ*(A6*BJ(5)+A5*BJ(5))
    STOR(NH4M,NH2A)=OAJ*(B5*BJ(7)+B6*BJ(3))
    STOR(NH4M,NH3A)=OAJ*(B6*BJ(7)+B5*BJ(3))
    STOR(NH2M,N)=OAJ*(A19*AJ(5)+A20*AJ(6))
    STOR(NH2M,NH1N)=OAJ*(-A20*AJ(5)+A19*AJ(5))
    STOR(NH2M,NH2N)=OAJ*(B19*AJ(7)+B20*AJ(3))
    STOR(NH2M,NH3N)=OAJ*(-B20*AJ(7)+B19*AJ(3))
32  CO(NH2M,NH4A)=OAJ*(A17*AJ(5)+A18*AJ(6))
    CO(NH2M,NH5A)=OAJ*(-A18*AJ(5)+A17*AJ(6))
    CO(NH2M,NH6A)=OAJ*(B17*AJ(7)+B18*AJ(3))
    CO(NH2M,NH7A)=OAJ*(-B18*AJ(7)+B17*AJ(3))
    CO(NH6M,N)=BJ2*(A7*AJ(1)+R1K3*AJ(2))
    CO(NH6M,NH1A)=OB2*(R1K3*AJ(1)+A7*AJ(2))
    CO(NH6M,NH2A)=OB2*(B7*AJ(3)+R1K3*AJ(4))
    CO(NH6M,NH3A)=OB2*(-R1K3*AJ(3)+B7*AJ(4))
    STOR(NH13M,N)=OAJ*(A17*BJ(5)+A18*BJ(6))
    STOR(NH13M,NH1A)=OAJ*(-A18*BJ(5)+A17*BJ(5))
    STOR(NH13M,NH2A)=OAJ*(B17*BJ(7)+B18*BJ(3))
    STOR(NH13M,NH3A)=OAJ*(-B18*BJ(7)+B17*BJ(3))
    STOR(NH7M,N)=OB2*(A7*BJ(1)+R1K3*BJ(2))
    STOR(NH7M,NH1A)=OB2*(R1K3*BJ(1)+A7*BJ(2))
    STOR(NH7M,NH2A)=OB2*(B7*BJ(3)+R1K3*BJ(4))
    STOR(NH7M,NH3A)=OB2*(-R1K3*BJ(3)+B7*BJ(4))
33  AM2=AN*AM
    AM1=AN2*AM
    AM=AN2*AM2
    GAMCAYUM
    OO 57 L=1,NL
    RMN=OX*AM4+JCA*AM2+BN2+SCB*BN4
    SMN=(SCC*AM4+SCD*BN2)*AM*BN
    SVI=UN*VL(L,2)
    CVI=CC3(SVI)
    SVI=GIN(SVI)
    AUI=AN*VL(L,1)
    CUI=CC3(AUI)

```

```

0000 381
0000 382
0000 383
0000 384
0000 385
0000 386
0000 387
0000 388
0000 389
0000 390
0000 391
0000 392
0000 393
0000 394
0000 395
0000 396
0000 397
0000 398
0000 399
0000 400
0000 401
0000 402
0000 403
0000 404
0000 405
0000 406
0000 407
0000 408
0000 409
0000 410
0000 411
0000 412
0000 413
0000 414
0000 415
0000 416
0000 417
0000 418
0000 419
0000 420
0000 421
0000 422
0000 423
0000 424
0000 425
0000 426
0000 427
0000 428
0000 429
0000 430
0000 431
0000 432
0000 433
0000 434
0000 435
0000 436
0000 437
0000 438
0000 439
0000 440
0000 441
0000 442
0000 443
0000 444
0000 445
0000 446
0000 447
0000 448
0000 449
0000 450
0000 451
0000 454
0000 455
0000 456
0000 457
0000 458

```

```

SUI=SIN(AUI)
Q1MN=CL1*CVI
Q2MN=CL1*SVI
Q3MN=CL1*CVI
Q4MN=CL1*SVI
ALR=AL*VL(L,3)/2.
BLS=BN*VL(L,4)/2.
SAA=SIN(ALR)/ALR
SBB=BSIN(BLS)/BLS
R9=CM/(RMN**2-SMN**2)*SAA*SBB*CO(L)
R9R=R9*RMN
R9S=R9*SMN
XMN=Q1MN*RS1-Q2MN*RSS
L1MN=Q2MN*RS1-Q1MN*RSS
P1MN=Q3MN*RS1+Q4MN*RSS
Q1MN=Q4MN*RS1+Q3MN*RSS
NCL=NC+L
NAL=NS4+L
IF (X-1) 45,34,46
IF (N-1) 40,35,40
IF (ZB) 36,33,37
34 CD(NC,NCL)=-COS(L)*884/180.
GO TO 40
35 CD(NC,NCL)=-COS(L)*334/30.
IF (ZB) 40,33,39
36 CD(NB1,NCL)=E1*COS(L)/4.
CD(NB1,NCL)=FV1
39 CD(NB2,NCL)=R9*COS(L)*83/12.+FV1
40 CD=CCO*CVI
TN=CCO*SVI
CD(NB1,NCL)=CD(NB1,NCL)-T6N*ON/BN4
IF (Z2) 41,44,42
41 CD(N,NCL)=-COS(L)*((13N-2.)*(1N)*884/94.-T6N/BN4
CD(NH3N,NCL)=BBTN*COS(L)*((17N-15N)-T6N/BN3*TN
C CD(NH3N,NCL) = 38TN*COS(L)*((17N-3.)*(15N)-T6N/BN3*TN
STOR(NH2N,NAL)=TN*T6N/BN3
STOR(NC,NAL)=STOR(NC,NAL)-T6N*ON/BN3/C
GO TO 43
42 CD(N,NCL)=-COS(L)*((13N/5.-1N)*834/15.-T6N/BN4
43 STOR(NH4N,NAL)=-T6N/BN4
IF (Z9) 46,44,45
44 SM1=-COS(L)*3*TSN/4.-T6N/BN
CD(N,NCL)=E1*TN
CD(NH4N,NCL)=R5*SM1
CD(NH3N,NCL)=R10*SM1
STOR(N,NAL)=46*T6N/BN
STOR(NH4N,NAL)=E1*TSN
STOR(NH21,NAL)=R10*T6N/BN
45 DO 206 K=1,4V
206 VMC(L)=VMC(L)+2.*FV(K)*((-1.)**N)*COS(2.*N*P[(K-0.5)/MV])
CD(NH2N,NCL)=-R9*(COS(L)*9B*(1N/8.-T6N/BN2)-C*VMC(L)/(2.*B)
CD(NB3,NCL)=CD(NB3,NCL)+R2*T6N*ON/BN2
DO 209 K=1,4V
209 VMC1(L)=VMC1(L)+2.*FV(K)*((-1.)**N)*SIN(2.*N*P[(K-0.5)/MV])
STOR(NH3N,NAL)=R9*T6N/BN2-C*VMC1(L)/(2.*B)
46 IF (N-1) 47,47,52
47 CDO=CO(L)*SAA/OX/2.
TSM=CCO*CVI
T7M=CCO*3UI
CD(NH4M,NCL)=-T7M/444
STOR(NH5M,NAL)=-T7M/444
IF (Z5) 48,50,49
48 CD(NH7M,NCL)=-T7M/AM3*TN
STOR(NH6M,NAL)=T7M/AM3*TN
STOR(NB2,NAL)=STOR(NB2,NAL)-T7M*OM/AM3/C
49 CD(NC,NCL)=CD(NC,NCL)-T5M*OM/AM4
IF (Z3) 52,50,51
50 STOR(NB1,NAL)=STOR(NB1,NAL)+R3*T7M*OM/AM
DO 207 K=1,4V
207 UMC(L)=JMC(L)+2.*FU(K)*((-1.)**N)*COS(2.*N*P[(K-0.5)/MU])
CD(NH6M,NCL)=UMC(L)/(2.*A)
DO 208 K=1,4V
208 UMC1(L)=JMC1(L)+2.*FU(K)*((-1.)**N)*SIN(2.*N*P[(K-0.5)/MU])
STOR(NH7M,NAL)=UMC1(L)/(2.*A)
51 CD(NB2,NCL)=CD(NB2,NCL)+R7*T5M*OM/AM2
52 SK1=E1*BN4
SK2=-(R4*AM1+R5*BN2)*BN

```

459  
 460  
 461  
 462  
 463  
 464  
 465  
 466  
 467  
 468  
 469  
 470  
 471  
 472  
 473  
 474  
 475  
 476  
 477  
 478  
 479  
 480  
 482  
 483  
 484  
 485  
 486  
 487  
 488  
 489  
 490  
 491  
 492  
 493  
 494  
 495  
 496  
 497  
 498  
 499  
 500  
 501  
 502  
 503  
 504  
 505  
 506  
 507  
 509  
 511  
 512  
 513  
 514  
 515  
 516  
 517  
 518  
 519  
 520  
 521  
 522  
 523  
 524  
 525  
 526



```

SKJ1=(R1)*AMN+I5*(BN2)*AM
CK1=(R7)*AMN+I9*(BN2)
CK2=(R2)*AMN+I3
CK3=(R1)*AMN+I4
CK4=(R1)*AMN+I3
CK5=(R1)*AMN+I3
CK6=(R1)*AMN+I3
CD(NH4M,NCL)=CD(NH4M,NCL)-KMN*Q1M
STOR(NH5M,NAL)=STOR(NH5M,NAL)-PMN*Q1M
IF (ZB) 53,55,54
53 CD(NH3N,NCL)=CD(NH3N,NCL)-(TN*(R1)*KMN+AM/C*L1M)
   CD(NH7M,NCL)=CD(NH7M,NCL)-(TN*(R1)*KMN+BN/C*L1M)*Q1M
   STOR(NH2M,NAL)=STOR(NH2M,NAL)-AM/C*PMN+TN*(R1)*Q1M
   STOR(NH6M,NAL)=STOR(NH6M,NAL)+(TN*(R1)*PMN+BN*(R1)*Q1M)*Q1M
54 CD(N,NCL)=CJ(N,NCL)-KMN
   STOR(NH7,NAL)=STOR(NH7,NAL)-Q1M
   IF (ZB) 57,55,56
55 CD(N,NCL)=CJ(N,NCL)+SK1*KMN
   CD(NH1N,NCL)=CD(NH1N,NCL)+SK2*KMN+SKJ*L1M
   CD(NH3N,NCL)=CD(NH3N,NCL)+CKJ*KMN+CK4*L1M
   STOR(N,NAL)=STOR(N,NAL)+SK3*PMN+SK2*Q1M
   STOR(NH2,NAL)=STOR(NH2,NAL)+SK1*Q1M
56 STOR(NH2N,NAL)=STOR(NH2N,NAL)+CK4*PMN-CKJ*Q1M
   CD(NH2N,NCL)=CD(NH2N,NCL)+CK1*KMN+CK3*L1M
   CD(NH6M,NCL)=CD(NH6M,NCL)+CK5*KMN+CK6*L1M
   STOR(NH3N,NAL)=STOR(NH3N,NAL)-CK2*PMN+CK1*Q1M
   STOR(NH7M,NAL)=STOR(NH7M,NAL)+CK5*PMN-CK6*Q1M
57 CONTINUE
   STAY=1.
   RETURN
C
58 FORMAT (3X,'RNP',13X,'RNP0',12X,'RNP5',12X,'SNA2',12X,'ANB2',1X,5
1F16.3/9X,'JAX2',12X,'9NY2',12X,'ANX2',12X,'ANY2',12X,'A2BN',3X,'B2
2BN',12X,'A2AX',12X,'S2AY',1X,8F16.3/9X,'BX',12X,'BY',12X,'AX
3',12X,'AY',12X,'TA1',12X,'TB1',12X,'TX1',12X,'TY1',1X,8F16.3/5X811
4S/6X,'1',3X,8F15.8)
59 FORMAT (/13X,'NH',15,5X,'N',15,5X,'4',15/)
60 FORMAT (3X,'RMP',13X,'RMP0',12X,'RMP2',12X,'R424',12X,'R225',12X,'Q
1MR',1X,8F16.3/9X,'SAA',13X,'SBA',13X,'SA',13X,'SYA',13X,'SA1',13X
2,'SB1',13X,'SX1',13X,'SY1',1X,8F16.8/9X,'SA2',13X,'SB2',13X,'SX2',
313X,'SY2',13X,'TA2',13X,'TB2',13X,'TX2',13X,'TY2',1X,8F15.8/9X,'TA
43',13X,'TB3',13X,'TX3',13X,'TY3',13X,'TA4',13X,'TB4',13X,'TX4',13X
5,'TY4',1X,8F16.8)
61 FORMAT (5X,8F15.8/5X,'AJ',5X,8F15.8/6X,'BJ',5X,8F15.8)
   END

```

5527  
5528  
5529  
5530  
5531  
5532  
5533  
5534  
5535  
5536  
5537  
5538  
5539  
5540  
5541  
5542  
5543  
5544  
5545  
5546  
5547  
5548  
5549  
5550  
5551  
5552  
5553  
5554  
5555  
5556  
5557  
5558  
5559  
5560  
5561  
5562  
5563  
5564  
5565  
5566  
5567  
5568  
5569  
5570  
5571

```

C *****
C SUBROUTINE ASLA (NS1,NSL,SYAS,CC,DC,STOR,NS,JS,LN,NST1,NST2)
C DIMENSION CH,CC
C DIMENSION CC(NS,JS), DC(NS,LN), STOR(NST1,NST2)
C DIMENSION BL(4),AC(NB),NC(JC,NH2,NH3,NH4,NH5,NH6,NH7,NB,NB1,NB2,NL
C DIMENSION J(4),COK(4)
C DO 3 J=1,NH4
C NH4=NH4+J
C DO 1 I=1,NH4
C CO(I,NH4,J)=STOR(I,J)
1 CONTINUE
C NH4=NH4+1
C DO 2 I=NH4,1,NB
C CO(I,J)=STOR(I,J)
2 CONTINUE
C CO(NB1,J)=0.
C CO(NB1,NH4,J)=STOR(NB1,J)
C CO(NB2,J)=0.
C CO(NB2,NH4,J)=STOR(NB2,J)
C CO(NB3,J)=0.
C CO(NB3,NH4,J)=STOR(NB3,J)
C CO(NC,J)=0.
C CO(NC,NH4,J)=STOR(NC,J)
3 CONTINUE
C DO 5 N=1,NL
C NH4=NH4+N
C NH5=NH4+N
C NH6=NH4+N
C NH7=NH4+N
C NH8=NH4+N
C NH9=NH4+N
C DO 4 I=1,N
C NH4=NH4*(2*I-1)+N
C NH5=NH4*I
C NH6=NH4+I
C NH7=NH4+I+I
C NH8=(J+I)*I+I
C NH9=(J+I)*I+I+I
C X(L)=(J+I)*I+I
C X(L)=(J+I)*I+I
C CO(L,J)=CO(NH1,NH4)
C CO(X(L),J)=CO(NH2,NH4)
4 CONTINUE
C CO(INH1,N)=CO(INHN,NHN)
C CO(INH1,NH1)=CO(INHN,N)
C CO(INH1,NH2)=CO(INHN,NHN)
C CO(INH1,NH3)=CO(INHN,NHN)
C CO(INH1,NH4)=CO(INHN,NHN)
C CO(INH1,NH5)=CO(L,N)
C CO(INH1,NH6)=CO(L,1)
C CO(INH1,NH7)=CO(L,4)
C CO(INH1,NH8)=CO(L,14)
C INHN=INHN+I+I+I
C CO(INH1,NH9)=CO(INHN,NH5N)
C CO(INH2,NH1)=CO(INHN,NH4N)
C CO(INH2,NH2)=CO(INHN,NH4N)
C CO(INH2,NH3)=CO(INHN,NH6N)
C CO(INH2,NH4)=CO(INHN,NH6N)
C CO(INH2,NH5)=CO(COK(2))
C CO(INH2,NH6)=CO(COK(1))
C CO(INH2,NH7)=CO(COK(4))
C CO(INH2,NH8)=CO(COK(J))
5 DO 6 J=NS1,NL
C NH4=NH4+J
C DO 5 I=1,NH4
C CO(I,NH4,J)=STOR(I,J)
6 SYAS=1.
C RETURN
C END

```

```

0 1
0 2
0 3
0 4
0 5
0 6
0 7
0 8
0 9
0 10
0 11
0 12
0 13
0 14
0 15
0 16
0 17
0 18
0 19
0 20
0 21
0 22
0 23
0 24
0 25
0 26
0 27
0 28
0 29
0 30
0 31
0 32
0 33
0 34
0 35
0 36
0 37
0 38
0 39
0 40
0 41
0 42
0 43
0 44
0 45
0 46
0 47
0 48
0 49
0 50
0 51
0 52
0 53
0 54
0 55
0 56
0 57
0 58
0 59
0 60
0 61
0 62
0 63
0 64
0 65

```



```

C *****
C SUBROUTINE 4INV (A,N,D,L,M,NSS,NS)
C DIMENSION A(2),DABS,BIGA,HOLD
C DE=1.0
C KX=1
C DO 1 L=1,N
C   KX=KX+1
C   M(KX)=KX
C   KX=KX+1
C   STOP
C   GO TO 2
C   IN=2+(L-1)
C   OC=2+L
C   IL=IN+1
C   IF (ABS(BIGA)-ABS(A(IJ))) 15,20,20
C   IF (ABS(BIGA)-DABS(A(IJ))) 1,2,2
1  BIGA=ABS(A(IJ))
C   M(KX)=L
C   CONTINUE
2  J=L
C   IF (J-K) 3,3,3
3  KI=K+1
C   DO 4 I=1,N
C   KI=KI+1
C   HOLD(I)=A(KI)
C   J=K+1
C   A(KI)=A(J)
C   A(J)=HOLD(I)
C   CONTINUE
4  IF (M(K))
5  IF (I-K) 5,5,6
6  LP=N+(I-1)
C   DO 7 J=1,N
C   JK=K+J
C   J=J+1
C   HOLD(J)=A(JK)
C   A(JK)=A(J)
C   A(J)=HOLD(J)
C   CONTINUE
7  IF (BIGA) 10,9,10
8  DO 9
9  PRINT 27
C   RETURN
10 DO 12 (I=1,N
11 IF (I-K) 11,12,11
11 IX=K+I
C   A(IX)=A(K)/(-BIGA)
12 CONTINUE
C   DO 13 (I=1,N
11 IX=K+I
C   HOLD(I)=A(IX)
12 IJ=I-K
C   DO 15 (J=1,N
13 IF (I-K) 13,15,13
14 IF (J-K) 14,15,14
C   KJ=IJ-I+K
C   A(IJ)=HOLD(KJ)+A(IJ)
15 CONTINUE
C   KJ=K-I
C   DO 17 (J=1,N
16 KJ=KJ+J
C   IF (J-K) 15,17,16
C   A(KJ)=A(KJ)/BIGA
17 CONTINUE
C   HOLD(I)=A(KX)
18 CONTINUE
19 KX=K-1
C   IF (K) 25,25,20
20 L(K)

```

```

1
2
3
4
5
6
7
8
9
10
11
12
13
14
15
16
17
18
19
20
21
22
23
24
25
26
27
28
29
30
31
32
33
34
35
36
37
38
39
40
41
42
43
44
45
46
47
48
49
50
51
52
53
54
55
56
57
58
59
60
61
62
63
64
65
66
67
68
69
70
71
72
73
74

```

```

21  IF (I-K) 23,23,21
    JC=N-(K-1)
    JR=N-(I-1)
    DO 22 J=1,N
    JK=JC+J
    HOLD=A(JK)
    JI=JR+J
    A(JK)=-A(JI)
    A(JI)=HOLD
22  CONTINUE
23  J=M(K)
    IF (J-K) 19,19,24
24  KI=K-N
    DO 25 I=1,N
    KI=KI+I
    HOLD=A(KI)
    JI=KI-K+J
    A(KI)=-A(JI)
    A(JI)=HOLD
25  CONTINUE
26  GO TO 19
    RETURN
C
27  FORMAT (/10X'THE MATRIX IS SINGULAR')
    END

```

```

75
76
77
78
79
80
81
82
83
84
85
86
87
88
89
90
91
92
93
94
95
96
97
98
99

```

```

C *****
C SUBROUTINE DS2A (CD,DC,STUR,NS,JS,LN,NST1,NST2) G 1
C *****
C DOUBLE PRECISION CH,DC G 2
C COMPUTE DEFLECTIONS AND MOMENTS (OLD SERIES) G 3
C G 4
C REAL KMN,MK1,MK2,MK3,MK4,MK5,MK6,ML1,ML2,ML3,ML4,ML,K3,K4,K5,MF,LM G 5
C IN G 6
C COMMON A,PI,SA,C,S,TN,C4,AA,AA3,AA4,Z,SYAS,C2,C3,ST,SF,T,TS,MNH G 7
C COMMON /BLJ/ S,DX,DY,DXY,OYX,D1,D2,LI,GJ,H,VL(4,5),Z5 G 8
C COMMON /BLI/ P,CO(4),COS(4),K3,K4,K5,BB,BB3,BB4,X2,Y2,A1,A2,A3,A4, G 9
C B1,B2,B3,B4,SCA,SCB,SCC,SCD,S1(4),S2(4),S3(4),S4(4),S5(4), G 10
C S7(4)
C COMMON /BL5/ VHC,NB3,NC,JC,NH2,NH3,NH4,NH5,NH6,NH7,NH8,NB1,NB2,NH,NL
C COMMON /EX/ UC(24),VC(24),NGC,YA(400,24),NR,UH(9),VR(3),NP(10)
C DIMENSION CJ(NS,JS),DC(NS,LN),STO(NST1,NST2)
C DIMENSION P1(20),P2(20),P3(20),P4(20),P5(20),P6(20),P7(20),
C P8(20),CC(20,20),SS(20,20)
C LT=MNH*10
C DO 14 I=1,NJC
C U=UC(I)
C V=VC(I)
C DO 1 N=1,NH
C RN=N
C RNP2=RN*PI
C AN=RNP2/A
C EN=RNP2/B
C VN=BN*V
C AU=AN*U
C BU=BN*C
C AV=AN*V
C AVK=AV*K3
C U3N=K3*BJ
C V3N=AVK*X2
C V3Y=AVK*Y2
C U4V=K4*BJ+VN
C USV=K5*BJ-VN
C V4U=K4*X2*AV+AU
C V5U=K5*Y2*AV-AU
C CHUN=COSH(J3N)
C SHUN=SINH(J3N)
C P1(N)=CHUN*COS(U4V)
C P2(N)=SHUN*SIN(U4V)
C P3(N)=CHUN*COS(U5V)
C P4(N)=SHUN*SIN(U5V)
C P5(N)=COSH(V3N)*COS(V4U)
C P6(N)=SINH(V3N)*SIN(V4U)
C P7(N)=COSH(V3Y)*COS(V5U)
C P8(N)=SINH(V3Y)*SIN(V5U)
C CV=COS(VN)
C SV=SIN(VN)
C DO 1 N=1,NH
C RM=M
C UM=RM*PI*U/A
C CC(M,N)=COS(UM)*CV
C SS(M,N)=SIN(UM)*SV
C DO 14 L=1,NL
C LN* = NHC+(-1)*LT
C CO4=CC5(L)/4.
C WL=JC(NB1,L)+DC(NB2,L)*(U/A)**2+DC(NB3,L)*(V/B)**2+(T*U**4-V**4)/B
C B4*CC(NC,L)
C IF (ZB) 3,2,2
C 2 WL=WL+CO4*(V**4-(V*B)**2*6.+5.*DB4)/24.
C GO TO 4
C 3 WL=WL+CO4*(V**4-(V*B)**2*2.+BB4)/24.
C DO 13 K=1,3
C 4 LNM=LN+MNH*K
C ML=2.*S1(K)*DC(NB2,L)/AA+2.*S3(K)*DC(NB3,L)/BB+12.*(T*U**2*S1(K)-
C )**2*S2(K))*JC(NC,L)/BB4
C IF (ZE) 5,3,5
C 5 ML=ML+CO4*(V*V-BB)/2.*S3(K)
C GO TO 7
C 6 ML=ML+CO4*(V*V-BB/3.)/2.*S3(K)
C 7 MK1=S1(K)*A2-S2(K)*K4-S3(K)
C MK2=S1(K)*A1+S2(K)*K3

```

```

MKJ=S1(K)+S2(K)*X2*K4-S3(K)*X2**2*A2
MK4=(S2(K)*K3+S3(K)*X2*A1)*X2
ML1=S1(K)*J2+S2(K)*K5-S3(K)
ML2=S1(K)*J1-S2(K)*K3
ML3=S1(K)-S2(K)*Y2*K5-S3(K)*Y2**2*B2
ML4=(S2(K)*K3-S3(K)*Y2*B1)*Y2
DO 12 N=1,N1
RN=N
RNP2=RN*PI
AN=RN*PI/A
DN=RN*PI/B
AN2=AN**2
BN2=BN**2
BN4=BN2*BN2
BV1=BN*VL(L,2)
CV1=CCS(BV1)
SV1=SIN(BV1)
BL3=BN*VL(L,4)/2.
SBB=SIN(BL3)/BL3
DO 10 M=1,N1
RM=M
AM=RM*PI/A
AM2=AM*AM
AM4=AM2*AM2
AU1=AM*VL(L,1)
CU1=CCS(AU1)
Q1MN=CU1*CV1
C2MN=SIN(AU1)*SV1
RMN=DX*AM4+S3A*AM2+BN2+SCB*BN4
SMN=(SCC*AM4+SCD*BN2)*AM*BN
ALR=AM*VL(L,3)/2.
SAA=SIN(ALR)/ALR
RS=1./((RMN**2-SMN**2)*SAA*SBB*CO(L))
RSS=RS*RMN
RSS=RS*SMN
KMN=Q1MN*R5R-C2MN*R5S
LMN=Q2MN*K5X-Q1MN*R5S
IF (N.GT.1) GO TO 3
T5MB=CO(L)*CU1*SAA/2./DX/AM2*CDS(AM*U)
ML=ML-T5MB*S1(K)
IF (K.GT.1) GO TO 9
WL=WL+T5MB/AM2
IF (K.GT.1) GO TO 9
WL=WL+KMN*CC(M,N)+LMN*SS(M,N)
MK5=AM2*S1(K)+BN2*S3(K)
MK6=DN*A4*S1(K)
ML=ML-(MK5*(KMN-MK6*LMN)*CC(M,N)+(MK6*KMN-MK5*LMN)*SS(M,N))
CONTINUE
NH1=NH+N
NH2=NH2+N
NH3=NH3+N
NH4=NH4+N
NH5=NH5+N
NH6=NH6+N
NH7=NH7+N
T6NB=CCS(L)*CV1*SBB/2./BN2*CDS(DN*V)
IF (K.GT.1) GO TO 11
WL=T6NB/BN2+DC(N,L)*P1(N)+DC(NH1,L)*P2(N)+DC(NH2N,L)*P3(N)+DC(NH3N
1.L)*P4(N)+DC(NH4N,L)*P5(N)+DC(NH5N,L)*P6(N)+DC(NH6N,L)*P7(N)+DC(NH
27N,L)*P8(N)+WL
11 ML=ML+AN2*((-MK3*P5(N)-MK4*P6(N))*DC(NH4N,L)+(MK4*P5(N)-MK3*P6(N))
1*DC(NH5N,L)+(-ML3*P7(N)+ML4*P8(N))*DC(NH6N,L)+(-ML4*P7(N)-ML3*P8(N)
2))*DC(NH7N,L)
ML=ML+BN2*((MK1*P1(N)-MK2*P2(N))*DC(N,L)+(MK2*P1(N)+MK1*P2(N))*DC(
1NH1N,L)+(ML1*P3(N)-ML2*P4(N))*DC(NH2N,L)+(ML2*P3(N)+ML1*P4(N))*DC(N
2H3N,L))-T6NB*S3(K)
12 CONTINUE
YA(LNK,I)=L
13 CONTINUE
14 YA(LNK,I)=L
RETURN
END

```

74  
75  
76  
77  
78  
79  
80  
81  
82  
83  
84  
85  
86  
87  
88  
89  
90  
91  
92  
93  
94  
95  
96  
97  
98  
99  
100  
101  
102  
103  
104  
105  
106  
107  
108  
109  
110  
111  
112  
113  
114  
115  
116  
117  
118  
119  
120  
121  
122  
123  
124  
125  
126  
127  
128  
129  
130  
131  
132  
133  
134  
135  
136  
137  
138  
139  
140  
141  
142  
143  
144  
145

```

C *****
C SUBROUTINE JADA (CJ,DC,STOR,NS,JS,LN,NST1,NST2) ***** I 1
*****
DOUBLE PRECISION CJ,DC ***** I 2
REAL KM, MK1, MK2, MK3, MK4, MK5, MK6, ML1, ML2, ML3, ML4, ML, KJ, X4, X5, MF, LM ***** I 3
IN ***** I 4
COMMON /BL/ B,OX,OY,DX,Y,D1,D2,EI,GJ,H,VL(4,5),ZB ***** I 5
COMMON /BL1/ P,CO(4),COS(4),XJ,K4,X5,BB,BB3,BB4,X2,Y2,A1,A2,A3,A4, ***** I 6
I B1,B2,B3,B, SCA,SCB,SCC,SCD,S1(4),S2(4),S3(4),S4(4),S5(4),S6(4), ***** I 7
2 S7(4)
COMMON /BL2/ JC,NB3,NC,JC,NH2,NH3,NH4,NH5,NH6,NH7,NH8,N81,NS2,NH,NL ***** I 8
COMMON /EX/ JC(24),VC(24),NGC,YA(40,24),NR,UR(9),VR(3),NP(10) ***** I 9
DIMENSION CJ(NS,JS),DC(NS,LN),STO(NST1,NST2) ***** I 11
DIMENSION P(20),P10(20),P11(20),P12(20),P13(20),P14(20),P15 ***** I 12
1 (20),P16(20),SC(20,20),CS(20,20) ***** I 13
LT=MMH*10 ***** I 14
DO 8 I=1,NS ***** I 15
UE=UC(I) ***** I 16
V=VC(I) ***** I 17
DO 1 N=1,NH ***** I 18
RN=N ***** I 19
RNP2=RN*P1 ***** I 20
AN=RNP2/A ***** I 21
BN=RNP2/U ***** I 22
VN=BN*V ***** I 23
AV=AN*V ***** I 24
BU=BN*U ***** I 25
UV=VN*V ***** I 26
V4U=K4*X2*AV+AU ***** I 27
V5U=K5*Y2*AV-AU ***** I 28
CHUN=COSH(JJN) ***** I 29
SHUN= SINH(JJN) ***** I 30
P0(N)=SHUN*CO(U4V) ***** I 31
P10(N)=CHUN*V*SIN(U4V) ***** I 32
P11(N)=SHUN*COS(U5V) ***** I 33
P12(N)=CHUN*V*SIN(U5V) ***** I 34
P13(N)=SINH(V3N)*COS(V4U) ***** I 35
P14(N)=COSH(V3N)*SIN(V4U) ***** I 36
P15(N)=SINH(V3Y)*COS(V5U) ***** I 37
P16(N)=COSH(V3Y)*SIN(V5U) ***** I 38
CV=COS(VN) ***** I 39
SV=SIN(VN) ***** I 40
DO 1 N=1,NH ***** I 41
RM=M ***** I 42
UM=RM*P1*U/A ***** I 43
SC(X,N)=S1(LUM)*CV ***** I 44
CS(M,N)=COS(UM)*SV ***** I 45
DO 8 L=1,NL ***** I 46
LNK = NHG+(L-1)*LT ***** I 47
ML=DC(N81,L)*U/A+DC(N83,L)*(U/A)**3+DC(N82,L)*V/B+DC(NC,L)*(V/B)** ***** I 48
13 ***** I 49
DO 7 K=1,3 ***** I 50
LNH=LN+4NH*K ***** I 51
ML=6.0*S1(K)*U/A+3*DC(N83,L)+6.*S3(K)*V/B+3*DC(NC,L) ***** I 52
MK1=S1(K)*A1-S2(K)*K4-S3(K) ***** I 53
MK2=S1(K)*A1+S2(K)*K3 ***** I 54
MK3=S1(K)+S2(K)*X2*K4-S3(K)*X2**2*A2 ***** I 55
MK4=(S2(K)*K3+S3(K)*X2*A1)*X2 ***** I 56
ML1=S1(K)*B1+S2(K)*K5-S3(K) ***** I 57
ML2=S1(K)*B1-S2(K)*K3 ***** I 58
ML3=S1(K)-S2(K)*Y2*K5-S3(K)*Y2**2*B2 ***** I 59
ML4=(S2(K)*K3-S3(K)*Y2*B1)*Y2 ***** I 60
DO 6 N=1,NH ***** I 61
RN=N ***** I 62
RNP2=RN*P1 ***** I 63
AN=RNP2/A ***** I 64
UN=RNP2/U ***** I 65
AN2=AN*AN ***** I 66
BN2=UN*BN ***** I 67

```



```

BN4=BN2*JN2
BV1=BN*VL(L,2)
CV1=CCS(BV1)
SV1=SIN(BV1)
BL3=BN*VL(L,4)/2.
SBB=SIN(BL3)/BL3
DC 4 N=1,NH
RM=K
AM=RM*PI/A
AM2=AM*AM
AN4=A*2*AM2
AU1=AN*VL(L,1)
CU1=CCS(AU1)
SU1=SIN(AU1)
O3MN=SC1*CV1
O4MN=CCS(AU1)*SV1
PMN=DX*AA+SCA*AM2*BN2+SCB*BN4
SMN=(SCC*AM1+SCD*BN2)*AN*BN
ALR=AN*VL(L,3)/2.
SAA=SIN(ALR)/ALR
RS=1./((RMN**2-SMN**2)*SAA*SBB*CU(L)
RSR=RS*RMN
RSS=RS*SMN
PMN=O3MN*RSR+O4MN*RSS
OMN=O4MN*RSR+O3MN*RSS
IF (N.GT.1) GO TO 2
T74B=CO(L)+LJ1*SAA/2./DX/AM2*SIN(AM*U)
ML=ML-T74B*S1(K)
IF (K.GT.1) GO TO 3
WL=WL+T74B/AM2
2 IF (K.GT.1) GO TO 3
3 MK5=AM2*S1(K)+BN2*S3(K)
MK6=BN*AA*SC(K)
4 ML=ML-(MK5*PMN+MK6*OMN)*SC(M,N)-(MK6*PMN+MK5*OMN)*CS(M,N)
CONTINUE
NH2N=NH2+N
NH3N=NH3+N
NH4N=NH4+N
NH5N=NH5+N
NH6N=NH6+N
NH7N=NH7+N
T8NB=CCS(L)*SV1*SBB/2./BN2*S1N(BN*V)
IF (K.GT.1) GO TO 5
WL=WL+JC(N,L)*P9(N)+DC(NH2N,L)*P10(N)+DC(NH3N,L)*
1 P12(N)+JC(N44N,L)*P13(N)+DC(NH5N,L)*P14(N)+DC(NH6N,L)*P15(N)+DC(NH
27N,L)*P16(N)+T8NB/BN2
5 ML=ML+BN2*((4K1*P9(N)-4K2*P10(N))*DC(N,L)+(MK2*P9(N)+MK1*P10(N))*O
1C(NH2N,L)+(ML1*P11(N)-ML2*P12(N))*DC(NH2N,L)+(ML2*P11(N)+ML1*P12(N)
2)*DC(NH3N,L)-T8NB*S3(K)
ML=ML+AN2*((-MK3*P13(N)-MK4*P14(N))*DC(NH4N,L)+(MK4*P13(N)-MK3*P14
1(N))*DC(NH5N,L)+(-ML3*P15(N)+ML4*P16(N))*DC(NH6N,L)+(-ML4*P15(N)-M
2L3*P16(N))*DC(NH7N,L))
6 CONTINUE
YA(LNM,I)=AL+YA(LNM,I)
7 CONTINUE
8 YA(LNW,I)=WL+YA(LNW,I)
RETURN
END

```

```

IIII 74
IIII 75
IIII 76
IIII 77
IIII 78
IIII 79
IIII 80
IIII 81
IIII 82
IIII 83
IIII 84
IIII 85
IIII 86
IIII 87
IIII 88
IIII 89
IIII 90
IIII 91
IIII 92
IIII 93
IIII 94
IIII 95
IIII 96
IIII 97
IIII 98
IIII 99
IIII 100
IIII 101
IIII 102
IIII 103
IIII 104
IIII 105
IIII 106
IIII 107
IIII 108
IIII 109
IIII 110
IIII 111
IIII 112
IIII 113
IIII 114
IIII 115
IIII 116
IIII 117
IIII 118
IIII 119
IIII 120
IIII 121
IIII 122
IIII 123
IIII 124
IIII 125
IIII 126
IIII 127
IIII 128
IIII 129
IIII 130
IIII 131
IIII 132
IIII 133

```

```

*****
SUBROUTINE JSRA (CD,DC,STOR,NS,JS,LN,NST1,NST2)
*****
DOUBLE PRECISION CH,DC
      COMPUTE DEFLECTIONS AND MOMENTS (OLD SERIES)
      REAL KMN,MK1,MK2,MK3,MK4,MK5,MK6,ML1,ML2,ML3,ML4,ML,K3,K4,K5,MF,LM
1N
COMMON A,PI,SA,C,S,TN,C4,AA,AA3,AA4,Z,SYAS,C2,C3,ST,SF,T,TD,MNH
COMMON /BL0/ S,DX,DY,DXY,DYX,D1,D2,E1,GJ,H,VL(4,5),ZB
COMMON /BL1/ P,CQ(4),COS(4),K3,K4,K5,BB,BB3,BB4,X2,Y2,A1,A2,A3,A4,
1B1,B2,B3,B4,SCA,SCB,SCC,SCD,S1(4),S2(4),S3(4),S4(4),S5(4),S6(4),
2 S7(4)
COMMON /BL5/ NHC,NB3,NC,JC,NH2,NH3,NH4,NH5,NH6,NH7,NH8,NB1,NB2,NH,NL
COMMON /EXL/ UC(24),VC(24),NGC,YA(400,24),NR,UR(9),VR(3),NP(10)
DIMENSION CJ(NS,JS),DC(NS,LN),STOR(NST1,NST2)
DIMENSION P1(20),P2(20),P3(20),P4(20),P5(20),P6(20),P7(20),
1P8(20),CC(20,20),SS(20,20)
DIMENSION P9(20),P10(20),P11(20),P12(20),P13(20),P14(20),P15(20)
1 ,P16(20),
      CS(20,20),SC(20,20)
      LT=MNX*10
      DO 14 J=1,NR
      V = VR(J)
      DO 14 I=1,9
      U = UR(I)
      DO 1 N=1,N1
      RN=N
      RNP2=RN*PI
      AN=RNP2/A
      BN=RNP2/B
      VN=BN*V
      AU=AN*U
      BU=BN*U
      AV=AN*V
      AVK=AV*K3
      U3N=K3*BU
      V3N=AV*KX2
      V3Y=AV*Y2
      U4V=K4*BJ+V.N
      U5V=K5*BJ-V.N
      V4U=K4*X2*AV+AU
      V5U=K5*Y2*AV-AU
      CHUN=COSH(U3N)
      SHUN=SINH(U3N)
      CHVN = COSH(V3N)
      SHVN = SINH(V3N)
      CHVY = COSH(V3Y)
      SHVY = SINH(V3Y)
      CU4 = COS(U4V)
      SU4 = SIN(U4V)
      CU5 = COS(U5V)
      SU5 = SIN(U5V)
      CV4 = COS(V4U)
      SV4 = SIN(V4U)
      CV5 = COS(V5U)
      SV5 = SIN(V5U)
      P 1(N) = CHUN * CU4
      P 2(N) = SHUN * SU4
      P 3(N) = CHUN * CU5
      P 4(N) = SHUN * SU5
      P 5(N) = CHVN * CV4
      P 6(N) = SHVN * SV4
      P 7(N) = CHVY * CV5
      P 8(N) = SHVY * SV5
      P 9(N) = CHUN * CU4
      P10(N) = SHUN * SU4
      P11(N) = CHUN * CU5
      P12(N) = SHUN * SU5
      P13(N) = CHVN * CV4
      P14(N) = SHVN * SV4
      P15(N) = CHVY * CV5
      P16(N) = SHVY * SV5
      CV=COS(VN)
      SV=SIN(VN)
      DO 1 K=1,N1

```

```

      2
      3
      4
      5
      6
      7
      8
      9
     10
     11
     12
     13
     14
     15
     16
     17
     18
     19
     20
     21
     22
     23
     24
     25
     26
     27
     28
     29
     30
     31
     32
     33
     34
     35
     36
     37
     38
     39
     40
     41
     42
     43
     44
     45
     46
     47
     48
     49
     50

```

```

RNM=N
UM=RN
CU=CCS(U/A)
SU=SIN(U/A)
CC(N,7)=SU*CV
SS(N,7)=SU*SV
CC(X,7)=SU*SV
DO 14 L=1,N
LNZ=NR*(L-1)*LT+(J+6)*MNH
K=4
COA=CCS(L)/4.
IF (.NOT.(1.EQ.1.OR.1.EQ.9)) GO TO 20
ML=2.*S1(K)*DC(NB2,L)/AA+2.*S3(K)*DC(NS3,L)/BB+12.*(T*U**2*S1(K)-V
1**2*SJ(K))*JC(NC,L)/BB4+CO4*(V*V-BB)/2.*S3(K)
IF (ZB) 6,5,5
5 ML=ML+CO4*(V*V-BB)/2.*S3(K)
GO TO 7
6 ML=ML+CO4*(V*V-BB/3.)/2.*S3(K)
7 MK1=S1(K)*A2-S2(K)*K4-S3(K)
MK2=S1(K)*A1+S2(K)*K3
MK3=S1(K)+S2(K)*X2*K4-SJ(K)*X2**2*A2
MK4=(S2(K)*KJ+S3(K)*X2*A1)*X2
ML1=S1(K)*B2+S2(K)*K5-S3(K)
ML2=S1(K)*B1-S2(K)*K3
ML3=S1(K)-S2(K)*Y2*K5-S3(K)*Y2**2*B2
ML4=(S2(K)*K3-S3(K)*Y2*B1)*Y2
20 QL=24.*(S4(K)*T*U-S7(K)*V)/BB4+DC(NC,L)+CO4*V*S7(K)
OK1=S4(K)*A3-S5(K)*A1-S6(K)*K3
OK2=S4(K)*A4+S5(K)*A2-S6(K)*K4-S7(K)
OK3=X2*(S5(K)*K3+S6(K)*X2*A1-S7(K)*X2*X2*A3)
OK4=S4(K)+X2*S5(K)*K4-S6(K)*X2*X2*A2-S7(K)*X2**3*A4
OL1=S4(K)*B3+S5(K)*B1-S6(K)*K3
OL2=S4(K)*B4-S5(K)*B2-S6(K)*K5+S7(K)
OL3=Y2*(S5(K)*K3-S6(K)*Y2*B1-S7(K)*Y2*Y2*B3)
OL4=S4(K)-Y2*S5(K)*K5-S6(K)*Y2*Y2*B2+S7(K)*Y2**3*B4
DO 12 N=1,N4
RNM=N
RND2=RN*PI
AN=RN*PI/A
BN=RN*PI/3
AN2=AN**2
BN2=BN**2
AN3=AN**3
BN3=BN**3
BN4=BN**4
DV1=DN*VL(L,2)
CV1=CCS(BV1)
SV1=SIN(BV1)
BLS=BN*VL(L,4)/2.
SBB=SIN(BLS)/BLS
VN=EN*V
DO 10 N=1,N4
RNM=N
AM=RN*PI/A
AM2=AM**2
AM4=AM**4
AUJ=AN*VL(L,1)
CU1=CCS(AUJ)
SUJ=SIN(AUJ)
O1MN=CU1*CV1
O2MN=SU1*SV1
O3MN=SU1*CV1
O4MN=CU1*SV1
RMN=DX*AM4+SCA*AM2*BN2+SCB*BN4
SMN=(SCC*AM2+SCD*BN2)*AM*BN
ALR=AN*VL(L,3)/2.
SAA=SIN(ALR)/ALR
RS=1./(RMN**2-SMN**2)*SAA*SBB*CO(L)
RSR=RS*RMN
RSS=RS*SIN
KMN=C1MN*RSR-O2MN*RSS
LMN=C2MN*RSR-O1MN*RSS
PMN=C3MN*RSR+O4MN*RSS
OMN=C4MN*RSR+O3MN*RSS
UM=AM*U
IF (N.GT.1) GO TO 8
TSMJ=CC(L)*CUJ*SAA/2./DX/AM

```

G 51  
 G 52  
 G 55  
 G 57  
 G 66  
 G 68  
 G 69  
 G 70  
 G 71  
 G 72  
 G 73  
 G 74  
 G 75  
 G 76  
 G 77  
 G 78  
 G 79  
 G 80  
 G 81  
 G 82  
 G 83  
 G 84  
 G 85  
 G 86  
 G 87  
 G 88  
 G 89  
 G 90  
 G 91  
 G 92  
 G 93  
 G 94  
 G 95  
 G 96  
 G 97  
 G 98  
 G 99  
 G 102  
 G 103  
 G 104  
 G 105  
 G 106  
 G 107  
 G 108  
 G 111

```

IF (.NOT.(I.EQ.1.OR.I.EQ.9)) GO TO 21
ML=ML-T543*S1(K)/AM*COS(UM)
21 CL = CL+T543*S4(K)*SIN(UM)
8 IF (.NOT.(I.EQ.1.OR.I.EQ.9)) GO TO 22
MK5=AK2*S1(K)+BN2*S3(K)
MK6=BN1+A4*S2(K)
ML=ML-(MK5*(MN-MK6*LMN))*CC(M,N)+(MK6*KMN-MK5*LMN)*SS(M,N)
22 OK5 = AM*(A42*S4(K)+BN2*S6(K))
OK6 = BN*(A42*S5(K)+BN2*S7(K))
10 QL = QL+(JK5*(KMN-OK6*LMN))*SC(M,N)+(OK6*(KMN-OK5*LMN))*CS(M,N)
NH1=NH+N
NH2N=NH2+N
NH3N=NH3+N
NH4N=NH4+N
NH5N=NH5+N
NH6N=NH6+N
NH7N=NH7+N
T6NB=CCS(L)*CV1*SBB/2./BN
IF (.NOT.(I.EQ.1.OR.I.EQ.9)) GO TO 23
11 ML=ML+AN2*((-MK3*P5(N)-MK4*P6(N))*DC(NH4N,L)+(MK4*P5(N)-MK3*P6(N))
1*DC(NH5N,L)+(-ML3*P7(N)+4L4*P8(N))*DC(NH6N,L)+(-ML4*P7(N)-ML3*P8(N)
2))*DC(NH7N,L)
ML=ML+BN2*((MK1*P1(N)-MK2*P2(N))*DC(N,L)+(MK2*P1(N)+MK1*P2(N))*DC(
1NH2N,L)+(ML1*P3(N)-ML2*P4(N))*DC(NH2N,L)+(ML2*P3(N)+ML1*P4(N))*DC(N
2H3N,L))-T543*S3(K)/BN*COS(VN)
23 QL = CL+AN3*((-OK3*P13(N)+OK4*P14(N))*DC(NH4N,L)+
1 (-OK4*P13(N)-OK3*P14(N))*DC(NH5N,L)+
2 (-QL3*P15(N)-QL4*P16(N))*DC(NH6N,L)+
3 (QL4*P15(N)-QL3*P16(N))*DC(NH7N,L))+T6NB*S7(K)
4 *SIN(VN)
12 QL = CL+B43*((OK1*P9(N)-OK2*P10(N))*DC(N,L)+
1 (OK2*P9(N)+OK1*P10(N))*DC(NH2N,L)+
2 (QL1*P11(N)-QL2*P12(N))*DC(NH3N,L)+
3 (QL2*P11(N)+QL1*P12(N))*DC(NH3N,L))
YA(LNR,1) = QL
IF (I.EQ.1) YA(LNR,10) = -ML
IF (I.NE.9) GO TO 14
YA(LNR,11) = ML
YA(LNR,12) = (YA(LNR,1)+YA(LNR,9)+2.*(2.*(YA(LNR,2)+YA(LNR,4)+
1YA(LNR,6) + YA(LNR,8))+YA(LNR,3)+YA(LNR,5)+YA(LNR,7)))*A/12.
2 +YA(LNR,10)+ML
14 CONTINUE
RETURN
END
G 119
G 120
G 122
G 123
G 124
G 125
G 126
G 127
G 128
G 134
G 135
G 136
G 137
G 138
G 139
G 144
G 145-

```

```

*****
SUBROUTINE JARA (CU,DC,STOR,NS,JS,LN,NST1,NST2)
*****
DOUBLE PRECISION CH,DC
REAL XMN,MK1,MK2,MK3,MK4,MK5,MK6,ML1,ML2,ML3,ML4,ML,K3,K4,K5,MF,LM
1N
COMMON A,B1,SA,C,S,TN,C4,AA,AA3,AA4,I,SYAS,C2,CJ,ST,ST,T,TB,MNH
COMMON /BLU/ B,DX,DY,DX,YD,DYX,D1,D2,E1,GJ,H,VL(4,5),ZB
COMMON /BLI/ P,CQ(4),COS(4),K3,K4,K5,BB,BB3,BB4,X2,Y2,A1,A2,A3,A4,
1B1,B2,B3,B4,SCA,SCB,SCC,SCD,S1(4),S2(4),S3(4),S4(4),S5(4),
2 S7(4)
COMMON /BLV/ JHC,NB3,NC,JC,NH2,NH3,NH4,NH5,NH6,NH7,N13,NB1,NB2,NH,NL
COMMON /EX/ UC(24),VC(24),NGC,YA(400,24),NR,UR(9),VR(3),NP(10)
DIMENSION CU(NS,JS),DC(NS,LN),STOR(NST1,NST2)
DIMENSION P1(20),P2(20),P3(20),P4(20),P5(20),P6(20),P7(20),
1P8(20),CC(20,20),SS(20,20)
DIMENSION P9(20),P10(20),P11(20),P12(20),P13(20),P14(20),P15
1(20),P16(20),SC(20,20),CS(20,20)
LT=MNH*10
DO 1 J=1,N3
V = VR(J)
DO 3 I=1,9
U = UR(I)
DO 1 N=1,NH
2NEN
RNDP=RP*PI
AN=RN*PI/A
BN=RN*PI/B
VNE=SN*V
AUB=AN*U
BUB=BN*U
AVR=AN*V
AVK=AV*K3
UJN=KJ*UJ
VJN=AVK*VJ2
VJY=AVK*YJ2
UV=K4*UJ+VJ
UV=K5*UJ+VJ
VAU=K4*XJ*AV+AU
V5U=K5*YJ*AV+AU
CHUN=COSH(JJN)
SHUN=SINH(JJN)
CHVN = COSH(VJN)
SHVN = SINH(VJN)
CHVY = COSH(VJY)
SHVY = SINH(VJY)
CU4 = COS(UJ+V)
SU4 = SINH(UJ+V)
CU5 = COS(UJ+V)
SU5 = SINH(UJ+V)
CU4 = COS(VJ+U)
SU4 = SINH(VJ+U)
CU5 = COS(VJ+U)
SU5 = SINH(VJ+U)
P 1(N) = CHUN ** CU4
P 2(N) = SHUN ** SU4
P 3(N) = CHUN ** CU5
P 4(N) = SHUN ** SU5
P 5(N) = CHVN ** CU4
P 6(N) = SHVN ** SU4
P 7(N) = CHVY ** CU4
P 8(N) = SHVY ** SU4
P 9(N) = SHVN ** SU5
P10(N) = CHUN ** SU4
P11(N) = SHUN ** SU5
P12(N) = CHUN ** SU5
P13(N) = SHVN ** SU4
P14(N) = CHVN ** SU4
P15(N) = SHVY ** SU5
P16(N) = CHVY ** SU5
CV=COS(VN)
SV=SIN(VN)
DO 1 X=1,N4
3NEM
UM=RM*PI*U/A
CU = COS(UA)

```

I	2
I	3
I	4
I	5
I	6
I	7
I	8
I	9
I	10
I	11
I	12
I	13
I	14
I	15
I	16
I	17
I	18
I	19
I	20
I	21
I	22
I	23
I	24
I	25
I	26
I	27
I	28
I	29
I	30
I	31
I	32
I	33
I	34
I	35
I	36
I	37
I	38
I	39
I	40
I	41
I	42
I	43
I	44
I	45
I	46
I	47
I	48
I	49
I	50

```

SU = SIN(UM)
CC(X,N) = CU * CV
SS(X,N) = SU * SV
SC(X,N) = CU * CV
CS(X,N) = SU * SV
DO 8 L=1,NL
LNH = NHC + (L-1)*LT + (J+6)*MNH
K = 4
IF (.NOT. (I.EG.1.OR.I.EQ.9)) GO TO 20
ML=0.0*S1(K)*U/AA3+DC(NB3,L)+6.*S3(K)*V/BB3+DC(NC,L)
MK1=S1(K)*A1-S2(K)*K4-S3(K)
MK2=S1(K)*A1+S2(K)*K3
MK3=S1(K)+S2(K)*X2*K4-S3(K)*X2**2*A2
MK4=(S2(K)*K3+S3(K)*X2*A1)*X2
ML1=S1(K)*B1+S2(K)*K5-S3(K)
ML2=S1(K)*B1-S2(K)*K3
ML3=S1(K)-S2(K)*Y2*K5-S3(K)*Y2**2*B2
ML4=(S2(K)*K3-S3(K)*Y2*B1)*Y2
OL = C.*(J+K)*DC(NB3,L)/AA3+S7(K)*DC(NC,L)/BB3
OK1 = S4(K)*A3-S5(K)*A1-S6(K)*K3
OK2 = S4(K)*A4+S5(K)*A2-S6(K)*K4-S7(K)
OK3 = A2*(S5(K)*K3+S6(K)*X2) - A1-S7(K)*X2*X2*A3
OK4 = S4(K)*X2*S5(K)*K4-S6(K)*X2*X2*A2-S7(K)*X2**3*A4
OL1 = S4(K)*B3+S5(K)*B1-S6(K)*K3
OL2 = S4(K)*B4-S5(K)*B2-S6(K)*K5+S7(K)
OL3 = Y2*(S5(K)*K3-S6(K)*Y2) - B1-S7(K)*Y2*Y2*B3
OL4 = S4(K)-Y2*S5(K)*K5-S6(K)*Y2*Y2*B2+S7(K)*Y2**3*B4
DO 6 N=1,NH
RN=RN
RNP2=RN*PI
AN=RNF2/A
BN=RNF2/B
AN2=AN*AN
BN2=BN*BN
AN3 = AN2*AN
BN3 = BN2*BN
BN4=BN*BN2
BV1=BN*VL(L,2)
CV1=CCS(BV1)
SV1=SIN(BV1)
BLS=BN*VL(L,4)/2.
SBB=SIN(BLS)/BLS
VN = BN*V
DO 4 M=1,NH
RM=RM
AM=RM*PI/A
AM2=AM*AM
AM4=AM2*AM2
AU1=AM*VL(L,1)
CU1=CCS(AU1)
SU1 = SIN(AU1)
O1MN = CU1*CV1
O2MN = SU1*CV1
O3MN = SU1*SV1
O4MN = CU1*SV1
RMN=DX*AM4+SCA*AM2*BN2+SCB*BN4
SMN=(SCC*AM2+SCO*BN2)*AM*BN
ALR=AM*VL(L,3)/2.
SAA=SIN(ALR)/ALR
RS=1./((RMN**2-SMN**2)*SAA*SBB*CO(L))
RGR=RS*RMN
RSG=RS*SMN
XMN = O1MN*RGR-O2MN*RSS
LMN = O2MN*RGR-O1MN*RSS
PMN = O3MN*RGR+O4MN*RSS
OMN = O4MN*RGR+O3MN*RSS
UM = AM*J
IF (N.GT.1) GO TO 2
T7MB=CC(L)*SU1*SAA/2./DX/AM
IF (.NOT. (I.EG.1.OR.I.EQ.9)) GO TO -1
ML=ML-T7MB*S1(K)/AM*SIN(UM)
OL = OL-T7MB*S4(K)*COS(UM)
IF (.NOT. (I.EG.1.OR.I.EQ.9)) GO TO -2
MK5=AM2*S1(K)+BN2*S3(K)
MK6=BN2*A4*S2(K)
ML=ML-(MK5*PMN+MK6*OMN)*SC(N,N)-(MK6*PMN+MK5*OMN)*CS(M,N)
OK5 = AM*(A42*S4(K)+BN2*S6(K))
OK6 = BN*(A42*S5(K)+BN2*S7(K))

```

I 52  
 I 58  
 I 59  
 I 60  
 I 61  
 I 62  
 I 63  
 I 64  
 I 65  
 I 66  
 I 67  
 I 68  
 I 69  
 I 70  
 I 71  
 I 72  
 I 73  
 I 74  
 I 75  
 I 76  
 I 77  
 I 78  
 I 79  
 I 80  
 I 81  
 I 82  
 I 83  
 I 84  
 I 85  
 I 86  
 I 90  
 I 91  
 I 92  
 I 93  
 I 94  
 I 95  
 I 96  
 I 99  
 I 107  
 I 108

```

4      QL = QL - (JK5*PMN + OK6*QMN)*CC(M,N) + (CK6*PMN + GK5*QMN)*SS(M,N)
      NHN=NH+N
      NH2N=NH2+N
      NH3N=NH3+N
      NH4N=NH4+N
      NH5N=NH5+N
      NH6N=NH6+N
      NH7N=NH7+N
      TBNS=CCS(L)*SV1*SBB/2./BN
      IF (.NOT.(I.EQ.1.OR.I.EQ.9)) GO TO 23
5      ML=ML+DN2*((MK1*P9(N)-MK2*P10(N))*JC(N,L)+(MK2*P9(N)+MK1*P10(N))*D
      1C(NH,N,L)+(ML1*P11(N)-ML2*P12(N))*DC(NH2N,L)+(ML2*P11(N)+ML1*P12(N)
      2)*DC(NH3N,L))-TBNS*S3(K)/BN*SIN(VN)
      ML=ML+AN2*((-MK3*P13(N)-MK4*P14(N))*DC(NH4N,L)+(MK4*P13(N)-MK3*P14
      1(N))*DC(NH5N,L)+(-ML3*P15(N)+ML4*P16(N))*DC(NH6N,L)+(-ML4*P15(N)-M
      2L3*P16(N))*DC(NH7N,L))
23     QL = QL + AN3*((-OK3*P 5(N)+OK4*P 6(N))*DC(NH4N,L)+
      1      (-OK4*P 5(N)-OK3*P 6(N))*DC(NH5N,L)+
      2      (-OL3*P 7(N)-OL4*P 8(N))*DC(NH6N,L)+
      3      (OL4*P 7(N)-OL3*P 8(N))*DC(NH7N,L))-TBNS*S7(K)
      4      *COS(VN)
C     QL = QL + BN3*((OK1*P 1(N)-OK2*P 2(N))*DC(N,L)+
      1      (OK2*P 1(N)+OK1*P 2(N))*DC(NH,N,L)+
      2      (OL1*P 3(N)-OL2*P 4(N))*DC(NH2N,L)+
      3      (OL2*P 3(N)+OL1*P 4(N))*DC(NH3N,L))
      YA(LNR,1) = QL + YA(LNR,1)
      IF (I.EQ.1) YA(LNR,10) = -ML + YA(LNR,10)
      IF (I.NE.9) GO TO 8
      YA(LNR,11) = ML + YA(LNR,11)
      YA(LNR,12) = (YA(LNR,1) + YA(LNR,9) + 2.*(2.*(YA(LNR,2) + YA(LNR,4) +
      1YA(LNR,6) + YA(LNR,8)) + YA(LNR,3) + YA(LNR,5) + YA(LNR,7)))*A/12.
      2      + YA(LNR,10) + ML
8      CONTINUE
      RETURN
      END
      H 132
      H 133-

```

SLAB NUMBER HALF  
INPUT DATA

PROPERTIES OF SLAB 50.55  
 HALF-WIDTH OF SLAB 32.00  
 HALF-SPAN OF SLAB 45.00  
 SKEW ANGLE  
 DX 13.40  
 DY 11.35  
 D1 1.22  
 D2 1.22  
 DXY 1.17  
 DYX 1.17  
 EI 62.71  
 GJ 35.35

LOADING SYSTEM

GENERAL LOADING (SYMMETRIC & ANTISYMMETRIC LOADS)

LOADING CASE	J1	VI	WIDTH OF LOAD	WIDTH OF LOAD	WIDTH OF LOAD	TOTAL LOAD
1	0.0	0.0	7.07000	7.07000	6.00000	100.00000
2	23.12999	0.0	7.07000	7.07000	6.00000	100.00000
3	46.66999	0.0	7.07000	7.07000	6.00000	100.00000
4	0.0	14.00000	7.07000	7.07000	6.00000	100.00000

THE SLAB IS ELASTICALLY SUPPORTED ON TWO EDGES

THE SLAB IS FLEXURALLY STRONG AND TORSIONALLY WEAK

DEPTH OF N.A. FROM TOP FIBRE -1.3730 -1.3740 -1.3740  
 SLAB THICKNESS = 4.0000 INS  
 TOP GAGES 1 THRU 12  
 BOTTOM GAGES 13 THRU 24

LOADING CASE	J1	VI	WIDTH OF LOAD	WIDTH OF LOAD	WIDTH OF LOAD	TOTAL LOAD
1	0.0	0.0	7.07000	7.07000	6.00000	100.00000
2	23.13	0.0	7.07	7.07	6.00	100.00
3	46.67	0.0	7.07	7.07	6.00	100.00
4	0.0	14.00	7.07	7.07	6.00	100.00
5	0.0	0.0	7.07	7.07	6.00	100.00
6	23.13	0.0	7.07	7.07	6.00	100.00
7	46.67	0.0	7.07	7.07	6.00	100.00
8	0.0	14.00	7.07	7.07	6.00	100.00
9	0.0	0.0	7.07	7.07	6.00	100.00
10	23.13	0.0	7.07	7.07	6.00	100.00
11	46.67	0.0	7.07	7.07	6.00	100.00
12	0.0	14.00	7.07	7.07	6.00	100.00
13	0.0	0.0	7.07	7.07	6.00	100.00
14	23.13	0.0	7.07	7.07	6.00	100.00
15	46.67	0.0	7.07	7.07	6.00	100.00
16	0.0	14.00	7.07	7.07	6.00	100.00
17	0.0	0.0	7.07	7.07	6.00	100.00
18	23.13	0.0	7.07	7.07	6.00	100.00
19	46.67	0.0	7.07	7.07	6.00	100.00
20	0.0	14.00	7.07	7.07	6.00	100.00
21	0.0	0.0	7.07	7.07	6.00	100.00
22	23.13	0.0	7.07	7.07	6.00	100.00
23	46.67	0.0	7.07	7.07	6.00	100.00
24	0.0	14.00	7.07	7.07	6.00	100.00

DEFLECTION  
 MOMENT PARALLEL TO X-AXIS (HX)  
 MOMENT PARALLEL TO Y-AXIS (HY)  
 TWISTING MOMENT (MXY)  
 PRINCIPAL MOMENT M1  
 PRINCIPAL MOMENT M2  
 PRINCIPAL DIRECTION  
 STRAIN IN X-AXIS  
 STRAIN IN Y-AXIS  
 STRAIN IN U-AXIS



LOADING CASE	J1	VI	WIDTH OF LOAD	BREADTH OF LOAD	TOTAL LOAD							
2	21.33999	0.0	7.37000	6.00000	100.00000							
1	2	3	4	5	6	7	8	9	10	11	12	
U=	50.50	46.67	23.33	0.0	-23.33	46.67	23.33	0.0	-23.33	-46.67	-50.50	
V=	0.0	0.0	0.0	0.0	16.50	16.50	16.50	16.50	16.50	16.50	16.50	
DEFLECTION												
III=10:	514.9275:	001.1711:	796.3682:	543.4211:	400.3630:	447.5977:	605.5100:	601.6943:	520.4634:	373.6277:	364.6731:	304.3767:
MOMENT PARALLEL TO X-AXIS (MX)												
III=10:	-30.2967:	-16.6230:	23.7979:	9.0393:	3.9278:	16.9212:	-9.0908:	6.7506:	3.4668:	3.0619:	-4.9301:	51.0521:
MOMENT PARALLEL TO Y-AXIS (MY)												
III=10:	21.0620:	7.2133:	35.1260:	10.0072:	6.3325:	21.0310:	1.4576:	0.7869:	14.8120:	9.1508:	1.4632:	0.4819:
TWISTING MOMENT MAY												
III=10:	-2.2237:	1.2060:	1.2415:	1.0900:	0.0299:	0.4650:	-0.2231:	0.5799:	0.6753:	0.7308:	0.6173:	-1.5714:
PRINCIPAL MOMENT M1												
III=10:	23.9539:	7.2742:	35.4010:	11.3329:	6.5911:	21.0030:	1.4625:	0.9411:	14.0521:	9.2370:	3.5083:	53.1052:
PRINCIPAL MOMENT M2												
III=10:	-30.3070:	-16.6035:	21.5229:	0.5137:	3.6672:	16.0692:	-9.1035:	6.6055:	3.4267:	2.9754:	-4.9752:	0.4209:
PRINCIPAL DIRECTION												
III=10:	2.3472:	-2.0090:	-12.4917:	-25.5821:	-17.3072:	-6.3736:	1.2101:	-14.8874:	-3.3942:	-6.7490:	-4.1036:	-1.8192:
STRAIN IN X-AXIS												
III=10:	3.3570:	1.7063:	-2.7470:	-0.0321:	-0.3461:	-1.5501:	0.9342:	-0.6156:	-0.2103:	-0.2300:	0.5423:	-5.4700:
STRAIN IN Y-AXIS												
III=10:	-2.7636:	-0.9062:	-1.3629:	-1.0359:	-0.6199:	-2.0222:	-0.2375:	-0.8470:	-1.5043:	-0.9206:	-0.4061:	0.4529:
STRAIN IN U-AXIS												
III=10:	*****											

LOADING CASE	J1	VI	WIDTH OF LOAD	BREADTH OF LOAD	TOTAL LOAD							
3	46.00000	0.0	7.07000	6.00000	100.00000							
1	2	3	4	5	6	7	8	9	10	11	12	
U=	50.50	46.67	23.33	0.0	-23.33	46.67	23.33	0.0	-23.33	-46.67	-50.50	
V=	0.0	0.0	0.0	0.0	16.50	16.50	16.50	16.50	16.50	16.50	16.50	
DEFLECTION												
III=10:	1044.0545:	1603.3520:	703.3900:	447.0950:	361.7495:	402.5201:	1109.1970:	794.0920:	430.5667:	314.0842:	355.7027:	304.2104:
MOMENT PARALLEL TO X-AXIS (MX)												
III=10:	-56.9419:	-22.4782:	-3.3676:	4.3769:	2.9114:	29.0287:	-12.6092:	-14.7200:	-2.5572:	2.7774:	-9.0406:	97.0507:
MOMENT PARALLEL TO Y-AXIS (MY)												
III=10:	67.5071:	39.0759:	11.9491:	7.7043:	5.5092:	32.0005:	0.5422:	21.5336:	9.4400:	6.7459:	-1.1255:	-6.9303:
TWISTING MOMENT MAY												
III=10:	-4.3872:	1.2395:	1.2347:	0.9421:	0.7604:	0.4371:	-1.6704:	0.6674:	0.0109:	0.5940:	0.3830:	-3.7524:
PRINCIPAL MOMENT M1												
III=10:	67.6616:	39.1005:	13.1663:	7.9525:	5.7940:	32.0634:	0.6728:	21.5459:	9.5051:	6.0329:	-1.1063:	97.1938:
PRINCIPAL MOMENT M2												
III=10:	-57.0703:	-22.5031:	-3.2047:	4.1207:	2.7066:	29.7657:	-12.0190:	-14.7331:	-2.6516:	2.6904:	-9.0509:	-7.1234:
PRINCIPAL DIRECTION												
III=10:	2.0165:	-1.1931:	-0.4052:	-14.7613:	-14.9253:	-0.1948:	4.4711:	-1.0543:	-2.0334:	-0.3326:	-2.7707:	-2.0620:
STRAIN IN X-AXIS												
III=10:	6.3236:	2.6527:	0.4409:	-0.3796:	-0.2481:	-2.7729:	1.3923:	1.7251:	0.3570:	-0.2233:	0.9230:	-10.0079:
STRAIN IN Y-AXIS												
III=10:	-7.5455:	-4.2503:	-1.3767:	-0.7500:	-0.5524:	-3.1212:	-1.0060:	-2.3743:	-1.0054:	-0.6737:	0.0311:	1.6453:
STRAIN IN U-AXIS												
III=10:	*****											



## BIBLIOGRAPHY

1. American Concrete Institute, "Building Code Requirements for Reinforced Concrete," (ACI 318-71), 1971.
- ✓ 2. Bares, R. and Massonet, C., "Analysis of Beam Grids and Orthotropic Plates by the Guyon-Massonet-Bares Method," Frederick Unger Publishing Co., New York, 1968.
3. Burns, N.H., and Hemakom, R., "Test of Scale Model Post-Tensioned Flat Plate," Journal of the Structural Division, ASCE, Vol. 103, No. ST6, June, 1977.
4. Cardenas, A.E., and Sozen, M.A., "Flexural Yield Capacity of Slabs," ACI Journal, Feb., 1973.
5. Cardenas, A.E., Lenschow, R.J., and Sozen, M.A., "Stiffness of Reinforced Concrete Plates," Journal of the Structural Division, Proc., ASCE, Vol. 98, No. ST11, Nov., 1972, pp. 2587-2603.
6. Evans, R.H., and Kong, F.K., "The Extensibility and Microcracking of the In-Situ Concrete in Composite Prestressed Concrete Beams," The Structural Engineer Journal, Vol. 42, No. 6, June 1964, pp. 181-190.
- ✓ 7. Gupta, D.S.R., and Kennedy, J.B., "Continuous Skew Orthotropic Plate Structures," Journal of the Structural Division, ASCE, Vol. 104, No. ST2, Feb. 1978, pp. 313-328.
- ✓ 8. Gupta, D.S.R., "Orthotropic Continuous Skew Plates," Ph.D. Thesis, 1974, Dept. of Civil Engineering, University of Windsor, Windsor, Ontario, Canada.
9. Hondros, G., and Smith, G.C., "Model and Theoretical Analysis of a Post-Tensioned Diagrid Flat Plate," PCI Journal, April, 1969, pp. 63-87.
10. Huffington, N.J., Jr., "Theoretical Determination of Rigidity Properties of Orthogonally Stiffened Plates," Journal of Applied Mechanics, Transaction S, ASME, Vol. 87, March, 1956, pp. 15-20.
11. Jackson, N., "The Torsional Rigidities of Concrete Bridge Decks," Concrete V<sub>2</sub>, n11, Nov., 1968, pp. 465-474.
12. Kennedy, J.B. and Gupta, D.S.R., "Bending of Skew Orthotropic Plate Structures," Journal of the Structural Division, Proc., ASCE, Vol. 102, No. ST8, August, 1976, pp. 1559-1574.

13. Kennedy, J.B., and Bali, S.K., "Rigidities of Concrete Waffle-Type Slab Structures," Accepted for publication in the Canadian Journal of Civil Engineering, March, 1979.
14. Kennedy, J.B., and Martins, I.C., "Stresses Near Corners of Skewed Stiffened Plates," The Structural Engineer, Vol. 41, 1963.
15. Kennedy, J.B., and Huggins, M.W., "Series Solution of Skewed Stiffened Plates," Journal of the Engineering Mechanics Division, ASCE, Vol. 90, No. EMI, Feb., 1964.
16. Kennedy, J.B., and Ng., S.F., "Analysis of Skewed Plate Structures with Clamped Edges," Trans. of the Engrg. Inst. of Canada, paper EIC-6S-BR STR9, Dec., 1965.
17. Lenert, Louis, H., "Advanced Technical Mathematics," Charles E. Merrill Publishing Company, A. Bell and Howell Company, Columbus, Ohio, 1970.
18. Lin, T.Y., "Design of Prestressed Concrete Structures," Second Edition, John Wiley and Sons, Inc., 1963.
19. McDonald, J.L., "Design of a Two-Way Post-Tensioned Waffle Slab," Civil Engineering, ASCE, May, 1973.
20. Muspratt, M.A., "Behaviour of a Prestressed Concrete Waffle Slab With Unbonded Tendons," ACI Journal, December, 1969, pp. 1001-1004.
21. Perry, P.G., and Heins, C.P., "Rapid Design of Orthotropic Bridge Floor Beams," Journal of the Structural Division, Proc., ASCE, Vol. 98, No. ST11, 1972, pp. 2491-2506.
22. Portland Cement Association, "Design and Control of Concrete Mixtures," Eleventh Edition, 1968.
23. Rawles, R.H., "Dallas Bridge Has Post-Tensioned Concrete Deck," Civil Engineering, ASCE, April, 1973.
24. Rowe, R.E., "Concrete Bridge Design," C.R. Books Limited, 1962.
25. Rowe, R.E., "Load Distribution in Bridge Slabs (With Special Reference to Transverse Bending Moments Determined From Tests on Three Prestressed Concrete Slabs)," Magazine of Concrete Research, Vol. 9, No. 27, November, 1957.

26. Scordelis, A.C., Lin, T.Y., and Itaya, R., "Behaviour of a Continuous Slab Prestressed in Two Directions," Journal of the American Concrete Institute, Dec., 1959, pp. 441-459.
27. Scordelis, A.C., Samarzich, W., and Pirtz, D., "Load Distribution on a Prestressed Concrete Slab Bridge," PCI Journal, June, 1960, pp. 18-33.
28. Sherman, Z., "Testing Post-Tensioned Slab and Beam Without Grouting," Journal of the Structural Division, ASCE, Vol. 83, No. ST4, July, 1957, pp. 1317, 1-17.
29. Szilard, R., "A Simplified Method for Torsional Analysis of Gridworks," ACI SP-35, American Concrete Institute, Detroit, 1973.
30. Szilard, R., "Theory and Analysis of Plates: Classical and Numerical Methods," Prentice-Hall Inc. Englewood Cliffs, New Jersey, 1974.
31. Timoshenko, S., and Woinowsky-Krieger, S., "Theory of Plates and Shells," McGraw Hill Book Co., 1959.
32. Wang, C-H., "Direct Design Method for Prestressed Concrete Slabs," PCI Journal, 1968, pp. 62-72.
33. Wylie, C.R., "Advanced Engineering Mathematics," McGraw-Hill Book Company, Inc., 1960.

VITA AUCTORIS

IBRAHIM SAYED AHMED EL-SEBAKHY

- 1949 Born on 1st of January in TANTA, EGYPT.
- 1967 Matriculated from Ahmedia School, TANTA, EGYPT.
- 1968 Attended the Military Technical College for one year, CAIRO, EGYPT.
- 1973 Graduated with Bachelor of Science (Honour) in Civil Engineering, from Alexandria University, ALEXANDRIA, EGYPT.
- 1973 Appointed as an instructor in Civil Engineering Department, Alexandria University, ALEXANDRIA, EGYPT.
- 1973 Joined as a part-time designer Engineer with Drs. Ebiedo, Fahmy and Korish Consulting Firm for Civil Engineering, ALEXANDRIA, EGYPT.
- 1976 Enrolled in a Master's program in Civil Engineering Department, University of Windsor, WINDSOR, ONTARIO, CANADA.